Implicación de LRP5 en la enfermedad cardiovascular

July Carolina Romero Sandoval

UNIVERSIDAD DE BARCELONA

FACULTAD DE FARMACIA

PROGRAMA DE DOCTORADO EN BIOMEDICINA

IMPLICACIÓN DE LRP5 EN LA ENFERMEDAD CARDIOVASCULAR

Tesis presentada por:

JULY CAROLINA ROMERO SANDOVAL

Para optar al grado de:

Doctor por la Universidad de Barcelona

Instituto Catalán de Ciencias Cardiovasculares (CSIC-ICCC)

El director | El director | El doctorando

Prof. Lina Badimon | **Dra. Maria Borrell-Pagés** | **July Carolina Romero**

Septiembre de 2014

A mi querido Krishna,

Porque todos mis logros son fruto de su misericordia.

A mi familia,

Que ha sido mi inspiración y motivación.

AGRADECIMIENTOS

Después de cinco años intensos de continuo aprendizaje, dedicación y miles de experiencias lejos de casa, llega el día en el que se cumple uno de mis grandes sueños. Un sueño que no hubiera sido posible sin la ayuda de tantas personas que se cruzaron en mi camino y me aportaron además de sus conocimientos y experiencias, su amistad y apoyo incondicional, cruciales durante esta etapa de mi vida.

En primer lugar quiero agradecer a la Dra. Lina Badimon por brindarme la oportunidad de realizar esta tesis y formar parte de su grupo de investigación. Gracias por tu disposición y ayuda durante estos años.

De manera muy especial quiero agradecer a Maria Borrell, quien fue mi mentora durante estos años. Gracias por haber confiado en mí, por haberme transmitido tanto conocimiento y por haber contribuido enormemente en mi formación profesional. Gracias por tu gran dedicación y esfuerzo para sacar este trabajo adelante. Gracias por brindarme tu amistad, tu comprensión y por estar dispuesta a escucharme y ayudarme en todo momento.

Quiero agradecer en general a todos los miembros del ICCC, porque de una u otra manera contribuyeron al desarrollo de mi tesis. En especial a Huertis, que ha trabajado mano a mano conmigo durante estos años. Muchas gracias por todo tu trabajo, por todo el tiempo compartido, por tu disponibilidad y por tu amistad. Esther P, Oriol, Maria Angeles, Sandra y Crespo, muchas gracias por colaborar en el desarrollo de varios de los experimentos de mi tesis, sus conocimientos y consejos fueron importantes para la continuidad de mi trabajo. Esther P, ya planearemos un viaje juntas, que no sea casualidad jiji. Oriol, mi compi de diálogos interreligiosos jeje. Maria Angeles, gracias por tu trabajo y gran simpatía. Sandra, eres una excelente persona, gracias por todos tus consejos. Crespin, buuu, que días más divertidos pasamos, gracias por sacarme una sonrisa cada vez que te veía.

Jose, Roi, Laura, Elena, chicos del antiguo 111, gracias por la cordial acogida que me dieron en su grupo, por su gran simpatía y buena disposición. Muchas gracias a mis compis de labo, Montse, Olaya, Espi, Esther, Rosa, por sus consejos, charlas y buen carisma. Montse, fue genial el tiempo compartido contigo y tu familia, gracias por ser mi amiga y darme apoyo cuando lo necesité. Olaya, gracias por tu apoyo en el labo y por compartir momentos y charlas chulis conmigo. Espi, gracias por tu compañía, la pasamos muy bien de fiesta. Esther, muchas gracias por tu labor en cultivos y por ayudarme cuando podías. Rosa, excelente compañera de viaje,

gracias por tu cordialidad y atención. Chicas del Biobanco, Maribel muchas gracias por tus consejos y por compartir tantas anécdotas curiosas de tu vida conmigo. Moni, siempre me recibías con una linda sonrisa, muchas gracias.

Muchas gracias a mis compis de comida por su compañía, simpatía y buen sentido del humor. Sergi y Josep, gracias por compartir con nosotras y por hacernos reír con tanto chiste malo jiji. Reichel, muchas gracias por haberme brindado tu amistad y por compartir tantas experiencias graciosas! Mi Maite, me faltan palabras para agradecerte todo lo que has hecho por mí. Gracias por escucharme, por ser un apoyo, por comprenderme, por todos los consejos y por alegrarme cada mañana con tu sonrisa, te quiero demasiado y espero que la distancia no sea un obstáculo para nuestra amistad.

Mi Yey, muchas gracias por recibirme cada finde en tu casa y por aguantarme tan llorica durante los primeros meses. Gracias por estar pendiente de mí y por brindarme tu compañía y palabras de aliento. Olguis, mi primera amiga catalana!! Aunque costó al principio, luego me mostraste tu hermosa personalidad, gracias por todo el apoyo recibido durante mis primeros meses en España. Helen!!! Muchas gracias por todos los findes de esparcimiento y desconexión!!! Moni y Cami, mis amigos vecinos, muchas gracias por recibirme tantas veces después del trabajo y escucharme. Gracias por todas las cenas y chocolates que compartimos, fueron un apoyo muy grande para mí durante este tiempo. Bertis, mi mejor compi de piso, gracias por este último año, ha sido una experiencia muy bonita compartir un hogar contigo, gracias por todas las tardes de chicas, de fiesta, de helados, en fin, gracias por tu compañía y amistad. Mi Kari, aunque muy lejos, siempre estuviste a mi lado por medio de las videollamadas y tanto whatsapp, gracias por tus sabios consejos y palabras de aliento en los momentos oportunos, te quiero mucho.

Y como no agradecer a mis amigos espirituales, muchas gracias por haber sido mi familia sustituta durante estos años, gracias por darme a conocer ese mundo espiritual tan hermoso que es lo más lindo que me llevo de España. Jaja Lashmy y Nimay, gracias por sus consejos, amistad y simpatía. Mana Mohana, Pilar, Jahnavi y familia, gracias por recibirme en su hogar como un miembro más, los llevo en mi corazoncito. En general muchas gracias a todos los devotos del templo, que con su simpatía y amor recargaban mi corazón cada domingo para

continuar con este camino que hoy culmina, los llevo en mi corazón al igual que a mis hermosas Goura y Nitae.

Quiero agradecer inmensamente a mi familia, que ha sido mi motivación desde el inicio de mi carrera. Espero algún día poder retribuirles todo lo que han hecho por mí, ya que la persona que soy ahora es gracias a todo su servicio y dedicación, gracias por siempre haber puesto a Dios en mi camino, se los agradezco inmensamente. Papitos, nadie más que sus hijos saben todo el esfuerzo que les ha costado sacarnos adelante a todos y habernos formado tan bien como lo han hecho, no sólo a nivel personal y profesional, sino a nivel espiritual, son dignos de mucha admiración. Nanis, mi mejor amiga y confidente, gracias por todo tu apoyo, este doctorado es de las dos, porque sin tu ayuda no hubiera podido perseverar y alcanzar la meta. Gracias por todo lo que has cuidado a mis papis durante mi ausencia, te amo mucho. Gabi, gracias por ser tan bueno con toda mi familia, por aguantarlos y por brindarles tu hogar, eres una gran persona y te quiero mucho. Mi bebé, te agradezco la compañía y la satisfacción que das a mis padres por medio de tus logros. Camilo, muchas gracias por todo tu amor, compañía y apoyo durante los primeros años que fueron los más duros, estar a tu lado me reconfortaba y llenaba el vacío de estar lejos de casa. Agradezco a mis demás familiares y amigos por sus buenos deseos y grandes recibimientos cada vez que visitaba Colombia, los estimo y recuerdo mucho.

Finalmente, quiero expresar mis más sinceros agradecimientos a mi querido Krishna, mi padre y amigo incondicional que siempre estuvo guiando mis pasos, dándome fortaleza, tenacidad, tolerancia, alegría, compañía, confort y mucho amor. Gracias por poner en mi vida tantas personas hermosas que han hecho parte de este logro. Gracias por enseñarme a desarrollar buenas cualidades y por mostrarme que más allá de este mundo material estás Tú esperando que volvamos a tu lado. Te amo con todo mi corazón y espero poder servirte cada día de mi vida.

MUCHAS GRACIAS A TODOS!!!

ÍNDICE

ABREVIATURAS

ABCA	Transportadores con dominio de unión al ATP, subfamilia A
ABCG	Transportadores con dominio de unión al ATP, subfamilia G
ACAT	Acil-CoA:colesterol aciltransferasa
TIA	Ataque isquémico transitorio
APC	Poliposis adenomatosa coli
AV-FITC	Annexin V-isotiocianato de fluoresceína
BCA	Ácido bicinconínico
BMP2	Proteína morfogénica ósea-2
BrdU	Bromodesoxiuridina
BSA	Albúmina de suero bovino
CAD	Enfermedad de las arterias coronarias
CE	Ésteres de colesterol
CETP	Proteína de transferencia de esteres de colesterol
CHD	Cardiopatía coronaria
CM	Quilomicrones
CVD	Enfermedades cardiovasculares
Dvl	Dishevelled
EC	Células endoteliales
ECM	Matriz extracelular
EGF	Factor de crecimiento epidérmico
EGTA	Ácido etilenglicoltetraacético
F3	Factor III de coagulación
FC	Colesterol libre
FFA	Ácidos grasos libres
GSK3B	Glucógeno sintasa quinasa 3 beta
HC	Dieta hipercolesterolémica
HC+PSE	Dieta hipercolesterolémica suplementada con fitoesteroles esterificados
HDL	Lipoproteínas de alta densidad
HL60	Células de leucemia promielocítica humana
HM	Monocitos humanos
HMDM	Macrófagos derivados de monocitos humanos
HeFH	Hipercolesterolemia familiar heterocigota

HoFH	Hipercolesterolemia familiar homocigota
IDL	Lipoproteínas de densidad intermedia
IFNG	Interferón gamma
LCAT	Lecitina:colesterol acetiltransferasa
LDL	Lipoproteínas de baja densidad
LDLR	Receptor de lipoproteínas de baja densidad
LEF-1	Factor potenciador linfoide 1
LPL	Lipoproteína lipasa
LPS	Lipopolisacáridos
LRP5	LDL receptor tipo 5
Lrp5$^{-/-}$	Ratones deficientes para LRP5
MMPs	Metaloproteínasas de matriz
MI	Infarto de miocardio
NC	Dieta normocolesterolémica
OCT	Temperatura de corte óptima
OPN	Osteopontina
OPPG	Síndrome de osteoporosis-pseudoglioma
PLPT	Proteína de transferencia de fosfolípidos
PMA	Forbol 12-miristato 13-acetato
PSE	Fitoesteroles esterificados
siRNA	ARN pequeño de interferencia
SR	Receptor depurador (scavenger receptor)
TCF	Factor de células T
TG	Triglicéridos
TNFα	Factor de necrosis tumoral alfa
VLDL	Lipoproteínas de muy baja densidad
VSMC	Células musculares lisas vasculares
WHHL	Conejos Watanabe con hiperlipidemia hereditaria
Wt	Tipo silvestre (Wildtype)

INTRODUCCIÓN

1. ENFERMEDADES CARDIOVASCULARES (CVD)

1.1 Tipos de CVD

Las enfermedades cardiovasculares son la principal causa de discapacidad y muerte prematura en el mundo[1] (Figura 1). Los paros cardíacos y los accidentes cerebrovasculares son fenómenos agudos debido a obstrucciones que impiden el flujo de la sangre al corazón o al cerebro. Las causas más frecuentes son la formación de depósitos de grasa en las paredes de los vasos sanguíneos, las hemorragias de los vasos cerebrales y los coágulos de sangre[2].

Las ECV se pueden presentar clínicamente como:

- *Cardiopatía coronaria (CHD)*: Causada por enfermedades de los vasos sanguíneos que irrigan el músculo cardíaco.
- *Ictus y ataque isquémico transitorio (TIA):* Causadas por una alteración del flujo sanguíneo que irriga al cerebro. Pueden ser resultado de un bloqueo (ictus isquémico) o por la ruptura de un vaso sanguíneo (ictus hemorrágico).
- *Aneurisma aórtico:* Causado por la dilatación y ruptura de la aorta.
- *Arteriopatías periféricas:* Causadas por enfermedades en las arterias que irrigan los miembros superiores e inferiores.
- *Cardiopatía reumática:* Originada por lesiones del miocardio y de las válvulas cardíacas debidas a la fiebre reumática (causada por estreptococos).
- *Cardiopatías congénitas:* Se presentan por malformaciones en estructuras del corazón presentes desde el nacimiento, causadas por factores genéticos o por exposiciones adversas durante la gestación.
- *Trombosis venosa profunda y embolias pulmonares:* estas ocurren por la formación de coágulos de sangre en las venas de las piernas, que pueden desprenderse y alojarse en los vasos del corazón y en los pulmones.
- *Otras CVD:* tumores del corazón, tumores vasculares del cerebro, enfermedad de la válvula cardíaca[3].

El 42.5% de las defunciones por CVD están relacionadas con la cardiopatía isquémica y un 35.5% con las enfermedades cerebrovasculares (Figura 1).

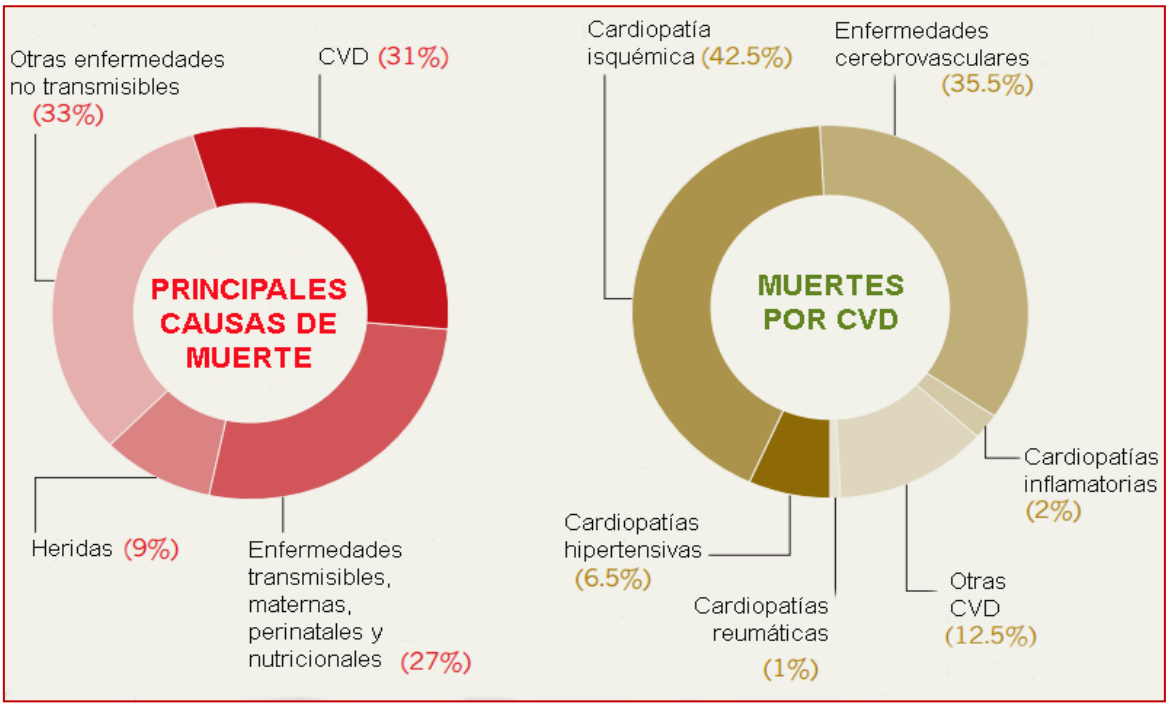

Figura 1: Principales causas de muerte a nivel mundial. Las enfermedades cardiovasculares son la principal causa de muerte, dentro de las cuales predominan la cardiopatía isquémica y los eventos cerebrovasculares. Modificado de Cannon et al, 2013[4].

1.2 Factores de riesgo de las CVD

Se han identificado 8 factores de riesgo que ocasionan el 61% de las muertes causadas por CVD: el consumo de alcohol y de tabaco, la hipertensión, el sobrepeso, los niveles altos de colesterol y glucosa en sangre, los malos hábitos alimentarios y el sedentarismo[5]. La modificación de estos factores de riesgo reduce la morbilidad y la mortalidad en personas con CVD diagnosticadas[6].

Varios estudios han demostrado que ciertos factores psicosociales, como la depresión, la ansiedad, la falta de apoyo social y las condiciones de estrés en el trabajo, incrementan la incidencia de los factores de riesgo principales y el curso de la enfermedad coronaria[7–10].

Una prevención efectiva depende de la identificación de los individuos con riesgo a desarrollar alguna enfermedad cardíaca. Mediante el uso de los factores de riesgo convencionales se intenta predecir el riesgo global de los pacientes, el diagnóstico y el tratamiento terapéutico. Además, se está implementando el uso de biomarcadores moleculares que permitan predecir eventos cardiovasculares[11]. Así, actualmente se utilizan biomarcadores de inflamación, de disfunción endotelial, de activación neurohormonal y de isquemia.

2. ATEROSCLEROSIS

Las complicaciones de la aterosclerosis se manifiestan en la edad adulta o en la vejez. Sin embargo, la aterosclerosis, que es el principal proceso patológico que da lugar a las CVD, comienza a una edad temprana y avanza gradualmente durante la adolescencia y la edad adulta[12]. Su progresión se encuentra modulada por la presencia de los factores de riesgo cardiovasculares.

La aterosclerosis es una enfermedad inflamatoria crónica caracterizada por la acumulación de lípidos y elementos fibrosos en las arterias[13], que surge por un desequilibrio en el metabolismo lipídico y por una mala respuesta inmune generada por la acumulación de macrófagos cargados de colesterol y la multiplicación y migración de las células musculares lisas en la pared vascular[14]. Los engrosamientos de las arterias se denominan placas y ocasionan un deterioro progresivo del vaso y una reducción del flujo sanguíneo[12].

Con el objetivo de estudiar la patogénesis de la aterosclerosis se han diseñado varios modelos animales. Entre los más usados se encuentra el modelo de ratones deficientes para el receptor de lipoproteínas de baja densidad (LDLR). Estos ratones presentan altos niveles de colesterol en plasma y concentraciones de lipoproteínas de densidad intermedia (IDL) y de baja densidad (LDL) 7-9 veces más altas que en los ratones silvestres (*Wt*). Además, cuando los ratones *Ldlr*$^{-/-}$ son alimentados con una dieta rica en colesterol desarrollan hipercolesterolemia severa y aterosclerosis aórtica[15]. Este modelo junto al de ratones deficientes para la Apolipoproteína E (*Apoe*$^{-/-}$) han sido de gran utilidad en la caracterización de los procesos y dianas clave en el desarrollo y progresión de la lesión aterosclerótica. En los siguientes apartados se explicará en términos generales el metabolismo de las lipoproteínas, la anatomía de la pared vascular y las principales etapas en el desarrollo de la aterosclerosis.

2.1 Lipoproteínas

2.1.1 Estructura y composición

La alteración del metabolismo lipídico (dislipemia) es un factor que contribuye al desarrollo y progresión de la placa aterosclerótica. De hecho, las lipoproteínas plasmáticas son la fuente principal de los lípidos que se encuentran en la placa[16]. Las lipoproteínas están formadas por

fosfolípidos, colesterol libre (FC), apoproteínas y un núcleo interno hidrofóbico compuesto por triglicéricos (TG) y ésteres de colesterol (CE) (Figura 2).

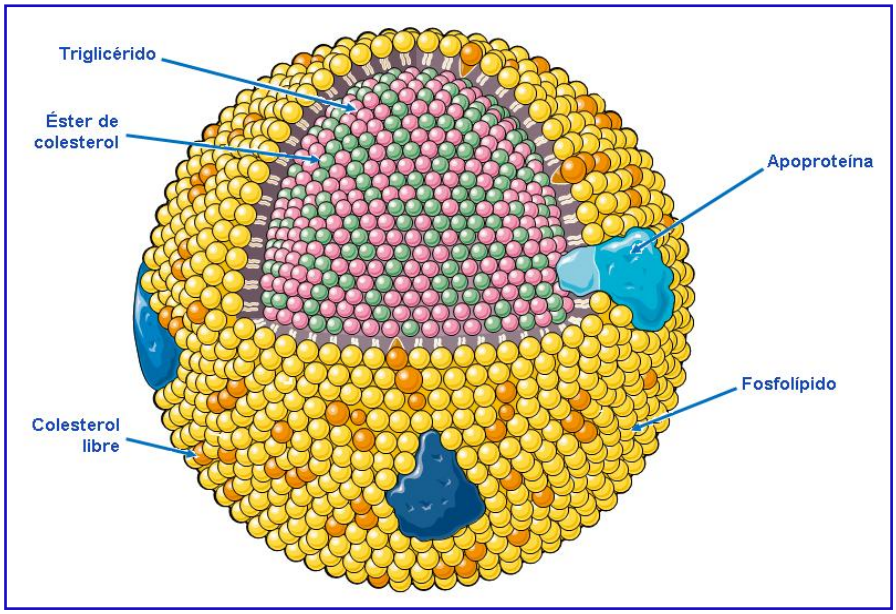

Figura 2: Estructura de las lipoproteínas. El colesterol libre (FC), las apoproteínas y los fosfolípidos se localizan en el exterior de la partícula. En el interior se encuentran los triglicéridos (TG) y los ésteres de colesterol (CE).

Las lipoproteínas se clasifican principalmente en 5 tipos según su composición y función: quilomicrones (CM), lipoproteínas de muy baja densidad (VLDL), IDL, LDL y lipoproteínas de alta densidad (HDL) (Tabla 1).

Lipoproteínas plasmáticas humanas					
	Quilomicrón	**VLDL**	**IDL**	**LDL**	**HDL**
Densidad (g/mL)	0.95	0.95-1.006	1.006-1.019	1.019-1.063	1.063-1.210
Composición (% en peso seco)					
Proteína	2	7	15	20	40-55
Triglicéridos	83	50	31	10	8
Colesterol libre	2	7	7	8	4
Ésteres de colesterol	3	12	23	42	12-20
Fosfolípidos	7	20	22	22	22
Composición de apoproteínas	A-I,A-II,B-48, C-I,C-II,C-III	B-100,C-I, C-II,C-III,E	B-100,C-I, C-II,C-III,E	B-100	A-I,A-II,C-I, C-II,C-III,D,E
Origen	Intestino	Hígado	Metabolismo de VLDL	Metabolismo de VLDL	Intestino, hígado (CM y VLDL)

Tabla1: Composición química de las principales clases de lipoproteínas humanas aisladas por gradiente de ultracentrifugación[17].

2.1.2 Metabolismo de las lipoproteínas

El colesterol proviene de la ingesta (300-500mg/día en una persona con dieta occidental) y de la producción hepática (800-1300mg/día). El colesterol absorbido es procesado en un 50% por los enterocitos del intestino delgado (duodeno y yeyuno), mientras que el otro 50% es eliminado en las heces[18,19]. En el enterocito, el colesterol es esterificado por la enzima acil-CoA:colesterol aciltransferasa (ACAT) e incorporado junto con los TG en los CM. Los CM son liberados a la linfa y entran a la circulación sistémica por medio del conducto torácico. Ya en la sangre, los CM adquieren algunas apolipoproteínas de las HDL y transfieren su contenido de TG al tejido adiposo y muscular, donde son hidrolizados a ácidos grasos libres (FFA) por la lipoproteína lipasa (LPL) y así, usados como fuente de energía (Figura 3). Después de perder los TG, los CM interactúan de nuevo con las HDL, que los convierten en CM residuales que son transportados al hígado y absorbidos por las células parenquimales hepáticas[20].

En el hígado, el colesterol de los CM residuales, junto con el colesterol de síntesis endógena es empaquetado en las VLDL y exportado a la sangre; de manera similar a los CM, las VLDL transportan TG a los diferentes tejidos. Además, las VLDL liberan FC, fosfolípidos y apolipoproteínas que son tomadas por las HDL. Cuando el contenido de las VLDL en la sangre cambia, estas partículas son transformadas en IDL y LDL, que son los principales transportadores de colesterol a través de la sangre[20].

En la pared vascular, la internalización de lípidos aumenta en presencia de altas concentraciones de LDL en sangre. Una vez internalizados, los lípidos son modificados por mecanismos oxidativos y no oxidativos[21]. Los macrófagos presentes en la pared arterial participan en la acumulación de colesterol como se explicará en la siguiente sección.

En la célula, las LDL son degradadas en los lisosomas y el colesterol es utilizado para sus necesidades específicas. El colesterol residual es eliminado por medio del transporte reverso del colesterol. Este proceso lo realizan mayoritariamente las HDL. Las HDL nacientes en la sangre (formadas por ApoA-1) reciben colesterol y fosfolípidos de las células cargadas de colesterol de los tejidos extra-hepáticos mediante el receptor transportador con dominio de unión al ATP-A1 (ABCA1). El FC de las HDL es esterificado por la lecitina:colesterol acetiltransferasa (LCAT) y la HDL naciente se convierte en una HDL madura (Figura 3). Esta HDL

provee CE a diferentes lipoproteínas en un intercambio por TG y las HDL residuales son transportadas al hígado para su eliminación por la bilis y las heces.

Otro mecanismo para eliminar el exceso de colesterol es la metabolización del colesterol en oxiesteroles solubles, los cuales salen por difusión de la célula hacia la circulación y son rápidamente transportados al hígado para su degradación[22].

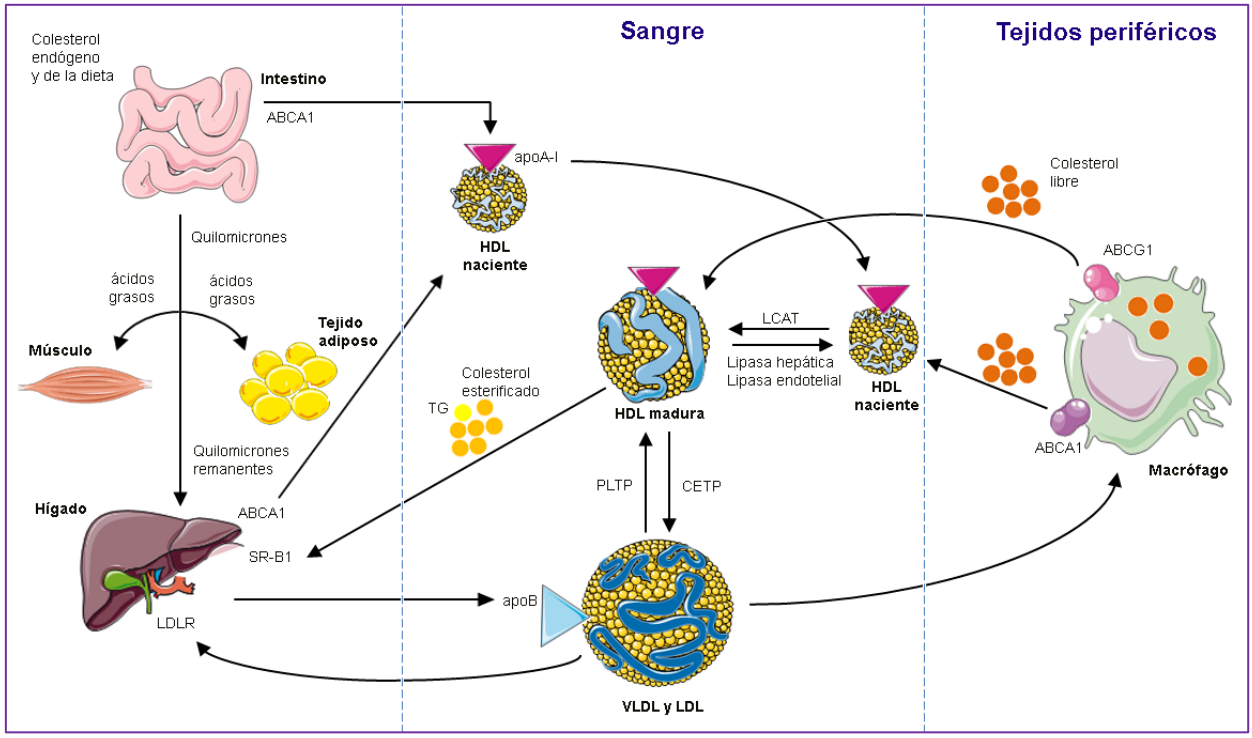

Figura 3: Metabolismo de las lipoproteínas. El intestino absorbe los lípidos endógenos y los de la dieta y los almacena en quilomicrones (CM), los cuales son transportados por la sangre a los tejidos periféricos donde liberan su contenido de ácidos grasos. Los CM residuales son absorbidos por el hígado y secretados en sangre donde se transforman a VLDL o LDL mediante la adición de ApoB. Las LDL son de nuevo absorbidas por el hígado a través de LDLR. Por otro lado, las HDL son producidas por el intestino y el hígado. En los tejidos periféricos, las HDL nacientes estimulan la salida del colesterol de los tejidos, por medio de ABCA1 y las HDL maduras por medio de ABCG1. El colesterol libre (FC) en las HDL nacientes es esterificado a CE por medio de la enzima lecitina:colesterol acetiltransferasa (LCAT), creando HDL maduras. El colesterol de las HDL es devuelto al hígado mediante la unión al receptor de depuración-B1 e indirectamente por la transferencia de CE a las LDL y VLDL mediada por la proteína de transferencia de CE (CETP). El contenido lipídico de las HDL depende de las enzimas lipasa hepática, lipasa endotelial, CETP y de la proteína de transferencia de fosfolípidos (PLPT). Modificado de Rader and Daugherty, 2008 [23].

2.2 La pared vascular

La pared vascular está compuesta por tres capas: la íntima, la media y la adventicia (Figura 4). Cada una presenta unas características funcionales, bioquímicas e histológicas específicas, contribuyendo al mantenimiento de la homeostasis vascular y a la regulación de la respuesta inflamatoria provocada por estrés o daño[24].

La íntima es la capa más interna de la arteria y está compuesta por el endotelio y el subendotelio. El endotelio está formado por una monocapa de células endoteliales (EC) que conforman la interface física entre la sangre y el tejido, y el subendotelio, es la lámina basal compuesta por proteoglicanos y colágeno, que limita con la lámina elástica interna. Las EC regulan el paso de nutrientes y componentes de la sangre y participan en varios procesos fisiológicos como son la homeostasis, la inflamación y la angiogénesis[25].

La capa media está compuesta por las células musculares lisas vasculares (VSMC) y proteínas de la matriz extracelular (ECM), como elastina, colágeno y proteoglicanos[25]. Esta capa está limitada exteriormente por la lámina elástica externa que permite el paso de sustancias en ambas direcciones.

La adventicia es la capa exterior de la arteria y está formada principalmente por fibroblastos, fibrocitos y fibras de colágeno. El grosor de la adventicia depende de la función fisiológica y la ubicación del vaso sanguíneo. El colágeno contribuye a la estabilidad y firmeza de la pared arterial[26].

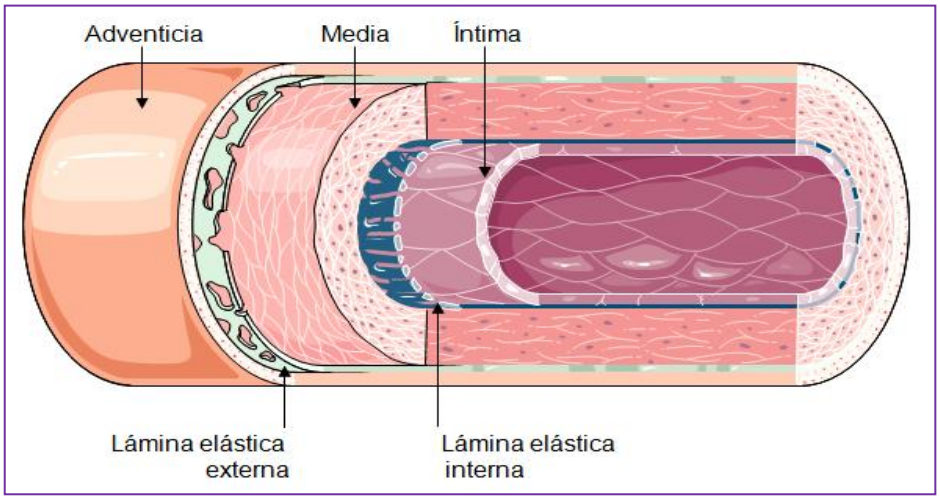

Figura 4: Representación de la estructura de la pared vascular.

2.3 Desarrollo de la lesión aterosclerótica

2.3.1 Activación endotelial:

Los cambios más tempranos que preceden la formación de la lesión aterosclerótica tienen lugar en el endotelio[12]. Esta capa está formada por células endoteliales, que en condiciones fisiológicas normales son resistentes a la adhesión y agregación de plaquetas, y a la adhesión de células inflamatorias[27]. Cuando el endotelio es activado por diversos factores, como la dislipemia, cambios en la velocidad del flujo sanguíneo, la hipertensión, la obesidad, la resistencia a la insulina o las dietas y hábitos poco saludables, se induce la secreción de citoquinas/quimioquinas y la expresión de receptores de adhesión (integrinas y selectinas) que aumentan la permeabilidad del endotelio y favorecen la adhesión y transmigración de leucocitos dentro de la pared arterial[27,28] (Figura 5A).

2.3.2 Adhesion e infiltración de monocitos:

Los monocitos son las principales células inflamatorias que participan en la progresión de la lesión aterosclerótica. Tras la activación del endotelio, los monocitos circulantes comienzan a rodar lentamente por la superficie del endotelio activado mediante su unión a los receptores de adhesión (selectina P y selectina E). A continuación los monocitos se adhieren firmemente a la superficie del endotelio mediante la unión a moléculas de adhesión celular vascular e intercelular (VCAM1 e ICAM1). Las quimioquinas (proteínas pro-inflamatorias) generan un estímulo quimiotáctico que induce la migración de los monocitos hacia la capa íntima (Figura 5A) donde se diferencian a macrófagos y comienzan a internalizar lípidos por medio de la expresión de receptores depuradores (SR, scavenger receptor) y receptores tipo Toll en la membrana celular [27,29].

2.3.3 Formación de las células espumosas y la capa fibrosa:

La continua internalización de lipoproteínas por parte de los macrófagos lleva a la formación de gotas de lípidos dentro de su citoplasma, generando una apariencia espumosa (Figura 5B). Estas células espumosas liberan factores de crecimiento, citoquinas, especies de oxígeno reactivas y otras enzimas que pueden destruir la ECM arterial, como las metaloproteinasas de matriz (MMPs) y el factor III de coagulación (F3)[27,28]. Este proceso está acompañado de la proliferación

y migración de las VSMC, de la activación de las células T, y de la adhesión y agregación de plaquetas[12]. Finalmente, las células espumosas sufren apoptosis y mueren, liberando todo su contenido lipídico y contribuyendo al desarrollo del centro necrótico[30] (Figura 5C). La proliferación de células musculares lisas conduce a la formación del tejido fibroso aumentando el tamaño de la lesión y reestructurándola. La lesión estará cubierta por una capa fibrosa, formada por una mezcla de leucocitos, lípidos y restos celulares, que rodea el centro lipídico y el tejido necrótico[12].

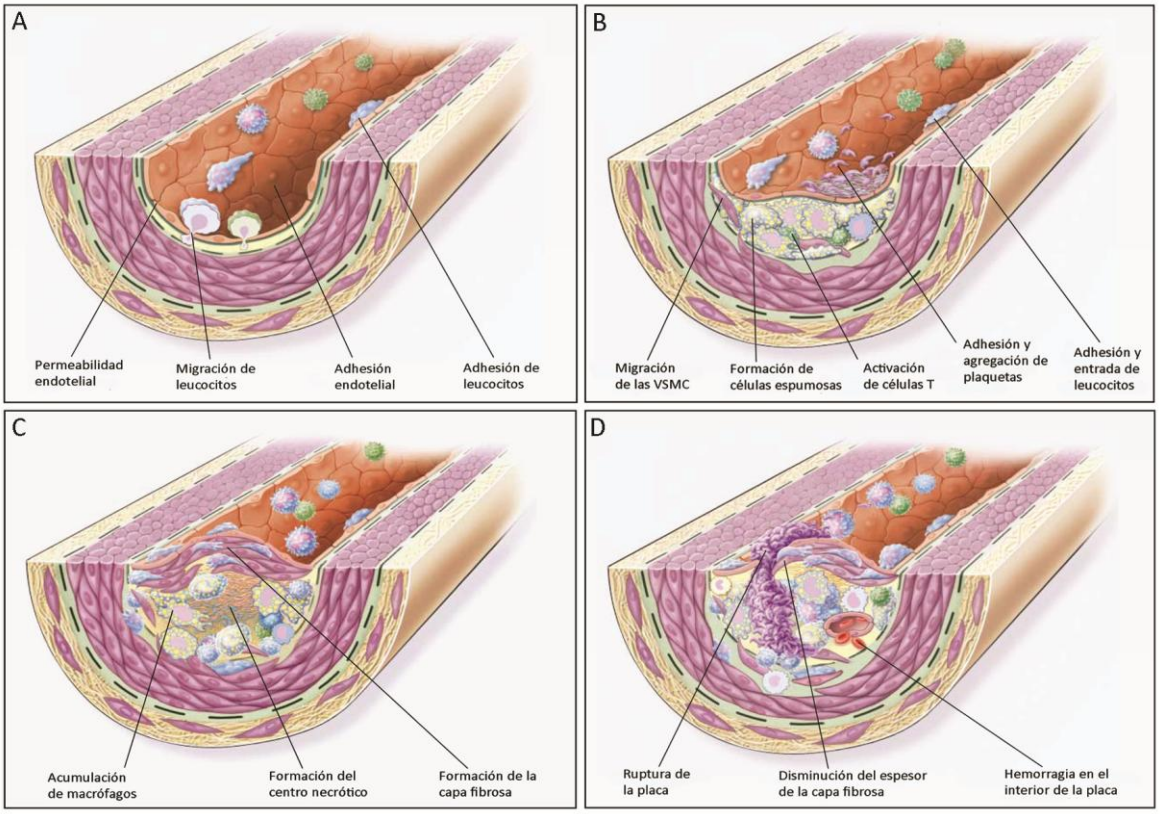

Figura 5: Desarrollo de la placa aterosclerótica. La activación del endotelio está provocada por diversos factores que incluyen la hipertensión, la dislipemia, el estrés de fricción y las infecciones. El endotelio activado permite la entrada de lípidos y aumenta la expresión de moléculas de adhesión que facilitan la migración de leucocitos en el espacio subendotelial **(A)**. En la capa íntima, los monocitos se diferencian a macrófagos que fagocitan lípidos ocasionando la acumulación de colesterol y la formación de células espumosas **(B)**. Los continuos ciclos de inflamación, acumulación y muerte de macrófagos, junto con la proliferación y migración de las VSMC, llevan a la formación de la capa fibrosa y a la progresión de la placa aterosclerótica **(C)**. El incremento en la liberación de MMPs y otras enzimas proteolíticas por parte de los macrófagos degradan la matriz y pueden llevar a una hemorragia desde el interior de la placa o desde el lumen de la arteria produciendo la formación de un trombo y la oclusión de la arteria **(D)**. Modificado de Ross, 1999[12].

2.3.4 Lesión avanzada y trombosis:

En el estadio avanzado de la aterosclerosis, las células endoteliales se deterioran y desprenden creando un ambiente propicio para el desarrollo de trombosis (Figura 5D). La túnica media reduce su grosor debido a la continua entrada de macrófagos que liberan MMPs y otras enzimas proteolíticas. Estas enzimas degradan la ECM y pueden iniciar una hemorragia desde el interior de la placa o desde el lumen de la arteria resultando en la formación de un trombo y en la oclusión de la arteria[12,30].

3. INFLAMACIÓN Y DIFERENCIACIÓN CELULAR EN LA ATEROSCLEROSIS

El avance de la aterosclerosis incluye diferentes respuestas celulares y moleculares específicas, que en conjunto son características de una enfermedad inflamatoria[12]. La participación de los monocitos y los macrófagos en el desarrollo de la lesión y su compleja interacción con las EC y las VSMC han sido claves para la descripción de la aterosclerosis como un proceso inflamatorio[30].

En el modelo murino los niveles elevados de colesterol en sangre inducen un aumento en los niveles de células madre hematopoyéticas y su diferenciación a monocitos y neutrófilos, que participan en la progresión de la lesión aterosclerótica[31]. Además, las células espumosas presentes en la lesión secretan mediadores de la inflamación que estimulan la desdiferenciación, proliferación y migración de las VSMC contribuyendo al desarrollo y a la ruptura de la placa[32,33].

La infiltración de células inflamatorias en la pared vascular y su diferenciación a macrófagos juegan un papel muy importante durante todos las etapas de la progresión de la lesión[27]. Los monocitos son clasificados en dos grupos en base a la expresión de CD14 -un antígeno de superficie que participa en el reconocimiento de moléculas externas como lipopolisacáridos (LPS)- y de CD16 –un miembro de la familia de receptores Fc (fragmento cristalizable)- en su superficie celular[34]. Los monocitos clásicos, $CD14^{++}CD16^{-}$ representan el 85-95% del total de monocitos; y los no-clásicos $CD14^{+}CD16^{+}$ comprenden cerca del 5-15%[35,36]. En ratón, los monocitos son diferenciados en base a la expresión de Ly-6C, un epítopo del antígeno de diferenciación mieloide Gr1, y son llamados $Ly\text{-}6C^{hi}$ y $Ly\text{-}6C^{lo}$ or $Gr1^{hi}$ y $Gr1^{lo}$, respectivamente[37,38]. Se ha propuesto que los monocitos de ratón $Ly\text{-}6C^{hi}$ y $Ly\text{-}6C^{lo}$ son análogos

de los monocitos clásicos $CD14^{++}CD16^{-}$ y no-clásicos $CD14^{+}CD16^{+}$ humanos, respectivamente[39]. Durante la progresión de la lesión aterosclerótica los monocitos clásicos son más abundantes y promueven la formación de macrófagos en la placa aterosclerótica mientras que los no-clásicos, también llamados monocitos controladores ("patrolling"), son menos abundantes, disminuyen la inflamación y promueven la angiogénesis[38].

A pesar de que la aterosclerosis ha sido ampliamente descrita por su fuerte componente inflamatorio, las terapias actuales están enfocadas a reducir la hiperlipemia y a prevenir la trombosis[40]. Aunque se puede observar ciertos efectos pleiotrópicos anti-inflamatorios en algunas terapias, como la del ácido acetilsalicílico y las estatinas, en general las terapias actuales para el tratamiento de la aterosclerosis no tienen como diana principal la inflamación[40]. El continuo análisis del potencial de diferenciación de los monocitos y su función en la inflamación durante la aterosclerosis puede dar lugar a futuras dianas terapéuticas para combatir la aterosclerosis y sus complicaciones.

4. FAMILIA DE RECEPTORES DE LAS LDL

Los miembros de la familia de receptores de las LDL son glicoproteínas transmembrana reconocidos como receptores endocíticos de superficie, los cuales se unen e internalizan ligandos extracelulares para su degradación por lisosomas[41]. Estos receptores participan en diversos procesos que incluyen: el transporte de lipoproteínas, la eliminación de complejos inhibidores de proteasas del plasma, el transporte y la eliminación de las LDL plasmáticas, y la transducción de señales biológicas durante el desarrollo y la diferenciación[41].

La familia de LDLR está compuesta por: LDLR, VLDLR, LRP1, LRP2, LRP3, LRP4, LRP5, LRP6, LRP8, LRP10 y LR11. En relación a la estructura, estos receptores tienen varios dominios en común, tales como los dominios de unión al ligando, los dominios homólogos al factor de crecimiento epidérmico (EGF) y los dominios transmembrana y citoplasmático (Figura 6). Los dominios de unión al ligando son repeticiones tipo A de 40 aminoácidos, con seis residuos de cisteína formando tres enlaces disulfuro ubicados en el extremo NH_2; las repeticiones homólogas al EGF, junto con un dominio de hélice enrollada β, están involucrados en la disociación dependiente de pH del complejo receptor-ligando[42,43]. Los dominios transmembrana participan en el anclaje de estos receptores a la membrana, mientras los dominios citoplasmáticos, que

contienen motivos NPxY o PPPSP, participan en la endocitosis mediada por receptor y en las vías de transducción de señales intracelulares[41,43].

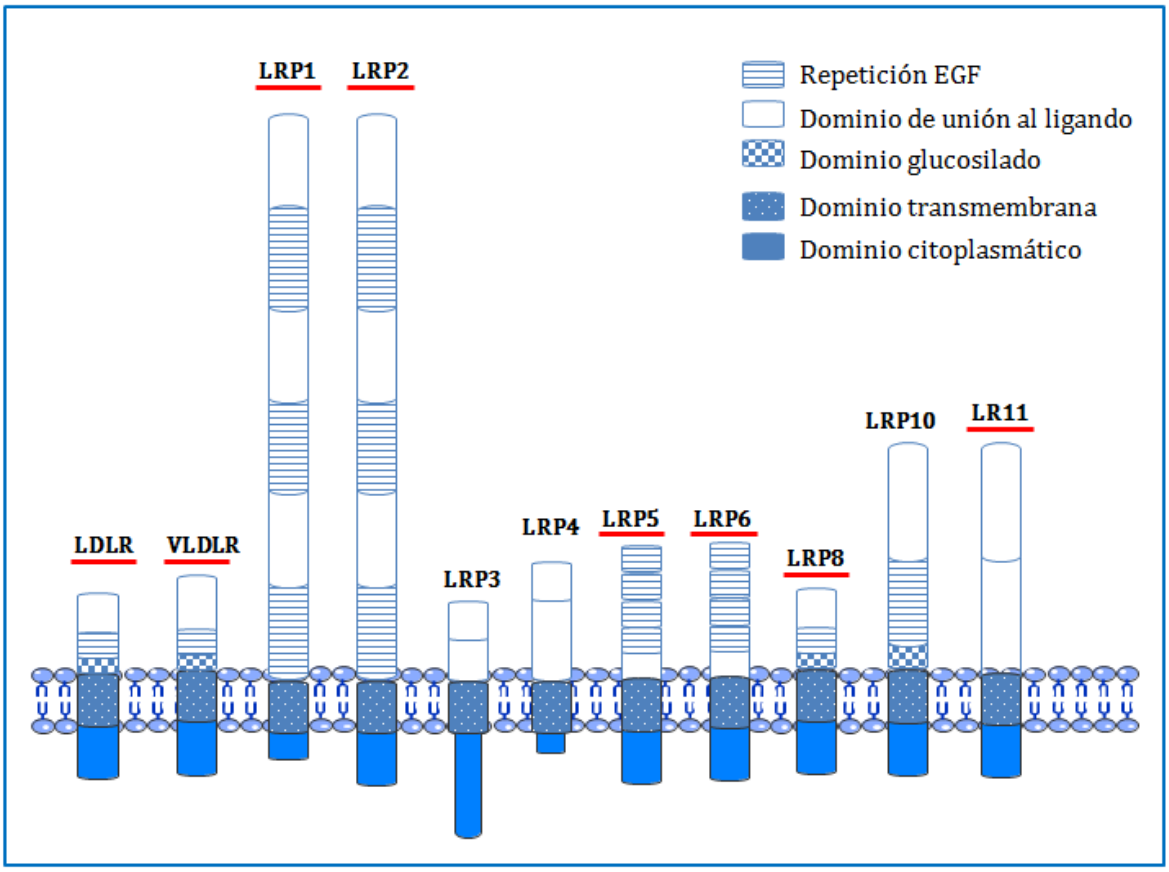

Figura 6: Comparación de los dominios estructurales en la familia de LDLR. Los receptores que participan en distintas enfermedades cardiovasculares están subrayados en rojo.

4.1 LDLR y VLDLR

LDLR fue el primer miembro de la familia descrito por su papel en la eliminación de las LDL y CE de la sangre[44]. Las mutaciones en el receptor de las LDL son la causa más común de hipercolesterolemia familiar (FH)[45], una enfermedad metabólica hereditaria, que presenta diferentes manifestaciones clínicas como aterosclerosis prematura y CHD[46]. Los pacientes con ambos alelos de LDLR mutados (FH homocigota, HoFH) están más afectados que los pacientes con sólo un alelo mutado (FH heterocigota, HeFH)[47].

VLDLR está expresado en el endotelio capilar del músculo esquelético, corazón, tejido adiposo e hígado[48], y se une a las VLDL y a los quilomicrones residuales[49]. La unión de estas partículas de lipoproteínas a VLDLR es estimulada por APOE y LPL e inhibida por la proteína de 39-kDa

asociada al receptor [50]. En el tejido vascular humano sano, VLDLR está expresado en las EC y VSMC. Estudios en ratones deficientes para VLDLR han mostrado un papel importante de este receptor en la migración de las VSMC y en la formación de células espumosas[51]. De hecho, la reconstitución de la expresión de VLDLR en los macrófagos de ratones *Vldlr*$^{-/-}$ aumenta significativamente el tamaño de la lesión, sugiriendo un papel facilitador para VLDLR de macrófagos en el desarrollo de la lesión aterosclerótica[51].

4.2 LRPs

La subfamilia de LRPs participa en el metabolismo de los lípidos, la neurotransmisión, el desarrollo embrionario, la formación ósea y las enfermedades cardiovasculares. La importancia de estos receptores radica en su habilidad para unirse a diferentes ligandos (e.g. glicoproteínas y lípidos) y de esta forma modular diversos procesos iniciados en respuesta a estímulos de daño o estrés[41,52,53]. Los receptores de esta subfamilia con un papel en la aterosclerosis u otras CVD son LRP1, LRP2, LRP5, LRP6, LRP8 and LR11 (Figura 6).

La sobreexpresión de LRP1 causa alteraciones en la función de las células cardiovasculares debido a una acumulación de lípidos intracelulares[54,55], al cambio a un fenotipo pro-trombótico[56,57] y a alteraciones en el transporte de calcio[58]. Por otro lado, la deficiencia de LRP1 provoca un aumento de la apoptosis de macrófagos[59] y de la captación de monocitos en las lesiones ateroscleróticas[59,60]. LRP2 regula el metabolismo de las HDL por medio de la internalización de sus componentes estructurales[61–63]. Estudios poblacionales muestran que una mutación de LRP5 (A1330V) ocasiona una reducción en la interacción de la proteína con sus ligandos[64,65] y está asociada con hipercolesterolemia[66,67]. Además, variaciones genéticas de *LRP6* resultan en CVD y CAD tempranas[68] y mutaciones de *LRP8* incrementan el riesgo de CAD y MI prematuros[69,70]. Por último, varios estudios poblacionales han identificado al receptor LR11 como un biomarcador potencial para la predicción de la aterosclerosis cerebral y/o coronaria[71–73].

5. LDL RECEPTOR-RELATED PROTEIN 5 (LRP5)

5.1 Estructura y función de LRP5

El gen de LRP5 codifica para una proteína de 1615 aa que contiene dominios conservados característicos de la familia de receptores de LDL (Figura 7). En su extremo N-terminal LRP5 contiene un dominio que consta de cinco repeticiones de aprox. 50 aa con la secuencia característica de Tyr-Trp-Thr-Asp (motivo YWTD) seguido por un dominio de repetición de EGF. Una unidad, definida por el dominio de motivos YWTD y una repetición de EGF, se encuentra repetida cuatro veces en el LRP5[74]. La última repetición de EGF esta adyacente a tres repeticiones de unión a ligandos (LDLR), las cuales tienen residuos de Cys conservados y el motivo Ser-Asp-Glu (SDE). El dominio transmembrana de LRP5 consta de 23 aa. En la familia de los LDLR las repeticiones LDLR normalmente se encuentran antes de las repeticiones de EGF, pero en LRP5 y LRP6 este patrón es inverso. Curiosamente, la organización de toda la porción extracelular de LRP5 corresponde exactamente a las repeticiones de EGF 7-10 separadas por los dominios de motivos YWTD y a las repeticiones de LDLR 11-13 en la región extracelular de LRP1[74,75].

El dominio citoplasmático de LRP5 está formado por 207 aa y está compuesto por un 16% y un 15% de residuos de Pro y Ser, respectivamente. Es interesante que el dominio citoplasmático de LRP5 y LRP6 no muestra ninguna similitud con los dominios citoplasmáticos de la familia de LDLR y tampoco es similar al de ninguna otra proteína conocida[74]. Este dominio contiene varios residuos aromáticos que pueden estar relacionados con la endocitosis[74] y un motivo dileucina, que podría funcionar como mediador de la internalización de un número de receptores de citoquinas y del receptor de la vitelogenina[76,77].

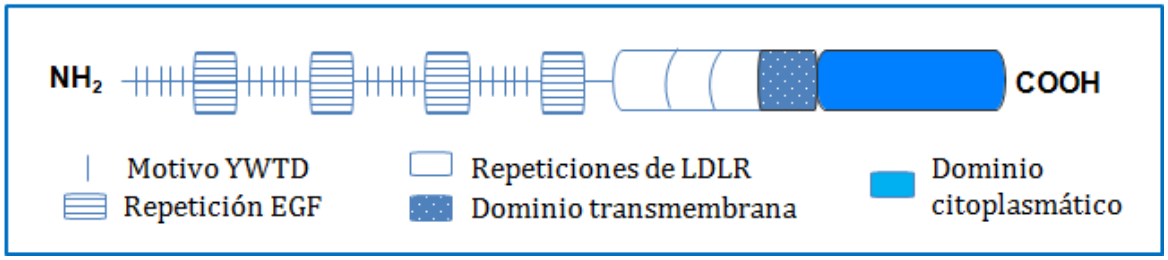

Figura 7: Representación gráfica de los dominios estructurales de LRP5.

LRP5 participa en diferentes patologías, como la osteoporosis, la osteoartritis, la neovascularización retiniana, la resistencia a la insulina y la aterosclerosis[78–85]. LRP5 funciona como un co-receptor con la proteína frizzled para las glicoproteínas extracelulares Wnt, que inducen la vía canónica de Wnt[52,86] (descrita en el siguiente apartado).

LRP5 se encuentra en una región cromosómica que contiene dos marcadores asociados a la diabetes tipo 1[74,87,88]. Así, alteraciones en la expresión de LRP5 pueden ser responsables de la susceptibilidad a desarrollar diabetes[78]. Además, LRP5 está altamente expresado en varios tipos celulares involucrados en el inicio y progresión de la diabetes, las células beta de los islotes de Langerhans, los monocitos y las células metabolizadoras de retinoides[78].

LRP5 es un regulador clave en la proliferación osteoblástica y en la formación ósea[79,80]. Mutaciones en este receptor causan el síndrome de osteoporosis-pseudoglioma (OPPG), un transtorno autosómico recesivo muy poco frecuente caracterizado por anormalidades oculares que causan ceguera congénita o que aparece durante la infancia y provoca osteoporosis juvenil severa con fracturas espontáneas[79,89]. Estas mutaciones de LRP5 ocasionan una pérdida de función del receptor y consecuentemente una reducción de la masa ósea. Por otro lado, un aumento de la función del receptor causado por el cambio del aminoácido de glicina por una valina (G171V) ocasiona el síndrome de alta densidad ósea (HBM)[81,90].

LRP5 tiene un papel esencial en la destrucción del cartílago en la osteoartritis[85]. De hecho, la expresión de LRP5 está aumentada en el cartílago articular de pacientes con osteoartritis[91] y este aumento se correlaciona con la sobreexpresión de factores catabólicos (MMP3 y MMP13), con la inhibición de la síntesis del factor anabólico colágeno tipo II y con la estimulación de la apoptosis en los condrocitos, que contribuyen al desarrollo de la enfermedad[85]. Estos efectos se producen por medio de la señalización de Wnt/β-CATENINA[85].

Recientemente se ha descrito que LRP5 también participa en la neovascularización de la retina[84]. Así, ratones deficientes para LRP5 presentan una vasculatura intraretinal subdesarrollada asociada a la acumulación y reducción de la migración de las EC[84], mientras que los ratones deficientes para VLDLR presentan neovascularización en la retina[92]. Los ratones deficientes para LRP5 y VLDLR no presentan neovascularización en la retina demostrando que LRP5 es necesario para este proceso. Estos resultados sugieren que LRP5 puede ser una diana efectiva para prevenir y tratar enfermedades de la retina causadas por la neovascularización[84].

5.2 Vía de señalización por Wnt

Las proteínas Wnt son una familia de glicoproteínas modificadas por lípidos conservadas a través de la evolución[93,94]. Las Wnt son de gran importancia en la regulación de procesos de desarrollo como el modelado de tejidos, la proliferación y la migración celular[95,96]. En adultos, la vía de señalización por Wnt es clave para la homeostasis de los tejidos ya que regula el mantenimiento de las células madre[97]. Su desregulación está asociada con varias patologías humanas pero donde extiste más documentación es en cáncer[98].

Existen dos vías de señalización por Wnt, la vía canónica (dependiente de β-CATENINA) y la no canónica, activadas por diferentes ligandos Wnt y receptores[99]. La vía de señalización no canónica se divide a su vez en dos tipos: la vía Wnt/Ca^{2+}, que estimula la liberación de Ca^{2+} intracelular y la activación de quinasas dependientes de Ca^{2+} y esta mediada por proteínas de señalización G; y la vía de polaridad planar celular (Wnt/PCP), que participa en la organización del citoesqueleto, en la motilidad celular, en la gastrulación y en la orientación de células sensoriales, por medio de la activación de pequeñas GTPasas, incluyendo RhoA, Rac, Cdc42 y JNKs (quinasas c-Jun N-terminal)[100].

La vía de señalización Wnt/β-CATENINA controla múltiples procesos celulares como la diferenciación celular, la inflamación, la carcinogénesis, la fibrosis y la angiogénesis[86,101]. En ausencia de Wnt, β-CATENINA es fosforilada por un complejo compuesto por AXINA, APC (poliposis adenomatosa coli) y GSK3β (glucógeno sintasa quinasa 3 beta), y degradada por ubiquitinas manteniendo así unos niveles bajos de β-catenina citoplasmática[100,102]. La unión de Wnt a sus receptores Frizzled y LRP5/6 estimula la fosforilación del dominio citoplasmático de LRP5/6 mediada por CK1 (caseína quinasa 1) o GSK3β[103]. LRP5/6 fosforilado actúa como un sitio de anclaje para AXINA, lo cual permite la disociación de β-CATENINA del complejo de degradación dependiente de Dishevelled (Dvl). Estos eventos resultan en la acumulación de β-CATENINA en el citoplasma y su posterior translocación al núcleo, donde se une a los factores de transcripción TCF (factor de células T) y LEF-1 (factor potenciador linfoide 1) y activa los genes diana de la vía de señalización por Wnt[104] (Figura 8). Entre los genes diana de esta vía se encuentran ciclo-oxigenasa 2, c-jun, conexina 43, ciclina D1, osteopontina (OPN) y la proteína morfogénica ósea-2 (BMP2)[105–110].

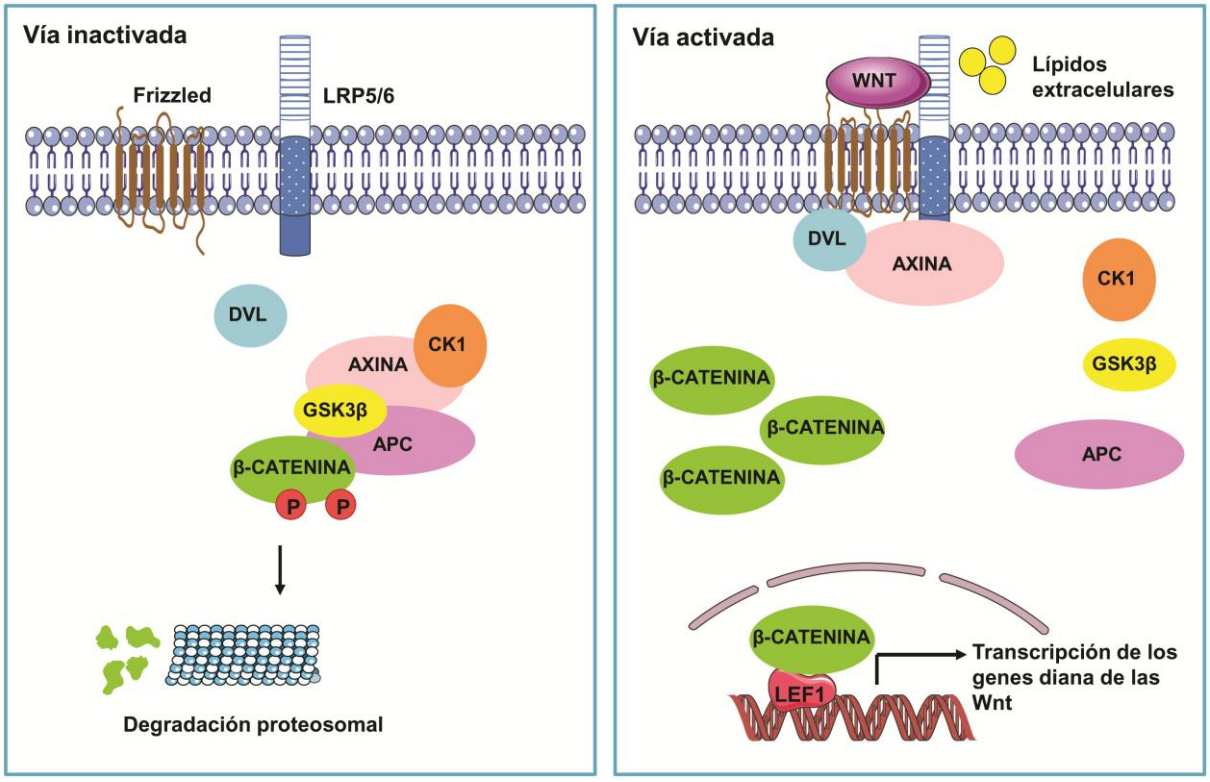

Figura 8: La vía canónica de señalización por Wnt se activa por la unión de glicoproteínas Wnt a sus receptores LRP5/6 y Frizzled evitando la fosforilación y degradación de β-CATENINA por parte del complejo de GSK3β. β-CATENINA se acumula en el citoplasma y se transloca al núcleo donde interacciona con los factores de transcripción LEF1/TCF para activar la transcripción de los genes diana.

5.2.1 Participación de la vía canónica de señalización por Wnt en la aterosclerosis: inflamación y diferenciación celular.

La vía canónica de señalización por Wnt ha sido caracterizada como un regulador de la proliferación, supervivencia y diferenciación celular[111–113]. Participa en la diferenciación de células madre mesenquimales, en la osteoblasteogénesis e inhibe la adipogénesis en humanos[79,114]. La vía canónica es una de las primeras vías moleculares de repuesta al daño celular[115]; sin embargo su papel en la inflamación no está definido todavía. De hecho existe cierta controversia sobre si la activación de la vía canónica induce un aumento o una disminución de la inflamación local. Así, se ha descrito que IL-1β y LPS causan una acumulación citoplasmática de β-CATENINA en las EC vasculares humanas[116] y que se observa una activación de los genes de la vía canónica Wnt en las EC de un modelo murino de trasplante de riñon[117], sugiriendo la implicación de la vía en la respuesta inflamatoria.

Se ha demostrado recientemente que la vía canónica participa en la resolución de la inflamación por medio de la regulación de genes anti-inflamatorios. Así, inhibidores de la vía

canónica de señalización por Wnt, como el GSK3β, aumentan la expresión de genes pro-inflamatorios en células endoteliales (EC) y en monocitos activados[118,119], y por el contario, la inhibición de GSK3β en macrófagos murinos disminuye la secreción de TNFa, IL6 e IL2[120]. La vía canónica de señalización por Wnt también parece regular la diferenciación de las células T[121] ya que TCF1 y β-CATENINA son necesarios para la diferenciación de las células T hacia células T efectoras Th2[122].

Los niveles de expresión de β-CATENINA activa en las placas ateroscleróticas vulnerables son mayores que en las placas estables, sugiriendo que la activación de la vía canónica contribuye a la inestabilidad de la placa[123]. Sin embargo, niveles bajos de expresión de LRP6 en las lesiones ateroscleróticas de carótida humana podrían indicar que una reducción de la señalización canónica de Wnt estaría contribuyendo a la aterosclerosis[124]. Además existen datos indicativos de que el efecto protector de la vía canónica podría involucrar la resolución de la inflamación[118–120].

Se ha descrito también que la vía canónica de señalización por Wnt promueve la calcificación vascular por medio del aumento de la expresión de BMP2[125]. Dicha señalización estaría estimulada por factores de riesgo aterosclerótico como la hipertensión y la diabetes[126]. BMP2 junto con las especies reactivas de oxígeno genera señales paracrinas que promueven la expresión vascular de los ligandos Wnt3a y Wnt7a, activando la vía canónica de señalización por Wnt y la calcificación vascular[126,127].

5.3 Participación de LRP5 en la homeostasis de lípidos

Los estudios de la función de LRP5 en el metabolismo lipídico comenzaron con el descubrimiento de la unión LRP5-APOE. APOE es un componente importante de varias lipoproteínas plasmáticas, como los CM residuales, las IDL y las VLDL[128]. La unión de LRP5 a APOE parece indicar que LRP5 participa en la eliminación de aquellas lipoproteínas que contienen APOE. Además, conejos Watanabe con hiperlipidemia hereditaria (WHHL), presentan mayor expresión hepática de LRP5 que conejos normales, sugiriendo que la expresión de LRP5 podría ser regulada por los niveles de colesterol *in vivo*[128].

Estudios con ratones deficientes para LRP5 (*Lrp5*$^{-/-}$) mostraron que este receptor es necesario para la homeostasis de la glucosa y el colesterol[82]. Así, ratones *Lrp5*$^{-/-}$ alimentados con una

dieta hipercolesterolémica (HC) presentan niveles de colesterol elevados en comparación con ratones *Wt* alimentados con la misma dieta, debido a una menor eliminación hepática de CM residuales. Además, los ratones *Lrp5*$^{-/-}$ alimentados con una dieta normocolesterolémica (NC) presentaron una menor tolerancia a la glucosa resultando en una secreción reducida de insulina[82]. El cultivo de islotes de Langerhans de ratones *Wt* con medio condicionado conteniendo Wnt3a, un activador específico de la vía, estimula la secreción de insulina inducida por glucosa mientras que este efecto no se observa en los islotes de Langerhans de ratones *Lrp5*$^{-/-}$[82].

La participación de LRP5 en la progresión de la lesión aterosclerótica se ha sugerido en un modelo de ratones transgénicos deficientes para *Apoe* y *Lrp5*[83]. Los ratones *Apoe*$^{-/-}$ alimentados con una dieta normal presentan hipercolesterolemia y desarrollan aterosclerosis espontánea[129]. Tras la eliminación de *Lrp5* (*Apoe*$^{-/-}$*:Lrp5*$^{-/-}$) los ratones presentan niveles de colesterol aún más altos que los ratones *Apoe*$^{-/-}$. El efecto deletéreo de la ausencia de LRP5 también se evidencia en el tamaño de las lesiones ateroscleróticas, las cuales son tres veces más grandes que las observadas en los ratones *Apoe*$^{-/-}$[83]. Sin embargo, los niveles de colesterol extremadamente altos de los ratones *Apoe*$^{-/-}$*:Lrp5*$^{-/-}$ (~750mg/dL) podrían estar enmascarando los efectos de la ausencia de LRP5. Finalmente, estudios poblaciones en China y Japón han mostrado que un polimorfismo en el dominio extracelular de LRP5 (A1330V), que causa la pérdida de su función, está asociado con altos niveles de colesterol en plasma[66,67].

6. FITOESTEROLES ESTERIFICADOS (PSE)

6.1 Estructura y mecanismos de acción

Los esteroles vegetales son alcaloides esteroideos de origen vegetal estructuralmente similares y análogos funcionalmente al colesterol, con capacidad de reducir los niveles de colesterol en sangre[130–134]. Las principales fuentes de fitoesteroles y fitoestanoles son los aceites vegetales, las margarinas, el pan, los cereales, las frutas y los vegetales[135]. Los fitoesteroles más abundantes son el sitosterol, el campesterol y el estigmasterol, y en una menor proporción se encuentran el brassicasterol, el 5 y 7-avenasterol y el ergosterol[131]. Al igual que el colesterol, los esteroles vegetales se presentan principalmente en forma libre y esterificada. Los fitoesteroles y los fitoestanoles se diferencian del colesterol por tener una cadena lateral unida al anillo de esterol (Figura 9). Los fitoestanoles son esteroles vegetales saturados sin doble enlace en el anillo esterol, debido a esta saturación, tienen una menor absorción que los fitoesteroles[136]. Cuando son empleados como ingrediente alimentario los esteroles vegetales y los estanoles son esterificados con un éster de ácido graso para incrementar la solubilidad en la matriz alimentaria, dando lugar a los fitoesteroles esterificados (PSE) y a los fitoestanoles esterificados[137,138].

El principal mecanismo que utilizan los PSE para reducir los niveles de colesterol es mediante la inhibición competitiva de la absorción del colesterol en los enterocitos del intestino[139–141]. Los fitoesteroles tienen una alta afinidad físicoquímica por las micelas resultando en una absorción menor de colesterol[142]. En el enterocito, una gran parte del colesterol y otros esteroles son esterificados por la enzima acil-CoA:colesterol aciltransferasa-2 (ACAT2) y liberados en la linfa dentro de los CM. Y otra parte es excretada de nuevo hacia el lumen del intestino por heterodímeros de los transportadores con dominio de unión al ATP, ABCG5 y ABCG8, que se encuentran en la parte apical del enterocito[143,144]. Otro mecanismo por el cual los PSE disminuyen la concentración del colesterol plasmático ocurre a través de la ruta de excresión transintestinal del colesterol (TICE), la cual presenta un sistema activo en la parte proximal del intestino delgado e implica el transporte del colesterol presente en la parte basolateral y apical del enterocito hacia el lumen intestinal[142,145]. Se ha descrito la participación del heterodimero ABCG5/ABCG8 en la ruta de TICE, provocando un aumento de la movilización del colesterol hacia el lumen del intestino para ser excretado por las heces[146,147].

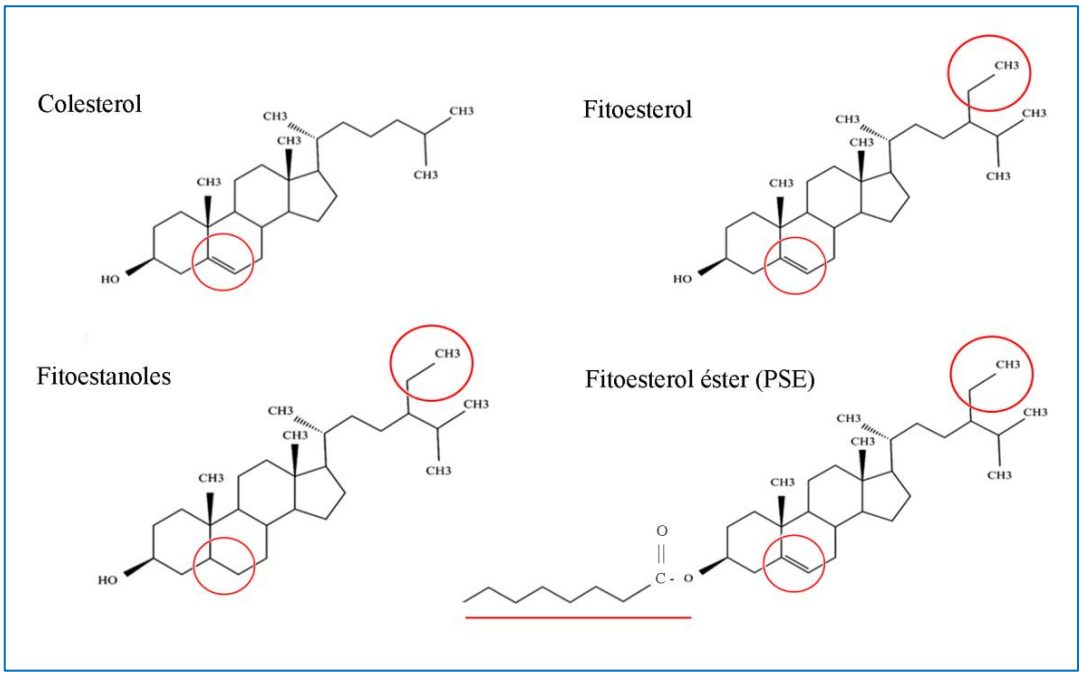

Figura 9: Estructura química del colesterol, fitoesterol (sitoesterol), fitoestanol (sitoestanol) y fitoesterol éster. Los fitoesteroles y fitoestanoles se diferencian del colesterol por tener una cadena lateral unida al anillo esterol. Los fitoestanoles son esteroles vegetales saturados sin doble enlace en el anillo esterol. Debido a esta saturación, tienen una menor absorción que los fitoesteroles. Cuando los fitoesteroles son utilizados como suplemento para reducir los niveles de colesterol se esterifican con ácidos grasos de cadena larga para aumentar su solubilidad y absorción, dando lugar a los fitoesteroles esterificados (PSE)[130,136].

6.2 Propiedades de los PSE en el desarrollo de la aterosclerosis

Durante los últimos años se han realizado muchos esfuerzos para elucidar el papel de los PSE más allá de su capacidad de reducir los niveles de colesterol en sangre. Estudios iniciales del rol de los PSE en la progresión de la lesión aterosclerótica se han realizado en ratones *Apoe*$^{-/-}$ alimentados con una dieta HC suplementada o no con fitoesteroles derivados de aceite de pino. Se observa que el consumo diario de los fitoesteroles reduce la formación de lesiones ateroscleróticas y los niveles de colesterol en plasma[148]. De forma similar, hámsteres alimentados con una dieta pro-aterogénica suplementada con PSE, presentan un área de células espumosas en la aorta menor que los que sólo recibieron la dieta pro-aterogénica, confirmando así el efecto benéfico de los PSE en el desarrollo de la aterosclerosis[149].

Además, los ratones *Ldlr*$^{-/-}$ alimentados con una dieta aterogénica durante 33 semanas seguida de la administración de atorvastatina, PSE o fitoestanoles durante 12 semanas muestran que los animales alimentados con dieta suplementada con PSE o fitoestanoles y aquellos

alimentados con PSE o fitoestanoles y atorvastatina tienen una inhibición de la progresión de la lesión e incluso inducen una regresión de esta[150]. Debido a sus efectos sobre el colesterol, los PSE tienen propiedades anti-inflamatorias[132]. En modelos murinos se ha observado que el consumo de PSE produce un descenso en los niveles de citoquinas pro-inflamatorias, como IL-6 y TNFα (factor de necrosis tumoral alfa) y un incremento de citoquinas anti-inflamatorias, como IL-2, IL-10 e IFNG (interferón gamma) asociado a su reducción en los niveles de colesterol plasmático[151,152].

En algunas situaciones los PSE no mostraron ningún efecto, como en ratones *Ldlr*$^{-/-}$ con niveles de fitoesteroles 20 veces más altos que lo normal debido a la inactivación de los genes ABCG5/8, los cuales alimentados durante 7 meses con dieta pro-aterogénica, no mostraron diferencias en el tamaño de la lesión en comparación con los controles (ratones alimentados con la misma dieta pero sin la mutación)[153]. Mientras que en algún caso se han descrito efectos nocivos. Así, ratas espontáneamente hipertensas susceptibles a presentar infartos (SHRSP) demuestran un efecto negativo de los PSE [154]. Se ha descrito que los niveles elevados de fitoesteroles en plasma incrementan la rigidez del eritrocito y acortan la vida media en las ratas[154]. De hecho, la sitosterolemia es una enfermedad genética caracterizada por presentar altos niveles de fitoesteroles y colesterol en plasma que cursan con la aparición de CHD prematura[143,155]. Estudios epidemiológicos en pacientes sin sitoesterolemia sugieren que un leve aumento de los niveles de fitoesteroles en plasma puede ser un factor de riesgo adicional para desarrollar CHD[156,157]. Además, ratones alimentados con dieta normal suplementada con PSE (2%) presentan disfunción endotelial y un incremento del daño cerebral durante la isquemia[158].

Finalmente, la Sociedad de Aterosclerosis Europea (EAS) ha determinado que el consumo de PSE puede ser considerado beneficiosos en individuos con niveles altos de colesterol plasmático y con un riesgo cardiovascular medio o bajo que no requieren farmacoterapia; en pacientes con riesgo alto o muy alto, que son intolerantes al tratamiento con estatinas o similares como una terapia farmacológica auxiliar; y en adultos y niños (mayores de 6 años) con FH[135]. Sin embargo se incentiva a continuar con estudios para establecer con seguridad el efecto beneficioso del consumo de los PSE.

7. RESUMEN DE LA INTRODUCCIÓN

Las CVD son la primera causa de discapacidad y muerte prematura en el mundo[1]. La aterosclerosis es el principal proceso patológico que da lugar a las CVD[159]. Esta patología cursa con altos niveles de colesterol en sangre y está caracterizada por la acumulación de lípidos en la pared vascular[13]. Las lipoproteínas son la fuente principal de los lípidos que se encuentran en la lesión aterosclerótica y están formadas por fosfolípidos, FC, apoproteínas, TG y CE[17]. Las lipoproteínas son absorbidas por el hígado y los tejidos periféricos a través de los receptores de LDL[23]. LDLR ha sido ampliamente caracterizado por su participación en el metabolismo de las lipoproteínas y mutaciones en este receptor alteran la homeostasis del colesterol provocando enfermedades como la FH[45]. Recientemente se ha descrito la participación de los LRPs, una subfamilia de los receptores de LDL, en diferentes patologías cardiovasculares. En particular, LRP5, descrito inicialmente por su papel en la osteoporosis y en la neovascularización de la retina, también participa en la homeostasis del colesterol y de la insulina[82,83]. De hecho, un modelo murino deficiente para ApoE y LRP5 presentó mayores niveles de colesterol en sangre y mayor tamaño de las lesiones ateroscleróticas que los ratones deficientes sólo para ApoE[83]. Sin embargo, el estudio aislado del efecto de LRP5 en la progresión de la aterosclerosis y de los mecanismos implicados en su función no se ha realizado aún. LRP5 es un correceptor de la vía canónica de señalización por Wnt[86], que controla múltiples procesos celulares como la diferenciación celular, la inflamación, la carcinogénesis, la fibrosis y la angiogénesis[86,101], por lo cual su modulación podría regular los procesos celulares que ocurren durante la progresión de la lesión aterosclerótica tanto a nivel sistémico como vascular.

HIPÓTESIS Y OBJETIVOS

La aterosclerosis, caracterizada por la acumulación de lípidos y elementos fibrosos en las arterias, es el principal proceso patológico que da lugar a las CVD[159]. En el desarrollo de esta patología participan la diferenciación, la proliferación y la migración celular, dando lugar a diferentes respuestas celulares y moleculares, que son características de una enfermedad inflamatoria[12]. La internalización de lípidos por las células de la pared vascular es crucial para la progresión de la lesión y es realizada en parte a través de los receptores de las LDL[13]. LRP5, un miembro de la familia de receptores de LDL y correceptor de la vía canónica de señalización por Wnt, se ha descrito por su participación en la homeostasis de lípidos[83]. Nuestra hipótesis de trabajo es que LRP5 participa en el desarrollo de las lesiones ateroscleróticas humanas, y que la modulación de la vía canónica de señalización por Wnt es clave para su función. Por lo tanto, nos planteamos los siguientes objetivos:

1. Investigar el papel de LRP5 y de la vía canónica de señalización por Wnt en las células inflamatorias.

2. Investigar la participación de LRP5 en la formación de la lesión aterosclerótica.

3. Investigar la implicación de LRP5 y la vía canónica de señalización por Wnt en la modulación de la inflamación *in vivo*.

4. Investigar el efecto de altos niveles de colesterol plasmático en la expresión de LRP5 *in vivo*.

METODOLOGÍA

1. NOMENCLATURA

Las abreviaturas de los genes y de las proteínas siguen las pautas establecidas por el "Comité Internacional sobre Nomenclatura Genética Estandarizada para Ratones" (www.informatics.jax.org) y el "Comité de Nomenclatura de la Organización del Genoma Humano" (www.genenames.org), resumidas en la siguiente tabla:

	Ratón	Humano
Gen	*Lrp5*	*LRP5*
Proteína	LRP5	LRP5

Tabla 2: Nomenclatura usada en las abreviaturas de los genes y proteínas utilizados.

2. CULTIVOS CELULARES

2.1 Células musculares lisas vasculares humanas (HVSMC)

Los cultivos primarios de las HVSMC se obtuvieron a partir de arterias coronarias humanas procedentes de corazones extraídos en los transplantes de corazón realizados en el Hospital de la Santa Creu i Sant Pau de Barcelona, siguiendo la técnica de explantes establecida por nuestro grupo[160]. El protocolo de obtención de muestras fue aprobado por el comité ético del hospital en concordancia con el tratado de Helsinki. Las coronarias se extrajeron del corazón explantado, se abrieron longitudinalmente y mediante el raspado de la cara interna se eliminó la capa de células endoteliales. A continuación, se separó la capa media de la adventicia y se cortó la media en explantes de 1-2mm^2, estos se distribuyeron en placas de cultivo con medio M199 (Gibco) suplementado con 20% de FBS, 2% de suero humano, 2mM de Glutamina, 100U/mL de penicilina y 100U/mL de estreptomicina e incubaron a 37°C con un 5% de CO_2. Cuando las VSMC migraron de los explantes hacia la placa se tripsinizaron (Tripsina/EDTA) y subcultivaron. Estas células se incubaron con nLDL o agLDL como se describirá más adelante en la sección de tratamiento con lipoproteínas.

2.2 Células endoteliales de la vena umbilical humana (HUVEC)

Las células HUVEC se compraron a ATCC y se cultivaron en medio M199 (Gibco) suplementado con 20% de FBS, 2mM de Glutamina, 2mM de Hepes, 2mM de Piruvato, 1% de Heparina, 1% de suplemento para el crecimiento de células endoteliales (ECGS), 100U/mL de penicilina y 100U/mL estreptomicina. Las placas se trataron con gelatina al 1% durante 30 min antes de sembrar las células. Para los experimentos con nLDL o agLDL se usaron HUVEC entre los pases 1 y 5.

2.3 Aislamiento de monocitos humanos (HM) y macrófagos derivados de monocitos humanos (HMDM)

Las células mononucleares de sangre periférica humana (PBMCs) fueron obtenidas a partir de residuos leucocitarios (15-20mL) de donantes sanos y aisladas por centrifugación por gradiente de densidad utilizando Ficoll-Hypaque. La sangre se añadió sobre 15mL de Ficoll y se centrifugó a 300g durante 1h a temperatura ambiente. Se aisló la capa leucocitaria que corresponde a la banda central blanca del gradiente y se hicieron de 3-4 lavados con 1X PBS centrifugando 5min a 300g. Las células se resuspendieron en medio RPMI1640 (Gibco) suplementado con 10% de suero humano AB (Immunogenetics), 100U/mL de penicilina y 100U/mL de estreptomicina. Se realizó el conteo de monocitos en un contador Coulter (250-350x10^6células) y se sembraron en placas de 100x20mm (20x10^6células) y en placas de 6 pocillos (4x10^6células/pocillo). Los monocitos sembrados en placas de 100x20mm se utilizaron al día siguiente de su aislamiento para la transfección de LRP5 y posterior análisis de la adhesión y diferenciación celular. Por otro lado, los monocitos cultivados en placas de 6 pocillos se incubaron durante 7 días para permitir su diferenciación a macrófagos (HMDM) y se usaron para la transfección de LRP5 y los ensayos de migración.

2.4 Células promielocíticas derivadas de leucemia humana (HL60)

Las células HL60 (human promyelocytic leukaemia cells) son una línea celular inmortalizada que proviene de leucocitos de sangre periférica de una paciente con leucemia promielocítica aguda. Estas células se diferencian a macrófagos tras el tratamiento con PMA (phorbol 12-myristate 13-acetate). Se caracterizan por la expresión de proteínas presentes en macrófagos y por la

capacidad de realizar actividades típicas de los macrófagos como la fagocitosis, la actividad de esterasas inespecíficas (NSE) y la adhesión[161–163]. Las HL60 fueron cultivadas en el medio RPMI1640 (Gibco) con Glutamax, suplementadas con 10% de FBS, 100U/mL de penicilina y 100U/mL de estreptomicina, e incubadas a 37°C con un 5% de CO_2. En esta tesis estas células se usaron para los ensayos de sobreexpresión y silenciamiento de LRP5 y su efecto en la adhesión, la diferenciación, la proliferación y la apoptosis celular.

2.5 Células PC3 y U87MG

Las células PC3 son derivadas de cáncer de próstata humano y las U87MG de glioblastoma. Se cultivaron en medio DMEM/F12 suplementado con 10% de FBS, 2mM de glutamina, 100U/mL de penicilina y 100U/mL de estreptomicina, e incubaron a 37°C con un 5% de CO_2. Estas células fueron usadas para la transfección de LRP5 y posterior análisis de la proliferación celular.

3. MODELO DE RATONES TRANSGÉNICOS

3.1 Obtención y caracterización de la colonia de ratones deficientes para *Lrp5*

Ratones heterocigotos para *Lrp5* (*Lrp5*$^{+/-}$) fundadores de la colonia fueron cedidos por el Dr. Bart Williams[164–166]. Se estabularon en jaulas con temperatura controlada (21±2ºC), en un ciclo de 12h luz/oscuridad y con comida y agua *ad libitum*.

Al cumplir 4 semanas de edad los ratones se genotiparon. Para ello fueron sedados con isofluorano y se les tomó una biopsia de la cola (0.5cm). Esta muestra se dividió en dos segmentos, uno se almacenó a -20°C y el otro se utilizó para la extracción del DNA. El tejido se incubó con 400µL de buffer (0.1M Tris pH 8; 0.3M NaCl; 0.4% SDS; 5mM EDTA; 100ug/mL Proteinasa K) toda la noche a 55°C en agitación constante. Al día siguiente se realizó una agitación vigorosa, seguida de centrifugación a 13.400g durante 5 min a temperatura ambiente. El pellet se descartó y el sobrenadante se incubó con 400µL de isopropanol y 40µL de 3M acetato sódico durante 30 min a -80°C. Se centrifugó a máxima velocidad durante 15 min a 0°C y el pellet resultante se lavó con etanol al 70%, se volvió a centrifugar y se evaporaron los restos de etanol a 95°C. El DNA se diluyó en agua destilada estéril y la calidad y concentración se determinaron con el Nanodrop ND-1000 (Nanodrop Technologies, Inc., Willington, DE, USA).

La PCR se realizó con la Taq polimerasa "Expand High Fidelity^{PLUS} PCR System" (Roche), los cebadores utilizados fueron S17 (GGC TCG GAG GAC AGA CCT GAG), S23 (CTG TCA GTG CCT GTA TCT GTC C) e IRES31 (AGG GGC GGA ATT CGA TAG CT) (Tabla 3). Los productos de la PCR fueron analizados en un gel de agarosa al 2%.

	Tiempo	Temperatura (°C)	
Activación inicial	2 min	92	
Desnaturalización	30 seg	94	40 ciclos
Alineamiento	30 seg	58	
Elongación	30 seg	72	
Elongación Final	10 min	72	

Tabla 3: Condiciones de la PCR para analizar el genotipo de los ratones.

3.2 Administración de dietas

Los ratones *Wt* y *Lrp5*$^{-/-}$ fueron alimentados con una dieta normocolesterolémica (NC, Tekland diet, Harland Labs) durante 10 semanas y posteriormente los animales de cada genotipo se dividieron en dos grupos para ser alimentados con la dieta NC o hipercolesterolémica (HC, TD.88137, Harland Labs) durante 8 semanas más (n=8-12 ratones/grupo). La composición detallada de las dietas utilizadas se muestra en la Tabla 4.

En los estudios con PSE los ratones *Wt* y *Lrp5*$^{-/-}$ fueron alimentados con la dieta NC durante 10 semanas y posteriormente los animales de cada genotipo se dividieron en tres grupos para ser alimentados con la dietas NC, HC ó HC suplementada con fitoesteroles esterificados al 2% (HC+PSE) durante 8 semanas más (8-12 ratones/grupo, Tabla 4). Los PSE fueron suministrados por DANONE y tienen un contenido de esteroles totales de mínimo 73%, del cual el 60% son fitoesteroles esterificados y el 40% son ácidos grasos. Teniendo en cuenta estos datos se calculó el volumen necesario para conseguir un consumo diario de PSE del 2%. Los PSE se suministraron diariamente en cuadritos de gelatina de 0.5cm^2. La administración se realizó mediante la preparación de forma convencional de gelatina Royal sin sabor baja en grasa (2,32g/mL) con agua estéril. Cuando la gelatina estaba totalmente disuelta se añadían los PSE (9.3mL/100mL) y se mantenía en agitación hasta que se disolvieran completamente. Después se dispensó 1mL de la gelatina en moldes de plástico de 1cm^2, se guardó a 4°C toda la noche y al día siguiente los cuadritos se extrajeron y cortaron por la mitad (volumen final 0.5mL). A los ratones alimentados sólo con dieta HC se les suministró la gelatina sin PSE.

Composición	Dieta NC	Dieta HC	Dieta HC+PSE
Grasa total %	3,5	22	22
Colesterol %	0	0,25	0,25
Sacarosa %	4,3	34	34
Calorías provenientes de las proteínas %	18	17	17
Calorías provenientes de la grasa %	11	40	40
PSE %	0	0	2

Tabla 4: Composición de las dietas normocolesterolémica (NC), hipercolesterolémica (HC) e HC suplementada con fitoesteroles esterificados (HC+PSE).

Al final de los experimentos los ratones fueron anestesiados con una mezcla de medetomidina y ketamina (dosis 1mg/kg y 75mg/kg, respectivamente). Cuando no se observaron reflejos podales se realizó punción cardiaca y la sangre obtenida se utilizó para los análisis bioquímicos y la extracción de mRNA. Los órganos de interés para el estudio (aorta, hígado, bazo, intestino) se recolectaron en nitrógeno líquido y después se almacenaron a -80°C. Aortas de cada grupo experimental se utilizaron para la extracción de mRNA, otras se fijaron en paraformaldehido (PFA) para posterior análisis inmunohistoquímico y otras se tiñeron para análisis de la lesión aterosclerótica.

Todos los protocolos realizados durante la manipulación de los animales fueron aprobados por el comité de investigación animal de la institución (ICCC051/5422) y siguen la guía para el uso y cuidado de animales de laboratorio publicada por el Instituto Nacional de Salud de los Estados Unidos.

4. LÍPIDOS

4.1 Aislamiento y modificación de lipoproteínas humanas

Las lipoproteínas utilizadas en los tratamientos celulares (LDL) fueron obtenidas de sueros normolipémicos de donantes del Banco de Sangre y Tejidos de Barcelona. El método utilizado consistió de una serie de ultracentrifugaciones que separan las fracciones de lipoproteínas sanguíneas en base a su densidad[167] (Tabla 5).

LIPOPROTEÍNAS	DENSIDAD (g/mL)
Quilomicrones (CM)	< 0.96
VLDL	0.96-1.006
IDL	1.006-1.019
LDL	1.019-1.063
HDL	1.063-1.210

Tabla 5: Clasificación de las lipoproteínas en función de su densidad.

Se prepararon tres soluciones de distinta densidad para el aislamiento de las fracciones, la composición de la solución de densidad 1.006g/mL se muestra en la tabla 6. Las soluciones de densidad 1.019g/mL y 1.063g/mL se prepararon añadiendo bromuro de potasio (KBr) a la solución de densidad 1.006g/mL. La cantidad de KBr añadida para alcanzar la densidad correspondiente se calculó a partir de la fórmula X=V(df-di)/(1-V'df), donde: X=gramos de KBr; V=volumen de la solución en mL; df=densidad final; di=densidad inicial y V'=volumen específico parcial de KBr, que para las fracciones de 1.006g/mL, 1.019g/mL y 1.063g/mL es 0.290mL, 0.291mL y 0.299mL respectivamente.

COMPOSICIÓN	Concentración Solución en H_2O destilada, pH 7.4
Cloranfenicol	15.5 mM
NaCl	0.2 M
EDTA tetrasodio	1 mM
EDTA disodio	0.8 mM
Sulfato de Gentamicina	0.1 mM
Azida de sodio	8 mM

Tabla 6: Composición de la solución de densidad 1.006g/mL para el aislamiento de lipoproteínas humanas.

4.1.1 Aislamiento de LDL

El suero se centrifugó a 117.791g (Rotor Beckman Type 50.2Ti) durante 30 min a 4°C y se descartó la fase superior blanca menos densa que corresponde a los CM. Se añadió la cantidad correspondiente de KBr al suero para llevar su densidad de 1.006g/mL a 1.019g/mL y se distribuyó en tubos de ultracentrífuga. Sobre el suero se añadió la solución de densidad 1.019g/mL lentamente y se centrifugó a 117.791g durante 18h a 4°C. Se recogió la fase superior blanca que está compuesta por VLDL e IDL, se eliminó la solución de densidad de la parte

superior de los tubos y se juntaron los sueros restantes. Se añadió KBr al suero para llevar su densidad de 1.019g/mL a 1.063g/mL y se distribuyó en tubos de ultracentrífuga. Sobre el suero se añadió la solución de densidad 1.063g/mL lentamente y se centrifugó 117.791g durante 18h a 4°C. Se recolectó la fase superior que corresponde a las LDL y se almacenaron protegidas de la luz a 4°C.

Una vez aisladas, las fracciones lipoproteicas se dializaron en tampón de diálisis 1X (150mM NaCl, 20mM Trizma Base, 1mM EDTA disodio) durante 2 horas a 4°C, se renovó el tampón de diálisis 1X y se dializaron durante 18 horas más. Finalmente, las fracciones lipoproteicas se dializaron en 150mM NaCl durante 2 horas a 4°C.

La cuantificación de las lipoproteínas se realizó mediante el kit de Pierce de determinación de proteína que utiliza el ácido bicinconínico (BCA) y se basa en el método de Lowry[168]. La recta patrón de albúmina bovina (BSA) y las muestras diluidas se incubaron durante 30 min a 60°C para romper las estructuras lipoproteicas y permitir que el BCA reaccione con los aminoácidos produciendo así un compuesto coloreado que absorbe a una longitud de onda de 562nm. La absorbancia se leyó en un espectofotómetro usando el programa SoftMax.

4.1.2 Modificación de LDL a LDL agregadas (agLDL)

La modificación de las LDL por agregación se realizó de forma mecánica como hemos descrito previamente en nuestro grupo[169]. Las LDL nativas (LDLn, obtenidas en el aislamiento de LDL sin modificaciones) se llevaron a una concentración de 1mg/ml con 1X PBS en tubos eppendorf de 2 mL y se agitaron en un vortex a máxima velocidad durante 4min a temperatura ambiente. A continuación se centrifugaron a 10.000g durante 10 min, el sobrenadante se recolectó en otro tubo y el pellet (compuesto 100% por agLDL) se resuspendió en 400µL del sobrenadante, obteniendo agLDL a una concentración final de 1mg/ml[170,171].

4.2 Análisis bioquímico de lipoproteínas en suero

La mitad del volumen de sangre extraído de los ratones por punción cardíaca (~350µL) se utilizó para calcular los niveles de lipoproteínas en suero. La sangre se centrifugó a 1.200g durante 20 min a 4°C y el suero se recolectó en otro tubo para posterior análisis. Los niveles de colesterol, triglicéridos y HDL fueron medidos enzimáticamente con kits disponibles comercialmente

(GERNON®) en un espectrofotómetro (MC-15 SOFT; RAL). Los niveles de LDL fueron calculados indirectamente con la fórmula de Friedewald (LDL=CT-HDL-(TG/5)[172].

4.3 Tinción de lípidos con ORO y DiI

Tras el sacrificio, cada ratón (n=6-8/grupo) se ubicó en un estereoscopio para limpiar la grasa perivascular y extraer la aorta que se cortó longitudinalmente ubicando la superficie luminal hacia arriba y se fijo toda la noche con PFA al 4%. Al día siguiente se lavó con ddH_2O durante 1h con agitación suave y se tiñó con "Oil Red-O" (ORO) durante 30min. Se lavó con etanol al 70% y ddH_2O, se hizo el montaje en un portaobjetos y las imágenes fueron captadas en el microscopio Nikon Eclipse 80i y digitalizadas con la cámara Retiga1300i Fast. Las imágenes se cuantificaron con el programa Image J y los resultados se presentaron como porcentaje de área cubierta por lípidos / área total de la aorta.

Para el marcaje de lípidos con DiI, los HMDM se fijaron con PFA al 4% durante 20 minutos, se bloquearon 2 veces durante 15 min en 1X PBS/BSA1% y se incubaron con 5 µl/ml de DiI (30 mg/mL en DMSO, Sigma) durante 1h. A continuación se lavaron y el montaje se realizó con el reactivo Prolong Gold Antifade. Las imágenes fueron captadas con microscopía confocal (Leica TCS SP2-AOBS), en un formato de 1024x1024 pixeles con un set de datos espacial (xyz) y procesadas con el programa Leica Standard TCS-AOBS.

4.4 Análisis del contenido de lípidos en los HMDM y aortas de ratones por cromatografía en capa fina

El protocolo de extracción lipídica que se utilizó es una modificación del método descrito por Bligh and Dyer[173]. Se añadió 1mL de 0.1N NaOH a 5mg de tejido pulverizado de aorta o a las células recolectadas en tampón de lisis (10mM Tris HCl pH 7.5; 150mM KCl; suplementado con el complejo inhibidor de proteasas, Roche) y se almacenaron a -20°C. Al día siguiente se añadieron 3mL de diclorometano-metanol (1:2), se agitó intensamente en un vortex durante 10seg, se añadió 1mL de diclorometano y se repitió la agitación. Esta mezcla se centrifugó a 1.500g durante 15min y se observaron 2 fases separadas por la fase proteica: la fase acuosa (superior) y la fase orgánica (inferior). Se recogió la fase orgánica, que es la que contiene los lípidos, en un nuevo tubo. A la fase acuosa se la añadió 1mL más de diclorometano, seguido de

agitación y centrifugación a 1.500g durante 15min. La nueva fase orgánica se juntó con la anterior. La muestra se concentró evaporando el solvente orgánico bajo una corriente de N_2 para evitar la oxidación de los lípidos.

Las muestras concentradas se resuspendieron en 100µL de diclorometano, se agitaron en un vortex y se cargaron en una placa de sílica de cromatografía (DC-Fertigplatten SIL G-24 UV). En cada placa se cargó un estándar de FC, CE y TG con concentración conocida para cuantificar las muestras. Se corrieron dos fases móviles: la primera, compuesta por una mezcla de heptano: dietil-éter: ácido acético (72:21:4) separa los lípidos; y la segunda, compuesta de heptano, arrastra posibles contaminantes con el frente. Se dejó que el frente subiera 4cm por encima del frente de la primera fase móvil. Las placas se dejaron secar y se tiñeron con una solución de 5% ácido fosfomolíbdico y 5% ácido sulfúrico durante 2min. Posteriormente se ubicaron en un horno a 100°C durante 7min. Las imágenes de las placas se captaron por densitometría con el Chemidoc XRS (Bio Rad) y se cuantificaron con el programa Quantity One (Bio Rad).

5. BIOLOGÍA CELULAR Y MOLECULAR

5.1 Tratamientos con LDL

Tras el aislamiento y cuantificación de las lipoproteínas humanas, las células HUVEC, HVSMC, HM y HMDM se incubaron con 100 ug de nLDL o agLDL durante 24 horas. A continuación, las células se lavaron exhaustivamente (dos lavados con 1X PBS, dos lavados con PBS/1%BSA, dos lavados con PBS/1%BSA/100U/mL de heparina, dos lavados con PBS/1%BSA y dos lavados con PBS) y se recogieron para la extracción de mRNA y de proteína.

5.2 Ensayos de migración *in vitro*: cierre de la herida y cámara Boyden

Los ensayos de migración se realizaron en los HMDM previamente transfectados con siRNA-LRP5, siRNA-LRP1 o siRNA-Random. 24 horas tras la transfección, se realizó una herida con una punta amarilla de pipeta estéril de 200µL. Las células se lavaron con 1X PBS y se incubaron con o sin agLDL en medio sin suero. Las fotos fueron tomadas en el momento de hacer la herida (t=0h) y 24h después en un microscopio invertido (Nykon) equipado con una cámara digital (Spot Diagnostic Instruments, Inc., Sterling Heights). La motilidad de los macrófagos se calculó

como la proporción del área libre de células a las 24h respecto al área del tiempo inicial (t=0h) mediante el programa Image J.

Los HMDM transfectados se sembraron en cámaras Boyden de 24 pocillos (Corning Costar Corporation). Este sistema consiste de dos cámaras, una inferior y otra superior que contienen una membrana de policarbonato con poros de 8µm. Los HMDM se tripsinizaron, se lavaron tres veces con 1X PBS y se sembraron en la cámara superior durante 24h en medio sin suero. El medio de la cámara inferior tampoco contenía suero, con el fin de descartar posibles interferencias provocadas por las múltiples proteínas presentes en el suero y ver un resultado irreal debido a las proteínas del suero y no al efecto de la sobreexpresión/inhibición de LRP5. Tras 24h, se eliminaron las células de la membrana de la cámara superior con un bastoncillo de algodón, y el fondo fue teñido con Giemsa. Las células que migraron hacia la cámara inferior se contaron en un microscopio de luz con un aumento de 20X.

5.3 Transfección de las células HL60, HM y HMDM

Se utilizaron diferentes métodos de transfección para el silenciamiento y sobreexpresión de LRP5 en los tipos celulares estudiados.

Células HL60: El silenciamiento y sobreexpresión de LRP5 en HL60 se realizó mediante nucleofección (kit Nucleofector®, Amaxa Co). Las células se mantuvieron en crecimiento hasta alcanzar una densidad de 5-7x10^5células/mL. 4x10^6 células se resuspendieron en 100µL de Cell Line Nucleofector® Solution V, se añadió el plásmido o el siRNA correspondiente y se transfirió a una cubeta de nucleofección. El programa utilizado en el nucleofector fue el T-019. Para el silenciamiento de LRP5 se utilizó el siRNA-LRP5 (s8293, Applied Biotechnologies) y como control de la transfección el siRNA-Random2 (4390843, Ambyon) ambos a una concentración de 300nM. La sobreexpresión de LRP5 se realizó con el plásmido pcDNA3-LRP5 y como control de la transfección el plásmido pcDNA3 (0.4ug/cubeta). Las células nucleofectadas se colocaron en medio completo pre-calentado a 37°C y se incubaron el tiempo específico según el procedimiento a realizar, ya fuese el análisis de la proliferación, de la apoptosis o de la diferenciación celular.

Monocitos humanos (HM): 24 horas después del aislamiento de los monocitos a partir de la muestra de leucocitos, fueron despegados con 0.53mM EDTA en 1X PBS durante 10min a 37°C.

$1x10^7$células/mL se nucleofectaron con 0.25µg de cDNA o 300nM de siRNA, con el programa X-001, seguido de 48h de incubación en medio completo y recolección para extracción de mRNA y de proteína.

Macrófagos derivados de monocitos humanos (HMDM): Los macrófagos obtenidos tras el cultivo de los HM aislados a partir del residuo leucocitario fueron transfectados con liposomas. Los ensayos de sobreexpresión se realizaron con Metafectene® Easy$^+$ (Biontex) siguiendo las instrucciones del fabricante. El silenciamiento se realizó mediante la transfección de 100nM de cada uno de los siRNAs con el reactivo HiPerfect (Qiagen), siguiendo las instrucciones del fabricante.

La eficiencia de los diferentes métodos de transfección fue verificada 48 horas después por medio de PCR a tiempo real de LRP5 y normalizada con el gen r18S.

5.4 Ensayos de proliferación en las células HL60, PC3 y U87MG

El efecto de LRP5 en la proliferación celular fue evaluado por medio del kit BrdU Cell Proliferation Assay (Calbiochem). Las células se transfectaron y ubicaron en placas de 96 pocillos. 24h después se añadieron 20µL/pocillo de una dilución 1:2000 de bromodesoxiuridina (BrdU). Tras 24h, las células se lavaron dos veces con 1X PBS, se fijaron e incubaron con el anticuerpo anti-BrdU durante 1h, seguido de tres lavados e incubación con el conjugado peroxidasa Goat anti-mouse IgG HRP durante 30 min. A continuación la placa se lavó con dH_2O, se adicionó el sustrato y una solución para detener la reacción (stop solution). La intensidad del color es proporcional a la cantidad de BrdU incorporado por las células, la cual se cuantificó en un espectrofotómetro a una longitud de onda de 450-595nm.

5.5 Apoptosis en células HL60

48h tras la transfección las células se colectaron, lavaron y tiñeron con Annexin V-isotiocianato de fluoresceína (AV-FITC) y yoduro de propidio (PI) siguiendo las instrucciones del fabricante (BD Pharmingen™). Las células fueron analizadas por citometría de flujo (FACSCalibur).

5.6 Ensayos de adhesión y diferenciación en HM y en células HL60.

24 horas tras la transfección, las células HL60 se recolectaron y contaron en la cámara de Neubauer para sembrar la misma cantidad de células en los diferentes tratamientos (sin transfección, pcDNA3, pcDNA3-LRP5, siR, siLRP5) y se trataron con 10nM PMA (Sigma) durante 24h. Se recolectaron las células en suspensión y las células adheridas al pocillo, y se contaron en cámaras de Neubauer.

Un día después del aislamiento los monocitos se nucleofectaron y se incubaron durante 7 días con medio completo a 37°C para su diferenciación a macrófagos. Al día 7, se captaron imágenes de los macrófagos y se contó el número de células por campo de visión para el análisis del efecto de los diferentes tratamientos en la diferenciación. 48h después de la transfección un grupo de células fue utilizado para extraer el mRNA y verificar la eficiencia de la transfección.

5.7 Inmunofluorescencia en HL60, HMDM y lesiones ateroscleróticas humanas

Los HMDM y las HL60 diferenciadas se lavaron dos veces con 1X PBS, se fijaron con paraformaldehido al 4% durante 20min y se permeabilizaron 5min con 0.5% Tween 20/1X PBS, seguido de bloqueo con 1% BSA/1X PBS durante 15 min 2 veces. A continuación se lavaron con 1X PBS, se añadió Signal Enhancer durante 30min y se lavó de nuevo. Las células se incubaron 1h con los anticuerpos primarios para LRP5 y CD68 (Abcam), seguido de 2 lavados con 1X PBS e incubación con Alexa Flour anti-mouse 488 IgG, Alexa Flour anti-rabbit 633 IgG y la tinción de núcleos (Hoechst, 33342) durante 1h. Se realizaron dos lavados con 1X PBS y el montaje con el reactivo Prolong® Gold Antifade (Life Thechnologies).

Las arterias coronarias humanas fueron obtenidas de corazones extraídos en los transplantes de corazón que se llevan a cabo en el Hospital de la Santa Creu i Sant Pau de Barcelona. El protocolo de extracción de muestras fue aprobado por el comité ético del hospital en concordancia con el tratado de Helsinki. Las lesiones de las arterias coronarias humanas fueron caracterizadas por la tinción tricrómica de Masson de acuerdo con los criterios de la Asociación Americana del Corazón[174]. Las lesiones se clasificaron en tres grupos: grupo I (lesiones iniciales, tipos I y II, n=7); grupo II (lesiones leves en desarrollo, tipos III-V, n=6); y grupo III (lesiones avanzadas de alto riesgo, tipos VI-VIII, n=6).

Las aortas fueron fijadas, incluidas en OCT y cortadas en secciones de 5µm de grosor. Las secciones de aortas se incubaron con los anticuerpos mouse monoclonal anti-human macrophage (HAM56; Dako) y rabbit policlonal anti-human LRP5 (Abcam). A continuación se incubaron con sus correspondientes anticuerpos secundarios, Alexa Fluor anti-mouse 633 IgG, Alexa Fluor anti-rabbit 488 IgG y con la tinción de núcleos (Hoechst, 33342). Las imágenes fueron captadas con microscopía confocal (Leica TCS SP2-AOBS), en un formato de 1024x1024 pixeles con un set de datos espacial (xyz) y procesadas con el programa Leica Standard TCS-AOBS. Los controles sin anticuerpo primario no presentaron marcaje fluorescente.

5.8 Inmunohistoquímica en arterias coronarias humanas y aortas de ratón

Las arterias coronarias humanas y las aortas de ratón se extrajeron rápidamente, se fijaron con PFA al 4% e incluyeron en parafina. Luego se cortaron en secciones seriadas de 5µm de grosor, se ubicaron en portaobjetos previamente tratados con poli-L-lisina y se desparafinizaron. Las secciones se lavaron, se suprimió la actividad peroxidasa con H_2O_2 y se bloquearon las uniones inespecíficas con suero equino. En el caso de las coronarias humanas, se realizó la técnica de recuperación del antígeno. Los anticuerpos primarios utilizados se muestran en la siguiente tabla:

Tejido	Anticuerpos
Arterias coronarias humanas	Mouse Monoclonal anti-human macrophage, Ham56 (Dako) Rabbit polyclonal anti-LRP5 (Abcam)
Aorta de ratón	Rabbit polyclonal anti-Matrix Metalloproteinase-7, MMP-7 (Abcam) Rabbit polyclonal anti-β-catenin (Millipore) Mouse Monoclonal anti-human macrophage, Ham56 (Dako)

Tabla 7: Anticuerpos utilizados para las tinciones mediante inmunohistoquímica de arterias humanas y de ratón.

Los anticuerpos se detectaron usando la técnica de inmunoperoxidasa con avidina-biotina. Las secciones se incubaron 1h con los anticuerpos secundarios biotinilados apropiados (1:200, Vector Laboratories). El cromógeno usado fue 3,3'-diaminobencidina. Después de varios lavados con 100mM PBS pH7.4, se realizó el montaje con medio Histomount (National Diagnostics). Las muestras se analizaron en el microscopio Nikon Eclipse 80i a través de la cámara Retiga 1300i Fast y las imágenes se capturaron en el programa Visilog 5.4 Noesis©. La hematoxilina de Mayer se usó para las tinciones nucleares y para visualizar estructuras.

5.9 Extracción y análisis de la expresión de mRNA

Las extracciones de mRNA de ésta tesis se realizaron mediantes dos métodos distintos dependiendo del sustrato. El kit de extracción de RNA Total (Qiagen) se utilizó en los experimentos realizados con cultivos celulares; y el reactivo de aislamiento TriPure (Roche), para la extracción de mRNA de los órganos extraídos del modelo experimental de ratones transgénicos. La concentración de mRNA fue determinada con el espectrofotómetro NanoDrop ND-1000 (NanoDrop Technologies) y la pureza verificada por el cociente 260/280 que ha de tener un valor entre 1.8 y 2. La integridad de mRNA se comprobó a través del análisis de un gel de agarosa al 1%.

El cDNA fue sintetizado a partir de 0.5ug de RNA con el kit de transcripción reversa de cDNA (Qiagen) y amplificado por PCR a tiempo real (DNA termal cycler, MJ Research). Las sondas específicas para los genes de interés en el estudio se muestran en la Tabla 8 y el programa utilizado se detalla en la Tabla 9. Los resultados fueron normalizados con la sonda 18S rRNA (4319413E) de Applied Biosystems.

Estudio	Gen	Nombre completo del gen	Casa Comercial*	Referencia
Apoptosis	BAX	BCL2-associated X protein	Applied	Hs00180269-m1
	DUSP6	dual specificity phosphatase 6	Applied	Hs00169257-m1
	$G0S_2$	G0/G1switch 2	Applied	Hs00274783-s1
	BCL2	B-cell CLL/lymphoma 2	Applied	Hs00608023-m1
	CDK1	cyclin-dependent kinase 1	Applied	Hs00938777-m1
	CD180	CD180 molecule	Applied	Hs01069872-m1
Diferenciación y adhesión	CD11B	integrin, alpha M	Applied	Hs00355885-m1
	CD44	CD44 molecule	Applied	Hs01075861-m1
Vía de señalización por Wnts	Ctnnb1	Catenin beta 1	Applied	Mm00483039-m1
	Bmp2	bone morphogenetic protein 2	Applied	Mm01340178-m1
	Lef1	lymphoid enhancer binding factor 1	Applied Applied	Hs01547250-m1 Mm00550265-m1
	Opn	secreted phosphoprotein 1	Applied	Mm00436767-m1
	c-Myc	v-myc avian myelocytomatosis viral oncogene homolog	Applied	Hs00153408-m1
	c-Jun	jun proto-oncogene	Applied	Hs99999141-s1
Captación de lípidos	Ldlr	low density lipoprotein receptor	IDT	Mm.PT.49a.9930556
	Vldlr	very low density lipoprotein receptor	Applied	Mm00443298-m1
	Lrp1	low density lipoprotein receptor-related protein 1	IDT	Mm.PT.49a.7750137
	Lrp2	low density lipoprotein receptor-related protein 2	IDT	Mm.PT.49a.11916154
	Lrp5	low density lipoprotein receptor-	Applied	Hs00182031-m1

		related protein 5	IDT	Mm.PT.49a.8045420
	Lrp6	low density lipoprotein receptor-related protein 6	IDT	Mm.PT.56a.6383636
	Lrp8	low density lipoprotein receptor-related protein 8	IDT	Mm.PT.49a.6553055
Absorción intestinal	Abcg5	ATP-binding cassette, sub-family G (WHITE), member 5	IDT	Mm.PT.56a.8809476
	Abcg8	ATP-binding cassette, sub-family G (WHITE), member 8	IDT	Mm.PT.56a.7910478

Tabla 8: Sondas utilizadas en la PCR a tiempo real para analizar la expresión de mRNA de los genes distintos. *Applied: Applied Biosystems; IDT: Integrated DNA Technologies.

	Tiempo	Temperatura (°C)	
Activación inicial	5 min	95	
Desnaturalización	15 seg	95	40 ciclos
Alineamiento	30 seg	60	
Elongación	30 seg	72	

Tabla 9: Condiciones de la PCR a tiempo real.

5.10 PCR array de citoquinas comunes de ratón

El análisis de la expresión de las citoquinas liberadas por los leucocitos circulantes en ratones se realizó mediante un PCR-array de citoquinas comunes de ratón. La mitad del volumen de sangre extraído de los ratones por punción cardíaca (~350µL) se recolectó en tubos PAX para obtener mRNA usando el kit PAXgene Blood RNA Kit (Qiagen). La concentración y pureza del mRNA se determinó con el espectrofotómetro NanoDrop ND-1000 (NanoDrop Technologies). El cDNA se sintetizó como se describió en el apartado anterior y se realizó el array "PCR RT2 Profiler PAMM-021" (SABiosciences, Qiagen) en un termociclador de RT-PCR (Applied Biosystems 7900HT).

5.11 Extracción y cuantificación proteica de las células HL60, HM y HMDM

La extracción proteica de células HL60 en suspensión se realizó mediante centrifugación, lavados con 1X PBS y resuspensión en buffer RIPA (suplementado con un complejo inhibidor de proteasas, Roche). En el caso de las HL60 diferenciadas, se lavaron, se tripsinizaron y tras 3min a 37°C se añadió medio completo para detener la acción de la tripsina. Las células se centrifugaron, se lavaron con 1X PBS y se resuspendieron en buffer RIPA. Para la extracción proteica de los HM Y HMDM se realizó el mismo procedimiento descrito para las HL60 en

suspensión y diferenciadas, respectivamente, pero el buffer utilizado para la resuspensión de las proteínas fue el buffer de lisis.

La proteína se cuantificó usando el método del ácido bicinconínico (BCA) siguiendo las instrucciones del fabricante. Se realizó una recta patrón de albúmina bovina (BSA, Pierce) y tanto las muestras diluidas como la recta patrón se incubaron con el reactivo durante 30min a 37°C. La absorbancia se leyó a una longitud de onda de 562nm en un espectrofotómetro usando el programa SoftMax. Todos los extractos proteicos fueron almacenados a -20°C hasta su utilización.

5.12 Fraccionamiento celular

La obtención de las fracciones de interés (núcleo, membrana, citoplasma) se realizó mediante dos métodos. Para obtener la fracción nuclear, las células se lavaron con 1X PBS y se añadió el buffer CSK (50nM NaCl, 10mM Pipes pH6.8, 3mM $MgCl_2$, 0.5% Triton X-100, 300mM sacarosa e inhibidores de proteasas). Las células se incubaron 20min con agitación constante a 4°C, se recolectaron con una espátula y se centrifugaron a 15.700g durante 10min. El pellet (fracción nuclear) se resuspendió en 50µL del buffer Sol/Insol (15mM pH7.5, 5mM EDTA, 2.5mM EGTA y 1% SDS), se incubó durante 10min a 100°C y se añadieron 50 µL del buffer CSK.

La obtención de las dos fracciones restantes se realizó siguiendo el protocolo de fraccionamiento subcelular de Abcam. Las células se lisaron con el buffer de fraccionamiento (250mM sacarosa, 20mM Hepes pH7.4, 10mM KCl, 1.5mM $MgCl_2$, 1mM EDTA y 1mM EGTA con inhibidores de proteasas), se pasaron 10 veces por una jeringa de 1mL con una aguja de 25G y se incubaron en hielo durante 20min. En este paso se recogieron 50µL (lisado total) y se almacenaron a -20°C. Se continuó con una centrifugación a 800g durante 5min a 4°C, se recogió el sobrenadante (citoplasma) y se centrifugó a 5.900g 5 min a 4°C (se descartó el pellet, fracción mitocondrial). El sobrenadante se centrifugó a 100.000g (Rotor MLA130) durante 55 min a 4°C y se recogió el sobrenadante que corresponde a la fracción citosólica. El pellet (fracción de membrana) se resuspendió en el buffer de fraccionamiento y se centrifugó de nuevo en las mismas condiciones. Se descartó el sobrenadante y el pellet se resuspendió en el buffer RIPA. Las fracciones subcelulares se analizaron por Western Blot para la detección de GAPDH e Histona H1, en sus correspondientes fracciones, citoplasma y núcleo, respectivamente.

5.13 Análisis de la expresión proteica por Western Blot.

La proteína se cargó en un gel de poliacrilamida con SDS para obtener una separación en función del peso molecular. El porcentaje de poliacrilamida de cada gel se determinó según el peso molecular de la proteína de estudio. A continuación las proteínas se transfirieron a una membrana de nitrocelulosa y se comprobó su eficiencia por medio de la tinción reversible Ponceau (Fluka) al 0.2% en ácido acético al 1%. Se lavó la membrana con dH_2O y se incubó durante 1h a temperatura ambiente con la solución de bloqueo (BSA o leche desnatada al 5% en buffer TBS/Tween20: 0.1M NaCl, 10mM Tris Base, pH7.4; 0.05% Tween 20) según las especificaciones de cada anticuerpo (ver Tabla 10). La membrana se incubó con el anticuerpo primario específico disuelto en la solución de bloqueo correspondiente durante toda la noche (16h) a 4°C. Se realizaron 3 lavados de 10min con el buffer TBS/Tween20 y se incubó durante 1h el anticuerpo secundario (Dako) disuelto en la solución de bloqueo a la concentración recomendada por el fabricante. Finalmente, se realizaron 3 lavados de 10min con el buffer TBS/Tween20 y la membrana se reveló incubándola 5min con el reactivo Super Signal® West Dura (Thermo Scientific). Este reactivo reacciona con la peroxidasa de rábano conjugada al anticuerpo secundario dando lugar a un sustrato quimioluminiscente. La señal fue captada con el equipo Chemidoc XRS (BioRad) y la densidad de las bandas cuantificada con el programa Quantity One (BioRad).

Estudio	Proteína	Anticuerpo	Condiciones del WB
Apoptosis	BAX	Rabbit Polyclonal anti-Bax (Δ21) (Santa Cruz)	Gel al 15% de poliacrilamida; condiciones reductoras (CR); Dilución 1:1000 en leche al 5% en TBS/Tween20.
	DUSP6	Mouse Monoclonal anti-MKP-3 (R&D Systems)	Gel al 15% de poliacrilamida; CR; Dilución 1:500 en BSA al 5% en TBS/Tween20.
	G0S2	Rabbit Polyclonal anti-G0S2 (N-13) (Santa Cruz)	Gel al 15% de poliacrilamida; CR; Dilución 1:100 en leche al 5% en TBS/Tween20.
	BCL2	Mouse Monoclonal anti-human BCL2 (Dako)	Gel al 15% de poliacrilamida; CR; Dilución 1:1000 en leche al 5% en TBS/Tween20.
	CDK1	Mouse Monoclonal anti-Cdc2 p34 (POH-1) (Santa Cruz)	Gel al 12% de poliacrilamida; CR; Dilución 1:200 en leche al 5% en TBS/Tween20.
	CD180	Goat Polyclonal anti-RP105(C-20) (Santa Cruz)	Gel al 12% de poliacrilamida; CR; Dilución 1:200 en leche al 5% en TBS/Tween20.

Captación de lípidos	LDLR	Rabbit Monoclonal anti-LDLR (Abcam)	Gel al 10% de poliacrilamida; CR; Dilución 1:500 en leche al 5% en TBS/Tween20.
	VLDLR	Mouse Monoclonal anti-VLDLR (Santa Cruz)	Gel al 7.5% de poliacrilamida; CNR; Dilución 1:200 en leche al 5% en TBS/Tween20.
	LRP1	Mouse Monoclonal anti-LRP/A2MR (Fitzgerald)	Gel al 7.5% de poliacrilamida; CNR; Dilución 1:50 en leche al 5% en TBS/Tween20.
	LRP2	Rabbit Monoclonal anti-LRP2/Megalin (Abcam)	Gel al 7.5% de poliacrilamida; CR; Dilución 1:500 en leche al 5% en TBS/Tween20.
	LRP5	Mouse Monoclonal anti-LRP5 (Abcam); Rabbit Polyclonal anti-LRP5 (Abcam)	Gel al 10% de poliacrilamida; CR; Dilución 1:1000 en leche al 5% en TBS/Tween20.
	LRP6	Mouse Monoclonal anti-LRP6 (Abcam)	Gel al 10% de poliacrilamida; CR; Dilución 1:2000 en leche al 5% en TBS/Tween20.
Vía de señalización por Wnts	β-catenina	Rabbit Polyclonal anti-β-catenin (Millipore)	Gel al 12% de poliacrilamida; CR; Dilución 1:500 en leche al 5% en TBS/Tween20.
	LEF1	Rabbit Polyclonal anti-LEF1 (Abnova)	Gel al 10% de poliacrilamida; CR; Dilución 1:500 en BSA al 5% en TBS/Tween20.
	C-JUN	Mouse Polyclonal anti-C-JUN (Millipore)	Gel al 12% de poliacrilamida; CR; Dilución 1:500 en BSA al 5% en TBS/Tween20
	CICLINA D1	Mouse Monoclonal anti-Cyclin D1 unconjugated (Invitrogen)	Gel al 12% de poliacrilamida; CR; Dilución 1:500 en leche al 5% en TBS/Tween20.
	OPN	Rabbit Polyclonal anti-OPN (Millipore)	Gel al 12% de poliacrilamida; CR; Dilución 1:500 en BSA al 5% en TBS/Tween20
	BMP2	Mouse Monoclonal anti-BMP2 (R&D Systems)	Gel al 12% de poliacrilamida; CR; Dilución 1:500 en leche al 5% en TBS/Tween20
Fraccionamiento celular	GAPDH	Chicken Polyclonal anti-GAPDH (Millipore)	Gel al 12% de poliacrilamida; CR; Dilución 1:20000 en leche al 5% en TBS/Tween20.
	Histona H1	Mouse Monoclonal anti-Nuclei & chromosomes, histone H1protein (Millipore)	Gel al 15% de poliacrilamida; CNR; Dilución 1:1000 en leche al 5% en TBS/Tween20.
Normalización WB	β-actina	Mouse Monoclonal anti-beta Actin (Abcam)	CR; Dilución 1:5000 en BSA al 5% en TBS/Tween20.
	β-Tubulina	Rabbit Polyclonal anti-beta Tubulin (Abcam)	CR; Dilución 1:500 en leche al 5% en TBS/Tween20

Tabla 10: Anticuerpos utilizados para la detección de proteínas por medio de la técnica de Western Blot.

Las membranas se deshibridaron con Restore Western Blot Stripping Buffer (Thermo Scientific) siguiendo las instrucciones del fabricante. Se volvieron a bloquear y se incubaron con el anticuerpo para detectar β-actina o β-tubulina, usados como control del total de proteína cargada en la membrana ya sea en células, tejido humano o en tejido de ratón.

6. ANÁLISIS ESTADÍSTICO

Los resultados de esta tesis son presentados como la media ± S.E.M. de experimentos realizados 3 veces por duplicado o triplicado como mínimo. Los datos han sido analizados con el programa estadístico StatView. Las comparaciones entre grupos se realizaron con análisis paramétrico mediante el test ANOVA de dos factores. Se realizaron análisis de regresión lineal aplicando la fórmula Y=a+b*X y las pendientes se compararon mediante el *t-test*. Un valor de $p<0.05$ se consideró estadísticamente significativo.

RESULTADOS

Los artículos que han sido publicados o están en proceso de publicación y que son resultado de esta tesis son los siguientes:

1. Wnt pathway activation, cell migration, and lipid uptake is regulated by low-density lipoprotein receptor-related protein 5 in human macrophages. Borrell-Pagès M, Romero JC, Juan-Babot O, Badimon L. Eur Heart J. 2011;32(22):2841-50. doi: 10.1093/eurheartj/ehr062. PMID: 21398644. FI: 14.10

2. LRP5 negatively regulates differentiation of monocytes through abrogation of Wnt signalling. Borrell-Pagès M, Romero JC, Badimon L. J Cell Mol Med. 2014; 18(2):314-25. doi: 10.1111/jcmm.12190. PMID: 24266894. FI: 4.75

3. LRP5 deficiency downregulates Wnt signaling and promotes aortic lipid infiltration in hypercholesterolemic mice. Borrell-Pagès M[±], Romero JC[±], Badimon L. J Cell Mol Med. 2014. Aceptado. FI: 4.75
   [±] Co-primeros autores

4. Cholesterol modulates LRP5 expression in the vessel wall. Borrell-Pages M[±], Romero JC[±], Badimon L. Atherosclerosis. 2014; 235(2):363-70. doi: 10.1016/j.atherosclerosis.2014.05.922. PMID: 24929284. FI: 3.71
   [±] Co-primeros autores

5. LRP5 and serum colesterol levels modulate the canonical Wnt pathway in peripherical blood leukocytes. Borrell-Pagès M[±], Romero JC[±], Badimon L. En revisión en Immunology and Cell Biology.
   [±] Co-primeros autores

ARTÍCULO 1

Wnt pathway activation, cell migration, and lipid uptake is regulated by low-density lipoprotein receptor-related protein 5 in human macrophages.

Autores: María Borrell-Pagés, July Carolina Romero, Oriol Juan-Babot , Lina Badimon.

Centro de Investigación Cardiovascular CSIC-ICCC, Hospital de la Santa Creu i Sant Pau, Barcelona, España.

Revista: European Heart Journal 2011; 32(22): 2841-50.

Factor de impacto: 14.10

RESUMEN

La activación de la vía de señalización por Wnt, la migración celular y la absorción de lípidos en macrófagos humanos está regulada por el receptor Low-density lipoprotein receptor-related protein 5.

El desarrollo de la placa aterosclerótica incluye la infiltración de células inflamatorias, la acumulación de lípidos y la formación de una capa fibrosa. El receptor LDL receptor-related protein 1 (LRP1) está expresado en los macrófagos y en las células musculares lisas vasculares presentes en las lesiones ateroscleróticas. El objetivo de este estudio es analizar la función de otro miembro de la familia de proteínas receptoras de LDL, LDL receptor-related protein 5 (LRP5), en la progresión de la lesión aterosclerótica.

El análisis de la expresión de los tipos celulares implicados en la formación de la lesión muestra que LRP5 está expresado en las células inflamatorias y en las células vasculares humanas. Los experimentos se han realizado en cultivos primarios de monocitos humanos (HM) y en macrófagos derivados de HM (HMDM) tratados con LDL. LRP5 está transcripcionalmente regulado por las LDL agregadas (agLDL), participando en la internalización de lípidos y en la transformación de macrófagos en células espumosas, un paso clave en la progresión de la lesión aterosclerótica. Los macrófagos tratados con agLDL mostraron una sobrexpresión de LRP5 que se correlaciona con una sobreexpresión de proteínas diana de la vía de señalización por Wnt, como son β-CATENINA, LEF1, C-JUN, CICLINA D1, proteína morfogenética osea 2

(BMP2) y osteopontina (OPN). Además, los experimentos de migración de cierre de la herida y la cámara Boyden muestran que los macrófagos deficientes para LRP5 tienen una migración defectuosa sugiriendo que LRP5 tiene un rol en la motilidad celular.

Estos resultados evidencian la participación de LRP5 en la internalización de lípidos y en la migración celular en macrófagos, procesos claves para el desarrollo de la lesión aterosclerótica.

European Heart Journal (2011) **32**, 2841–2850
doi:10.1093/eurheartj/ehr062

BASIC SCIENCE

Wnt pathway activation, cell migration, and lipid uptake is regulated by low-density lipoprotein receptor-related protein 5 in human macrophages

Maria Borrell-Pagès, July Carolina Romero, Oriol Juan-Babot, and Lina Badimon*

Cardiovascular Research Center, CSIC-ICCC, Hospital de la Santa Creu i Sant Pau (UAB), Barcelona, Spain

Received 1 October 2010; revised 11 January 2011; accepted 1 February 2011; online publish-ahead-of-print 12 March 2011

Aims Atherosclerosis plaque development includes infiltration of inflammatory cells, accumulation of lipids and fibrous cap formation. Low-density lipoprotein receptor-related protein 1 (LRP1) is expressed on atherosclerotic lesions associated with macrophages and vascular smooth muscle cells. The aim of this work is to analyse the role in atherosclerosis lesion progression of another member of the LDL receptor protein family, low-density lipoprotein receptor-related protein 5 (LRP5), a co-receptor with Frizzled known to activate the Wnt signalling pathway in several cell types.

Methods and results LRP5 is expressed in human vascular and innate inflammatory cells. LRP5 is transcriptionally regulated by aggregated LDL (agLDL), participating in the lipid uptake and transformation of macrophages into foam cells, a critical step in atherosclerosis progression. AgLDL-treated macrophages show up-regulated expression of β-catenin, LEF1, c-jun, cyclinD1, bone morphogenetic protein 2 (BMP2), and osteopontin (OPN), proteins and targets of the Wnt signalling pathway, whereas LRP5-silenced macrophages show a significant down-regulation of OPN and BMP2 expression. Furthermore, LRP5-deficient macrophages exhibit an impaired migration both in wound-repair and modified Boyden chambers models.

Conclusion These results demonstrate the involvement of LRP5 in the innate inflammatory reaction to lipid infiltration in atherosclerosis.

Keywords Atherosclerosis • LRP5 • Human macrophages • Wnt signalling • Lipid uptake

Introduction

Atherosclerosis is an inflammatory process characterized by the accumulation of lipids and fibrous elements in large arteries. High levels of plasma lipids, particularly low-density lipoproteins (LDL), are prominent risk factors for atherosclerosis because of their accumulation in the subendothelial space of the vascular wall.[1,2] Aggregation is one of the most important initial LDL modifications in the vascular wall where particles become aggregated by binding to extracellular matrix proteoglycans in the arterial intima.[2–4] Unlike native LDL (nLDL), agLDL are a potent inducer of massive intracellular cholesteryl ester (CE) accumulation both in macrophages[5–7] and vascular smooth muscle cells (VSMC),[8–11] two key cell types that determine the fate of the arterial wall during atherosclerotic transformation.

We and others have described that low-density lipoprotein receptor-related protein 1 (LRP1) is highly expressed on atherosclerotic lesions in association with macrophages and VSMC[9–12] and that it is involved in the progression of human coronary lesions.[13] Our group demonstrated that agLDL up-regulates LRP1 expression at a transcriptional level leading to a large increase in LRP1 protein expression. We also proved that LRP1 is involved in agLDL uptake which leads to an increase in intracellular CE accumulation in human VSMC and macrophages.[9–11,14]

LRP1 belongs to the LDL family of receptors. They share extracellular homology domains such as ligand-binding repeats, and

* Corresponding author: Cardiovascular Research Center, C/Sant Antoni Maria Claret 167, 08025 Barcelona, Spain. Tel: +34 935565880, Fax: +34 935565559, Email: lbadimon@csic-iccc.org

harbour in their cytoplasmic tails recognition sites for adaptor proteins, that upon activation of the receptor will induce different signal transduction pathways. Other members of this family include the LDL receptor, LRP2/megalin, LRP4, LRP5, LRP6, LRP8/ApoE receptor2, LRP9, and LRP10. In this report, we demonstrate that another member of this family, LRP5 is involved, through its presence in macrophages, in two processes essential for atherosclerotic progression: agLDL uptake and monocyte/macrophage migration.

LRP5 is known to function as a co-receptor with the protein frizzled to bind extracellular Wnt glycoproteins which activate the canonical β-catenin signalling pathway that mediates vital biological processes like embryogenesis, organogenesis, and tumorigenesis.[15,16] Upon Wnt binding, the LRP5-frizzled complex triggers several intracellular phosphorylation events that ultimately lead to an increase in the intracellular concentration of β-catenin. β-catenin is free to translocate to the nucleus where it interacts with the TCF/LEF1 family of transcription factors to promote transcription. There are several downstream target genes whose expression is known to be regulated by the Wnt signalling pathway including cyclo-oxygenase-2,[17] c-jun,[18] connexin43,[19] cyclinD1,[20] osteopontin (opn),[21] and bone morphogenetic protein 2 (bmp2).[22]

The aim of this study was to analyse the expression and function of LRP5 in the different cell types present in atherosclerotic lesions with and without agLDL-mimicking arterial lesions. Our findings show that (i) LRP5 is expressed in human endothelial cells, vascular smooth muscle cells, monocytes, and macrophages, (ii) LRP5 expression is transcriptionally regulated by agLDL only in monocytes/macrophages, (iii) CE uptake from agLDL is reduced in siRNA-LRP5-treated macrophages, (iv) agLDL induce an increase in mRNA and protein levels of the Wnt pathway including β-catenin, LEF1, cyclinD1, c-jun, OPN, and BMP2, (v) siRNA-LRP5-treated macrophages show a reduced motility in two models. These results show, for the first time, the role of LRP5 in lipid internalization, triggering the Wnt signalling cascade and in macrophage motility.

Methods

Experiments were mainly performed on primary cultures of human monocytes (HM) and HM-derived macrophages (HMDM) treated with LDL and the expression levels of genes and proteins of interest were measured.

For protocol description of primary cultures, LDL treatments, western blot (WB), flow cytometry, real-time polymerase chain reaction (PCR), thin-layer chromatography (TLC), immunohistochemistry, and migration assays, see the 'Detailed methods' section in Supplementary material online.

Results

Low-density lipoprotein receptor-related protein 5 expression in the major cell types present in atherosclerotic lesions

LRP5 is expressed in the four major cell types present in atherosclerotic lesions. Human monocytes (HM) and HMDM primary cultures were cultured in the absence or presence of LDL (natives, nLDL, or aggregated, agLDL) for up to 48 h. Although all the cell types showed detectable basal mRNA LRP5 levels, only inflammatory cells underwent a significant increase in the mRNA LRP5 levels after agLDL, but not nLDL treatment (*Figure 1A*). Indeed, neither human vein endothelial cells nor human coronary VSMC showed changes in mRNA LRP5 levels when treated with agLDL.

Immunohistochemical analysis of macrophages (measured as HAM56 staining), VSMC (stained with α-actin), and LRP5 were performed in initial (where macrophage infiltration is almost absent) and advanced human atherosclerotic lesions as described under the Methods section. LRP5 expression was detected independently of aetiological myocardial disease. As shown in *Figure 1B*, intimal HAM56 and LRP5 staining increased in advanced lesions. Furthermore, a $62 \pm 1\%$ increase in LRP5-positive macrophages is detected in advanced plaques respect to initial lesions. Colocalization between HAM56 and LRP5 staining is detected in sections where macrophage infiltration is observed (*Figure 1C*), suggesting a role for LRP5 in atherosclerosis progression.

Western blot and immunofluorescence experiments confirmed that the increase in LRP5 mRNA levels due to agLDL treatment was concomitant with an increase in the protein expression in both HM (*Figure 2A*) and HMDM (*Figure 2B*) primary cultures. Furthermore, flow cytometry analyses show a $42 \pm 1\%$ and a $48 \pm 1\%$ increase in LRP5 intensity after agLDL treatment in HM and HMDM, respectively (*Figure 2A* and *B*).

Cell viability and apoptosis in human monocyte and human monocyte-derived macrophage cultures following aggregated low-density lipoprotein treatment

We treated HM and HMDM with increasing concentrations of agLDL to determine a concentration range of LRP5 expression levels; 100 μg/mL agLDL induced the maximum mRNA LRP5 expression and was chosen for further experiments (*Figure 2C*).

To test whether agLDL-treated cells and LRP5-mediated processes induced apoptosis, levels of pro-apoptotic Bax protein and anti-apoptotic Bcl-2 protein were measured because an increase in the Bax:Bcl-2 ratio would indicate cell commitment to apoptotic death via mitochondria-mediated pathway. We could not detect any changes in the Bax:Bcl-2 ratio in HM or HMDM after 100 μg/mL nLDL or agLDL treatments, indicating that the apoptotic pathway was not induced (*Figure 2D*).

Blocking of low-density lipoprotein receptor-related protein 1 does not affect low-density lipoprotein receptor-related protein 5 mRNA levels

It has been recently reported that LRP1 participates in the uptake of LDL in macrophages[23,24] and human VSMC.[10,11]

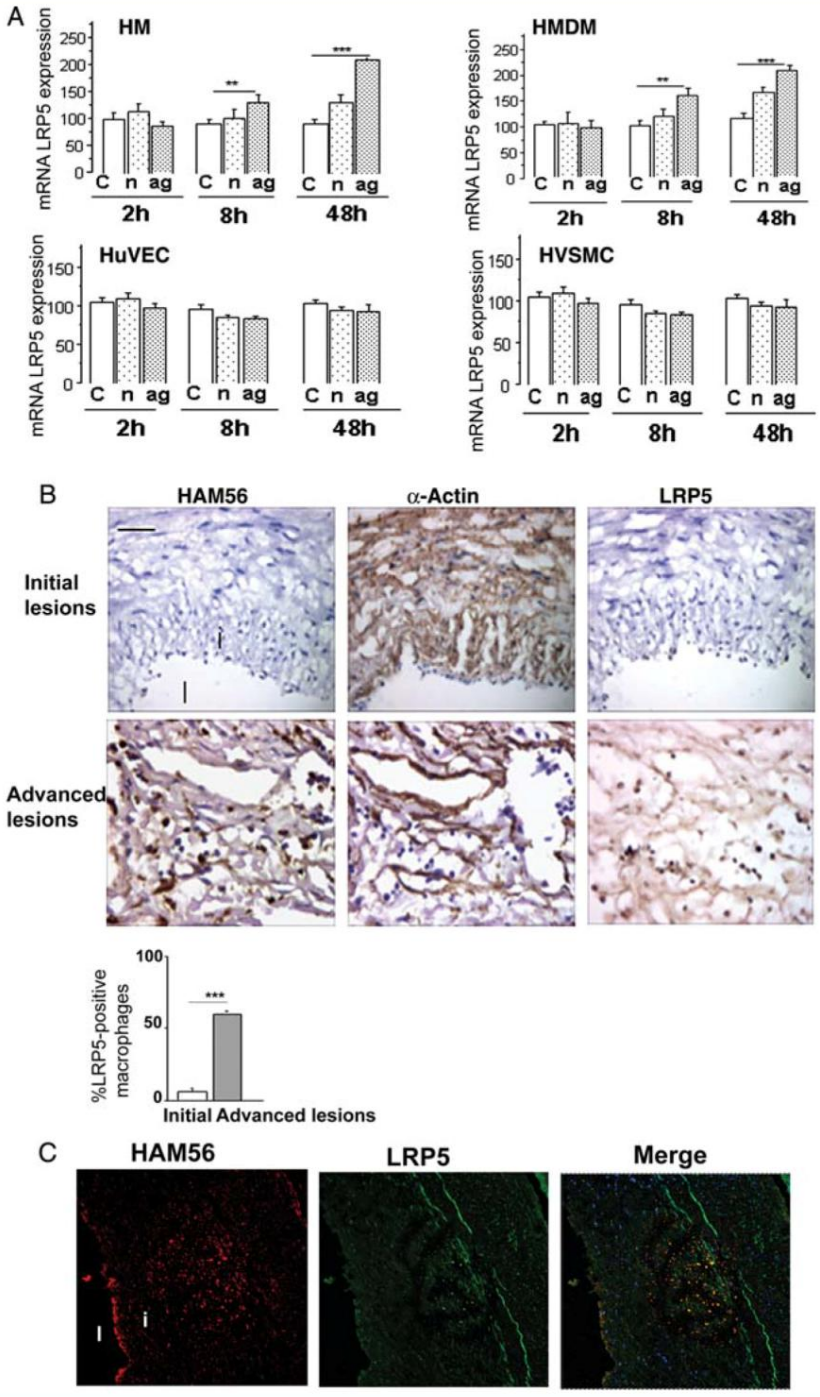

Figure 1 Low-density lipoprotein receptor-related protein 5 expression in primary cultures and in atherosclerotic lesions in human arteries. (*A*) human monocytes, human monocyte-derived macrophages, human vein endothelial cells, and human vascular smooth muscle cells were serum-free treated or incubated with 100 μg/mL native low-density lipoprotein or aggregated low-density lipoprotein for the indicated times. Low-density lipoprotein receptor-related protein 5 mRNA levels from RNA extracts were quantified by real-time polymerase chain reaction and normalized to 18srRNA; $^{**}P < 0.01$, $^{***}P < 0.005$. Experiments were performed three independent times in triplicates. (*B*) Representative images of lesions from deparaffinized human coronary arteries were classified into initial lesions (types I–II, $n = 6$) and advanced lesions, (types VII–VIII, $n = 6$) and immunostained with monoclonal anti-HAM56 for macrophages, anti-α-Actin for vascular smooth muscle cells, and anti-low-density lipoprotein receptor-related protein 5. Bar 100 μm; l, lumen, i, intima. Quantitative analysis of low-density lipoprotein receptor-related protein 5-positive macrophages $^{***}P < 0.005$. (*C*) Confocal image of intimal advanced lesion double-labelled with anti-HAM56 and anti-low-density lipoprotein receptor-related protein 5. l, lumen, i, intima.

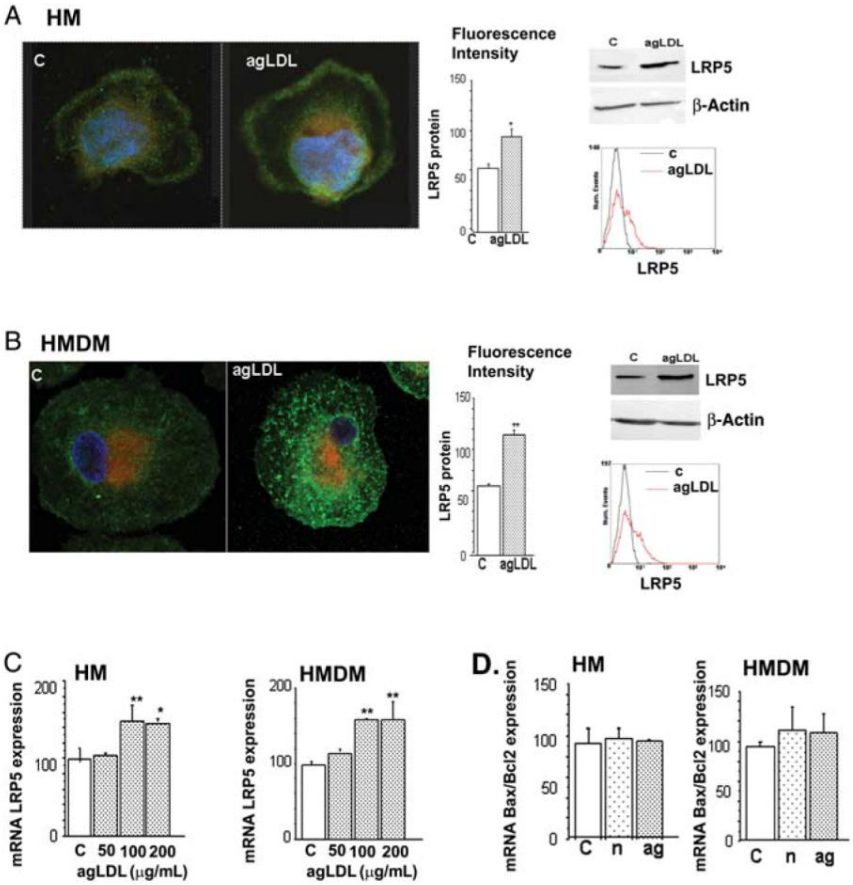

Figure 2 Low-density lipoprotein receptor-related protein 5 protein expression and cell viability after aggregated low-density lipoprotein treatment in human monocytes and human monocyte-derived macrophages. (*A*) Human monocytes were incubated or not with 100 μg/mL aggregated low-density lipoprotein for 8 h and stained with mouse anti-low-density lipoprotein receptor-related protein 5, rabbit anti-CD68 followed by Alexa Fluor anti-mouse 488 IgG, Alexa Fluor anti-rabbit 633 IgG, and Hoechst. Fluorescence intensity for low-density lipoprotein receptor-related protein 5 staining measured with the Leica Standard Software TCS-AOBS; $*P < 0.05$. Representative western blot and flow cytometry analysis of low-density lipoprotein receptor-related protein 5 expression in untreated and aggregated low-density lipoprotein-treated human monocytes. (*B*) Same procedures as (*A*) in human monocyte-derived macrophages $**P < 0.01$. (*C*) Human monocytes and human monocyte-derived macrophages incubated with the indicated concentrations of aggregated low-density lipoprotein for 8 h. Low-density lipoprotein receptor-related protein 5 mRNA levels from RNA extracts were quantified by real-time polymerase chain reaction and normalized to 18srRNA; $*P < 0.05$, $**P < 0.01$. Experiments were performed three times in triplicates. (*D*) Human monocytes and human monocyte-derived macrophages serum-free treated or incubated with 100 μg/mL of native or aggregated low-density lipoprotein for 8 h. Bax and Bcl2 mRNA levels from RNA extracts were quantified by real-time polymerase chain reaction and normalized by 18srRNA. Experiments were performed three times in duplicates.

Specific inhibition of LRP1 with small interfering RNA resulted in a significant reduction in intracellular CE in both HMDM and VSMC.[10,11,23,24] To eliminate a possible interaction between LRP1 and LRP5, we used monoclonal antibodies against the α-chain of LRP1, which has been described to bind to LRP1 extracellular domain. Both IgG and anti-LRP1-treated HMDM showed a significant increase in LRP5 mRNA levels after 8 h agLDL treatment, indicating that LRP5 increased expression in the presence of agLDL is independent from LRP1 (*Figure 3A*).

Low-density lipoprotein receptor-related protein 5 silencing decreases cholesteryl ester accumulation after aggregated low-density lipoprotein treatment in human monocyte-derived macrophages

Specific inhibition of either LRP1 or LRP5 expression (with siRNA) or scavenger receptors (with polyinosinic acid) was used to demonstrate an involvement for LRP5 in agLDL uptake in HMDM. Western blot analysis showed a reduction in LRP5

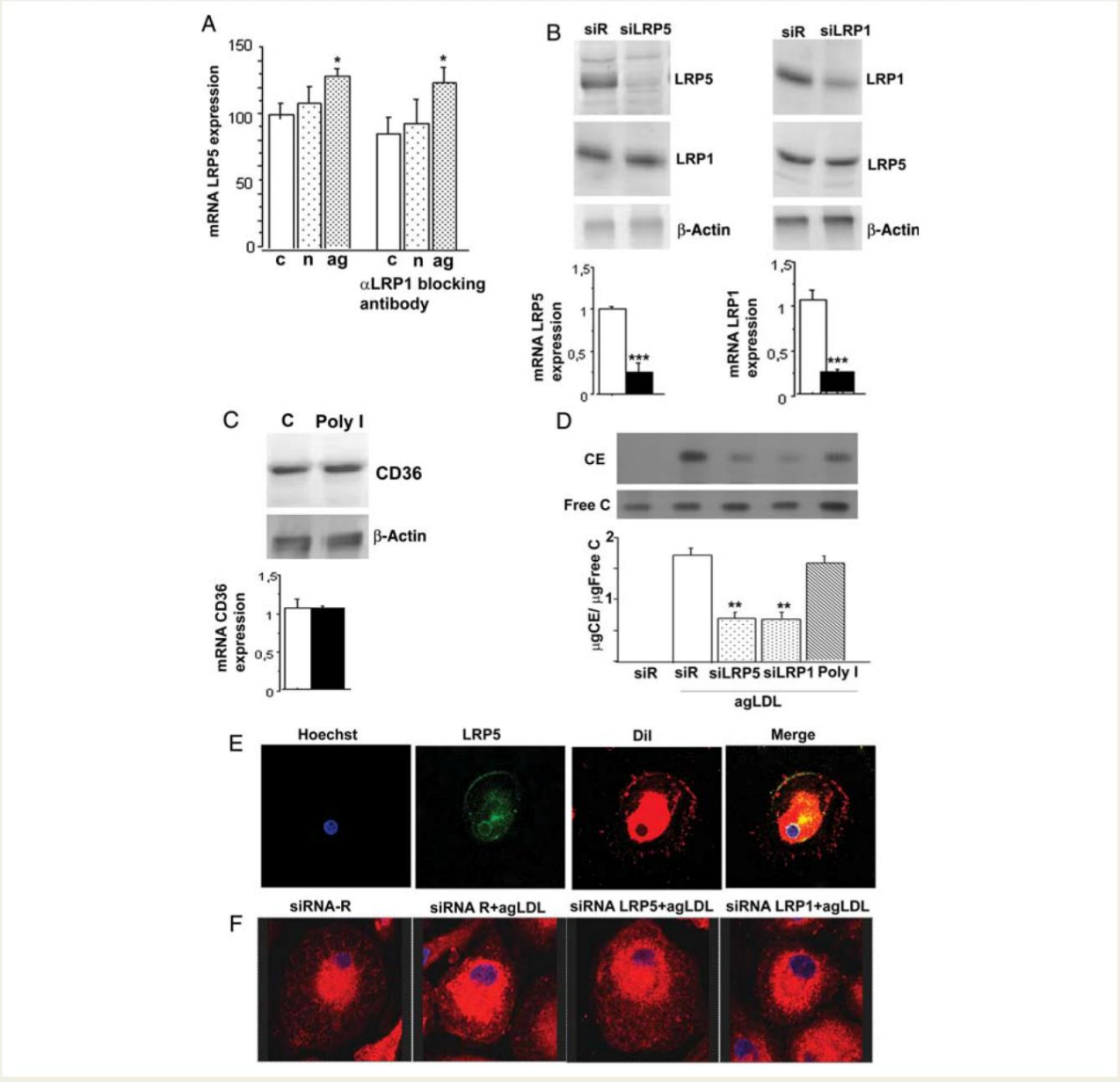

Figure 3 Low-density lipoprotein receptor-related protein 5 and lipid uptake in human monocyte-derived macrophages. (*A*) human monocyte-derived macrophages were arrested and pre-treated for 2 h with 25 μg/mL of monoclonal anti-low-density lipoprotein receptor-related protein 1 antibody or non-immune IgG antibody, incubated in serum-free medium or with 100 μg/mL of native or aggregated low-density lipoprotein for further 8 h. Samples were collected and low-density lipoprotein receptor-related protein 5 mRNA levels from RNA extracts were quantified by real-time polymerase chain reaction and normalized to 18srRNA. Experiments were performed three times in triplicates. $^{*}P < 0.05$. (*B*) Low-density lipoprotein receptor-related protein 1 and 5 protein and mRNA levels in siRNA-Random, siRNA-low-density lipoprotein receptor-related protein 5, and siRNA-low-density lipoprotein receptor-related protein 1 transfected human monocyte-derived macrophages. Protein extracts were blotted against monoclonal anti-low-density lipoprotein receptor-related protein 1 or 5, and β-actin was used for normalization. RNA extracts detected mRNA levels from low-density lipoprotein receptor-related protein 1 and 5, normalized to 18srRNA. $^{***}P < 0.005$. (*C*) CD36 expression in human monocyte-derived macrophages treated or not with 100 μg/mL polyinosinic acid for 8 h. Protein extracts were blotted with CD36 primary antibody and β-actin. CD36 mRNA levels from RNA extracts were quantified by real-time polymerase chain reaction and normalized to 18srRNA. (*D*) Human monocyte-derived macrophages containing siRNA-Random, siRNA-low-density lipoprotein receptor-related protein 1, and siRNA-low-density lipoprotein receptor-related protein 5 or treated with polyinosinic acid (100 μg/mL) were aggregated low-density lipoprotein incubated (100 μg/mL) for 8 h. Human monocyte-derived macrophages were then exhaustively washed and harvested to measure intracellular Free C and EC by TLC. Bar graph showing the quantification of cholesteryl esters respect to Free C. $^{**}P < 0.01$. (*E*) Confocal microscopy of aggregated low-density lipoprotein-treated human monocyte-derived macrophages stained with DiI and anti-low-density lipoprotein receptor-related protein 5. (*F*) Confocal microscopy of low-density lipoprotein receptor-related protein 1- and 5-silenced human monocyte-derived macrophages and treated or not with 100 μg/mL aggregated low-density lipoprotein, washed, fixed, and stained with DiI.

protein levels by 97 ± 1% in siRNA-LRP5-treated HMDM, whereas LRP1 expression was inhibited by 92 ± 0.5% by siRNA-LRP1 treatment (*Figure 3B*). Analysis of mRNA expression by reverse transcriptase–PCR showed a 75 ± 3% LRP1 reduction in siRNA-LRP1-treated cells and a 76 ± 2% LRP5 reduction in siRNA-LRP5-treated cells (*Figure 3B*). A scavenger receptor blockade was assessed by polyinosinic acid, a known ligand of this family of receptors used at an inhibitory concentration of 100 μg/mL[9] (*Figure 3C*). CD36 is a class B scavenger receptor that facilitates oxidized but not agLDL uptake in macrophages and is involved

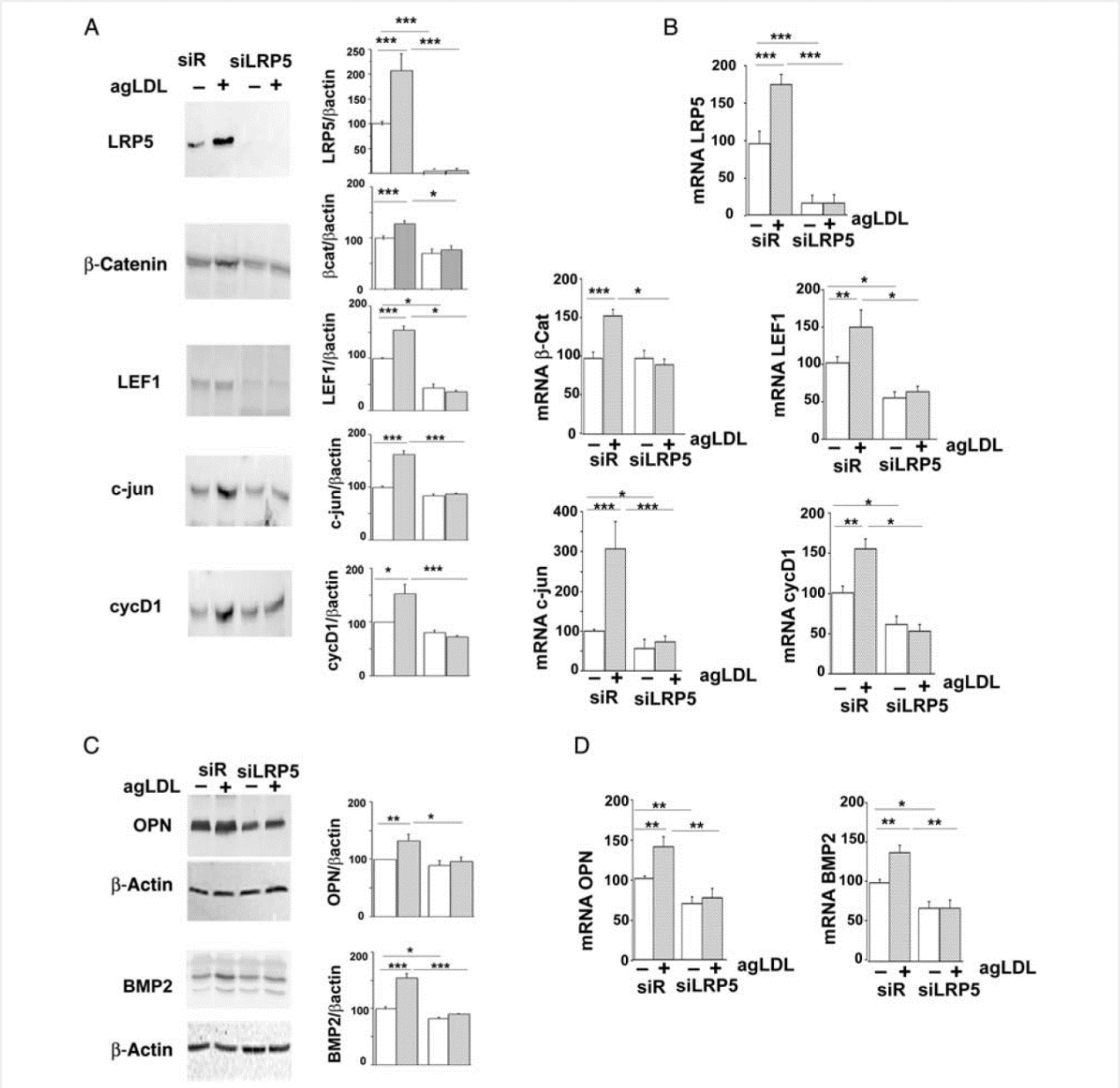

Figure 4 Aggregated low-density lipoprotein fails to induce an increase in Wnt pathway proteins in low-density lipoprotein receptor-related protein 5-deficient human monocyte-derived macrophages. siRNA-Random and siRNA-low-density lipoprotein receptor-related protein 5-treated human monocyte-derived macrophages were incubated in the presence or absence of 100 μg/mL aggregated low-density lipoprotein for 24 h. (*A*) Representative western blot and quantitative analysis (control cells, white boxes; aggregated low-density lipoprotein-treated cells, hatched boxes) of low-density lipoprotein receptor-related protein 5, β-catenin, LEF1, c-jun, and cyclinD1. (*B*) Real-time polymerase chain reaction quantification of low-density lipoprotein receptor-related protein 5, β-catenin, LEF1, c-jun, and cyclin D1 mRNA expression levels normalized to 18srRNA. (*C*) Representative western blot and quantitative analysis (control cells, white boxes; aggregated low-density lipoprotein-treated cells, hatched boxes) of OPN and BMP2. (*D*) Real-time polymerase chain reaction quantification of opn and bmp2 mRNA expression levels normalized to 18srRNA; $*P < 0.05$, $**P < 0.01$, $***P < 0.005$.

in the development of atherosclerotic lesions.[25] Indeed, as shown in *Figure 3D*, no decrease in CE accumulation could be detected after polyinosinic acid treatment.

AgLDL (100 μg/mL) induced high levels of intracellular CE accumulation in HMDM and siRNA-LRP5 treatment inhibited CE accumulation from agLDL by 1 μg CE/μg FC (*Figure 3D*). Confirming previous results from our lab, siRNA-LRP1 treatment also diminished CE accumulation.[14] We further analysed the effect of siRNA-LRP1 and siRNA-LRP5 treatment in an agLDL excess content (400 μg/mL; Supplementary material online, *Figure S1*). Under these conditions, although both receptors can promote CE accumulation, LRP5 is more effective probably due to an early saturation of LRP1's lipid uptake activity. These results show that in lipid-saturating conditions, both receptors have different capacities of lipid uptake in HMDM.

Colocalization of LRP5 with agLDL was observed by confocal microscopy experiments in agLDL-treated HMDM (*Figure 3E*). Furthermore, total lipid content was measured in HMDM transfected with siRNA-LRP5 or siRNA-LRP1, treated or not with agLDL and labelled with DiI. In control conditions, when no agLDL is present in the media, little or no DiI staining can be observed. In contrast, when agLDL are added, a strong vesicular DiI staining can be observed in non-transfected conditions. This labelling is dramatically reduced in the presence of siRNA-LRP5 or siRNA-LRP1, showing a decrease in agLDL uptake in macrophages silenced for LRP1 or LRP5 (*Figure 3F*).

Effect of aggregated low-density lipoprotein on Wnt signalling pathway

We then searched for intracellular pathways modulated by agLDL treatment in HMDM. We have shown that both HM and HMDM primary cultures show increased LRP5 levels after agLDL treatment. Therefore, there seems to be no differences in LRP5 modulation in these primary cultures. To characterize LRP5 signalling pathway, we decided to use HMDM as they are easier to transfect. We focused on the canonical Wnt signalling pathway as LRP5 has been described to activate the Wnt pathway in several cell types ranging from adipocytes,[26] to osteoblasts[27]and hepatocytes.[28] We analysed the mRNA and protein levels of several Wnt proteins in control and agLDL-treated HMDM in the presence and absence of LRP5. Results show that both mRNA and protein levels of β-catenin and LEF1 are increased 24 h after agLDL treatment in HMDM. This increase is abrogated in siRNA-LRP5-treated cells (*Figure 4A* and *B*). Furthermore, LRP5-deficient macrophages show a reduction in LEF1 mRNA levels in control conditions ($50 \pm 3\%$) and in agLDL-treated cells ($62 \pm 2\%$). mRNA and protein levels of c-jun and cyclinD1, two well-known Wnt targets, are also increased only in the presence of LRP5 in agLDL-treated cells (*Figure 4A* and *B*). As for LEF1, their mRNA and protein levels are reduced in the absence of LRP5, regardless of treatment (50 ± 1 and $76 \pm 2\%$ in untreated and agLDL-incubated HMDM c-jun mRNA levels, and 30 ± 2 and $56 \pm 3\%$ in cyclinD1 mRNA expression). These results indicate that LRP5 interaction with agLDL triggers the activation of the Wnt signalling pathway.

Aggregated low-density lipoprotein induces transcriptional and protein levels of osteopontin and bone morphogenetic protein 2

Osteopontin and BMP2 have been described to participate in the progression of atherosclerotic plaques.[29–32] They have also been reported to be Wnt target genes.[21,22] Here, we show that agLDL treatment induces an increase in mRNA levels of bmp2 and opn. LRP5 silencing abrogates the effect of agLDL (37 ± 1 and $52 \pm 2\%$ in untreated and agLDL-incubated HMDM opn mRNA levels and 25 ± 3 and $35 \pm 3\%$ in bmp2 mRNA expression). A direct effect for LRP5 silencing was also observed in protein levels of OPN and BMP2 (*Figure 4C* and *D*). These results indicate a direct role for LRP5 in atherosclerosis progression.

Silencing of low-density lipoprotein receptor-related protein 5 decreases migration of human monocyte-derived macrophage cells in a wound-healing assay

c-jun and cyclinD1 are known to play a role in cell motility.[33,34] Therefore, we tested whether cell motility of HMDM was affected in a wound-healing assay by LRP5 modulation.

To this end, HMDM were transfected with siRNA-Random, siRNA-LRP5, or siRNA-LRP1. The wound-repair model was performed as described in the Methods section. Pictures were taken immediately after the wound was inflicted to the plated cells and 24 h later (*Figure 5A*). Twenty-four hours after wounding, control and siRNA-LRP1-treated cells had migrated from the outermost cell row into the wound, whereas siRNA-LRP5-treated cells were significantly less motile (*Figure 5A*), suggesting a role for LRP5 in human macrophage migration. Image analysis allowed the quantification of the infiltration of macrophages to the wound (*Figure 5B*). LRP1 and LRP5 mRNA and protein levels were analysed, showing an efficient inhibition by siRNA-LRP1 and siRNA-LRP5 (*Figure 5C*).

To analyse the role of agLDL treatment in our cell motility assay, the model system with siRNA-Random, siRNA-LRP1, and siRNA-LRP5 was challenged with agLDL. Pictures were taken 24 h after incubation. Contrary to non-treated cells, none of the agLDL-treated conditions were able to significantly reduce the scratch within 24 h, showing a reduced motility of the cells. However, silencing of LRP5 showed the higher inhibition (*Figure 5D*). *Figure 5E* shows that the motility decreased by almost $40 \pm 2\%$ in agLDL-treated cells compared with non-treated cells.

Low-density lipoprotein receptor-related protein 5-deficient human monocyte-derived macrophage cells show a decreased migration in modified Boyden chambers

LRP5 involvement in HMDM migration was further analysed by modified Boyden chambers. Cells devoid of LRP1, LRP5, and siRNA-Random cells were trypsinized, resuspended in serum-

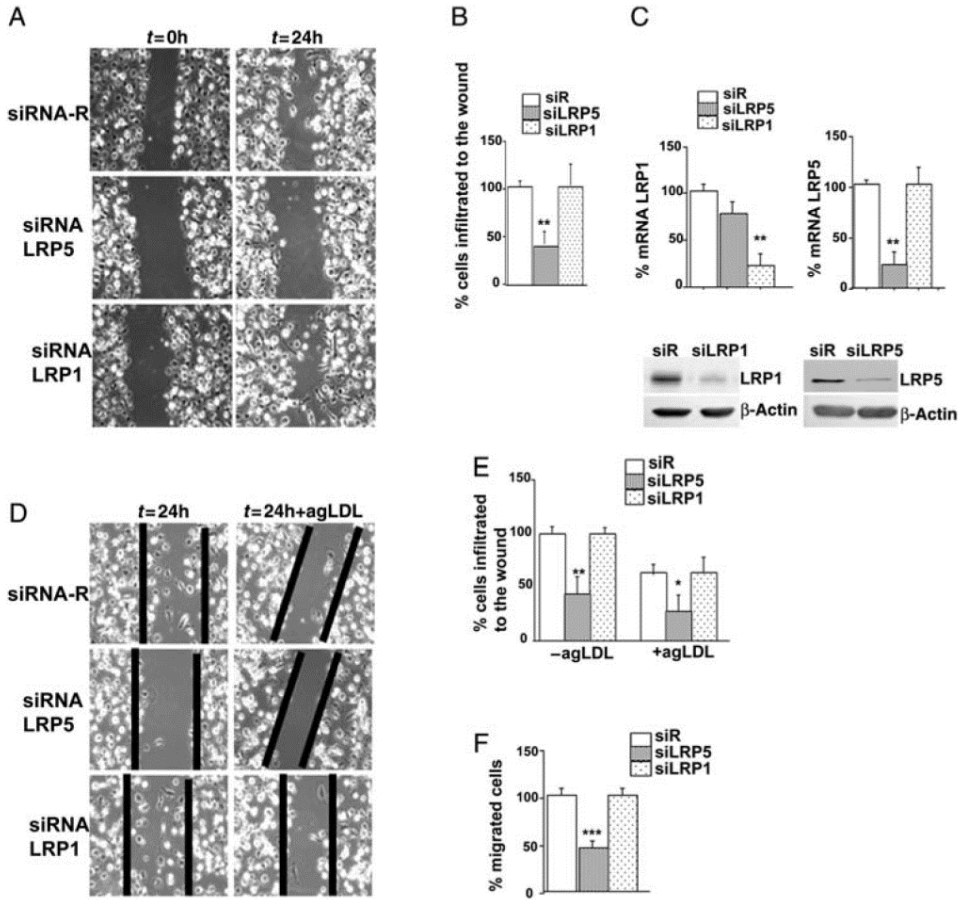

Figure 5 Low-density lipoprotein receptor-related protein 5-deficient human monocyte-derived macrophages cells show a decrease in migration in a wound-healing assay and in modified Boyden chambers. (*A*) siRNA-Random, siRNA-low-density lipoprotein receptor-related protein 5, and siRNA-low-density lipoprotein receptor-related protein 1 transfected human monocyte-derived macrophages immediately after ($t = 0$ h) and 24 h after ($t = 24$ h) wounding. Representative images of $n = 4$ experiments. (*B*) Bar graph showing the infiltration of human monocyte-derived macrophages cells to the wound; $^{**}P < 0.01$. (*C*) Real-time polymerase chain reaction quantification and western blot analysis of low-density lipoprotein receptor-related protein 5 and low-density lipoprotein receptor-related protein 1 mRNA expression levels in siRNA-Random, siRNA-low-density lipoprotein receptor-related protein 5, and siRNA-low-density lipoprotein receptor-related protein 1 transfected human monocyte-derived macrophages cells; $^{**}P < 0.01$. (*D*) Human monocyte-derived macrophages containing siRNA-Random, siRNA-low-density lipoprotein receptor-related protein 5, and siRNA-low-density lipoprotein receptor-related protein 1 incubated or not with 100 μg/mL aggregated low-density lipoprotein for 24 h immediately after wounding. The solid line indicates the position of the cell border at $t = 0$ h. Representative images of $n = 4$ experiments. (*E*) Bar graph showing the infiltration of human monocyte-derived macrophages cells to the wound; $^{**}P < 0.01$, $^{*}P < 0.05$. (*F*) Transfected human monocyte-derived macrophages containing siRNA-Random, siRNA-low-density lipoprotein receptor-related protein 5, or siRNA-low-density lipoprotein receptor-related protein 1 in modified Boyden chambers (24 h). Results are expressed as % of migrated cells. The experiments were run in triplicate and five fields from each chamber were counted and averaged; $^{***}P < 0.005$.

free medium, and added to the top chamber for 24 h. The medium in the lower chamber did not contain any chemoattractants in order to ascertain that the variation detected in HMDM migration was only due to the lack of LRPs. After incubation for 24 h at 37°C, the top side of the insert membrane was scrubbed free of cells with a cotton swab, and the bottom side was stained with Giemsa. Cells that migrated to the bottom side of the membrane were counted, revealing that LRP5-deficient cells show a 51 ± 1% reduction in macrophage migration respect to controls (*Figure 5F*).

Discussion

The development of atherosclerotic lesions is characterized by the accumulation of modified LDL in the vascular wall. agLDL are able to induce massive intracellular CE accumulation in two cell types involved in atherosclerosis, human VSMC, and macrophages.[5–8,10,11,23,24] In this report, we demonstrate that agLDL strongly up-regulates a new member of the LDL receptor family, LRP5, at a transcriptional level in human monocytes and macrophages. The increase in LRP5 mRNA transcription leads to an

increase in LRP5 protein expression. This increase in LRP5 levels after agLDL incubation is specific of inflammatory cells as agLDL does not regulate LRP5 levels in human endothelial or VSMC. Consequently, by inducing LRP5 expression in human macrophages and monocytes, agLDL could lead to a progressive intracellular accumulation of cholesterol in these cells.

Our group has recently demonstrated that agLDL increases LRP1 expression in VSMC and macrophages. In order to ascertain that the uptake of agLDL by LRP5 in human macrophages is independent of LRP1, we assessed the effect of monoclonal antibodies against the α-chain of LRP1, showing that when LRP1 is blocked, LRP5 expression in agLDL-incubated macrophages is still increased. Therefore, LRP1 does not interfere in agLDL induction of LRP5.

In this report, we show for the first time the functional involvement of LRP5 in LDL uptake in human macrophages. As shown by TLC, inhibition of LRP5 by siRNA treatments dramatically decreases the uptake of agLDL, and consequently, the total lipid content is also severely reduced. This suggests a role for this receptor in the accumulation of CE in macrophages that are present from the earliest discernable fatty streak lesions to advanced plaques and that are key regulators of the pathological behaviour of plaques.[35,36] The lack of involvement of scavenger receptors on agLDL binding and internalization by macrophages has been demonstrated by several authors.[5–7]

One major question is the signalling pathway activated upon agLDL induction of LRP5 expression. Our data suggest that the stimulation effect of agLDL on LRP5 induces the activation of canonical Wnt/β-catenin pathway. After agLDL incubation, human macrophages showed an increase in the mRNA and protein levels of several Wnt/β-catenin pathway proteins and targets, including β-catenin, LEF1, c-jun, cyclinD1, bmp2, and opn. Importantly, the increase in all these Wnt signalling proteins was greatly reduced in the absence of LRP5, indicating that in human macrophages, agLDL triggers the Wnt pathway only in the presence of LRP5.

In the context of atherosclerosis, agLDL increased BMP2 and OPN expression in macrophages. These proteins have been described to be differentially expressed in human with increased levels of atherosclerotic plaques.[29–31]More importantly, a proteomic search of biomarkers of atherosclerotic plaque has identified OPN as a potential plaque biomarker as high plasma levels of OPN strongly predict the risk of a new vascular complication.[32] Since LRP5 is involved in agLDL uptake and OPN and BMP2 are up-regulated only in the presence of LRP5, our results reinforce the notion of LRP5 having a role in atherosclerotic progression through its presence in human macrophages. Therefore, the use of nanoparticles for the therapeutic administration of siRNA-LRP5 targeted to macrophages at sites of injury could have potential relevant applications in an attempt to reduce infiltration and accumulation of inflammatory cells.

c-jun and cyclinD1 have been involved in cell motility and are up-regulated after agLDL treatment in macrophages. We hypothesized that LRP5 and the Wnt pathway could participate in the macrophage motility associated with an atherosclerotic process. We found that in LRP5-deficient macrophages, the repair or migration of cells to the wounded area was greatly impaired. This did not occur in LRP1-defective cells, suggesting that it is a specific function for LRP5. These results were confirmed by modified Boyden chambers where LRP5-defective macrophages showed a slower migration rate than control or LRP1-defective cells.

When treated with agLDL, human macrophages showed a lower migratory capacity under all the conditions tested. We here report a significant effect of agLDL on scratch assays in human macrophages, suggesting that agLDL may likely have a major functional effect on the formation of the atherosclerotic plaque. Indeed, in macrophages, agLDL up-regulate the expression of LRP5 and internalize significant amounts of CE contributing to the transformation of macrophages into lipid-loaded immune cells. From a mechanistic standpoint, the fact that agLDL exert inhibitory effects on human macrophage migration, regardless of the LRP inhibited, indicates that part of the observed functional effects are due to the accumulation of CE.

LRP5 involvement in lipoprotein uptake is being studied in animal models. In contrast to apoE knockout mice or LDL-receptor knockout mice, LRP5-deficient mice do not show an increase in plasma cholesterol levels on a normal diet. However, LRP5 knockout mice fed a high-fat diet develop high plasma cholesterol levels.[37] Furthermore, double knockout mice deficient in LRP5 and ApoE fed a normal diet exhibiting 60% higher plasma cholesterol levels compared to apoE knockout mice.[38] Atherosclerotic lesions on the double knockouts were three times greater than those in apoE knockout mice.[38] Presently, we are performing studies in LRP5-deficient mice to better understand innate inflammatory reaction in dyslipaemic conditions.

Since LRP5 seems to play a role in promoting the formation of macrophage-derived foam cells, our results indicate a previously unidentified mechanism by which intimal aggregated LDL are internalized in human macrophages and contribute to the advancement of atherosclerosis. We also show that LRP5-deficient cells have a reduced migratory capacity, supporting a role for LRP5 in the accumulation of macrophage-derived foam cells in the arterial wall.

Supplementary material

Supplementary material is available at *European Heart Journal* online.

Acknowledgements

We thank Laura Nasarre, Ester Peña, and Sonia Huertas for technical assistance.

Funding

This work was supported by the Spanish Ministry of Science (SAF2006-10091 to L.B.), Instituto de Salud CarlosIII (CIBEROBN-CB06/03 to L.B.), and RyC (RyC2007-01466 to M.B.-P.).

Conflict of interest: none declared.

References

1. Fuster V, Badimon L, Badimon JJ, Chesebro JH. The pathogenesis of coronary artery disease and the acute coronary syndromes (1). *N Engl J Med* 1992;**23**: 242–250.

2. Hurt-Camejo E, Olsson U, Wiklund O, Bondjers G, Camejo G. Cellular consequences of the association of apoB lipoproteins with proteoglycans. Potential contribution to atherogenesis. *Arterioscler Thromb Vasc Biol* 1997;**17**:1011–1017.
3. Frank JS, Fogelman AM. Ultrastructure of the intima in WHHL and cholesterol-fed rabbit aortas prepared by ultra-rapid freezing and freeze-etching. *J Lipid Res* 1989;**30**:967–978.
4. Williams KJ. Arterial wall chondroitin sulfate proteoglycans: diverse molecules with distinct roles in lipoprotein retention and atherogenesis. *Curr Opin Lipidol* 2001;**12**:477–487.
5. Khoo JC, Miller E, McLoughlin P, Steinberg D. Enhanced macrophage uptake of low-density-lipoprotein after self-aggregation. *Arteriosclerosis* 1988;**8**:348–358.
6. Zhang WY, Ishii I, Kruth HS. Plasmin-mediated macrophage reversal of low-density-lipoprotein aggregation. *J Biol Chem* 2000;**275**:33176–33183.
7. Kruth HS. Sequestration of aggregated low-density-lipoproteins by macrophages. *Curr Opin Lipidol* 2002;**13**:483–488.
8. Tertov VV, Orekhov AN, Sobenin IA, Gabbasov ZA, Popov EG, Yaroslavov AA, Smirnov VN. Three types of naturally occurring modified lipoproteins induce intracellular lipid accumulation due to lipoprotein aggregation. *Circ Res* 1992;**71**: 218–228.
9. Llorente-Cortés V, Martínez-González J, Badimon L. LDL-receptor-related-protein mediates uptake of aggregated LDL in HVSMC. *Arterioscler Thromb Vasc Biol* 2000;**20**:1572–1579.
10. Llorente-Cortés V, Otero-Viñas M, Sánchez S, Rodríguez C, Badimon L. Low-density-lipoprotein upregulates low-density lipoprotein-receptor-related protein expression in VSMC: possible involvement of SRBP-2-dependent mechanism. *Circulation* 2002;**106**:3104–3110.
11. Llorente-Cortés V, Otero-Viñas M, Camino-López S, Costales P, Badimon L. Cholesteryl esters of aggregated-LDL are internalized by selective uptake in HVSMC. *Arterioscler Thromb Vasc Biol* 2006;**26**:117–123.
12. Hiltunen TP, Luoma JS, Nikkari T, Ylä-Herttuala S. Expression of LDL-receptor, VLDL-receptor, LDL-receptor-related protein, and scavenger receptor in rabbit atherosclerotic lesions: marked induction of scavenger receptor and VLDL-receptor expression during lesion development. *Circulation* 1998;**97**: 1079–1086.
13. Llorente-Cortés V, Otero-Viñas M, Berrozpe M, Badimon L. Intracellular lipid accumulation, low-density-lipoprotein-receptor-related protein expression, and cell survival in VSMC derived from normal and atherosclerotic human coronaries. *Eur J Clin Invest* 2004;**34**:182–190.
14. Llorente-Cortés V, Royo T, Otero-Viñas M, Berrozpe M, Badimon L. Sterol regulatory element binding proteins downregulate LRP1 expression and LRP1-mediated aggregated LDL uptake by human macrophages. *Cardiovasc Res* 2007;**74**:526–536.
15. Mao J, Wang J, Liu B, Pan W, Farr G, Flynn C, Yuan H, Takada S, Kimelman D, Li L, Wu D. LRP5 binds to axin and regulates the canonical Wnt signaling pathway. *Mol Cell* 2001;**7**:801–809.
16. Johnson ML. The high bone mass family—the role of Wnt/Lrp5 signaling in the regulation of bone mass. *J Musculoskelet Neuronal Interact* 2004;**4**:135–138.
17. Howe LR, Subbaramaia K, Chung WJ, Dannenberg AJ, Brown AM. Transcriptional activation of cyclooxygenase-2 in Wnt-1-transformed mouse mammary epithelial cells. *Cancer Res* 1999;**59**:1572–1577.
18. Mann B, Gelos M, Siedow A, Hanski ML, Gratchev A, Ilyas M, Bodmer WF, Moyer MP, Riecken EO, Buhr HJ, Hanski C. Target genes of beta-catenin-T cell-factor/lymphoid-enhancer-factor signaling in human colorectal carcinomas. *Proc Natl Acad Sci USA* 1999;**96**:1603–1608.
19. Van Der Heyden MA, Rook MB, Hermans MM, Rijksen G, Boonstra J, Defize LH, Destree OH. Identification of connexin 43 as a functional target for Wnt signalling. *J Cell Sci* 1998;**111**:1741–1749.
20. Shtutman M, Zhurinsky J, Simcha I, Albanese C, D'Amico M, Pestell R, Ben-Ze'ev A. The cyclinD1 gene is a target of the beta-catenin/LEF-1 pathway. *Proc Natl Acad Sci USA* 1999;**96**:5522–5527.
21. Müller T, Bain G, Wang X, Papkoff J. Regulation of epithelial cell migration and tumor formation by beta-catenin signaling. *Exp Cell Res* 2002;**280**:119–133.
22. Dell'Accio F, De Bari C, El Tawil NM, Barone F, Mitsiadis TA, O'Dowd J, Pitzalis C. Activation of WNT and BMP signaling in adult human articular cartilage following mechanical injury. *Arthritis Res Ther* 2006;**8**:139.
23. Sakr SW, Eddy RJ, Barth H, Wang F, Greenberg S, Maxfield FR, Tabas I. The uptake and degradation of matrix-bound lipoproteins by macrophages require an intact actin Cytoskeleton, Rho family GTPases, and myosin ATPase activity. *J Biol Chem* 2001;**276**:37649–37658.
24. Morita SY, Kawabe M, Sakurai A, Okuhira K, Vertut-Doï A, Nakano M, Handa T. Ceramide in lipid particles enhances heparan-sulfate proteoglycan and low-density-lipoprotein-receptor-related protein-mediated uptake by macrophages. *J Biol Chem* 2004;**279**:24355–24361.
25. Silverstein RL. Inflammation, atherosclerosis, and arterial thrombosis: role of the scavenger receptor CD36. *Cleve Clin J Med* 2009;**76**:S27–S30.
26. Qiu W, Hu Y, Andersen TE, Jafari A, Li N, Chen W, Kassem M. Tumor necrosis factor receptor superfamily member 19 (TNFRSF19) regulates differentiation fate of human mesenchymal (stromal) stem cells through canonical WNT signaling and C/EBP. *J Biol Chem* 2010;**285**:14438–14449.
27. Haÿ E, Nouraud A, Marie PJ. N-cadherin negatively regulates osteoblast proliferation and survival by antagonizing Wnt, ERK and PI3K/Akt signalling. *PLoS One* 2009;**4**:e8284.
28. Yuzugullu H, Benhaj K, Ozturk N, Senturk S, Celik E, Toylu A, Tasdemir N, Yilmaz M, Erdal E, Akcali KC, Atabey N, Ozturk M. Canonical Wnt signaling is antagonized by noncanonical Wnt5a in hepatocellular carcinoma cells. *Mol Cancer* 2009;**8**:90.
29. Dhore CR, Cleutjens JP, Lutgens E, Cleutjens KB, Geusens PP, Kitslaar PJ, Tordoir JH, Spronk HM, Vermeer C, Daemen MJ. Differential expression of bone matrix regulatory proteins in human atherosclerotic plaques. *Arterioscler Thromb Vasc Biol* 2001;**21**:1998–2003.
30. Lund SA, Giachelli CM, Scatena M. The role of osteopontin in inflammatory processes. *J Cell Commun Signal* 2009;**3**:311–322.
31. Boström K, Watson KE, Horn S, Wortham C, Herman IM, Demer LL. Bone morphogenetic protein expression in human atherosclerotic lesions. *J Clin Invest* 1993; **91**:1800–1809.
32. de Kleijn DP, Moll FL, Hellings WE, Ozsarlak-Sozer G, de Bruin P, Doevendans PA, Vink A, Catanzariti LM, Schoneveld AH, Algra A, Daemen MJ, Biessen EA, de Jager W, Zhang H, de Vries JP, Falk E, Lim SK, van der Spek PJ, Sze SK, Pasterkamp G. Local atherosclerotic plaques are a source of prognostic biomarkers for adverse cardiovascular events. *Arterioscler Thromb Vasc Biol* 2010; **30**:612–9.
33. Jiao X, Katiyar S, Willmarth NE, Liu M, Ma X, Flomenberg N, Lisanti MP, Pestell RG. c-Jun induces mammary epithelial cellular invasion and breast cancer stem cell expansion. *J Biol Chem* 2010;**285**:8218–8226.
34. Zhong Z, Yeow WS, Zou C, Wassell R, Wang C, Pestell RG, Quong JN, Quong AA. CyclinD1/cyclin-dependent kinase-4 interacts with filamin-A and affects the migration and invasion potential of breast cancer cells. *Cancer Res* 2010;**70**:2105–2114.
35. Webb NR, Moore KJ. Macrophage-derived foam cells in atherosclerosis: lessons from murine models and implications for therapy. *Curr Drug Targets* 2007;**8**: 1249–1263.
36. Choudhury RP, Lee JM, Greaves DR. Mechanisms of disease: macrophage-derived foam cells emerging as therapeutic targets in atherosclerosis. *Nat Clin Pract Cardiovasc Med* 2005;**2**:309–315.
37. Fujino T, Asaba H, Kang MJ, Ikeda Y, Sone H, Takada S, Kim DH, Kamataki A, Magoori K, Miyamoto Y, Oishi H, Nose M, Okazaki M, Usui S, Imaizumi K, Yanagisawa M, Sakai J, Yamamoto TT. LRP5 is essential for normal cholesterol metabolism and glucose-induced secretion. *Proc Natl Acad Sci USA* 2003;**100**: 229–234.
38. Magoori K, Kang MJ, Ito MR, Kakuuchi H, Ioka RX, Kim DH, Asaba H, Iwasaki S, Takei YA, Takahashi S, Ono M, Nose M, Sakai J, Fujino T, Yamamoto TT. Severe hypercholesterolemia, impaired fat tolerance, and advanced atherosclerosis in mice lacking both LRP5 and apolipoprotein E. *J Biol Chem* 2003;**278**: 11331–11336.

SUPPLEMENTARY FIGURE

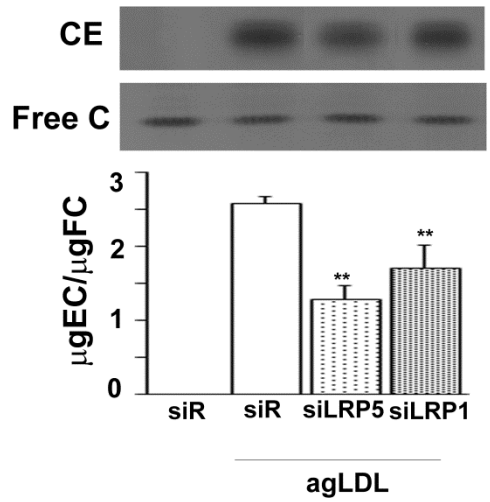

Sup. Fig: LRP5 and lipid uptake in HMDM. HMDM containing siRNA-R, siRNA-LRP1 or siRNA-LRP5 were incubated with an excess of agLDL (400µg/ml) for 8h. HMDM were exhaustively washed and harvested to measure Free C and EC by thin layer chromatography. Experiments were run in triplicate. Bar graph showing the quantification of EC respect to Free C in µg. **p<0.01

SUPPLEMENTARY DATA

DETAILED METHODS

Tissue Immunohistochemistry and Immunofluorescence

Human coronary arteries were obtained from explanted hearts immediately after surgical excision. All procedures were approved by the Institutional Review and Ethics Committee. Paraffin-embedded specimens were cut into 5-µm-thick serial sections, placed on poly-L-lysine-coated slides and deparaffinised. Lesions were characterized in Masson's trichrome-stained sections according to American Heart Association criteria.[1] Masson trichromic staining allowed classification of lesions into initial lesions, types I and II, n=6, and advanced lesions, types VII-VIII, n=6.

Consecutive sections were deparaffinised, after target retrieval, and the sections were washed, suppressing endogenous peroxidase activity with H_2O_2, hydrated and blocked. The following primary antibodies were detected using the avidin-biotin immunoperoxidase technique: monoclonal mouse anti-human smooth muscle actin (α-SMC, clone 1A4; Dako); monoclonal

mouse anti-human macrophage, HAM56 (HAM56; Dako); and polyclonal rabbit anti-human LRP5 (Abcam 38311), for 2 h (dilution 1:100) at room temperature. After several washes, the sections were incubated with an appropriate biotinylated secondary antibody (1:200, Vector®). 3, 3'-diaminobenzidine was used as a chromogen and haematoxylin was used for nuclear staining. The sections were washed in PBS 100 mM, pH 7.4 and mounted in Glicergel® mounting medium (DAKO A/S). Images were captured by Nicon Eclipse 80i microscope and digitized by Retiga 1330i Fast camera. Controls with the appropriate secondary antibody only were run with each set of specimens. 3 sections/ plaque were analyzed for each antibody and individual. For double-labelling immunofluorescence experiments, OCT included human coronary arteries were cut into5-µm-thick sections and stained with monoclonal mouse anti-human macrophage, HAM56 (HAM56; Dako); and polyclonal rabbit anti-human LRP5 (Abcam 38311) (1:50), followed by Alexa Fluor anti-mouse 633, Alexa Fluor anti rabbit 488 (1:100) and Hoechst (1:1000). Images of immunostained tissues were recorded on a Leica inverted fluorescence confocal microscope (Leica TCS SP2-AOBS, Germany). Tissues were viewed with HCX PL APO 63x/1.2W Corr/0.17 CS objective. Fluorescent images were acquired in a scan format of 1024x1024 pixels in a spatial data set (xyz) and were processed with the Leica Standard Software TCS-AOBS. Controls without primary antibodies showed no fluorescence labeling.

50 images of immunostained tissues with HAM56 or LRP5 from initial and advanced atherosclerotic lesions were analyzed by counting HAM56 and LRP5-stained macrophages respectively. The amount of LRP5 positive macrophages was calculated as the ratio of LRP5 expressing macrophages to HAM56 expressing macrophages.

Isolation of human monocytes (HM) and human monocyte-derived macrophages (HMDM) primary cultures.

This protocol has been previously described.[2] Briefly, human monocytes (HM) were obtained by standard protocols from buffy coats (40-45ml) from healthy donors. Cells were applied on 15 ml of Ficoll-Hypaque and centrifuged at 300 g for 1hour at 22°C, with no brake. Mononuclear cells were obtained from the central white band of the gradient, exhaustively washed in Dulbecco's phosphate buffer saline, and resuspended in RPMI medium (Gibco) supplemented with 10% human serum AB (Immunogenetics). A set of cells was left overnight in culture,

washed and treated with nLDL or agLDL for the described times and concentrations. A second set of cells was left 7 days in culture and allowed to differentiate into macrophages. HMDM were then incubated with nLDL or agLDL for the described times and concentrations. At the end of the experiments, HM and HMDM were exhaustively washed and collected for both mRNA and protein detection.

HVSMC culture

Primary cultures of human coronary vascular smooth muscle cells (HVSMC) were prepared from nonatherosclerotic areas of human coronaries from explanted hearts at transplant operations at the Hospital de la Santa Creu i Sant Pau. HVSMC were obtained by a modification of the explants technique previously described.[3] Outgrown cells were suspended in a trypsin/EDTA solution and subcultured in 199 medium containing 20% FBS plus 2% human serum, and incubated with nLDL or agLDL for the described times and concentrations. All procedures were approved by the Hospital Ethics Committee. Three independent experiments were carried out per condition.

HuVEC culture

Human umbilical vein endothelial cells (HuVEC) were purchased from ATCC and cultured in M199 medium supplemented with 20% FBS, 2mM Glutamine, 1%Hepes, 1% Pyruvate, 1%Heparine, 1% endothelial cell growth supplement (ECGS), and antibiotics. Plates were coated with gelatin 30 minutes prior to seeding the cells. For experiments, HuVEC at passages 1–5 were used.

LDL isolation and modification

Human LDLs (d1.019–d1.063 g/ml) were obtained as previously described.[2] Briefly human LDL were obtained from pooled sera of normocholesterolemic volunteers, isolated by sequential ultracentrifugation, and dialyzed. LDL protein concentration was determined by the bicinchoninic acid method, and cholesterol concentration was determined using a commercial kit (Boehringer). The purity of LDL was assessed by agarose gel electrophoresis. The model system of agLDL was generated by vortexing LDL (1 mg/ml) for 4 min at room temperature at maximal speed. agLDL was then centrifuged at 10,000 g for 10 min, and the precipitated fraction composed of 100% agLDL was added to cell cultures.[3,4]

LDL treatment

After LDL (native or aggregated) incubation, cells were exhaustively washed (twice with PBS, twice with PBS/1% BSA, twice with PBS/1%BSA/heparin 100 U/ml, twice with PBS/1% BSA, and twice with PBS) before collection for mRNA or protein detection.

RNA isolation and Real time PCR

Total RNA was isolated from cultured HM, HMDM, HVSMC or HuVEC using the Total RNA extraction kit (Qiagen). Total RNA concentration was determined on NanoDrop ND-1000 spectrophotometer (NanoDrop Technologies, Inc., Wilmington, DE, USA) and purity was checked by the A260/A280 ratio (ratios between 1.8 and 2.1 were considered acceptable), in addition, an agarose gel was run to assess the quality. cDNA was synthesized from 1 μg RNA with cDNA Reverse transcription kit (Qiagen) The resulting cDNA samples were amplified by polymerase chain reaction (PCR) using a DNA thermal cycler (MJ Research, Watertown, MA, USA) and the following specific human probes from Applied Biotechnologies: LRP5 (Hs00182031-m1), LRP1 (Hs00233899-m1), 18S rRNA (4319413E), Bax (Hs00180269-m1), Bcl2 (Hs00241824-m1), β-catenin (Hs00170025-m1), LEF1 (Hs01547250-m1), cyclinD1 (Hs00277039-m1), c-jun (Hs99999141-s1), CD36 (Hs00169627-m1), OPN (Hs00960942-m1) and BMP2 (Hs00154192)

LRP1 blocking antibody

Monoclonal antibody against the α-chain of LRP1 (Servicios Hospitalarios) and normal mouse IgG (sc-2025, Santa Cruz) were used at 25μg/ml for 8h in HMDM.

Obtaining LRP5-, LRP1- -deficient HMDM and inhibition of Scavenger Receptor

To inhibit LRP1 or LRP5 expression in HMDM small anti-LRP1 interfering RNA (siRNA-LRP1) or siRNA-LRP5 synthesized by Ambion were used to transfect HMDM. Briefly, HMDM obtained from buffy coats were transfected with the HiPerfect Transfection Reagent (QiAGEN) following manufacturers instructions. 24h later, HMDM underwent the specified treatments for 8h or 24h were washed and collected. Silencer Selective negative control#2 siRNA (Ambion) was used as a control and did not exert any effect on LRP1 or LRP5 expression. To inhibit scavenger receptor expression polyinosinic acid (5') (Sigma) was used at an inhibitory concentration of 100μg/ml[4].

Determination of free and esterified cholesterol content

siRNA-LRP1, siRNA-LRP5, siRNA-Random (50nM) and polyinosinic acid (100µg/ml) treated HMDM were incubated for 8h with 100 or 400 µg/ml agLDL. Cells were exhaustively washed, twice with PBS, twice with PBS/1% BSA, and twice with PBS/1%BSA/heparin 100 U/ml before harvesting into 1ml of 0.1N NaOH. Lipid extraction and thin layer chromatography were performed as previously described.[5,6] The spots corresponding to free cholesterol (Free C) and cholesteryl esters (CE) were quantified by densitometry against a standard curve of cholesterol and cholesterol palmitate respectively, with the use of a computing densitometer (Molecular Dynamics).

Western blot and flow cytometry

Sample extracts (50µg protein) were resolved by SDS-PAGE and transferred to nitrocellulose membranes, blocked with 5% skim milk and probed for monoclonal (LRP5 and βactin from Abcam, CD36 from Biocytex, LEF1 and BMP2 from Sigma, cyclin D1 from Millipore, LRP1 from Servicios Hospitalarios) or polyclonal (β-catenin and OPN from Millipore, c-jun from R+D Systems) primary antibodies. Membranes were then washed and blotted with anti-mouse or anti-rabbit secondary antibodies (Dako). Band densities were determined with the ChemiDoc XRS system (Bio-Rad) in chemiluminescence detection modus and Quantity-One software (Bio-Rad). Normalization was performed against β-actin.

LRP5 expression was also assessed by staining HM and HMDM primary cultures with LRP5 monoclonal antibody (1:50) followed by Alexa Fluor anti-mouse 488 (1:100) and analysis by flow cytometry (FACSCalibur). Controls were run without primary antibodies.

Immunofluorescence and DiI labellingin cells

HM and HMDM incubated or not with agLDL were fixed with 4% paraformaldehyde and permeabilized with 0.5% Tween in PBS at room temperature. After incubation in blocking buffer (3% bovine serum albumin in PBS) primary LRP5 (Biovision) and CD68 (Abcam) antibodies were added 1h at room temperature in a moist chamber. Appropriate secondary antibodies (Alexa Fluor anti-mouse 488 IgG (H+L), Alexa Fluor anti-rabbit 633 IgG (H+L), and Hoechst 33342) were added for 1h and stained cells were washed and covered with Prolong Gold antifade reagent (Molecular Probes). Images of immunostained cells were recorded on a

Leica inverted fluorescence confocal microscope (Leica TCS SP2-AOBS, Germany). Cells were viewed with HCX PL APO 63x/1.2W Corr/0.17 CS objective. Fluorescent images were acquired in a scan format of 1024x1024 pixels in a spatial data set (xyz) and were processed with the Leica Standard Software TCS-AOBS. Controls without primary antibodies showed no fluorescence labeling.

For DiI labeling, cells were fixed, blocked, incubated with 5 µl/ml medium of DiI (30 mg/mL in DMSO, SIGMA) for 1h, washed and covered with Prolong Gold antifade reagent.

Wound migration assay

Transfected HMDM containing siRNA-LRP5, siRNA-LRP1 or siRNA-Random were scratched with a soft sterile 200µl pipette tip to create a double sided wound. After being rinsed with PBS, cells were incubated with or without agLDL and allowed to migrate in serum-free medium. Pictures were taken directly after scratching and 24h later. The area of cell-free wound was photographed with an inverted microscope (Nikon, Tokyo, Japan) equipped with a digital camera (Spot, Diagnostic Instruments, Inc., Sterling Heights, MI) at indicated time points. The macrophage motility was calculated as the ratio of cell-free area at 24h (with or without agLDL) to initial wound length. The experiments were performed four times.

In vitro Boyden chamber migration assay

Transfected HMDM containing siRNA-LRP5, siRNA-LRP1 or siRNA-Random were plated into modified Boyden chamber assay using 24-transwell unit (Corning Costar Corporation). This system consists of a lower and an upper chamber containing a polycarbonate filter with 8µm pores. HMDM cells were trypsinized and, to eliminate the effects of serum, rinsed three times in PBS and added to the top chamber for 24h in serum-free medium. The medium in the lower well also contained serum-free medium in order to discard possible interferences from other than the lack of LDL receptors. After incubation for 24h at 37ºC, the top side of the insert membrane was scrubbed free of cells with a cotton swab, and the bottom side was stained with Giemsa. Cells that migrated to the bottom side of the membrane were counted at 20X magnification light microscopy. Three experiments were performed in triplicates.

Statistical analysis

Results are expressed as mean ± S.E.M. A Stat View statistical package was used for all the analysis. Comparisons among groups were performed by Fisher test after ANOVA. Statistical significance was considered when $p<0.05$.

SUPPLEMENTAL REFERENCES

1.Stary, H.C.Composition and classification of human atherosclerotic lesions.*Virchows.Arch. A. Pathol. Anat. Histopathol*.1992;**421**:277–290

2.Llorente-Cortés V,Royo T,Juan-Babot O,Badimon L.Adipocyte differentiation-related protein is induced by LRP1-mediated aggregated LDL internalization in human vascular smooth muscle cells and macrophages.*J Lipid Res*.2007;**48**:2133-40.

3.Llorente-Cortés, V,Otero-Viñas M,Badimon L.Differential role of heparan sulfate proteoglycans on aggregated LDL uptake in human vascular smooth muscle cells and mouse embryonic fibroblasts.*Arterioscler Thromb Vasc Biol*.2002;**22**:1905-11.

4.Llorente-Cortés V,Martínez-González J,Badimon L.LDL receptor-related protein mediates uptake of aggregated LDL in human vascular smooth muscle cells.*Arterioscler Thromb Vasc Biol.*2000;**20**:1572-9

5.Llorente-Cortés V,Martínez-González J,Badimon L.Esterified cholesterol accumulation induced by aggregated LDL uptake in human vascular smooth muscle cells is reduced by HMG-CoA reductase inhibitors.*Arterioscler Thromb Vasc Biol.*1998;**18**:738-46.

6.Asmis R,Llorente VC,Gey KF.Prevention of cholesteryl ester accumulation in P388D1 macrophage-like cells by increased cellular vitamin E depends on species of extracellular cholesterol. Conventional heterologous non-human cell cultures are poor models of human atherosclerotic foam cell formation.*Eur J Biochem.*1995;**233**:171-8.

ARTÍCULO 2

LRP5 negatively regulates differentiation of monocytes through abrogation of Wnt signalling.

Autores: María Borrell-Pagés, July Carolina Romero, Lina Badimon.

Revista: Journal of Cellular and Molecular Medicine 2014; 18(2): 314-25.

Factor de impacto: 4.75

Centro de Investigación Cardiovascular CSIC-ICCC, Hospital de la Santa Creu i Sant Pau, Barcelona, España.

RESUMEN

LRP5 regula negativamente la diferenciación de monocitos mediante el bloqueo de la señalización por Wnt.

Las células inflamatorias circulantes se infiltran y diferencian en tejidos diana específicos para combatir infecciones y/o daño tisular y restablecer la homeostasis celular. Estudiamos los mecanismos de diferenciación de células HL60 y de cultivos primarios de monocitos humanos y postulamos que LRP5 y la vía canónica de señalización por Wnt participan en el proceso de diferenciación de células monocíticas.

El silenciamiento de LRP5 incrementa la diferenciación de las células HL60 y de los monocitos humanos a macrófagos, sugiriendo que LRP5 bloquea la diferenciación. Demostramos que los mecanismos implicados incluyen el secuestro de β-CATENINA en la membrana celular, la inhibición de la vía canónica de señalización por Wnt y un incremento en la apoptosis celular. Además, confirmamos la participación de LRP5 y la vía canónica de señalización por Wnt en el proceso ya que la diferenciación celular puede ser rescatada por la adición de proteínas diana de la vía canónica en las células monocíticas.

Nuestro trabajo describe por primera vez un mecanismo por el cual LRP5 bloquea la activación de la vía de señalización por Wnt para mantener las células en un estado indiferenciado.

J. Cell. Mol. Med. Vol 18, No 2, 2014 pp. 314-325

LRP5 negatively regulates differentiation of monocytes through abrogation of Wnt signalling

Maria Borrell-Pagès [a], July Carolina Romero [a], Lina Badimon [a, b, c, *]

[a] *Cardiovascular Research Center, CSIC-ICCC, Hospital de la Santa Creu i Sant Pau, IIB-Sant Pau, Barcelona, Spain*
[b] *CIBERobn, Fisiopatología de la Obesidad y Nutrición, Instituto de Salud Carlos III, Barcelona, Spain*
[c] *Cardiovascular Research Chair, UAB, Barcelona, Spain*

Received: July 1, 2013; Accepted: October 17, 2013

Abstract

Molecular changes involved in cell differentiation are only partially known. Circulating inflammatory cells need to differentiate to perform specialized functions in target tissues. Here, we hypothesized that low-density lipoprotein receptor–related protein 5 (LRP5) is involved, through its participation in the canonical Wnt/β-catenin signalling, in the differentiation process of monocytic cells. To this aim, we characterized differentiation mechanisms of HL60 cells and primary human monocytes. We show that silencing the LRP5 gene increased differentiation of HL60 cells and human monocytes, suggesting that LRP5 signalling abrogates differentiation. We demonstrate that the mechanisms behind this blockade include sequestration of β-catenin at the cellular membrane, inhibition of the Wnt signalling and increase of apoptosis. We further demonstrate the involvement of LRP5 and the Wnt/β-catenin signalling in the process because cellular differentiation can be rescued by the addition of downstream Wnt target genes to the monocytic cells.

Keywords: LRP5 • apoptosis • cellular differentiation • macrophages • HL60

Introduction

Low-density lipoprotein receptor–related protein 5 (LRP5) belongs to the LDL receptor family and has been recognized as a multifunctional cell surface receptor [1]. From a mechanistic standpoint, LRP5 functions as a co-receptor with the protein frizzled to bind extracellular Wnt proteins resulting in the stabilization of intracellular β-catenin. The stabilized β-catenin is free to translocate to the nucleus and bind to lymphoid enhancer binding factor/T cell factor (LEF1/TCF) to regulate the transcription of Wnt-responsive genes. We have recently demonstrated that extracellular lipid binding to LRP5 in human macrophages can trigger the Wnt signalling cascade and induce macrophage motility [2]. The canonical Wnt/β-catenin signalling pathway regulates multiple biological events, including proliferation and development [3, 4].

*Correspondence to: Prof. Lina BADIMON,
Cardiovascular Research Center, C/Sant Antoni Maria Claret 167,
Barcelona 08025, Spain.
Tel.: 34935565880
Fax: 34935565559
E-mail: lbadimon@csic-iccc.org

Deregulation of Wnt signalling causes alterations in inflammatory mechanisms that will ultimately lead to several types of diseases, including cancer or Alzheimer disease [5]. Inflammation is a complex biological response of organs and tissues to harmful stimuli [6]. It is mainly orchestrated by monocytes and macrophages that respond to extracellular signals and induce inflammatory reactions by causing the release of cytokines and other inflammation mediators [7]. Although the role of Wnt signalling in the inflammatory response is poorly understood, β-catenin-dependent Wnt signalling is suggested to increase the inflammatory response to LPS in human macrophages [8]. Also, the proliferative effects of the Wnt/β-catenin pathway appear to enhance wound repair/healing responses. Indeed, during the wound healing process after myocardial infarction in adult male SD rats, the activated Wnt-frizzled-Dishevelled signalling pathway seems to contribute to the myofibroblast proliferation and migration [9]. Although the relevance of the Wnt signalling pathway in inflammatory processes is under constant study, the independent contribution of some of its components, specifically of LRP5, has never been addressed.

In the present paper, we have hypothesized that LRP5 negatively regulates monocytic cell differentiation. We have proven

J. Cell. Mol. Med. Vol 18, No 2, 2014

this hypothesis by investigating LRP5 function in the monocytic cell line HL60 and in primary cultures of human monocytes (HM).

Materials and methods

A complete description of the cell lines, antibodies, reagents and techniques used in this paper can be found in the Supplemental section.

Results

Differentiation is increased in LRP5-silenced PMA-treated HL60 cells

HL60 cells treated with 10 nM phorbol 12-myristate 13-acetate (PMA) differentiate to macrophages, as described previously [10, 11]. Immunofluorescence analysis of differentiated macrophages (measured as cd68 staining) showed expression of LRP5 (Fig. 1A). To understand the role of LRP5 in cell differentiation, we silenced its expression in undifferentiated inflammatory cells. HL60 cells were transfected with either control siRNA-Random (siR) or a siRNA against LRP5 (siRNA-LRP5), then were treated with PMA to differentiate them to macrophages (Fig. 1B, upper panels).Higher rates of cell differentiation were observed in LRP5-silenced HL60 cells (92.5 $\pm$ 3%, Fig. 1C). Undifferentiated HL60 cells were transduced with a plasmid containing LRP5 ($LRP5^{OE}$) or the vector alone (C) and treated as above. Opposed to siRNA-LRP5 results, $LRP5^{OE}$-HL60 cells showed lower differentiation rate, as only 22.3 $\pm$ 1% of cells were differentiated (Fig. 1B, lower panels and Fig. 1C). In these experiments, adhered and non-adhered cells were collected and viable cells were counted (Fig. S1A). Up-regulation of LRP5 reduced differentiation in a 37.5 $\pm$ 1% of cells, while silencing of LRP5 increased differentiation in a 30.3 $\pm$ 1% of cells (Fig. 1C), supporting a negative effect of LRP5 in cell differentiation. LRP5 mRNA analysis confirmed the overexpression or silencing of LRP5 in these cells (Fig. S1B).

To confirm the effects of LRP5 in cell differentiation, we analysed the expression levels of two well-established differentiation and adhesion markers, CD11b and CD44. CD11b and CD44 were down-regulated in LRP5-overexpressing cells (45 $\pm$ 3% and 38 $\pm$ 1% respectively, Fig. 1D) and CD44 was up-regulated in LRP5-silenced cells (63 $\pm$ 1%, Fig. 1D). Taken together, these results indicate that LRP5 blocks differentiation.

LRP5 overexpression inhibits cell proliferation and induces apoptosis

We then searched for the mechanisms by which LRP5 overexpression in undifferentiated HL60 cells inhibited cell differentiation. Wnt signalling has been widely described as an inducer of cell proliferation in several cell lines, including epithelial, stromal and endothelial cells [12]. HL60 proliferation, tested by measuring DNA replication by incorporation of the thymidine analogue BrdU, was inhibited by 44.5 $\pm$ 1% in LRP5-overexpressing HL60 cells (Fig. 2A, $P < 0.005$). Interestingly, LRP5 silencing did not affect cell proliferation rates. LRP5 mRNA and protein expression levels confirmed LRP5 expression levels in these cells (Fig. 2B and C).

To investigate whether the reduction in cell differentiation seen in Figure 1C and the inhibition of cell proliferation seen in Figure 2A were because of apoptotic cell death, LRP5 apoptotic features were measured by using the AnnexinV FITC/PI assay kit. Forty-eight hours after transfection, there was a threefold increase in apoptotic $LRP5^{OE}$ cells compared with control cells (cells transfected with an empty vector, Fig. 1D, $P < 0.01$). There was no significant apoptotic cell death induced in siRNA-LRP5 cells (Fig. 1D).

Apoptosis-related genes and proteins modulated by LRP5 expression levels

Apoptosis-related proteins were measured in LRP5-modified cells. We first analysed the expression levels of three pro-apoptotic genes and proteins: Bax, Dual Specific Phosphatase 6 (Dusp6) and G0/G1 switch gene 2 (G0S2). Figure 3A shows increased expression in Bax (49 $\pm$ 2%, $P < 0.005$), DUSP6 (41 $\pm$ 2%, $P < 0.005$) and G0S2 (75 $\pm$ 3%, $P < 0.005$) mRNA levels in $LRP5^{OE}$ cells respect to C cells. LRP5 silencing not only abrogated this effect but also promoted a down-regulation of these three pro-apoptotic genes (37 $\pm$ 1%, $P < 0.005$ in Bax, 26 $\pm$ 1%, $P < 0.005$ in DUSP6 and 49 $\pm$ 3%, $P < 0.005$ in G0S2 LRP5 mRNA levels). A direct effect for LRP5 silencing and overexpression was also observed at the protein expression level for Bax, DUSP6 and G0S2 (Fig. 3B).

We also determined the levels of expression of three anti-apoptotic genes and proteins, Bcl2, Cyclin-dependent kinase 1 (CDK1) and the Toll-like receptor CD180. Cells overexpressing $LRP5^{OE}$ had reduced mRNA levels of the anti-apoptotic proteins Bcl2 (19 $\pm$ 0.5%, $P < 0.005$), Cdk1 (52 $\pm$ 1%, $P < 0.005$) and CD180 (37.5 $\pm$ 2%, $P < 0.005$, Fig. 3C) *versus* controls. In these conditions, protein expression levels were also reduced for Bcl2, CDK1 and CD180 (Fig. 3D). LRP5-silenced cells showed an increased expression of Bcl2 and CD180 mRNA levels (24 $\pm$ 2%, $P < 0.01$ and 32 $\pm$ 1%, $P < 0.005$). Furthermore, CD180 protein levels were also increased in siRNA-LRP5-treated cells by 61 $\pm$ 3%, $P < 0.005$. Taken together, these results show increased expression levels of pro-apoptotic proteins and decreased expression levels of anti-apoptotic proteins in the presence of high levels of LRP5, supporting a key role for LRP5 in apoptotic processes.

LRP5 silencing does not affect proliferation in adhered cancer cells

Increased adhesion and differentiation capacity in differentiation condition was observed after LRP5 silencing of HL60 cells. Therefore, we investigated whether LRP5 overexpression could also play a role in

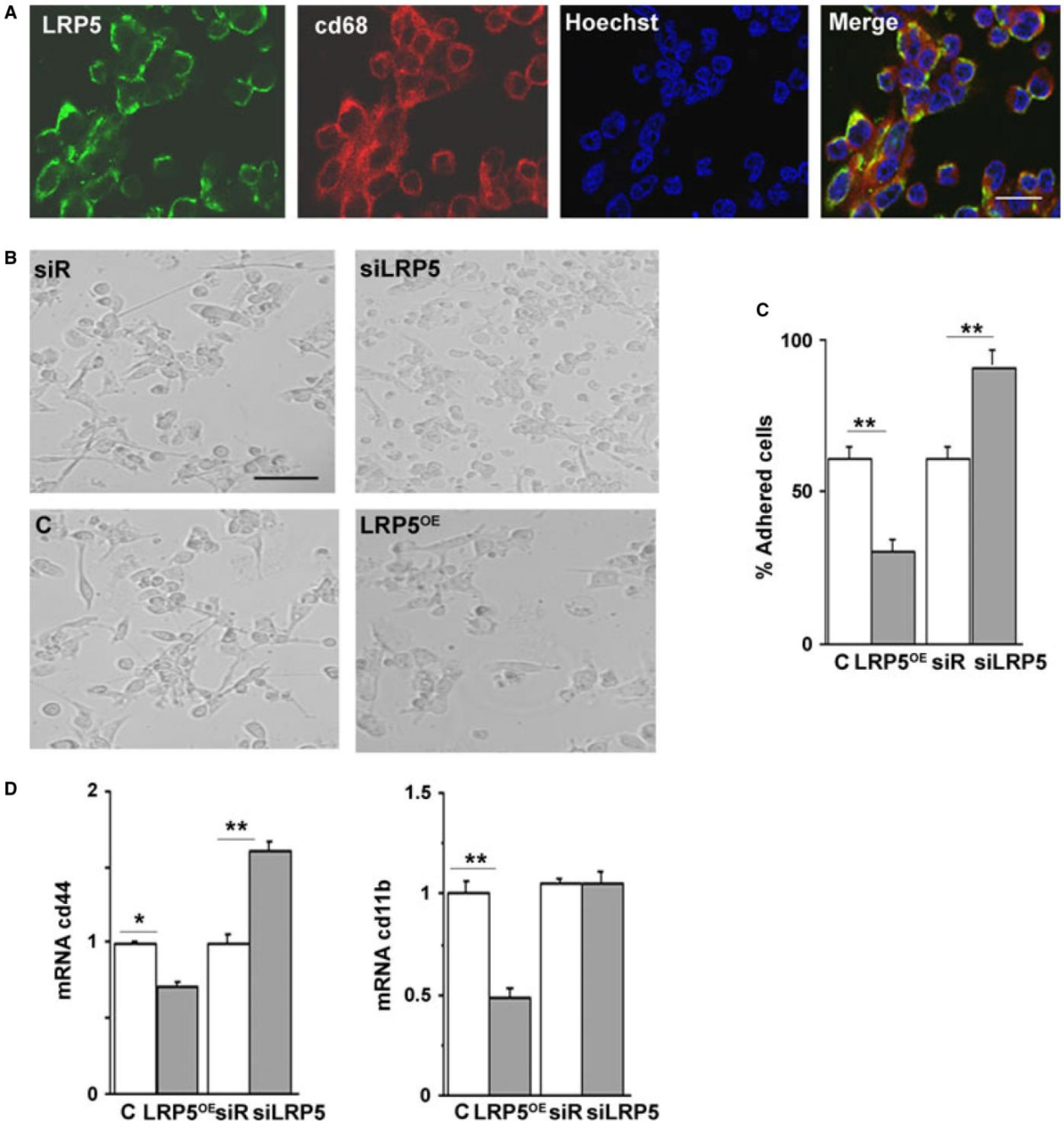

Fig. 1 Differentiation is increased in LRP5-silenced HL60 cells. (**A**) Representative image of PMA-treated HL60 cells fixed, permeabilized and immunostained with mouse anti-LRP5, rabbit anti-cd68 followed by Alexa Flour anti-mouse 488 IgG, Alexa Flour anti-rabbit 633 IgG and Hoechst. Scale bar: 20 μM. (**B**) HL60 cells transfected to either silence (siLRP5) or overexpress LRP5 ($LRP5^{OE}$) along with the controls (C, siR). 24 hrs after transfection, PMA (10 nM) was added to the supernatant for further 24 hrs when supernatants were collected and pictures were taken. Scale bar: 80 μM. (**C**) Bar graph showing the% of adhered cells in $LRP5^{OE}$ and siRNA-LRP5 HL60 cells (**D**) cd44 and cd11b mRNA levels, from RNA extracts from adhered cells in B, were quantified by real time PCR and normalized to 18srRNA, $^{**}P < 0.01$, $^{*}P < 0.05$.

preventing proliferation of adhered cancer cells. Two common cancer cells, known for their highly proliferative profiles, were studied: prostate cancer cells (PC3) and a glioblastoma cell line (U87MG) [13–15]. Neither overexpression nor silencing of LRP5 affected BrdU incorporation in either cell line (Fig. 4A). mRNA analysis was used as a control to confirm the overexpression or silencing of LRP5 (Fig. 4B).

J. Cell. Mol. Med. Vol 18, No 2, 2014

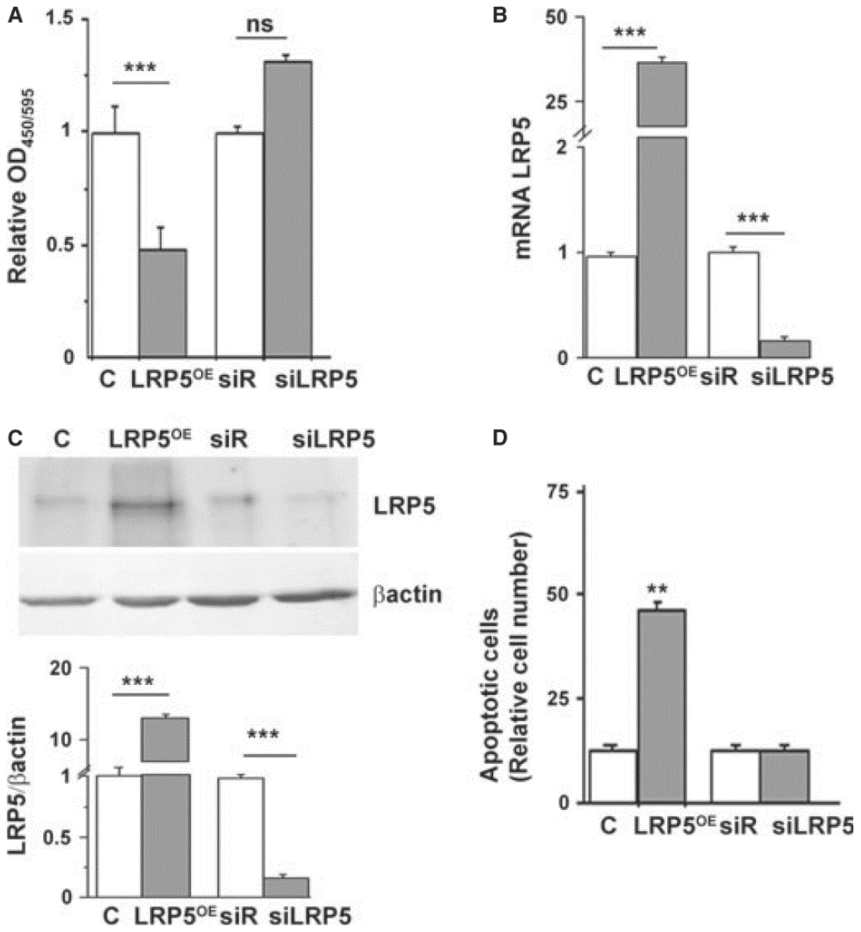

Fig. 2 LRP5 overexpression inhibits cell proliferation and induces apoptosis in HL60 cells. (**A**) HL60 cells containing C, LRP5^{OE}, siRNA-Random or siRNA-LRP5 were cultured in 96-well plates and 24 hrs after transfection BrdU was added for further 24 hrs. Results were read at 450–595 nm and the experiment was performed three times in duplicates. HL60 cells were transfected for 48 hrs to either silence (siLRP5) or overexpress LRP5 (LRP5^{OE}) along with the controls (empty vector, C and siRNA-Random, siR) and (**B**) LRP5 mRNA levels from RNA extracts were quantified by real time PCR and normalized to 18srRNA. (**C**) Representative western blots and quantitative analysis (control cells, white boxes; LRP5-treated cells, grey boxes) of HL60-transfected cells. (**D**) 48 hrs post-transfection, HL60 cells were collected, washed, stained with Annexin V and PI following manufacturer's instructions and analysed by flow cytometry, $^{**}P < 0.01$ all conditions respect to LRP5^{OE+}. Three experiments were performed in triplicates $^{***}P < 0.005$, $^{**}P < 0.01$.

LRP5 silencing increases differentiation in human primary monocytes

To determine if the effect of LRP5 silencing in cellular differentiation was restrained to a monocytic cell line (HL60 cells) or was a general mechanism for undifferentiated inflammatory cells, we used HM primary cultures. Human monocytes transfected with LRP5^{OE}, vector alone (C), siR or siRNA-LRP5 were spontaneously differentiated to macrophages (HMDM) in culture and analysed as before (Fig. 4C). Image analyses allowed the quantification of adhered HMDM (Fig. 4D) showing a significant reduction in adhesion of HMDM overexpressing LRP5 (166 ± 2% respect to C), while HM transfection of siRNA-LRP5 increased HM differentiation to HMDM (27 ± 1% with respect to siR). mRNA analysis was used as a control to confirm the overexpression or silencing of LRP5 (Fig. 4E). Taken together, these results further support an inhibitory role for LRP5 in monocyte to macrophage differentiation.

Canonical Wnt pathway activation in monocytes and macrophages

Canonical Wnt signalling pathway proteins and transcription factors, including β-catenin, LEF1, c-jun and c-myc [16–18], were investigated in LRP5-modified cells. PMA-treated HL60 cells, differentiated, adherent LRP5^{OE} cells (Fig. 1C and D) showed a significant increase in β-catenin, LEF1, c-jun and c-myc mRNA expression levels (29 ± 1%, 39 ± 2%, 19 ± 2%, and 28 ± 2%, with respect to

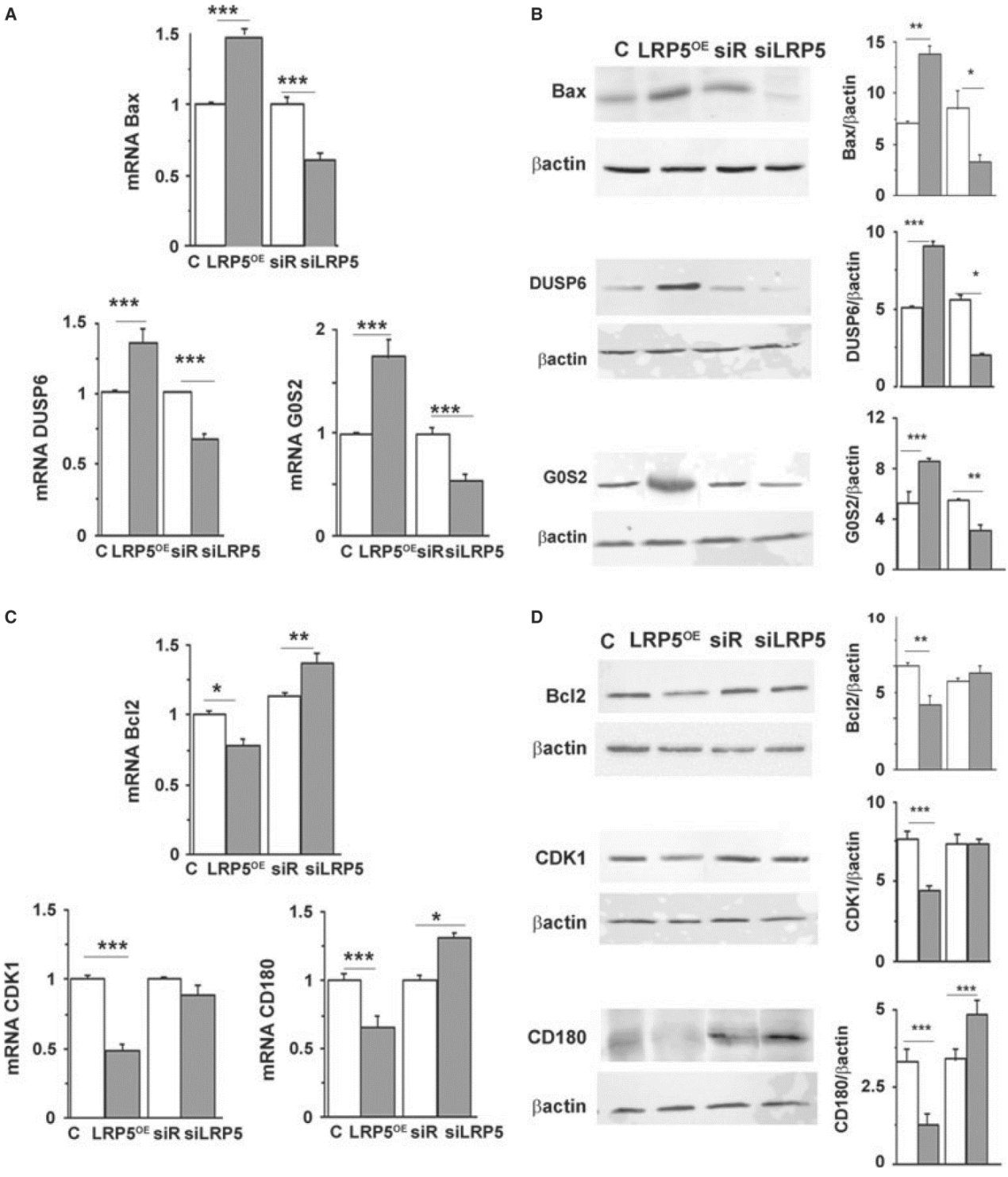

Fig. 3 Apoptosis-related genes and proteins modulated by LRP5 expression levels. siRNA-Random, siRNA-LRP5, vector (C) and LRP5^{OE} were transfected in HL60 cells for 48 hrs and (**A**), mRNA levels from RNA extracts were quantified by real time PCR and normalized to 18srRNA and (**B**) Representative western blots and quantitative analysis of pro-apoptotic proteins Bax, DUSP6 and G0S2 were measured (control cells, white boxes; LRP5-treated cells, grey boxes). (**C** and **D**) Same as in A and B for the anti-apoptotic proteins Bcl2, CDK1 and CD180, ***$P < 0.005$, **$P < 0.01$, *$P < 0.05$. Experiments were performed twice in duplicates.

J. Cell. Mol. Med. Vol 18, No 2, 2014

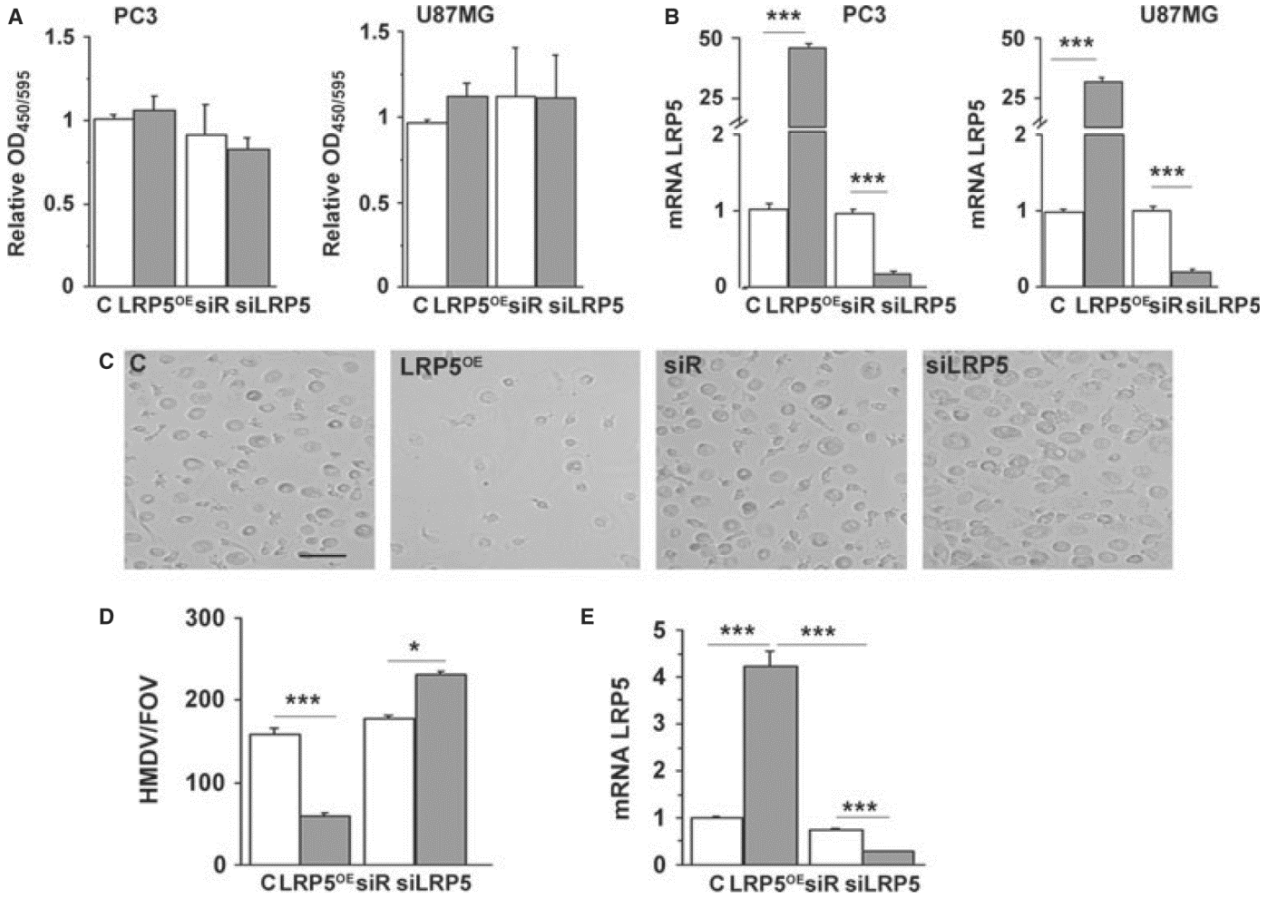

Fig. 4 LRP5^{OE} cells inhibit HM differentiation to HMDM. (**A**) PC3 and U87MG cells containing C, LRP5^{OE}, siRNA-Random or siRNA-LRP5 were cultured in 96-well plates and 24 hrs post-transfection BrdU was added for further 24 hrs. Results were read at 450–595 nm and the experiment was performed twice in triplicates. (**B**) Real time PCR quantification of LRP5 mRNA expression levels in C, LRP5^{OE}, siRNA-Random and siRNA-LRP5-transfected PC3 and U87MG cells after 48 hrs. (**C**) HM cells transfected with vector (C), LRP5 (LRP5^{OE}), siRNA-Random or siRNA-LRP5 and differentiated to HMDM when pictures were taken. Representative images of $n = 4$ experiments. Scale bar: 80 μM (**D**) Bar graph showing the analysis of number of HMDM/Field of Vision. (**E**) Real time PCR quantification of LRP5 mRNA expression levels in C, LRP5^{OE}, siRNA-Random and siRNA-LRP5-transfected HM cells after 48 hrs, $***P < 0.005$, $*P < 0.05$.

control), suggesting Wnt pathway activation (Fig. 5A). Correspondingly, LRP5-silenced cells showed a significant reduction in LEF1, c-jun and c-myc mRNA levels (33.3 ± 1%, 75 ± 1% and 48 ± 1% respectively). β-catenin gene expression levels were only slightly down-regulated. The analyses of the mRNA expression levels of β-catenin, LEF1, c-jun and c-myc in human macrophages overexpressing LRP5 revealed a 42 ± 2% increase in β-catenin, 63 ± 2% increase in LEF1, a 49 ± 1% increase in c-jun and a 32 ± 1% increase in c-myc mRNA expression levels (Fig. 5B). Again, in siRNA-LRP5 HMDM, there was a significant inhibition of LEF1, c-jun and c-myc (Fig. 5B), while β-catenin was only slightly down-regulated. Therefore, the canonical Wnt signalling pathway is activated in differentiated, PMA-treated HL60 cells and human macrophages with high LRP5 expression levels.

We then analysed the mRNA expression levels of β-catenin, LEF1, c-jun and c-myc in undifferentiated cells (HL60 and HM). β-catenin gene expression levels were increased by 49 ± 3% and 27 ± 1% in undifferentiated HL60 cells and HM respectively. However, silencing of LRP5 did not modulate β-catenin gene expression levels. Furthermore, LEF1, c-myc and c-jun were unchanged by LRP5 expression levels in undifferentiated HL60 and in HM, indicating that up-regulation or silencing of LRP5 does not affect β-catenin canonical downstream signalling (Fig. 5C and D).

Sequestering of β-catenin to the cell membrane induced by LRP5 overexpression in undifferentiated cells

We then searched for an explanation for the results observed in the undifferentiated cells (non-differentiated, non-adhered HL60 and HM). Wnt signalling can be interrupted by sequestering β-catenin at the plasma membrane [19, 20] and N-cadherin has been shown to interact with LRP5 and axin to negatively regulate

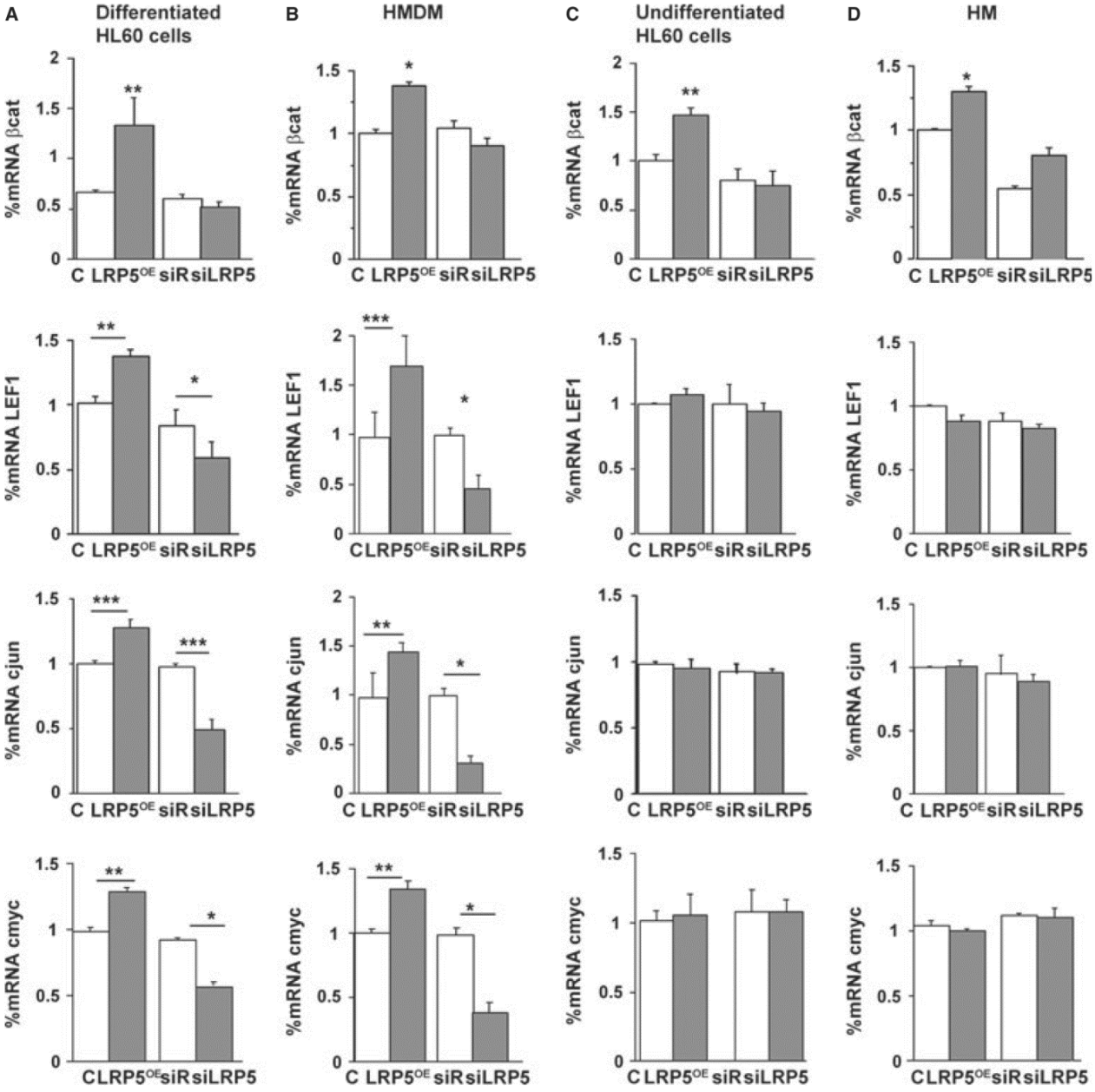

Fig. 5 Canonical Wnt pathway activation in differentiated and undifferentiated cells. Real time PCR quantification of β-catenin, LEF1, c-jun and c-myc was performed in samples from transfected differentiated HL60 (**A**), differentiated HMDM (**B**), undifferentiated HL60 (**C**) and HM (**D**) $***P < 0.005$, $**P < 0.01$, $*P < 0.05$.

Wnt signalling through β-catenin sequestration at the plasma membrane [21]. By cellular subfractionation experiments, we tested whether LRP5 overexpression was antagonizing Wnt signalling in undifferentiated cells. Consistent with the current model of the canonical Wnt signalling pathway, we found that overexpression of LRP5 in differentiated cells (PMA-differentiated HL60 cells and HMDM) increased β-catenin translocation to the nucleus with respect to control cells (Fig. 6A and B). In addition, cell membrane–associated β-catenin levels did not differ in control and LRP5-overexpressing differentiated cells (Fig. 6A and B). In contrast, LRP5 overexpression in undifferentiated cells (non-differentiated, non-adhered HL60 and HM) induced little β-catenin translocation to the nucleus, while a strong β-catenin staining could be observed in the membrane fraction of LRP5-overexpressing cells (Fig. 6C and D). These results show that the defective Wnt/β-catenin signalling induced by LRP5 overexpression in undif-

J. Cell. Mol. Med. Vol 18, No 2, 2014

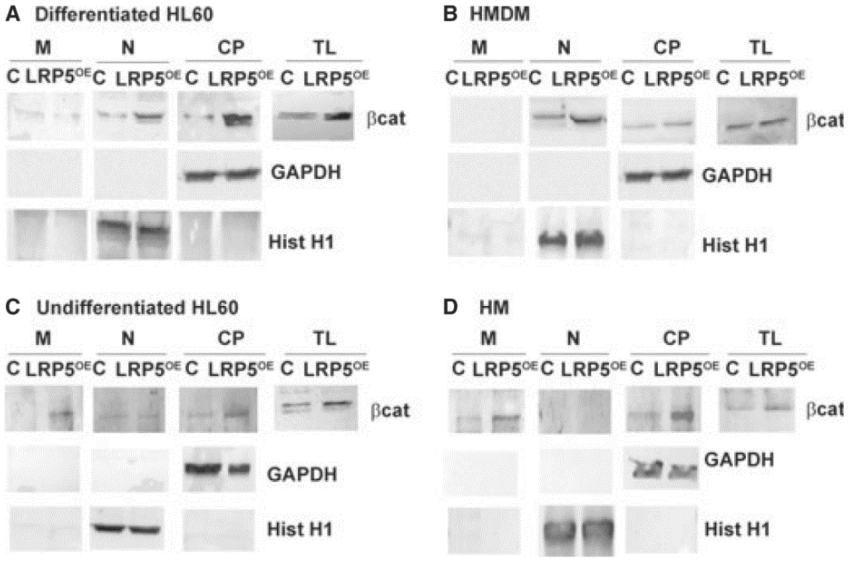

Fig. 6 β-catenin sequestering at the plasma membrane only in undifferentiated cells. PMA-differentiated HL60 cells (**A**), HMDM (**B**), undifferentiated HL60 cells (**C**) or HM (**D**) were transfected with LRP5 ($LRP5^{OE}$) or with the vector alone (C) and membrane (M), nuclear (N), cytoplasmic (CP) fractions and total lysates (TL) were analysed by Western blotting by using anti–β-catenin antibody. GAPDH and Histone H1 were used as quality controls for cytoplasmic/membrane and nuclear fractions respectively.

ferentiated cells results, in part, from β-catenin sequestering to the plasma membrane.

To further determine the role of LRP5 in β-catenin sequestration to the cell membrane, we performed cellular subfractionation experiments in cells without LRP5. Protein expression levels (Fig. S2) confirm gene expression levels (Fig. 5 upper panel), which shows that LRP5 depleted cells without further stimulus, do not modulate β-catenin expression levels in differentiated or undifferentiated cells. Therefore, in differentiated, adhered cells (differentiated HL60 and HMDM), β-catenin is mainly located in the cytoplasm (CP) and basal low levels of β-catenin are present in the nucleus (N). In undifferentiated cells (HL60 and HM), β-catenin is also mainly in the CP, while basal low levels are found at the plasma membrane (M). Contrarily, when LRP5 is overexpressed, Wnt signalling pathway is triggered.

c-myc or c-jun overexpression rescue differentiation in inflammatory cells

To further determine the involvement of LRP5 in cellular differentiation, we performed rescue experiments. We have shown that LRP5 overexpression in undifferentiated cells inhibits cellular differentiation (Fig. 1), increases cellular apoptosis (Fig. 2) and inhibits canonical Wnt pathway activation (Fig. 5) by the sequestering of β-catenin to the plasma membrane (Fig. 6). We now sought to determine if an increased expression of Wnt target genes that are downstream to β-catenin's translocation to the nucleus, and may induce a constitutive activation of the canonical Wnt signalling pathway, could rescue cellular differentiation.

Undifferentiated HL60 cells were transduced with control, $LRP5^{OE}$, $LRP5^{OE}$/c-myc or $LRP5^{OE}$/c-jun plasmids and differentiated with PMA to macrophages (Fig. 7A). Morphometric analyses show an increase in HL60 differentiation in $LRP5^{OE}$/c-myc and $LRP5^{OE}$/c-jun cotransfected cells. Differentiated (adhered, Fig. 7B upper panel) and non-differentiated (non-adhered, Fig. 7B lower panel) cells were collected and counted showing an increased adhesion in $LRP5^{OE}$/c-myc HL60 and $LRP5^{OE}$/c-jun HL60 cells (49 ± 1% and 61 ± 1% respectively). mRNA analysis was used as a control to confirm the overexpression of c-myc and c-jun in these cells (data not shown).

Similar results were observed when HM were transfected with $LRP5^{OE}$, $LRP5^{OE}$/c-myc or $LRP5^{OE}$/c-jun and differentiated to HMDM (Fig. 7C). Overexpression of $LRP5^{OE}$/c-myc or $LRP5^{OE}$/c-jun rescued HMDM differentiation by 28.5 ± 1% and 35.7 ± 0.5%, respectively, further demonstrating the negative regulation of LRP5 in cellular differentiation (Fig. 7D).

Discussion

In the present work, we have addressed the effect of LRP5 modulation and downstream activation of the Wnt signalling pathway in cell proliferation, adhesion and differentiation of monocytic cells. First, we have investigated the effect of LRP5 on cell differentiation in a monocytic cell model that requires PMA for differentiation to macrophages. The LRP5 levels of pro-myelocytic leukaemia cells (HL60) were genetically modified by silencing (siRNA-LRP5) or overexpression ($LRP5^{OE}$) experiments. siRNA-LRP5 undifferentiated HL60 cells, induced by PMA, showed increased cellular differentiation, suggesting

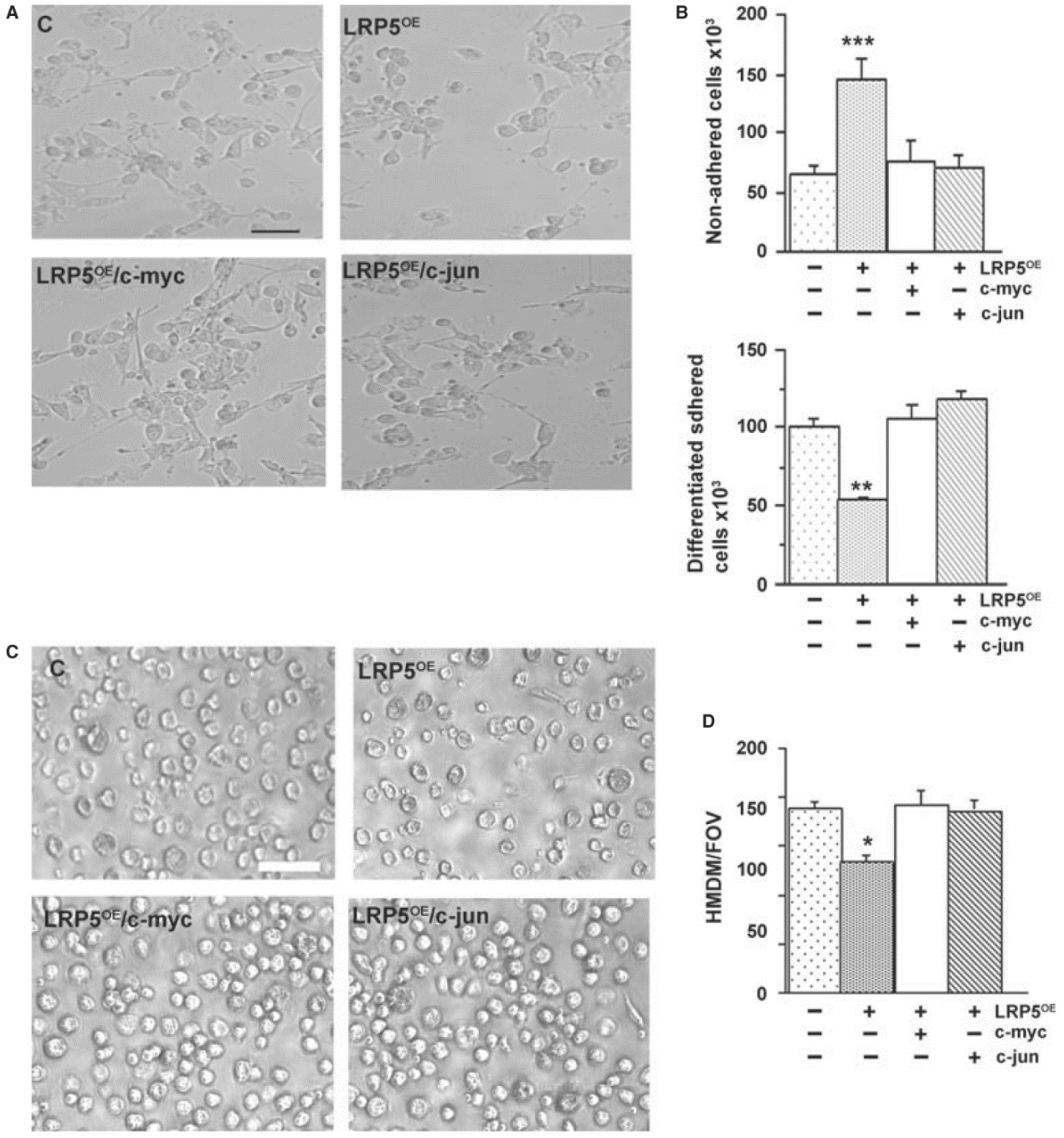

Fig. 7 Overexpression of Wnt target genes rescues cellular differentiation. (**A**) 24 hrs after transfection, HL60 cells containing C, LRP5^{OE}, LRP5^{OE}/c-myc or LRP5^{OE}/c-jun had 10 nM PMA added to the supernatant for further 24 hrs when supernatants were collected and pictures were taken. Scale bar: 80 μM. Representative images of $n = 3$ experiments (**B**) HL60 non-adhered and adhered cells were counted. Experiments were performed three times in triplicates, $***P < 0.005$, $**P < 0.01$ (**C**) HM cells transfected with C, LRP5^{OE}, LRP5^{OE}/c-myc or LRP5^{OE}/c-jun and differentiated to HMDM when pictures were taken. Representative images of $n = 4$ experiments.Scale bar: 40 μM (**D**) Bar graph showing the analysis of number of HMDM/Field of Vision $***P < 0.005$, $**P < 0.01$, $*P < 0.05$.

that LRP5 could be a negative differentiation regulator of cellular differentiation. Indeed, LRP5^{OE} HL60 cells, induced by PMA, showed less differentiation than control cells and the differentiation markers CD11b and CD44 were significantly reduced. The expression of the CD11b adhesion molecule is a maturation marker for HL60 cells in response to differentiation, as more than 90% of cells became CD11b-positive following PMA treatment [11]. On the other hand, the adhesion molecule CD44 is a cell surface transmembrane glycoprotein and its major physiological role is to maintain organ and tissue structure *via* cell–cell and cell–matrix adhesion (for a review, see Slevin *et al.* [22]). These results strongly suggest a negative role for LRP5 in HL60 PMA-induced differentiation that may be orchestrated by LRP5's direct or indirect interference with cellular adhesion molecules (Fig. S3).

Low-density lipoprotein receptor–related protein 5 is frequently characterized as a Wnt/β-catenin signalling activator that increases cell proliferation [23]. Surprisingly, LRP5^{OE} HL60 undifferentiated cells showed decreased proliferation, as determined by decreased BrdU incorporation. The activity of the signalling components of the Wnt pathway can either foster or restrain the processes of apoptosis, according to specific cellular environment stimuli [24, 25]. Wnt signalling regulates the early and late stages of apoptosis in both development and adult cell injury in neurons, endothelial cells, vascular smooth muscle cells and cardiomyocytes [26]. Thus, another explanation for the observed inhibition of LRP5^{OE} HL60 cell proliferation could be the activation of the apoptosis machinery. Indeed, increased apoptosis was observed in undifferentiated LRP5^{OE} HL60 cells, while siRNA-LRP5 cells did not vary their apoptotic ratio. This result is supported by studies with LRP5$^{-/-}$ mice, where osteoblast apoptosis was found to be reduced by lithium therapy in cultures of calvaria cells derived from LRP5$^{-/-}$ mice *ex vivo* [27], and the persistent embryonic eye vascularization of LRP5$^{-/-}$ mice as a result of a failure of macrophage-induced endothelial cell apoptosis [28].

Our results show that an increase in LRP5 cellular expression is accompanied of increased expression levels in other pro-apoptotic proteins, including Bax, DUSP6 and G0S2. Bax is a pro-apoptotic member of the Bcl-2 family that interferes with mitochondrial function by forming pores at the outer mitochondria membrane [29]. Dusp6 has been shown to participate in the pro-apoptotic pathway as its down-regulation mediates up-regulation of ERK (Extracellular signal-Regulated Kinase) and survival of endothelial cells by means of anti-apoptosis [30]. Moreover, analyses by flow cytometry and immunocytochemistry revealed that the exogenous expression of Dusp6 induced apoptosis in cultured pancreatic cancer cells [31]. G0S2 encodes a mitochondrial protein that specifically interacts with Bcl-2 and promotes apoptosis by preventing the formation of protective Bcl-2/Bax heterodimers [32]. Interestingly, the expression levels of three broad anti-apoptotic proteins, Bcl2, Cdk1 and CD180, were significantly reduced in cells overexpressing LRP5. Bcl2 is a well-known pro-survival protein that has an essential function in a wide variety of processes (for a review, see Kelly and Strasser [33]). Cdk1 interacts with cyclin B1 to form the 'mitosis-promoting factor' whose activity influences various pro-survival signalling pathways before entering mitosis [34, 35]. Also, inhibition of cyclin B1/Cdk1 activity has been shown to increase apoptosis in human tumour cells [36, 37]. The CD180 molecule is the transmitter of the activation signal that leads to massive proliferation as well as resistance against apoptosis [38, 39]. These results further support a role for high LRP5 expression levels in promoting apoptosis in undifferentiated HL60 cells.

We then analysed the highly proliferative cancer cells PC3 and U87MG to test if LRP5 overexpression could inhibit their proliferation. LRP5^{OE} PC3 or LRP5^{OE} U87MG cells did not show reduced proliferation rates, restricting the observed LRP5^{OE} role in proliferation inhibition to undifferentiated, non-adhered cells.

To confirm the inhibitory role of LRP5 overexpression in differentiation processes, we used HM primary cultures. LRP5 overexpression in HM reduced differentiation to macrophages. Wnt signalling target genes (LEF1, c-jun and c-myc) did not modulate their expression levels in LRP5^{OE} or siRNA-LRP5 HM. However, β-catenin gene expression levels were increased in the presence of LRP5^{OE}, indicating a disruption in Wnt signalling downstream of β-catenin. Contrarily, adherent, differentiated LRP5^{OE} macrophages showed a significant increase in the mRNA expression levels of these Wnt genes. PMA-treated undifferentiated HL60 cells that overexpress LRP5 show that, although most of the cells do not adhere, the ones that do attach (and will eventually differentiate to macrophages) show an incipient activation of the Wnt signalling pathway. Interestingly, LRP5 overexpression was shown to inhibit osteogenic differentiation in mesenchymal stem cells [40] and repression of canonical Wnt signalling has been described in poorly differentiated hepatocellular carcinoma cells [41]. Taken together, these results strongly suggest an activation of the Wnt signalling pathway only in LRP5^{OE} differentiated cells (Fig. S3).

To understand the mechanisms underlying the inhibition of cellular differentiation by LRP5^{OE}, we performed subfractionation experiments that showed that LRP5^{OE} maintains undifferentiated cells in an undifferentiated state by sequestering β-catenin at the plasma membrane. It has been reported in osteoblasts that N-cadherin association with β-catenin at the membrane forms a complex with axin and LRP5 cytoplasmic tail domain causing increased β-catenin degradation, blocking canonical Wnt signalling and resulting in defective osteoblast function [21]. We have demonstrated a similar process in undifferentiated monocytic cells. When cells are differentiated, LRP5 overexpression induces β-catenin translocation to the nucleus and increased expression levels of Wnt signalling genes (Fig. S3).

To further demonstrate that LRP5 is essential for cellular differentiation, we performed experiments to rescue cellular differentiation. To this end, we transfected Wnt target genes in undifferentiated cells that rescued differentiation indicating that the inhibition of the Wnt pathway and cellular differentiation in undifferentiated inflammatory cells signals *via* LRP5 (Fig. S3).

One major question raised in this study is the significance of an increased LRP5 expression in the absence of known LRP5 ligands. Several reports have shown that, in the absence of LRP5 ligands, overexpression of LRP5 lacking either the extracellular or both the transmembrane and extracellular domains leads to the activation of the Wnt signalling pathway by cytoplasmic dimerization of the recep-

tor [3, 42, 43]. This may explain our results in undifferentiated cells that show modulation of different biological processes in the presence of excess full-length LRP5 cDNA construct in the absence of known LRP5 ligands.

In summary, our results indicate a fine regulatory role for LRP5 in undifferentiated cells' fate. Usually, LRP5 binds its ligands (glycoproteins, extracellular lipids) and moderately increases its expression levels to activate the Wnt pathway machinery [2, 44, 45]. In this report, we show that when undifferentiated, non-adherent cells overexpress LRP5 there is inhibition of cell proliferation and activation of the apoptosis machinery. Furthermore, there is a down-regulation of the differentiation processes by the sequestration of β-catenin to the cell membranes. The inhibition of the Wnt signalling pathway can be rescued by the addition of exogenous Wnt target genes. This is the first time that the mechanism by which LRP5 shuts off the Wnt signalling pathway to maintain cells in an undifferentiated state is described.

Acknowledgements

This work was supported by grants from the Spanish Ministry of Science and Innovation (SAF 2010-16549 to LB), Instituto de Salud Carlos III (TERCEL - RD12/0019/0026 to LB), I3 Contract (to MBP), Danone Institute Fellowship (to CRS), and Fundación de Investigación Cardiovascular – Fundación Jesus Serra.

Conflicts of interest

None.

Supporting information

Additional Supporting Information may be found in the online version of this article:

Figure S1 HL60 cells transfected to either silence (siLRP5) or overexpress LRP5 ($LRP5^{OE}$) along with the controls (C, siR).

Figure S2 LRP5 silencing in differentiated and undifferentiated cells.

Figure S3 Schematic showing different LRP5-β-catenin regulation in differentiated and undifferentiated cells.

Data S1 Materials and methods.

References

1. **Li Y, Bu G.** LRP5, a multifunctional cell surface receptor. *Curr Opin Lipidol.* 2004; 3: 361–3.
2. **Borrell-Pagès M, Romero JC, Juan-Babot O, *et al.*** Wnt pathway activation, cell migration, and lipid uptake is regulated by LRP5 in human macrophages. *Eur Heart J.* 2011; 32: 2841–50.
3. **Mao J, Wang J, Liu B, *et al.*** LRP5 binds to Axin and regulates the canonical Wnt signalling pathway. *Mol Cell.* 2001; 7: 801–9.
4. **Logan CY, Nusse R.** The Wnt signalling pathway in development and disease. *Annu Rev Cell Dev Biol.* 2004; 20: 781–810.
5. **Clevers H.** Wnt/beta-catenin signaling in development and disease. *Cell.* 2006; 127: 469–80.
6. **Ferrero-Miliani L, Nielsen OH, Andersen PS, *et al.*** Chronic inflammation: importance of NOD2 and NALP3 in interleukin-1beta generation. *Clin Exp Immunol.* 2007; 147: 227–35.
7. **Lee H, Bae S, Choi BW.** YoonY.WNT/β-catenin pathway is modulated in asthma patients and LPS-stimulated RAW264.7 macrophage cell line. *Immunopharmacol Immunotoxicol.* 2012; 34: 56–65.
8. **Kim JS, Yeo S, Shin DG, *et al.*** GSK3beta and beta-catenin pathway is involved in TLR4-mediated NADPH oxidase 1 expression in macrophages. *FEBS J.* 2010; 277: 2830–7.
9. **Chen L, Wu Q, Guo F, *et al.*** Expression of Dishevelled-1 in wound healing after acute myocardial infarction: possible involvement in myofibroblast proliferation and migration. *J Cell Mol Med.* 2004; 8: 257–64.
10. **Padilla PI, Wada A, Yahiro K, *et al.*** Morphologic differentiation of HL-60 cells is associated with appearance of RPTPbeta and induction of Helicobacter pylori VacA sensitivity. *J Biol Chem.* 2000; 275: 15200–6.
11. **Sokoloski JA, Sartorelli AC, Rosen CA, *et al.*** Antisense oligonucleotides to the p65 subunit of NF-kappa B block CD11b expression and alter adhesion properties of differentiated HL-60 granulocytes. *Blood.* 1993; 82: 625–32.
12. **Davidson G, Niehrs C.** Emerging links between CDK cell cycle regulators and Wnt signalling. *Trends Cell Biol.* 2010; 20: 453–60.
13. **Morin A, Fritsch L, Mathieu JR, *et al.*** Identification of CAD as an androgen receptor interactant and an early marker of prostate tumor recurrence. *FASEB J.* 2012; 26: 460–7.
14. **Roca H, Craig MJ, Ying C, *et al.*** IL-4 induces proliferation in prostate cancer PC3 cells under nutrient-depletion stress through the activation of the JNK-pathway and survivin upregulation. *J Cell Biochem.* 2012; 113: 1569–80.
15. **Rooj AK, McNicholas CM, Bartoszewski R, *et al.*** Glioma specific cation conductance regulates migration and cell cycle progression. *J Biol Chem.* 2012; 287: 4053–65.
16. **Nead MA, Baglia LA, Antinore MJ, *et al.*** Rb binds c-Jun and activates transcription. *EMBO J.* 1998; 17: 2342–52.
17. **Mann B, Gelos M, Siedow A, *et al.*** Target genes of beta-catenin-TCF/LEF signalling in human colorectal carcinomas. *Proc Natl Acad Sci USA.* 1999; 96: 1603–8.
18. **Staal FJ, Weerkamp F, Baert MR, *et al.*** Wnt target genes identified by DNA microarrays in immature CD34 + thymocytes regulate proliferation and cell adhesion. *J Immunol.* 2004; 172: 1099–108.
19. **Linask KK, Knudsen KA.** Gui YH.N-cadherin-catenin interaction: necessary component of cardiac cell compartmentalization during early vertebrate heart development. *Dev Biol.* 1997; 185: 148–64.
20. **Xu G, Arregui C, Lilien J.** Balsamo J. PTP1B modulates the association of beta-catenin with N-cadherin through binding to an adjacent and partially overlapping target site. *J Biol Chem.* 2002; 277: 49989–97.

21. **Haÿ E, Laplantine E, Geoffroy V, *et al.*** N-cadherin interacts with axin and LRP5 to negatively regulate Wnt/beta-catenin signalling, osteoblast function, and bone formation. *Mol Cell Biol.* 2009; 29: 953–64.
22. **Slevin M, Krupinski J, Gaffney J, *et al.*** Hyaluronan-mediated angiogenesis in vascular disease: uncovering RHAMM and CD44 receptor signalling pathways. *Matrix Biol.* 2007; 26: 58–68.
23. **Angers S, Moon RT.** Proximal events in Wnt signal transduction. *Nat Rev Mol Cell Biol.* 2009; 10: 468–77.
24. **Yeo W, Gautier J.** Early neural cell death: dying to become neurons. *Dev Biol.* 2004; 274: 233–44.
25. **Brocardo M, Henderson BR.** APC shuttling to the membrane, nucleus and beyond. *Trends Cell Biol.* 2008; 18: 587–96.
26. **Li F, Chong ZZ, Maiese K.** Winding through the WNT pathway during cellular development and demise. *Histol Histopathol.* 2006; 21: 103–24.
27. **Clément-Lacroix P, Ai M, Morvan F, *et al.*** Lrp5-independent activation of Wnt signalling by lithium chloride increases bone formation and bone mass in mice. *Proc Natl Acad Sci USA.* 2005; 102: 17406–11.
28. **Kato M, Patel MS, Levasseur R, *et al.*** Cbfa1-independent decrease in osteoblast proliferation, osteopenia, and persistent embryonic eye vascularization in mice deficient in Lrp5, a Wnt coreceptor. *J Cell Biol.* 2002; 157: 303–14.
29. **Danial NN, Korsmeyer SJ.** Cell death: critical control points. *Cell.* 2004; 116: 205–19.
30. **Rossig L, Haendeler J, Hermann C, *et al.*** Nitric oxide down-regulates MKP-3 mRNA levels: involvement in endothelial cell protection from apoptosis. *J Biol Chem.* 2000; 275: 25502–7.
31. **Furukawa T, Sunamura M, Motoi F, *et al.*** Potential tumor suppressive pathway involving DUSP6/MKP-3 in pancreatic cancer. *Am J Pathol.* 2003; 162: 1807–15.
32. **Welch C, Santra MK, El-Assaad W, *et al.*** Identification of a protein, G0S2, that lacks Bcl-2 homology domains and interacts with and antagonizes Bcl-2. *Cancer Res.* 2009; 69: 6782–9.
33. **Kelly GL, Strasser A.** The essential role of evasion from cell death in cancer. *Adv Cancer Res.* 2011; 111: 39–96.
34. **Bernhard EJ, McKenna WG, Muschel RJ.** Cyclin expression and G2-phase delay after irradiation. *Radiat Res.* 1994; 138: S64–7.
35. **Maity A, Hwang A, Janss A, *et al.*** Delayed cyclin B1 expression during the G2 arrest following DNA damage. *Oncogene.* 1996; 13: 1647–57.
36. **Li Z, Xia L, Lee LM, *et al.*** Effector genes altered in MCF-7 human breast cancer cells after exposure to fractionated ionizing radiation. *Radiat Res.* 2001; 155: 543–53.
37. **Yuan J, Yan R, Krämer A, *et al.*** Cyclin B1 depletion inhibits proliferation and induces apoptosis in human tumor cells. *Oncogene.* 2004; 23: 5843–52.
38. **Good KL, Avery DT, Tangye SG.** Resting human memory B cells are intrinsically programmed for enhanced survival and responsiveness to diverse stimuli compared to naive B cells. *J Immunol.* 2009; 182: 890–901.
39. **Porakishvili N, Memon A, Vispute K, *et al.*** CD180 functions in activation, survival and cycling of B chronic lymphocytic leukaemia cells. *Br J Haematol.* 2011; 153: 486–98.
40. **Baksh D, Boland GM, Tuan RS.** Cross-talk between Wnt signalling pathways in human mesenchymal stem cells leads to functional antagonism during osteogenic differentiation. *J Cell Biochem.* 2007; 101: 1109–24.
41. **Yuzugullu H, Benhaj K, Ozturk N, *et al.*** Canonical Wnt signaling is antagonized by noncanonical Wnt5a in hepatocellular carcinoma cells. *Mol Cancer.* 2009; 8: 90.
42. **Hay E, Faucheu C, Suc-Royer I, *et al.*** Interaction between LRP5 and Frat1 mediates the activation of the Wnt canonical pathway. *J Biol Chem.* 2005; 280: 13616–23.
43. **Shahi P, Park D, Pond AC, *et al.*** Activation of Wnt signalling by chemically induced dimerization of LRP5 disrupts cellular homeostasis. *PLoS ONE.* 2012; 7: e30814.
44. **Rajamannan NM, Subramaniam M, Caira F, *et al.*** Atorvastatin inhibits hypercholesterolemia-induced calcification in the aortic valves *via* the Lrp5 receptor pathway. *Circulation.* 2005; 112: I229–34.
45. **Lindvall C, Evans NC, Zylstra CR, *et al.*** The Wnt signalling receptor Lrp5 is required for mammary ductal stem cell activity and Wnt1-induced tumorigenesis. *J Biol Chem.* 2006; 281: 35081–7.

Sup Fig. 1

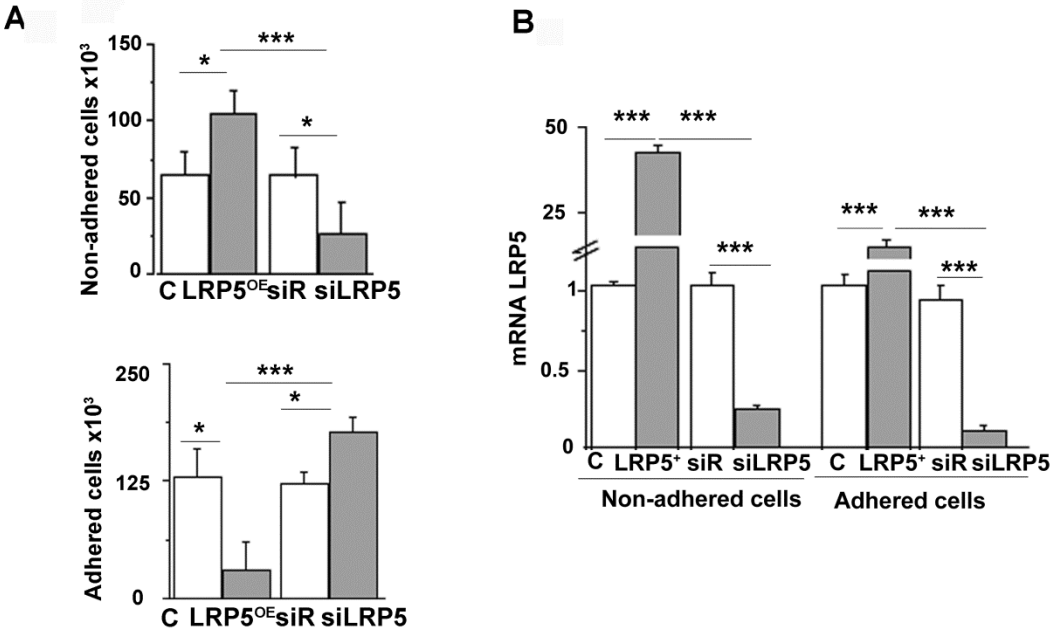

Sup Fig 1: HL60 cells transfected to either silence (siLRP5) or overexpress LRP5 ($LRP5^{OE}$) along with the controls (C, siR). 24h post transfection, PMA (10nM) was added to the supernatant for further 24h when (A) non-adhered and adhered cells were collected and viable cells were counted, (B) LRP5 mRNA levels from RNA extracts were quantified by real time PCR and normalized to 18srRNA. ***p<0.005, **p<0.01, *p<0.05. Experiments were performed three times in triplicates.

Sup Fig. 2

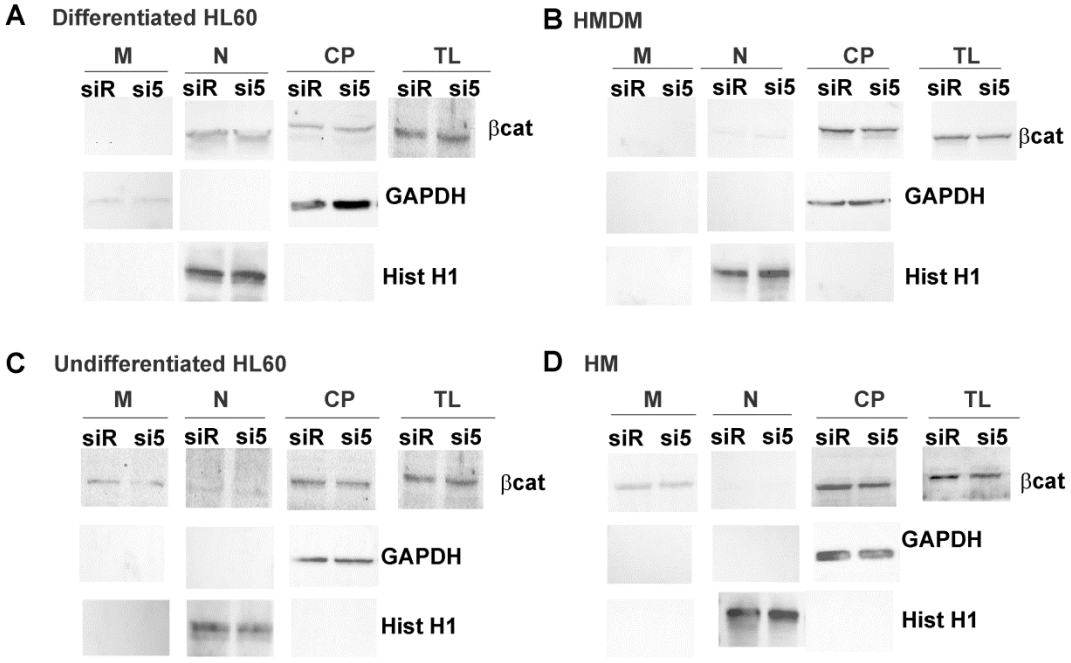

Sup. Fig. 2: LRP5 silencing in differentiated and undifferentiated cells. PMA-differentiated HL60 cells (A), HMDM (B), undifferentiated HL60 cells (C) or HM (D) were transfected with siRNA-LRP5 (si5) or siRNA-Random (siR) and membrane (M), nuclear (N), cytoplasmic (CP) fractions and total lysates (TL) were analyzed by Western blotting using anti-β-catenin antibody. GAPDH and Histone H1 were used as quality controls for cytoplasmic/membrane and nuclear fractions respectively.

Sup Fig. 3

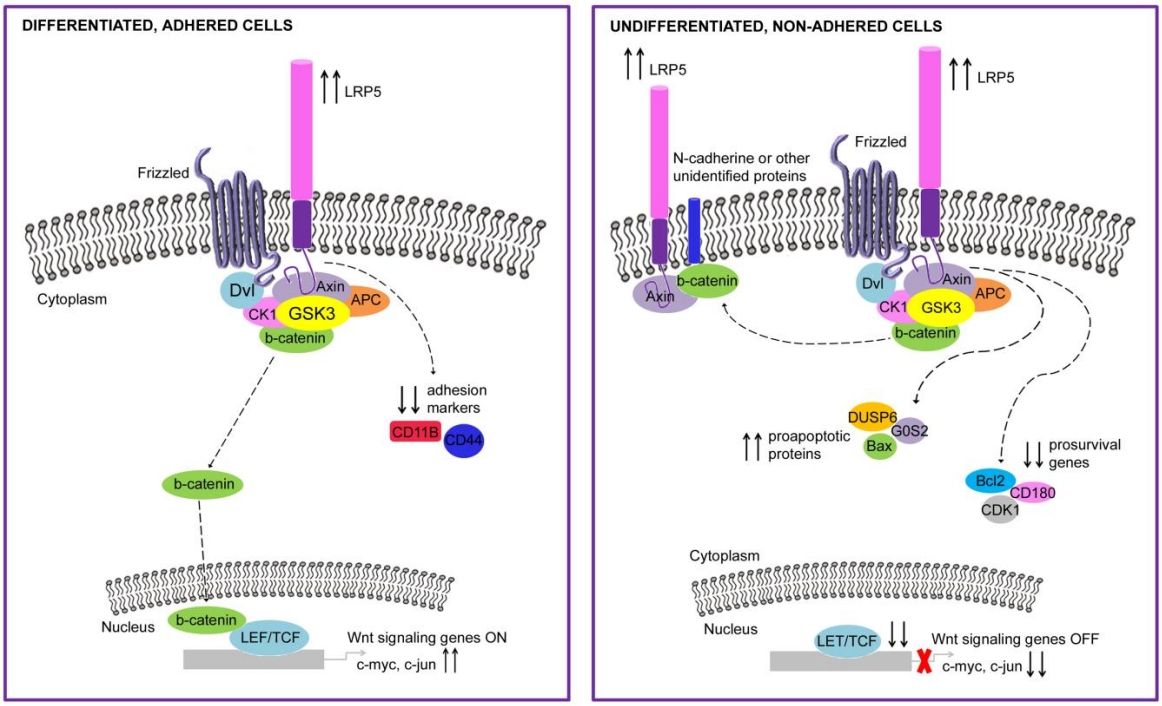

Sup Fig. 3: Squematic showing the different regulation pathways in differentiated and undifferentiated cells.

Supplemental materials and methods:

Cell culture

Human promyelocytic leukaemia cells (HL60) were grown in RPMI 1640 medium with Glutamax, supplemented with 10% heat-inactivated foetal bovine serum, 100U/mL penicillin and 100U/mL streptomycin during 3 days before treatment. When the culture reached a density of 7-8x10^5 cells/mL, cells were washed, subcultured in 6 well plates (5x10^5cells/well) and treated with PMA (10nM). 48 hours after treatment, cells achieved a macrophage phenotype, although the phagocytic function remained untested.

Human peripheral blood mononuclear cells (PBMCs) were obtained by standard protocols from buffy coats (15-20ml) from healthy donors. Cells were applied on 15 ml of Ficoll-Hypaque and centrifuged at 300g for 1 hour at 22°C, with no brake. Mononuclear cells were obtained from the central white band of the gradient, washed in phosphate buffer saline (PBS), and suspended in RPMI medium (Gibco) supplemented with 10% human serum AB (Immunogenetics) and antibiotics. Cells were seed in 6 well plates (4x10^6cells/well) and allowed to differentiate into macrophages by 7 days in culture, replacing medium each two days.

PC3 and U87MG were grown in DMEM/F-12 medium with 10%FBS, 2mM glutamine, 100U/mL P/S.

HL60, HM and HMDM silencing and overexpression.

$4x10^6$ HL60-cells/mL in 100µL of Cell Line Nucleofector® Solution V and 300nM of siR, siLRP5 or 0.4ug of pcDNA3 or pcDNA3-LRP5 were transfected with T-019 program.siR and pcDNA3 alone were used as controls and did not exert any effect on LRP5 expression. HM cells were nucleofected as described for HL60 cells with 0.25ug of cDNA, $1x10^7$cells/mL and X-001 transfection program. HMDM cells, PMA-treated HL60 cells, PC3 and U87MG were transfected using Metafectene® Easy$^+$ (Biontex) following the manufacturer's instructions.For silencing experiments, 100nM of each siRNA was transfected using HiPerFect Transfection Reagent (Quiagen). 48 hours after transfection efficiency was systematically analyzed by LRP5 RT-Real Time PCR and normalized to r18S.

RNA isolation and Real time PCR

RNA was isolated using Total RNA extraction kit (Qiagen). Concentration was determined with a NanoDrop ND-1000 spectrophotometer (NanoDrop Technologies) and purity was checked by the A260/A280 ratio. cDNA was synthesized from 0.5 µg RNA with cDNA Reverse transcription kit (Qiagen). The resulting cDNA samples were amplified by PCR using a DNA thermal cycler (MJ Research) and the following specific probes from Applied Biotechnologies: LRP5 (Hs00182031-m1), 18S rRNA (4319413E), CDK1 (Hs00938777-m1), G0S2 (Hs00274783-s1), CD180 (Hs01069872),DUSP6 (Hs00169257-m1), CD11b (Hs00355885-m1), CD44 (Hs01075861-m1), BAX (Hs00180269-m1), BCL2 (Hs00608023-m1), c-myc (Hs00153408_m1), c-jun (Hs99999141_s1), LEF1 (Hs01547250_m1).

Western Blot

Transfected HL60 cells were lysed in RIPA buffer containing protease inhibitor complex (Roche, Germany). Electrophoresis of SDS-polyacrylamide gels, transfer to nitrocellulose filters,incubation with primary antibodies (LRP5, Bcl2 and β-actin from Abcam, Cdc2p34, Bax, G0S2 and Cd180 from Santa Cruz, Dusp6 from R+D Systems) and with anti-mouse, anti-rabbit or anti-goat secondary antibodies (Dako) was performed.Band densities were determined with the ChemiDoc XRS system (Bio-Rad).Normalization was performed against β-actin.

Bromideoxyuridine (BrdU) labeling and detection

24 hours post-transfection BrdU (BrdU Cell Proliferation Assay, Calbiochem) was added (20uL/well of a 1:2000 dilution) for further 24 hours. Cells were fixed, incubated with anti-BrdU antibody, washed and incubated with peroxidise Goat anti-mouse IgG HRP conjugate.Substrate and stop solution were added and intensity was quantified using a spectrophotometric plate reader at dual wavelength of 450–595 nm.

Annexin V-FITC determination

48 hours post-transfection HL60 cells were collected, washed, stained with Annexin V fluorescein isothiocyanate (AV-FITC) and propidium iodide (PI) following manufacturer's instructions (BD Pharmingen) and analyzed by flow cytometry (FACSCalibur).

Immunofluorescence

PMA-treated HL60 were fixed with 4% paraformaldehyde and primary LRP5 (Biovision) and cd68 (Abcam) antibodies were added followed by Alexa Flour anti-mouse 488 IgG, Alexa Flour anti-rabbit 633 IgG and Hoechst (33342). Fluorescent images were acquired in a scan format of 1024x1024 pixels in a spatial data set (xyz) and were processed with the Leica Standard Software TCS-AOBS. Controls without primary antibodies showed no fluorescence labeling.

Adhesion assay

HL60 cells transfected with siRNA-Random, siRNA-LRP5, pcDNA3, pcDNA3-LRP5, pcDNA3-cmyc or c-jun were seeded in triplicates and treated with 10nM PMA for further 24h when supernatant and cell lysate were collected. A set of cells was counted on Neubahuer chambers while another set was used for RNA extraction.

Differentiation assay in HM.

One day after isolation, monocytes were nucleofected as described for HL60 cells with $1x10^7$cells/mL and X-001 transfection program. Cells were differentiated to HMDM for 7 days when pictures were taken and cells were counted. Transfection efficiency was analyzed 48 hours after transfection by LRP5 and r18S RT-PCR.

Subfractionation experiments

For nuclear extracts, cells were PBS washed,scraped with CSK buffer (50nM NaCl, 10mM Pipes pH6.8, 3mM $MgCl_2$, 0.5% Triton X-100, 300mM sucrose and protease inhibitors), incubated 20 minutes shaking at 4ºC and centrifuged. Supernatants (cytoplasmic fractions) were stored at -20ºC.Pellets (nuclear fractions) was suspended in 50uL of Sol/Insol Buffer (15mM pH7.5, 5mM EDTA, 2.5mM EGTA and 1% SDS) and heated for 10 minutes at 100°C. Membrane fraction isolation was performed as described[42]. Subcellular fractions were analyzed by western blot for β-catenin, GAPDH, Histone H1.

Statistical analysis

Results are expressed as mean ± S.E.M. A Stat View statistical package was used for all the analysis. When possible, comparisons among groups were performed by parametric (one factor ANOVA) analysis. Statistical significance was considered when $p<0.05$.

ARTÍCULO 3

LRP5 deficiency downregulates Wnt signaling and promotes aortic lipid infiltration in hypercholesterolemic mice.

Autores: María Borrell-Pagés[±], July Carolina Romero[±], Lina Badimon.

Revista: Journal of Cellular and Molecular Medicine 2014; Aceptado.

Factor de impacto: 4.75

Centro de Investigación Cardiovascular CSIC-ICCC, Hospital de la Santa Creu i Sant Pau, Barcelona, España.

[±] Co-primeros autores

RESUMEN

La deficiencia de LRP5 inhibe la señalización por Wnt y promueve la infiltración de lípidos en las aortas de ratones hipercolesterolémicos.

La participación de LRP5 y la vía de señalización por Wnt en la pared vascular de animales dislipémicos no está descrita. En este estudio analizamos la función de LRP5 y la vía de señalización por Wnt en ratones *Wt* y *Lrp5*$^{-/-}$ alimentados con una dieta hipercolesterolémica (HC) para provocar dislipemia.

Ratones *Lrp5*$^{-/-}$ presentan una mayor infiltración de lípidos en las aortas que la de los ratones *Wt*, indicando un rol protector para LRP5 en la pared vascular. Tres miembros de la familia de LDLR, *Lrp1*, *Vldlr* y *Lrp6*, están sobreexpresados en las aortas de los ratones *Lrp5*$^{-/-}$alimentados con una dieta HC con respecto a los *Wt,* indicando que estos receptores contribuyen al incremento de la acumulación de lípidos observada en estos ratones. La dieta HC en los ratones *Lrp5*$^{-/-}$ provoca una mayor infiltración de macrófagos en las aortas y un aumento de la expresión de citoquinas inflamatorias, sugiriendo que los ratones *Lrp5*$^{-/-}$ no pueden regular apropiadamente la respuesta inflamatoria durante la hipercolesterolemia. La expresión de proteínas de la vía de señalización Wnt/β-catenina está disminuida en las aortas de los ratones

Lrp5$^{-/-}$ HC, indicando que LRP5 regula la activación de la vía canónica de señalización por Wnt en la pared vascular.

Nuestros resultados muestran que la supresión de LRP5 y la vía canónica de señalización por Wnt aumentan el perfil dislipémico de ratones *Lrp5*$^{-/-}$ mediante el aumento de la infiltración de lípidos y macrófagos en la pared vascular y de la disminución de la respuesta inflamatoria de los leucocitos.

LRP5 deficiency down-regulates Wnt signalling and promotes aortic lipid infiltration in hypercholesterolaemic mice

Maria Borrell-Pagès [a, #], Carolina Romero [a, #], Lina Badimon [a, b, *]

[a] *Cardiovascular Research Center, CSIC-ICCC, Hospital de la Santa Creu i Sant Pau, IIB-Sant Pau, Barcelona, Spain*
[b] *Cardiovascular Research Chair, UAB, Barcelona, Spain*

Received: ??, ????; Accepted: ??, ????

Abstract

Low-density lipoprotein receptor-related protein 5 (LRP5) is a member of the LDLR family that orchestrates cholesterol homoeostasis. The role of LRP5 and the canonical Wnt pathway in the vascular wall of dyslipidaemic animals remains unknown. In this study, we analysed the role of LRP5 and the Wnt signalling pathway in mice fed a hypercholesterolaemic diet (HC) to trigger dyslipidaemia. We show that *Lrp5*$^{-/-}$ mice had larger aortic lipid infiltrations than wild-type mice, indicating a protective role for LRP5 in the vascular wall. Three members of the LDLR family, *Lrp1*, *Vldlr* and *Lrp6*, showed up-regulated gene expression levels in aortas of *Lrp5*$^{-/-}$ mice fed a hypercholesterolaemic diet. HC feeding in *Lrp5*$^{-/-}$ mice induced higher macrophage infiltration in the aortas and accumulation of inflammatory cytokines in blood. Wnt/β-CATENIN signalling proteins were down-regulated in HC *Lrp5*$^{-/-}$ mice indicating that LRP5 regulates the activation of Wnt signalling in the vascular wall. In conclusion, our findings show that LRP5 and the canonical Wnt pathway down-regulation regulate the dyslipidaemic profile by promoting lipid and macrophage retention in the vessel wall and increasing leucocyte-driven systemic inflammation.

Keywords: LRP5 • atherosclerosis • plasma cholesterol • canonical Wnt signalling • macrophages

Introduction

Hypercholesterolaemia is a causal factor for atherosclerosis, which predisposes individuals to the development of clinical cardiovascular diseases [1]. High levels of low-density lipoprotein (LDL) in plasma rapidly infiltrate the vessel wall triggering an inflammatory–immunomodulatory chain reaction [2, 3]. Members of the LDL receptor family are involved in lipoprotein transport and plasma LDL cholesterol clearance, modulating critical stages of atherosclerosis progression including inflammation, foam cell formation and endothelial activation [4, 5]. There is ongoing controversy on the role of LRP5 and the canonical Wnt/β-CATENIN pathway in lipid induced vascular damage and atherosclerosis. Indeed, activation of the β-CATENIN/lymphoid enhancer-binding factor 1 (LEF1) signalling in the endothelium occurs in response to atheroprone haemodynamic stimulations and precedes lesion development in *ApoE*$^{-/-}$ mice [6] and higher levels of active β-CATENIN are observed in disrupted atherosclerotic plaques compared to stable plaques from human carotid artery, suggesting a potential role for Wnt signalling in the evolution of atherosclerotic plaque [7]. However, *ApoE*$^{-/-}$*Lrp5*$^{-/-}$ mice fed a high-fat diet developed bigger atherosclerotic lesions that their *ApoE*$^{-/-}$ littermates [8], although the exceedingly high levels of cholesterol in these animals (almost 750 mg/dl) could have shadowed any effect of the canonical Wnt receptor, LRP5.

The canonical Wnt/β-CATENIN pathway has also been described to regulate inflammatory reactions although its role remains controversial. Indeed, Wnt/β-CATENIN pathway seems to inhibit inflammation as β-CATENIN inhibitors increase the expression of inflammatory genes in human aortic endothelial cells [9] and administration of GSK3β, an inhibitor of Wnt/β-CATENIN pathway in human monocytes triggers Toll-like receptor-mediated pro-inflammatory cytokine production [10]. However, IL-1β and LPS induced nuclear β-CATENIN accumulation in human vascular endothelial cells [6] and activation of canonical Wnt genes have been found in endothelial cells of a rejected kidney model [11] suggesting that activation of the pathway triggers the inflammatory response.

We have recently reported that LRP5 is involved in monocyte to macrophage differentiation [12], it regulates macrophage motility and

2 LRP5-expressing mononuclear cells are a fraction of the macrophag-

#Both authors contributed equally to this work.
*Correspondence to: Lina BADIMON,
Cardiovascular Research Center, CSIC-ICCC,
Hospital de la Santa Creu i Sant Pau,
IIB-Sant Pau, Barcelona, Spain.
Tel.: ???????
Fax: ???????
E-mail: ???????

doi: 10.1111/jcmm.12396

es found in human advanced coronary atherosclerotic plaques [13]. Still, the presence of LRP5-positive cells in these coronary plaques does not imply causality. Thus, to better understand the role of LRP5 and Wnt signalling in the early stages of lipid infiltration in the vessel wall, we studied the effects of a hyperlipidaemic diet inducing a mild increase in cholesterol serum levels in *Lrp5*$^{-/-}$ mice and in wild-type (WT) controls. We hypothesized that LRP5 and the Wnt signalling pathway have a role in the inflammatory process associated to atherosclerosis progression. Absence of LRP5, induced higher lipid infiltration in mouse thoracic aortas, increased the transcription of the LDLR family member *Lrp6*, induced higher macrophage infiltration and increased inflammatory cytokines secretion, supporting an anti-inflammatory role for LRP5 and the target genes of the Wnt/β-CATENIN pathway.

Materials and methods

Animals and experimental design

Lrp5$^{-/-}$ mice, a kind gift from Dr. Bart Williams [14–16] were maintained in a C57BL/6 background. Mice were housed in cages under controlled temperature (21 ± 2°C) on a 12 hrs light/dark cycle with food and water *ad libitum*. Homozygous WT *C57BL/6* mice (n = 22) and *Lrp5*$^{-/-}$ *C57BL/6* mice (LRP5$^{-/-}$; n = 22) were used for the protocols. The presence of *Lrp5* alleles was assessed by PCR amplification from DNA extracted from tail biopsies in WT, heterozygous and homozygous littermates. Primers used were S17 (GGC TCG GAG GAC AGA CCT GAG), S23 (CTG TCA GTG CCT GTA TCT GTC C) and IRES31 (AGG GGC GGA ATT CGA TAG CT). *Lrp5*$^{-/-}$ and *Wt* mice were fed a normal chow diet (NC, Tekland diet, Harland Labs) for 10 weeks. Animals were then divided into two groups to be fed NC or high cholesterol diet (HC, TD.88137, Harland Labs) for further 8 weeks (8–12 mice/group). Cardiac puncture was performed in mice under terminal anaesthesia (1 mg/kg Medetomidine and 75 mg/kg Ketamine, ip). The study protocol was conducted in conformity with the Public Health Service (PHS) Policy on Humane Care and Use of Laboratory Animals and approved by the local institutional animal research committee (ICCC051/5422).

Biochemical analysis and blood-derived mRNA

Blood samples were collected in serum separator gel tubes and PAX-tubes. Serum was obtained by centrifugation 3500 r.p.m., 20 min. at 4°C. Cholesterol, triglycerides and HDL levels were measured enzymatically by using commercially available kits (GERNON reagents) and read in a spectrophotometer (MC-15 SOFT; RAL). PAX-tubes were processed for preparation of blood-derived mRNA using PAXgene Blood RNA Kit (Qiagen). Real Time RT-PCR array was performed with RT2 Profiler PCR array PAMM-021 (SABiosciences, Qiagen).

Quantification of atherosclerotic lesions

Mice were anaesthetized and aortas were removed, carefully cleaned of adventitial fat under a stereoscopic microscope, and longitudinally cut with the luminal surface facing up (n = 6–8 mice/group). Aortas were fixed overnight in 4% paraformaldehyde, washed with ddH_2O 1 hr in gentle shaking and stained with Oil-red-O (ORO) for 30 min. Aortas were rinsed with 70% ethanol and ddH_2O; images were captured by Nikon Eclipse 80i microscope and digitized by Retiga 1300i Fast camera. ORO-stained area was quantified with Image J software and results are expressed as percentage of lipid area/total aortic area.

Thin layer chromatography

Aorta tissue (5 mg) was homogenized in NaOH 0.1 M. The organic solvent was removed under a N_2 stream, the lipid extract was suspended in dichloromethane and separated by thin layer chromatography (TLC). TLC was performed on silica G-24 plates. Concentrations of standards (a mix of cholesterol, cholesterol palmitate, triglycerides, diglycerides and monoglycerides) were applied to each plate. The chromatographic developing solution was heptane/diethylether/acetic acid (74:21:4, vol/vol/vol). The spots corresponding to cholesteryl esters (CE) were quantified by densitometry.

Real time RT-PCR

Aortas were frozen in liquid nitrogen and aortic RNA was isolated with Trizol® Reagent (Invitrogen; n = 5–7 mice/group). Concentration was determined with a NanoDrop ND-1000 spectrophotometer (NanoDrop Technologies, Inc., Wilmington, DE, USA) and purity was checked by the A260/A280 ratio (ratios between 1.8 and 2.1 were considered acceptable). cDNA was synthesized from 0.5 μg RNA with cDNA Reverse transcription kit (Qiagen). The resulting cDNA samples were amplified with a RT-PCR thermal cycler (Applied Biosystems 7900HT) and the following specific probes from CONDA: *Lrp5* (Mm.PT.49a.8045420), *Lrp1* (Mm.PT.49a.7750137), *Lrp2* (Mm.PT.49a.11916154), *Lrp6* (Mm.PT.56a.6383636), *Lrp8* (Mm.PT.49a.6553055), *Ldlr* (Mm.PT.49a.9930556) and *Cd36* (Mm.PT.49a.12111555). *Vldlr* (Mm00443298_m1) was purchased from Applied Biosystems. Results were normalized with *18S* probe from Applied Biosystems.

Immunohistochemistry

Immediately after surgical excision, aortas were immersed in fixative solution (4% paraformaldehyde) and embedded in paraffin, cut into 5 μm thick serial sections and placed on poly-L-lysine coated slides. Primary antibodies used were: Matrix Metalloproteinase-7, MMP-7 (Rabbit polyclonal; Abcam), β-CATENIN (Rabbit policlonal; Millipore) and HAM56 (Mouse monoclonal; Dako). Before incubation with primary antibodies, sections were washed and endogenous peroxidase activity was impressed with H_2O_2 and goat or horse serum block. Primary antibodies were detected using the avidin–biotin immunoperoxidase technique. Sections were incubated with an appropriate biotinylated secondary antibody (1:200; Vector Laboratories). The chromogen used was 3,3′-diaminobenzidine. Haematoxylin was used for nuclear stain. Images were captured by Nikon Eclipse 80i

microscope and digitized by Retiga 1300i Fast camera, magnification (×400).

Statistical analysis

Results are expressed as mean ± SEM. A Stat View statistical package was used for all the analysis. Comparisons among groups were performed by two-way ANOVA analysis. Regression analyses were performed by applying $Y = a + b*X$ lineal pattern selecting just highly adjusted equations. Slopes were compared by *t*-test. Statistical significance was considered when $P < 0.05$.

Results

Serum cholesterol profile

We analysed the differences in serum cholesterol profiles of *Wt* and *Lrp5*$^{-/-}$ mice fed a normocholesterolaemic (NC) or hypercholesterolaemic (HC) diet. Figure 1A shows an agarose gel with *Wt*, *Lrp5*$^{-/-}$ and *Lrp5*$^{+/-}$ alleles. Cholesterol serum levels of *Lrp5*$^{-/-}$ mice fed a NC diet containing 3.5% (w/w) fat and 0% cholesterol were lower than those of their *Wt* littermates (Fig. 1B). When mice were fed a HC diet containing 21% (w/w) fat and 0.25% cholesterol, total cholesterol levels were significantly increased in both *Lrp5*$^{-/-}$ and *Wt* mice (Fig. 1B). Interestingly, the overall increase in serum cholesterol levels in high-fat diet with respect to chow diet was double in *Lrp5*$^{-/-}$ (125.69 mg/dl) than in *Wt* mice (62.25 mg/dl, Fig. 1B). Non-HDL cholesterol increased by 42 ± 8% and 300 ± 23% in HC *Wt* and HC *Lrp5*$^{-/-}$ mice with respect to their NC littermates (Fig. 1C).

Lipid deposition in aortas

The administration of a HC diet in *Wt* and *Lrp5*$^{-/-}$ mice led to a significant increase in early lesions in the aortic area with lipid infiltration in both groups. Indeed, the aortic lipid rich coverage increased by 7 ± 0.5% and by 17 ± 1% in *Wt* and *Lrp5*$^{-/-}$ mice respectively (Fig. 1D and E). The increased lipid deposition in HC *Lrp5*$^{-/-}$ mice was over 70% higher than in HC *Wt* mice indicating a protective role for LRP5 in mice aortas. Furthermore, HC feeding induced higher levels of CE accumulation in *Lrp5*$^{-/-}$ (87 ± 8%) than in *Wt* (51 ± 6%) aortas with respect to NC mice (Fig. 1F).

Positive correlation between plasma cholesterol levels and aortic lipid deposition in Wt and Lrp5$^{-/-}$ mice

To analyse the effect of total plasma cholesterol on aortic lipid coverage, regression analyses were performed for *Wt* and *Lrp5*$^{-/-}$ mice results. Significantly higher aortic lipid deposition was observed with higher plasma cholesterol levels (Fig. 2A and B). The slope for this correlation was steeper for *Lrp5*$^{-/-}$ mice. Correlation analyses remained positive and significant between non-HDL cholesterol and aortic lipid coverage and slopes were significantly different with higher change in *Lrp5*$^{-/-}$ mice (Fig. 2C and D).

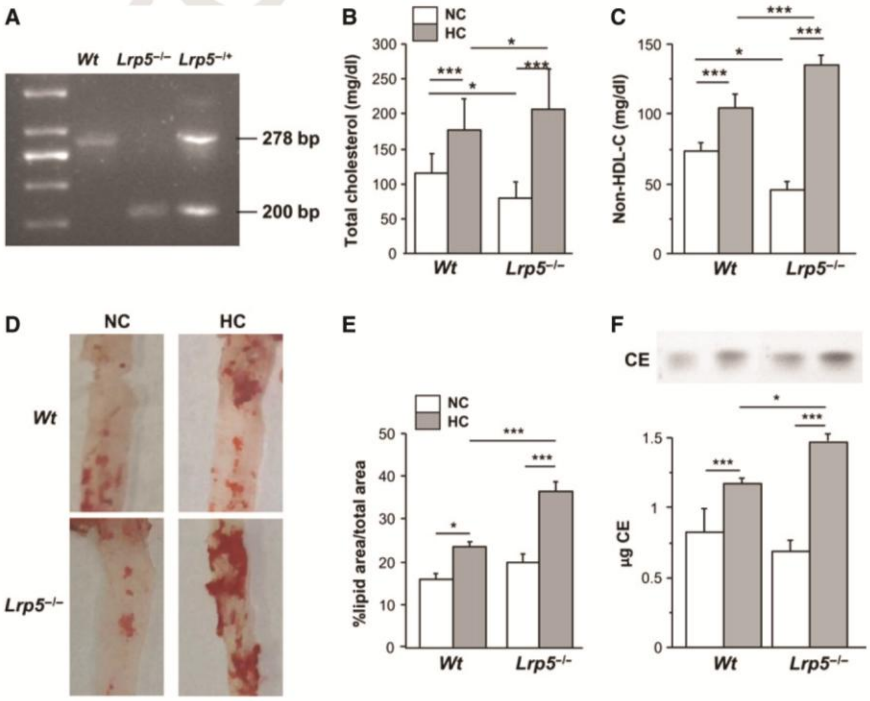

Fig. 1 Hypercholesterolaemic (HC) *Lrp5*$^{-/-}$ mice model characterization. (**A**) Agarose gel showing *Wt*, *Lrp5*$^{-/-}$ and *Lrp5*$^{-/+}$ alleles. (**B**) Serum cholesterol levels in *Wt* and *Lrp5*$^{-/-}$ mice fed a normocholesterolaemic (NC) or a HC diet. (**C**) Non-HDL-C in *Wt* and *Lrp5*$^{-/-}$ mice fed a NC or a HC diet. (**D**) Representative images of mouse thoracic aortas stained with ORO. (**E**) Quantification of lipid area in mice aortas. (**F**) Cholesteryl ester measurement by thin layer chromatography and bar graph showing CE quantification. $*P < 0.05$; $***P < 0.005$.

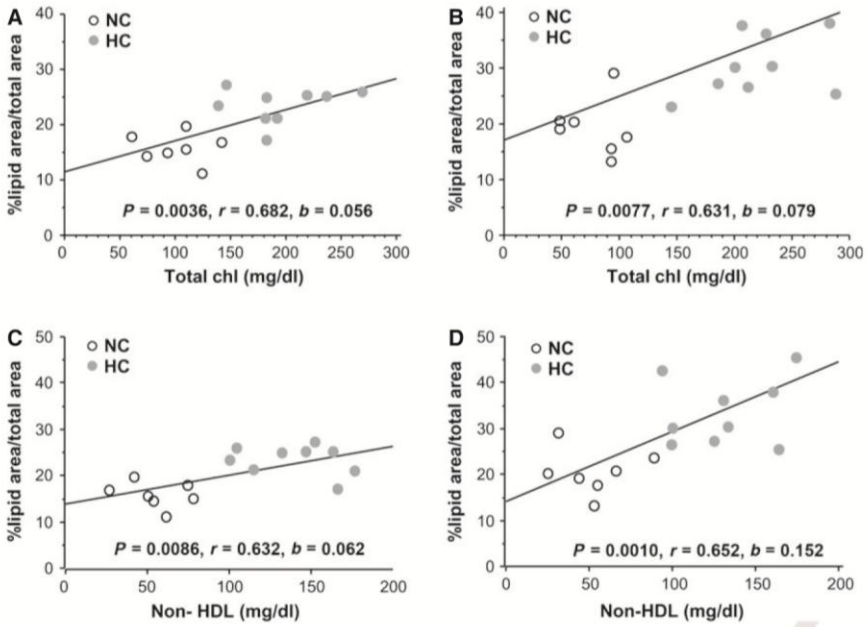

Fig. 2 Regression analyses between total cholesterol and aortic lipid coverage in *Wt* (**A**) and *Lrp5*$^{-/-}$ mice (**B**) and between non-HDL cholesterol and aortic lipid coverage in *Wt* (**C**) and *Lrp5*$^{-/-}$ mice (**D**) with their statistical significances (p), correlation coefficients (r) and slopes (b).

Increased macrophage infiltration in Lrp5$^{-/-}$ mice

Lrp5 mRNA expression in white blood cells showed a 77.5 ± 0.2% increase because of hypercholesterolaemia in *Wt* mice (Fig. 3A). *Lrp5* mRNA expression was negligible in white cells of *Lrp5*$^{-/-}$ mice. Immunostaining with HAM56 for macrophages (Fig. 3B) showed a 47.6 ± 2% increase in macrophage infiltration to the intima in HC *Lrp5*$^{-/-}$ mice compared with HC *Wt* mice (Fig. 3C). Monocytes–macrophages in aortic tissue were more abundant in *Lrp5*$^{-/-}$ mice.

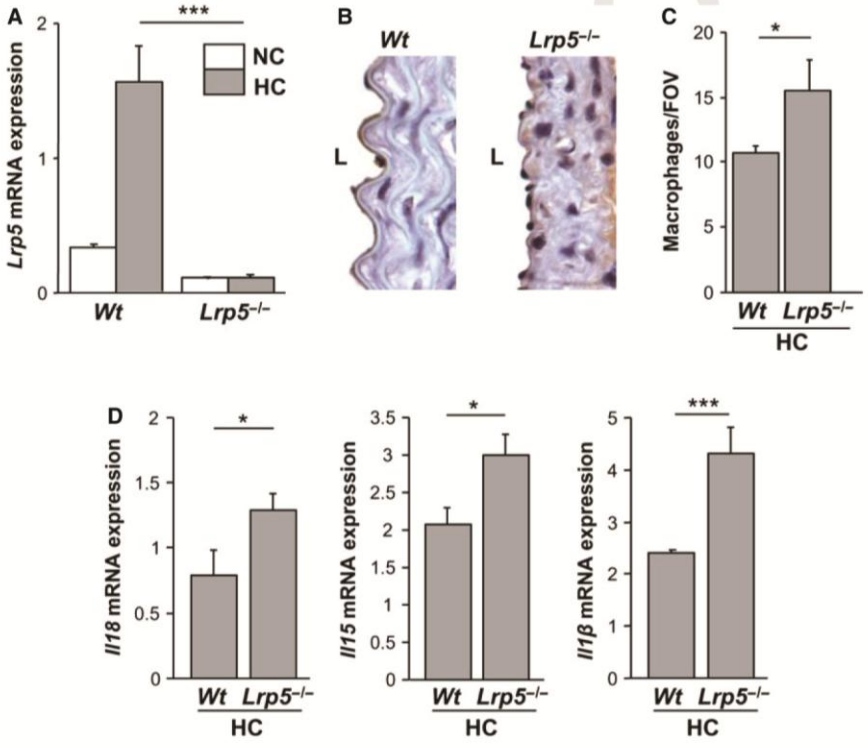

Fig. 3 Hypercholesterolaemic (HC) *Lrp5*$^{-/-}$ mice show increased aortic macrophage infiltration. (**A**) *Lrp5* expression levels in blood leucocytes in normocholesterolaemic (NC) or HC *Wt* and *Lrp5*$^{-/-}$ mice. (**B**) HC *Wt* and HC *Lrp5*$^{-/-}$ mice aortas labelled with HAM56, L, lumen. (**C**) Quantitative analysis of B expressed as number of macrophages/field of vision. (**D**) White blood cells gene expression of pro-inflammatory cytokines in HC *Wt* and HC *Lrp5*$^{-/-}$ mice. *$P < 0.05$; ***$P < 0.005$.

Expression of pro-inflammatory cytokines in white blood cells

We then analysed gene expression levels of pro-inflammatory cytokines in white blood cells from HC *Wt* and HC *Lrp5*$^{-/-}$ mice. Results show an increase of *Il18*, *Il15* and *Il1*β mRNA expression by 62.5 ± 2%, 43 ± 1% and 91 ± 2% respectively in HC *Lrp5*$^{-/-}$ compared with HC *Wt* mice (Fig. 3D). These results show increased inflammation in HC *Lrp5*$^{-/-}$ mice respect to their *Wt* littermates.

Wnt pathway activation in mice aortas

Levels of two proteins of the canonical Wnt pathway, β-CATENIN and MMP-7 were analysed in macroscopically ORO-stained areas of the aortas of *Wt* and *Lrp5*$^{-/-}$ mice. β-CATENIN staining was increased in aortas of HC *Wt* mice compared to NC *Wt* mice indicating an activation of the Wnt/β-CATENIN pathway by hypercholesterolaemia. As expected, there was no increase in β-CATENIN staining in HC *Lrp5*$^{-/-}$ mice (Fig. 4A and B). Similarly MMP-7, another downstream protein of the pathway, was up-regulated in HC *Wt* compared with NC *Wt* mice, while in aortas from HC *Lrp5*$^{-/-}$ mice, the area covered by MMP-7 staining was smaller (Fig. 4C and D). These results suggest that the canonical Wnt/β-CATENIN pathway is triggered by mild dyslipidaemia as a protective response and that this effect cannot be produced when LRP5 is absent.

LDL receptors in WT and LRP5$^{-/-}$ mice aortas

LRP5 belongs to the LDL receptor superfamily of proteins involved in lipoprotein trafficking [5]. To determine if other receptors were causing the lipid infiltration observed in aortas of *Lrp5*$^{-/-}$ mice, we analysed gene expression of receptors described to be involved in the initial stages of atherosclerosis lesions. Results show that *Lrp2* gene expression was strongly down-regulated in *Lrp5*$^{-/-}$ mice independently of diet (Fig. 5A), while *Lrp8* gene expression was down-regulated in *Wt* and *Lrp5*$^{-/-}$ mice after HC diet (21.05 ± 2% and 57.14 ± 2% respectively, Fig. 5B). Similarly, the classical *Ldlr* mRNA expression levels were reduced with HC feeding in both genotypes (21.4 ± 0.5% in HC *Wt* respect to NC *Wt* and 23.6 ± 1% in *Lrp5*$^{-/-}$, Fig. 5C). *Cd36* increased its mRNA expression by 48.2 ± 1% in HC *Wt* mice with respect to NC *Wt* animals, but showed a 41.6 ± 0.5% decrease in HC *Lrp5*$^{-/-}$ mice with respect to NC *Lrp5*$^{-/-}$ mice (Fig. 5D). On the contrary, *Lrp1* significantly increased by 37 ± 2% in HC *Wt* mice and 21 ± 9% in HC *Lrp5*$^{-/-}$ mice aortas with respect to their NC littermates, but there was no significant effect because of HC in the *Lrp5*$^{-/-}$ mice (Fig. 6A). The *Vldlr* mRNA levels were up-regulated by the HC diet in *Wt* and *Lrp5*$^{-/-}$ mice, although in a non-significant manner (Fig. 6B). Finally, *Lrp6* mRNA expression levels were increased by 31 ± 2% in HC *Lrp5*$^{-/-}$ mice with respect to NC *Lrp5*$^{-/-}$ mice (Fig. 6C). Regression analyses revealed a significant positive correlation between *Lrp6* gene expression levels and lipid rich coverage in aortas of *Lrp5*$^{-/-}$ mice, but not for *Lrp1* (Fig. 6D).

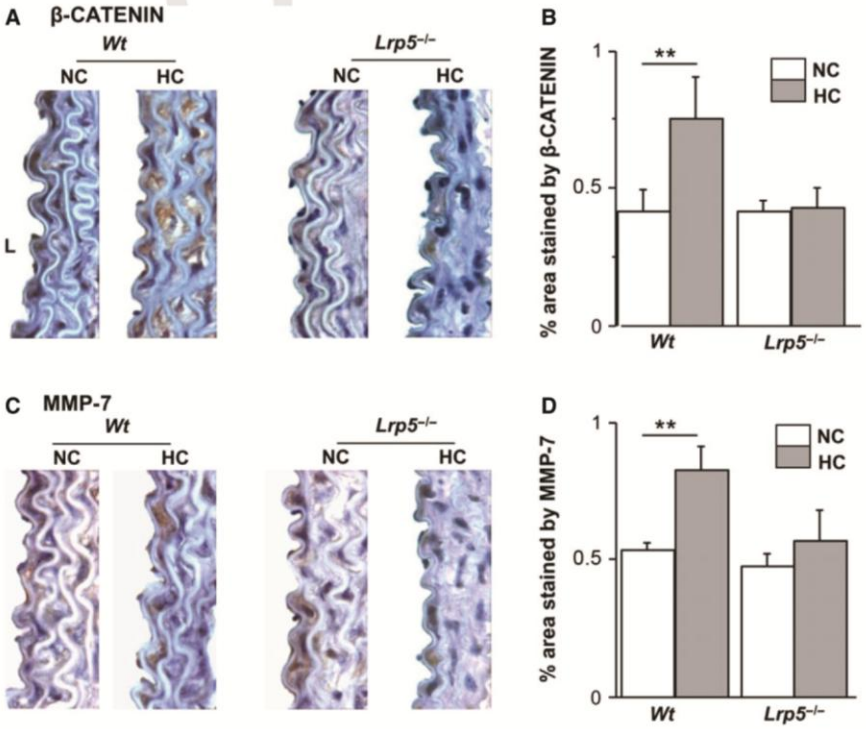

Fig. 4 Wnt pathway modulation in aortas from *Wt* and *Lrp5*$^{-/-}$ mice. (**A**) Representative images of aortas sections immunostained with β-CATENIN in normocholesterolaemic (NC) or hypercholesterolaemic (HC) *Wt* and *Lrp5*$^{-/-}$ mice. (**B**) % area stained by β-CATENIN. (**C**) Representative images of aortas sections immunostained with MMP-7 in NC or a HC *Wt* and *Lrp5*$^{-/-}$ mice. (**D**) Quantitative analysis of aortas in C. $^{**}P < 0.01$.

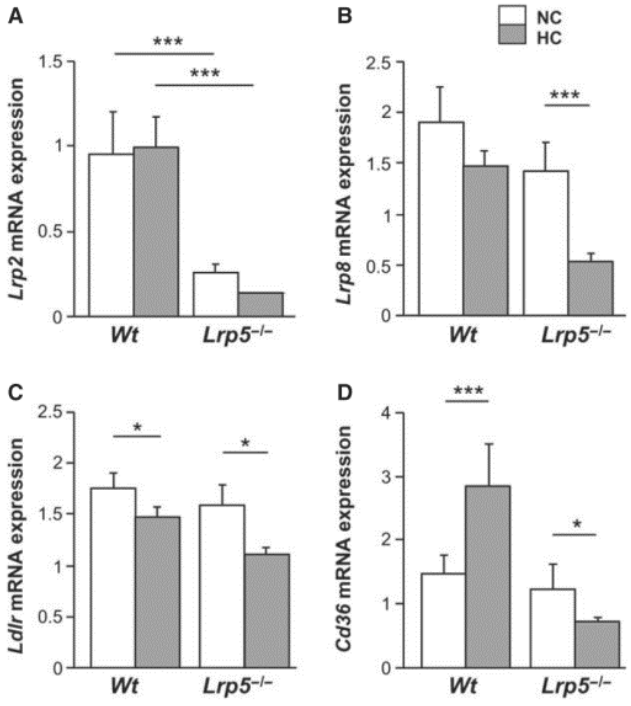

Fig. 5 Receptors expression in mice aortas. mRNA expression levels of *Lrp2* (**A**), *Lrp8* (**B**), *Ldlr* (**C**) and *Cd36* (**D**) in aortas from *Wt* and *Lrp5*$^{-/-}$ mice fed a normocholesterolaemic (NC) or a hypercholesterolaemic (HC) diet. $*P < 0.05$; $***P < 0.005$.

Discussion

Over the last decades, LRP5 has been involved in several pathways, including bone development, impaired fat tolerance and glucose metabolism [8, 17–19]. Impaired plasma clearance of chylomicron remnants and reduced glucose tolerance was observed in LRP5-deficient mice fed a high-fat diet compared with their *Wt* littermates [17]. Here, we have studied the role of LRP5 and the canonical Wnt pathway in mildly HC *Lrp5*$^{-/-}$ mice. Total cholesterol and non-HDL plasma levels increased after HC feeding in *Wt* and *Lrp5*$^{-/-}$ mice. However, total cholesterol levels in HC *Lrp5*$^{-/-}$ mice that had a significantly higher aortic lipid infiltration were higher than those in HC *Wt* mice, suggesting an involvement for LRP5 during dyslipidaemia, at the initial stages of atherosclerosis development. Similarly in humans, LPR5-rs3736228T alleles that cause loss-of-function in LRP5 protein show increased plasmatic cholesterol levels in Chinese Han population [20] and is considered an independent risk factor for hypercholesterolaemia in the male Japanese population [21].

Hypercholesterolaemic *Lrp5*$^{-/-}$ mice show larger lipid infiltration in the thoracic aorta compared with HC *Wt* animals. Accordingly, IHC analyses revealed an increase in macrophage staining in the intima layer of HC *Lrp5*$^{-/-}$ mice aortas confirming our previous *in vitro* results showing that monocytes that overexpress LRP5 show a down-regulation of the differentiation processes by the sequestration of β-CATENIN to the cell membranes [12]. Consequently, here we show that mice lacking LRP5 have more macrophages in the vascular wall. Activated monocytes/macrophages stimulate cytokine secretion

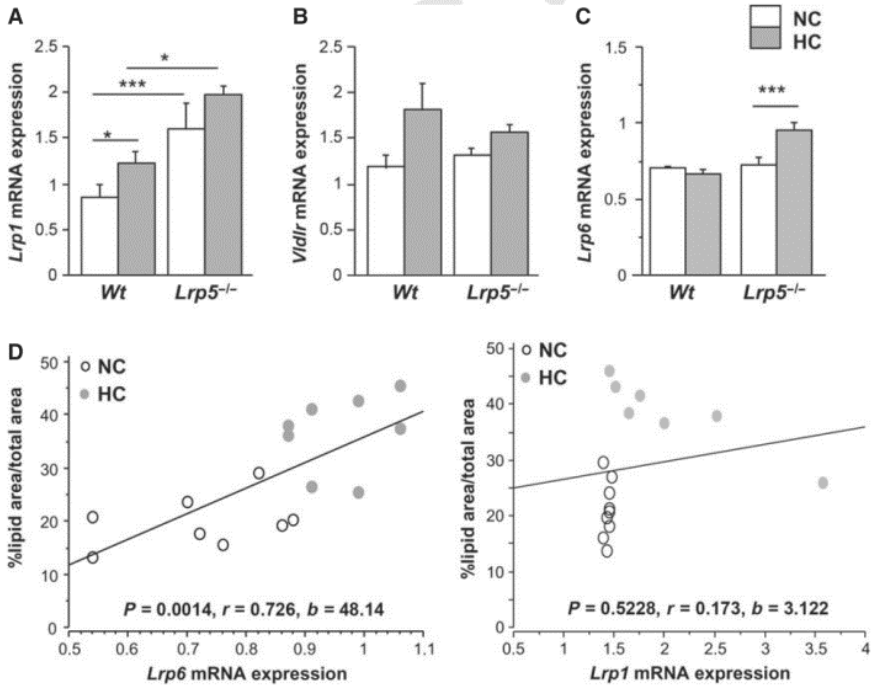

Fig. 6 Receptors expression in mice aortas. mRNA expression levels of *Lrp1* (**A**), *Vldlr* (**B**) and *Lrp6* (**C**) in aortas from *Wt* and *Lrp5*$^{-/-}$ mice fed a normocholesterolaemic (NC) or a hypercholesterolaemic (HC) diet. $*P < 0.05$; $***P < 0.005$. (**D**) Regression analyses between aortic lipid coverage and *Lrp6* or *Lrp1* gene expression levels in aortas of *Lrp5*$^{-/-}$ mice with their statistical significances (p), correlation coefficients (r) and slopes (b).

promoting pro-inflammatory chronic stimulation [1, 22, 23]. Therefore, we analysed the expression of pro-inflammatory and pro-atherogenic cytokines (*Il18*, *Il15* and *Il1*β) in white blood cells from HC *Wt* and HC *Lrp5*$^{-/-}$ mice [24–27]. Wnt/β-CATENIN activation inhibits the inflammatory response in endothelial cells [9] and enhances injury repair and healing responses in other inflammatory diseases including rheumatoid arthritis and colitis [28]. We found increased inflammatory cytokines gene expression in white blood cells from HC *Lrp5*$^{-/-}$ mice indicating increased inflammation.

IHC analyses revealed a down-regulation of the Wnt canonical pathway members, β-CATENIN and MMP7, in the absence of LRP5 evidencing a down-regulation of the canonical Wnt signalling pathway in HC *Lrp5*$^{-/-}$ mice aortas. This supports our previous *in vitro* findings showing that LRP5 silencing in human macrophages abrogates Wnt/β-CATENIN pathway activation [13].

Aortic *Lrp6* expression increased in *Lrp5*$^{-/-}$ animals fed the HC diet and directly correlated with aortic lesion area. LRP6 has been found overexpressed in human atherosclerotic lesions [29] and regulates LDLR-mediated LDL uptake as LDLR internalization is severely diminished in *Lrp6*$^{-/-}$ cells [30]. We analysed the expression of other receptors that have been described to participate in lipid internalization. Indeed, LRP2 contributes to HDL metabolism by internalizing ApoA-I and ApoA-II, which are structural components of HDLs [31]; LRP8 is a component of the interactions between the endothelium and monocytes and leucocyte transendothelial migration, foam cell formation and activation of platelet aggregation [32]; and the classical LDLR is known for its involvement in lipoprotein transport and plasmatic LDL cholesterol clearance [33]. *Lrp2*, *Lrp8* and *Ldlr* expression levels were down-regulated in aortas from HC *Lrp5*$^{-/-}$ indicating that they were not contributing to the observed lipid deposition in mice aortas. The atherogenicity of CD36 remains unclear, CD36 deficiency has been associated with enhanced atherosclerotic cardiovascular diseases [34], but cultured macrophages from these patients present a reduced uptake of oxidized LDL [35]. Our results do not support the contribution of *Cd36* to the lipid-rich phenotype of *Lrp5*$^{-/-}$ mice aortas as its expression is increased in HC *Wt* mice but reduced in HC *Lrp5*$^{-/-}$ mice. *Lrp1* is up-regulated in aortas from *Lrp5*$^{-/-}$ mice. LRP1 has been found up-regulated in advanced human atherosclerotic plaques where its up-regulation is induced by extracellular lipids in human smooth muscle cells and human macrophages [36, 37]. Up-regulated LRP1 expression is also found in the aorta of rabbits and pigs after HC diets suggesting a pro-atherogenic role for LRP1 overexpression [36, 38]. Consistently, here we show enhanced *Lrp1* expression levels in HC conditions in *Wt* and *Lrp5*$^{-/-}$ mice. *Vldlr*, a multiligand receptor that binds VLDL and chylomicron remnants [39] is not highly modified by mild hypercholesterolaemia or LRP5$^{-/-}$.

Interestingly, there was an increase in *Lrp6* gene expression levels in aortas of *Lrp5*$^{-/-}$ animals after HC feeding; however, *Lrp6* did not trigger the canonical Wnt pathway. *Lrp5*$^{-/-}$ and *Lrp6*$^{-/-}$ mice have different phenotypes suggesting that these receptors cannot compensate each other's function [40–42]. Also, mammary stem cells require LRP5 to trigger Wnt signalling despite of LRP6 co-expression [42]. In view of our results, we suggest that *Lrp1* and *Lrp6* contribute to the increased aortic lipid deposition observed in HC *Lrp5*$^{-/-}$ mice, but further analysis on the LRP1-LRP5 and LRP6-LRP5 interactions are needed to better characterize this hypothesis.

In conclusion, our findings show that lipid depositions in the aorta are larger in HC *Lrp5*$^{-/-}$ mice with mildly increased levels of blood cholesterol demonstrating a protector role for LRP5 in the vascular wall. LRP5 and proteins from the Wnt/β-CATENIN pathway are up-regulated in HC *Wt* aortas and this increase is lost when LRP5 is absent. The absence of LRP5 regulates the dyslipidaemic profile by promoting lipid and macrophage retention in the vessel wall and increasing leucocyte driven systemic inflammation.

Acknowledgements

We thank S Huerta, M Amado and S Florit for technical assistance, Dr. Camino for help with genes and proteins nomenclature and Dr. Juan for the IHC analyses. This work was supported by grants from the Spanish Ministry of Economy and Competitiveness (SAF 2010-16549 to LB), Institute of Health Carlos III, ISCIII (TERCEL RD12/0019/0026 and RIC RD12/0042/0027 to LB); I3 Contract (to MBP) and a Danone Institute Fellowship (to CRS). MBP designed the research, performed experiments, analysed, interpreted data and co-wrote the manuscript, CRS performed experiments, collected data and co-wrote the manuscript, LB co-wrote the manuscript and provided resources for the study.

Conflicts of interest

The authors confirm that there are no conflicts of interest.

References

1. **Badimon L, Storey RF, Vilahur G.** Update on lipids, inflammation and atherothrombosis. *Thromb Haemost*. 2011; 105(Suppl. 1): S34–42.
2. **Nissen SE, Tuzcu EM, Schoenhagen P, *et al.*** Statin therapy, LDL cholesterol, C-reactive protein, and coronary artery disease. *N Engl J Med*. 2005; 352: 29–38.
3. **Badimon L, Vilahur G.** LDL-cholesterol *versus* HDL-cholesterol in the atherosclerotic plaque: inflammatory resolution *versus* thrombotic chaos. *Ann N Y Acad Sci*. 2012; 1254: 18–32.
4. **Jeon H, Blacklow SC.** Structure and physiologic function of the low-density lipoprotein receptor. *Annu Rev Biochem*. 2005; 74: 535–62.
5. **Go G-W, Mani A.** Low-density lipoprotein receptor (LDLR) family orchestrates cholesterol homeostasis. *Yale J Biol Med*. 2012; 85: 19–28.
6. **Gelfand BD, Meller J, Pryor AW, *et al.*** Hemodynamic activation of beta-catenin and T-cell-specific transcription factor signaling in vascular endothelium regulates fibronectin expression. *Arterioscler Thromb Vasc Biol*. 2011; 31: 1625–33.
7. **Bedel A, Nègre-Salvayre A, Heeneman S, *et al.*** E-cadherin/beta-catenin/T-cell factor pathway is involved in smooth muscle cell proliferation elicited by oxidized

low-density lipoprotein. *Circ Res*. 2008; 103: 694–701.

8. **Magoori K, Kang M-J, Ito MR, *et al.*** Severe hypercholesterolemia, impaired fat tolerance, and advanced atherosclerosis in mice lacking both low density lipoprotein receptor-related protein 5 and apolipoprotein E. *J Biol Chem*. 2003; 278: 11331–6.
9. **Kim J, Kim J, Kim DW, *et al.*** Wnt5a induces endothelial inflammation *via* beta-catenin-independent signaling. *J Immunol*. 2010; 185: 1274–82.
10. **Martin M, Rehani K, Jope RS, *et al.*** Toll-like receptor-mediated cytokine production is differentially regulated by glycogen synthase kinase 3. *Nat Immunol*. 2005; 6: 777–84.
11. **Von Toerne C, Schmidt C, Adams J, *et al.*** Wnt pathway regulation in chronic renal allograft damage. *Am J Transplant*. 2009; 9: 2223–39.
12. **Borrell-Pagès M, Romero JC, Badimon L.** LRP5 negatively regulates differentiation of monocytes through abrogation of Wnt signalling. *J Cell Mol Med*. 2014; 18: 314–25.
13. **Borrell-Pagès M, Romero JC, Juan-Babot O, *et al.*** Wnt pathway activation, cell migration, and lipid uptake is regulated by low-density lipoprotein receptor-related protein 5 in human macrophages. *Eur Heart J*. 2011; 32: 2841–50.
14. **Holmen SL, Giambernardi TA, Zylstra CR, *et al.*** Decreased BMD and limb deformities in mice carrying mutations in both Lrp5 and Lrp6. *J Bone Miner Res*. 2004; 19: 2033–40.
15. **Lindvall C, Evans NC, Zylstra CR, *et al.*** The Wnt signaling receptor Lrp5 is required for mammary ductal stem cell activity and Wnt1-induced tumorigenesis. *J Biol Chem*. 2006; 281: 35081–7.
16. **Cui Y, Niziolek PJ, MacDonald BT, *et al.*** Lrp5 functions in bone to regulate bone mass. *Nat Med*. 2011; 17: 684–91.
17. **Fujino T, Asaba H, Kang M-J, *et al.*** Low-density lipoprotein receptor-related protein 5 (LRP5) is essential for normal cholesterol metabolism and glucose-induced insulin secretion. *Proc Natl Acad Sci USA*. 2003; 100: 229–34.
18. **Gong Y, Slee RB, Fukai N, *et al.*** LDL receptor-related protein 5 (LRP5) affects bone accrual and eye development. *Cell*. 2001; 107: 513–23.
19. **Little RD, Carulli JP, Del Mastro RG, *et al.*** A mutation in the LDL receptor-related protein 5 gene results in the autosomal dominant high-bone-mass trait. *Am J Hum Genet*. 2002; 70: 11–9.
20. **Jiang X-Y, Chen Y, Xu L, *et al.*** Association of LPR5 polymorphism with bone mass density and cholesterol level in population of Chinese Han. *Exp Clin Endocrinol Diabetes*. 2010; 118: 388–91.
21. **Urano T, Shiraki M, Usui T, *et al.*** A1330V variant of the low-density lipoprotein receptor-related protein 5 (LRP5) gene decreases Wnt signaling and affects the total body bone mineral density in Japanese women. *Endocr J*. 2009; 56: 625–31.
22. **Shalhoub J, Falck-Hansen MA, Davies AH, *et al.*** Innate immunity and monocyte-macrophage activation in atherosclerosis. *J Inflamm (Lond)*. 2011; 8: 9.
23. **Libby P, Ridker PM, Hansson GK.** Inflammation in atherosclerosis: from pathophysiology to practice. *J Am Coll Cardiol*. 2009; 54: 2129–38.
24. **Badimon L.** Interleukin-18: a potent pro-inflammatory cytokine in atherosclerosis. *Cardiovasc Res*. 2012; 96: 172–5; discussion 176–180.
25. **Kirii H, Niwa T, Yamada Y, *et al.*** Lack of interleukin-1beta decreases the severity of atherosclerosis in ApoE-deficient mice. *Arterioscler Thromb Vasc Biol*. 2003; 23: 656–60.
26. **Houtkamp MA, van Der Wal AC, de Boer OJ, *et al.*** Interleukin-15 expression in atherosclerotic plaques: an alternative pathway for T-cell activation in atherosclerosis? *Arterioscler Thromb Vasc Biol*. 2001; 21: 1208–13.
27. **Wuttge DM, Eriksson P, Sirsjö A, *et al.*** Expression of interleukin-15 in mouse and human atherosclerotic lesions. *Am J Pathol*. 2001; 159: 417–23.
28. **Whyte JL, Smith AA, Helms JA.** Wnt signaling and injury repair. *Cold Spring Harb Perspect Biol*. 2012; 4: a008078.
29. **Keramati AR, Singh R, Lin A, *et al.*** Wild-type LRP6 inhibits, whereas atherosclerosis-linked LRP6R611C increases PDGF-dependent vascular smooth muscle cell proliferation. *Proc Natl Acad Sci USA*. 2011; 108: 1914–8.
30. **Ye Z, Go G-W, Singh R, *et al.*** LRP6 protein regulates low density lipoprotein (LDL) receptor-mediated LDL uptake. *J Biol Chem*. 2012; 287: 1335–44.
31. **Dugué-Pujol S, Rousset X, Château D, *et al.*** Apolipoprotein A-II is catabolized in the kidney as a function of its plasma concentration. *J Lipid Res*. 2007; 48: 2151–61.
32. **Quinn KL, Henriques M, Tabuchi A, *et al.*** Human neutrophil peptides mediate endothelial-monocyte interaction, foam cell formation, and platelet activation. *Arterioscler Thromb Vasc Biol*. 2011; 31: 2070–9.
33. **Brown MS, Goldstein JL.** Receptor-mediated control of cholesterol metabolism. *Science*. 1976; 191: 150–4.
34. **Yuasa-Kawase M, Masuda D, Yamashita T, *et al.*** Patients with CD36 deficiency are associated with enhanced atherosclerotic cardiovascular diseases. *J Atheroscler Thromb*. 2012; 19: 263–75.
35. **Nozaki S, Kashiwagi H, Yamashita S, *et al.*** Reduced uptake of oxidized low density lipoproteins in monocyte-derived macrophages from CD36-deficient subjects. *J Clin Invest*. 1995; 96: 1859–65.
36. **Llorente-Cortés V, Otero-Viñas M, Sánchez S, *et al.*** Low-density lipoprotein upregulates low-density lipoprotein receptor-related protein expression in vascular smooth muscle cells: possible involvement of sterol regulatory element binding protein-2-dependent mechanism. *Circulation*. 2002; 106: 3104–10.
37. **Llorente-Cortés V, Badimon L.** LDL receptor-related protein and the vascular wall: implications for atherothrombosis. *Arterioscler Thromb Vasc Biol*. 2005; 25: 497–504.
38. **Llorente-Cortes V, Casani L, Cal R, *et al.*** Cholesterol-lowering strategies reduce vascular LRP1 overexpression induced by hypercholesterolaemia. *Eur J Clin Invest*. 2011; 41: 1087–97.
39. **Takahashi S, Suzuki J, Kohno M, *et al.*** Enhancement of the binding of triglyceride-rich lipoproteins to the very low density lipoprotein receptor by apolipoprotein E and lipoprotein lipase. *J Biol Chem*. 1995; 270: 15747–54.
40. **Pinson KI, Brennan J, Monkley S, *et al.*** An LDL-receptor-related protein mediates Wnt signalling in mice. *Nature*. 2000; 407: 535–8.
41. **Kato M, Patel MS, Levasseur R, *et al.*** Cbfa1-independent decrease in osteoblast proliferation, osteopenia, and persistent embryonic eye vascularization in mice deficient in Lrp5, a Wnt coreceptor. *J Cell Biol*. 2002; 157: 303–14.
42. **Goel S, Chin EN, Fakhraldeen SA, *et al.*** Both LRP5 and LRP6 receptors are required to respond to physiological Wnt ligands in mammary epithelial cells and fibroblasts. *J Biol Chem*. 2012; 287: 16454–66.

ARTÍCULO 4

Cholesterol modulates LRP5 expression in the vessel wall.

Autores: María Borrell-Pagés[a±], July Carolina Romero[a±], Lina Badimon[a,b,].

Revista: Atherosclerosis 2014; 235(2):363-70.

Factor de impacto: 3.71

Centro de Investigación Cardiovascular CSIC-ICCC, Hospital de la Santa Creu i Sant Pau, Barcelona, España.

[±] Co-primeros autores

RESUMEN

El colesterol modula la expresión de LRP5 en la pared de los vasos sanguíneos.

Los macrófagos son muy importantes en la formación y progresión de la lesión aterosclerótica. Hemos demostrado que los macrófagos cargados de lípidos tienen la vía canónica de señalización por Wnt activada. Para estudiar *in vivo* la función de la vía canónica de Wnt en la aterosclerosis utilizamos ratones deficientes para *Lrp5*$^{-/-}$ alimentados con una dieta hipercolesterolémica (HC) para inducir aterosclerosis. La dieta HC fue suplementada o no con fitoesteroles esterificados (PSE) al 2% y administrada durante 8 semanas.

Los ratones *Wt* HC presentaron un moderado incremento de los niveles de colesterol non-HDL en sangre, desarrollaron lesiones ateroscleróticas y mostraron altos niveles de expresión de LRP5 en la aorta. Los ratones *Lrp5*$^{-/-}$ HC desarrollaron lesiones ateroscleróticas de mayor tamaño que las de los ratones *Wt*, indicando que LRP5 tiene una función protectora en la progresión de la aterosclerosis. La administración de PSE reduce los niveles de colesterol en suero, elimina la sobreexpresión de LRP5 inducida por la dieta HC y reduce el tamaño de las placas ateroscleróticas en la aorta.

Nuestros resultados demuestran que los efectos proaterogénicos ocasionados por el exceso de lípidos en el plasma están mediados en parte por la modulación de LRP5 en la aorta y que LRP5

y la vía canónica de señalización por Wnt ejercen un mecanismo de defensa protector en contra de la hiperlipemia y la progresión de las lesiones ateroscleróticas.

Atherosclerosis 235 (2014) 363–370

Contents lists available at ScienceDirect

Atherosclerosis

journal homepage: www.elsevier.com/locate/atherosclerosis

Cholesterol modulates LRP5 expression in the vessel wall

M. Borrell-Pages [a, 1], J.C. Romero [a, 1], L. Badimon [a, b, *]

[a] Cardiovascular Research Center, CSIC-ICCC, Hospital de la Santa Creu i Sant Pau, IIB-Sant Pau, Barcelona, Spain
[b] Cardiovascular Research Chair, UAB, Barcelona, Spain

ARTICLE INFO

Article history:
Received 7 February 2014
Received in revised form
7 May 2014
Accepted 7 May 2014
Available online 2 June 2014

Keywords:
LRP5
Macrophages
Atherosclerosis
Plant sterol esters
Hypercholesterolemia
Wnt pathway

ABSTRACT

Objective: Macrophages are key players in atherosclerotic lesion formation and progression. We have recently demonstrated that lipid-loaded macrophages show activation of the canonical Wnt signaling pathway.
Methods: To test the *in vivo* role of the canonical Wnt pathway in atherosclerosis we used mice deficient in the Wnt signaling receptor LRP5 ($LRP5^{-/-}$) fed a hypercholesterolemic diet (HC) to induce atherosclerosis. These dietary groups were further subdivided into two subgroups receiving their respective diets supplemented with 2% plant sterol esters (PSE). All mice remained on their assigned diets until age 18 weeks.
Results: HC WT mice had mildly increased non-HDL cholesterol levels, developed aortic atherosclerotic lesions and showed upregulated expression levels of aortic Lrp5. HC $LRP5^{-/-}$ mice develop larger aortic atherosclerotic lesions than WT mice indicating that LRP5 has a protective function in atherosclerosis progression. The oral administration of PSE, a dietary cholesterol-lowering agent, had an effect in the expression levels of the Wnt signaling receptor and in atherosclerosis progression. We found that PSE reduced serum total cholesterol levels, abolished HC-induced LRP5 overexpression and reduced aortic atherosclerotic plaques.
Conclusion: The proatherogenic effects of the excess of plasma lipids are in part mediated by modulation of LRP5 in the aorta. LRP5 and canonical Wnt signaling exert a protective defense mechanism against hyperlipidemia and atherosclerosis lesion progression.

1. Introduction

Atherosclerotic lesions are formed by the accumulation of lipids and fibrous elements in large and medium size arteries in response to injury [1]. Under physiological conditions, cells store fatty acids and fatty alcohols in the form of neutral lipids (triacylglycerols, TAG and cholesteryl esters, CE) that are used for membrane formation and energy supply [2]. However, elevated cytoplasmic deposition of neutral lipids is a significant risk factor for several pathologies. For example, the accumulation of CE in smooth muscle cells and macrophages in the vessel wall comprises the earliest recognizable stage in atherosclerotic plaque formation [2]. Furthermore, serum levels of TAG and total cholesterol are independent risk factors for atherosclerosis. High low-density lipoprotein plasma levels (LDL) are also considered risk factors for atherosclerosis [3–5]. Atherosclerotic plaques are characterized by the accumulation of lipid-loaded foam cells, increased levels of oxidized-LDL, HDL, TAG, phospholipids, and oxysterols, and the accumulation of fibrinogen, apo-AI, clusterin and paraoxonase [6–8]. Lipid droplets in the intima wall contain about half the lipids in the lesions with a composition of 95% CE, 1.5% free cholesterol, 1% phospholipids and 2,5% TAG [9].

Lipid internalization in the vascular wall is mediated by the LDL superfamily of receptors including LDLR, VLDLR, LDL receptor-related proteins (LRPs) and scavenger receptors [10]. Our group showed that two LRPs, LRP1 and LRP5 are involved in lipid uptake leading to an increase in intracellular CE accumulation in human vascular smooth muscle cells and macrophages [11,12].

LRP5 is a receptor of the canonical Wnt/β-catenin pathway. LRP5 involvement in the modulation of glucose-induced insulin secretion was shown with $LRP5^{-/-}$ mice that had a decreased glucose-induced insulin secretion as a result of reduced cellular ATP and calcium levels in pancreatic islets [13]. LRP5 involvement in cholesterol metabolism comes from the observation that $ApoE^{-/-}LRP5^{-/-}$ mice have larger atherosclerotic lesions

* Corresponding author. Cardiovascular Research Center, C/Sant Antoni Maria Claret 167, 08025 Barcelona, Spain. Tel.: +34 935565880; fax: +34 935565559.
E-mail addresses: lbadimon@csic-iccc.org, smorato@csic-iccc.org (L. Badimon).
[1] Both authors contributed equally to this work.

http://dx.doi.org/10.1016/j.atherosclerosis.2014.05.922
0021-9150/

than their ApoE$^{-/-}$ littermates [14]. However, the exceedingly high levels of plasma cholesterol in ApoE$^{-/-}$LRP5$^{-/-}$ mice (almost 750 mg/dl) could have shadowed any effect of LRP5.

Several studies have evaluated the use of plant sterol esters (PSE) as a cholesterol-lowering strategy [15–18]. PSE reduce cholesterol absorption by competitively inhibiting its internalization and processing in enterocytes in the intestine [18,19]. Although the beneficial cardiovascular effects of PSE are mainly because their plasma lipid-lowering capacity, they can decrease growth and proliferation of smooth muscle cells and reduce foam cell formation [20]. PSE can also attenuate the inflammatory response by ameliorating endothelial dysfunction in ApoE$^{-/-}$ mice [21] and decrease aggregated LDL-induced secretion of pro-inflammatory cytokines (TNFα, IL-6 and IL1B) in cultured macrophages [22]. Furthermore, plant sterol feeding have been shown to have anti-inflammatory properties in different cohorts of healthy subjects although its association with reduced cholesterol absorption was not determined [17,23,24].

Our previous results show that LRP5 is overexpressed in cultured lipid-loaded macrophages [12]. Here, we investigated whether the modulation of plasma lipid levels by cholesterol-lowering strategies can modulate the canonical Wnt signaling receptor and cholesteryl ester content in aortic atherosclerotic plaques *in vivo*.

2. Materials and methods

2.1. Experimental design

LRP5$^{-/-}$ mice, a kind gift from Dr. Bart Williams [25–27] were maintained in a C57BL/6 background. Mice were housed in cages under controlled temperature (21 ± 2 °C) on a 12 h light/dark cycle with food and water *ad libitum*. Homozygous wild-type C57BL/6 mice (WT; $n = 34$) and LRP5$^{-/-}$C57BL/6 mice (LRP5$^{-/-}$; $n = 34$) were used for the protocols. The presence of LRP5 alleles was assessed by PCR amplification from DNA extracted from tail biopsies in wild type, heterozygous and homozygous littermates. Primers used were S17 (GGC TCG GAG GAC AGA CCT GAG), S23 (CTG TCA GTG CCT GTA TCT GTC C) and IRES31 (AGG GGC GGA ATT CGA TAG CT). LRP5$^{-/-}$ and WT mice were fed a normal chow diet (NC, Tekland diet, Harland Labs) for 10 weeks. Animals were then divided into 3 groups to be fed with NC diet, high cholesterol diet (HC, TD.88137, Harland Labs) or HC diet supplemented with 2% Plant Sterol Esters (w/w) for further 8 weeks ($n = 8$–12/group). PSE were provided by Danone (Barcelona, Spain). All sterol analyses were performed by gas liquid chromatography. The study protocol was approved by the local institutional animal research committee (ICCC051/5422) and was performed in agreement with the Guide for the Care and Use of Laboratory Animals published by the US National Institutes of Health.

2.2. Biochemical analysis

Blood samples were collected in serum separator gel tubes. Serum was obtained by centrifugation 3500 rpm, 20 min at 4 °C. Cholesterol, triglycerides and HDL levels were measured enzymatically by using commercially available kits (GERNON reagents) and read in a spectrophotometer (MC-15 SOFT; RAL).

2.3. Quantification of atherosclerotic lesions

Mice were anesthetized and aortas were removed, carefully cleaned of adventitial fat under a stereoscopic microscope and longitudinally cut with the luminal surface facing up ($n = 6$–12 mice/group). Aortas were fixed overnight in 4% paraformaldehyde, washed with ddH_2O 1 h in gently shaking and stained with Oil-red-O (ORO) for 30 min. Aortas were rinsed with 70% ethanol and ddH_2O; images were captured by Nikon Eclipse 80i microscope and digitized by Retiga 1300i Fast camera. ORO-stained area was quantified with Image J software and results are expressed as percentage of lipid area/total aortic area.

2.4. Thin layer chromatography (TLC)

Aortas (5 mg) were homogenized in NaOH 0.1 M. The organic solvent was removed under a N_2 stream; the lipid extract was suspended in dichloromethane and TLC was performed on silica G-24 plates. Different concentrations of standards (a mix of cholesterol, cholesterol palmitate, triglycerides, diglycerides and monoglycerides) were applied to each plate. The chromatographic developing solution was heptane/diethyl ether/acetic acid (74:21:4, vol/vol/vol). The spots corresponding to cholesteryl esters (CE), triacylglycerides (TAG), diacylglycerides (DAG), monoacylglycerides (MAG) and free cholesterol (FC) were quantified by densitometry.

2.5. Real-time RT-PCR

Aortas were frozen in liquid nitrogen and aortic RNA was isolated with Trizol® Reagent (Invitrogen) ($N = 5$–8 mice/group). Concentration was determined with a NanoDrop ND-1000 spectrophotometer (NanoDrop Technologies, Inc., Wilmington, DE, USA) and purity was checked by the A260/A280 ratio (ratios between 1.8 and 2.1 were considered acceptable). cDNA was synthesized from 0.5 μg RNA with cDNA Reverse transcription kit (Qiagen). The resulting cDNA samples were amplified with a with RT-PCR thermal cycler (Applied Biosystems 7900HT) and LRP5 (Mm.PT.49a.8045420) and LDLR (Mm.PT.49a.9930556) specific probes. Results were normalized with 18S probe from Applied Biosystems.

2.6. Statistical analysis

Results are expressed as mean ± S.E.M. A Stat View statistical package was used for all the analysis. When possible, comparisons among groups were performed by parametric analysis (one factor ANOVA). Statistical significance was considered when $p < 0.05$.

3. Experimental results

3.1. Hypercholesterolemic diet increases serum cholesterol and aortic lipid deposition

To determine whether cholesterol-lowering strategies modulated serum cholesterol profile in LRP5$^{-/-}$ mice, WT and LRP5$^{-/-}$ mice were fed a hypercholesterolemic (HC) diet supplemented or not with 2% plant sterol esters (HC + PSE). A normocholesterolemic (NC) control group was also analyzed. Diet composition details are shown in Table 1.

Serum levels of total cholesterol, HDL and non-HDL were significantly increased in HC WT mice and HC LRP5$^{-/-}$ mice with respect to their NC littermates (Sup. Table 1). Plant sterol esters supplementation to HC diets in WT mice reduced total cholesterol and non-HDL-C serum concentrations without affecting HDL-C levels as previously described [28]. However, PSE feeding in LRP5$^{-/-}$ mice induced an increase in HDL-C serum levels respect to HC LRP5$^{-/-}$ mice. Serum triglycerides (TAG) concentrations were reduced after PSE + HC diets with respect to HC diets in WT mice while TAG levels did not differ significantly among dietary treatment groups in LRP5$^{-/-}$ mice (Sup. Table 1).

Table 1
Composition of experimental diets.

	Chow diet (NC) %	Hypercholesterolemic diet (HC)	Plant sterol esters diet (HC + PSE)
% Total fat	3,5	22	22
% Cholesterol	0	0,25	0,25
% Sucrose	4,3	34	34
% Calories from protein	18	17	17
% Calories from fat	11	40	40
% PSE	0	0	2

Serum cholesterol levels increased after 8 weeks of HC feeding in both WT and LRP5$^{-/-}$ mice (Fig 1A). Interestingly, the overall increase in serum cholesterol levels in high-fat diet respect to chow diet was double in LRP5$^{-/-}$ mice (125.69 mg/dl) than in their WT littermates (62.25 mg/dl, Fig 1B). The measurement of the formation of lipid-rich plaques in mice aortas showed that HC feeding induced a significant increase in aortic plaque in WT and LRP5$^{-/-}$ mice. However, the extent of lipid aortic coverage was significantly higher in HC LRP5$^{-/-}$ mice (12.8 ± 1.5%) than in HC WT mice (Fig 1C). Regression analyses in HC WT and HC LRP5$^{-/-}$ mice showed a positive correlation ($p = 0.0217$, $r = 0.498$; Fig 1D); LRP5$^{-/-}$ mice had higher serum cholesterol levels and larger atherosclerotic plaques in the aorta.

3.2. Hypercholesterolemic diet increases aortic CE and neutral acylglycerides accumulation

We performed thin layer chromatography (TLC) to analyze the cholesteryl ester (CE) and neutral acylglyceride lipid content in WT and LRP5$^{-/-}$ mice aortas. CE content in WT and LRP5$^{-/-}$ mice increased respectively 49 ± 5% and 87 ± 9% after HC feeding (Fig 2A). Interestingly, LRP5$^{-/-}$ mice showed more aortic neutral acylglyceride lipid accumulation than WT mice independently of diet (Fig 2B).

3.3. LRP5 is overexpressed in aortas of hypercholesterolemic WT mice

We then analyzed Lrp5 and Ldlr gene expression levels in aortas of WT and LRP5$^{-/-}$ mice. Results showed 89 ± 13% increase in Lrp5 gene expression levels in aortas of WT mice after HC diets while Lrp5 expression was almost undetectable in LRP5$^{-/-}$ mice (Fig 2C). As expected, Ldlr expression levels were reduced after HC feeding by 16 ± 1% and 30 ± 2% in WT and LRP5$^{-/-}$ mice respectively (Fig 2D).

3.4. PSE downregulate serum cholesterol levels, reduce aortic plaque coverage and Lrp5 expression induced by hypercholesterolemia in WT mice

Serum cholesterol levels in WT and LRP5$^{-/-}$ mice fed a HC diet were reduced by dietary PSE supplementation (Fig 3A). PSE also reduced the extent in aortic plaque coverage by 8% and 23 ± 1% in WT and LRP5$^{-/-}$ mice respectively (Fig 3B). TLC analyses in mice aortas after dietary PSE feeding showed a 17 ± 2% decrease in CE accumulation in WT mice and a 32 ± 5% reduction in LRP5$^{-/-}$ mice (Fig 3C). Dietary PSE did not modify the neutral acylglyceride content in WT mice, however a decrease was observed in LRP5$^{-/-}$ mice (Fig 3D). Finally, PSE feeding significantly reduced Lrp5 gene expression levels in the aortas of WT mice by 55 ± 2% (Fig 3E) without modifying Ldlr gene expression levels in WT or LRP5$^{-/-}$ mice (Fig 3F). Taken together these results show that PSE reduce

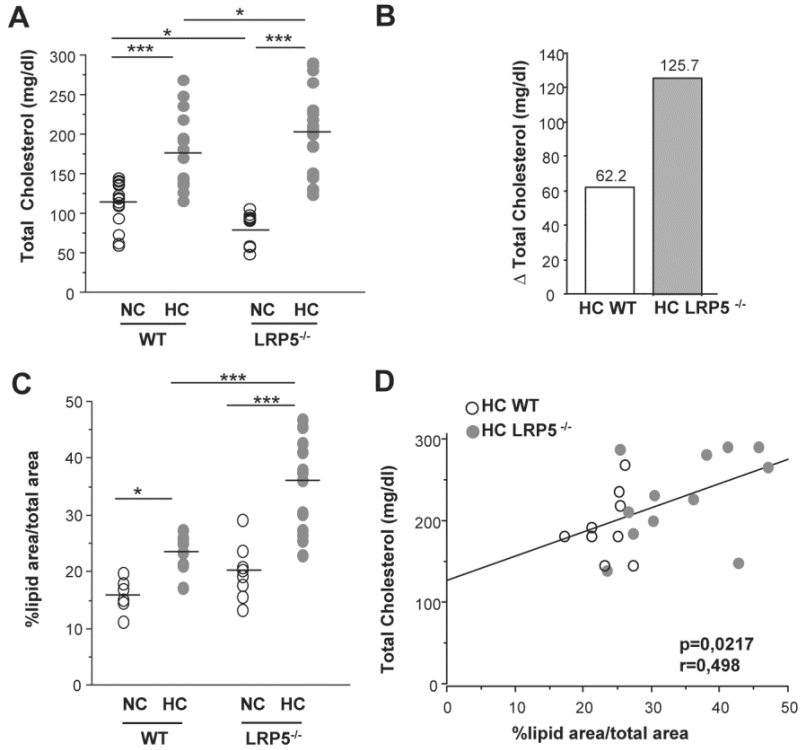

Fig. 1. Lipid profile in WT and LRP5$^{-/-}$ mice. (A) Serum cholesterol levels in WT and LRP5$^{-/-}$ mice. (B) Total serum cholesterol increase in HC WT and HC LRP5$^{-/-}$ mice. (C) Scattergram of aortic lipid coverage in WT and LRP5$^{-/-}$ mice aortas. (D) Linear regression analyses between total cholesterol and %lipid area/total area in HC WT and LRP5$^{-/-}$ mice with p statistical significance and r correlation coefficient $^{*}p < 0.05$; $^{***}p < 0.005$.

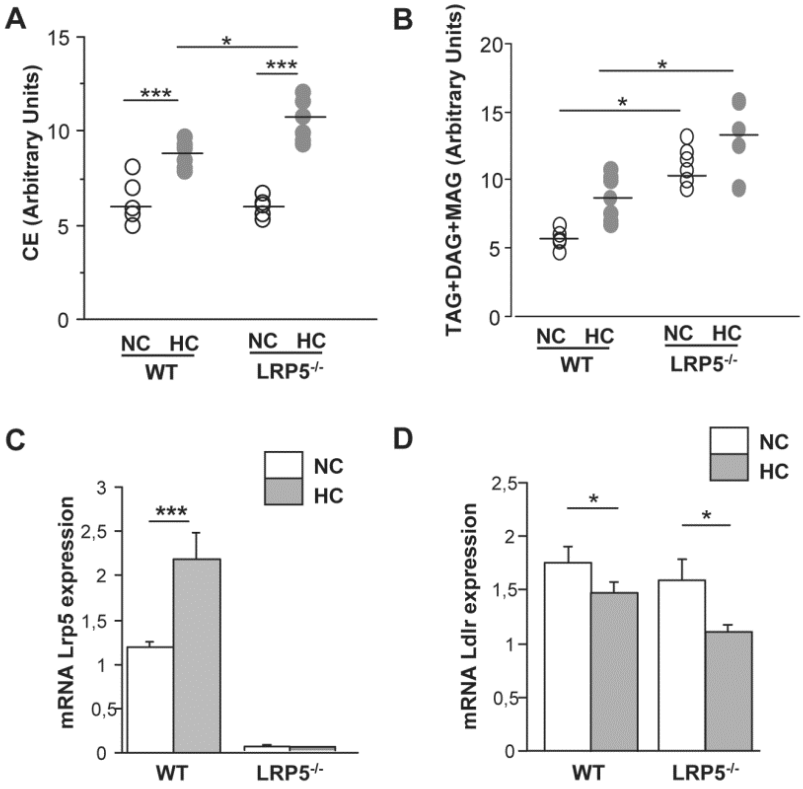

Fig. 2. Lipid composition and gene expression in mice aortas. (A) Cholesteryl esters and (B) acylglycerol content in aortas of WT and LRP5$^{-/-}$ mice. (C) Lrp5 and (D) Ldlr expression levels in aortas of WT and LRP5$^{-/-}$ mice fed an NC or an HC diet. *$p < 0.05$, ***$p < 0.005$.

plasma lipid levels and the lowering of plasma cholesterol induces downregulation of Lrp5 expression levels.

3.5. PSE reduce LRP5 overexpression induced by hypercholesterolemia in aortas of WT mice

Linear regression analyses revealed significant correlation between aortic Lrp5 gene expression and aortic plaque coverage in hypercholesterolemic WT mice ($p = 0.042$; $r = 0.628$, Fig 4A) while no significance could be detected in LRP5$^{-/-}$ mice ($p = 0.491$; $r = 0.210$, Fig 4B). Plotting aortic lipid coverage against non-HDL cholesterol levels after dietary PSE feeding in WT mice reveals a significant correlation ($p = 0.002$; $p = 0.749$, Fig 4C). Moreover, the correlation remains significant between non-HDL cholesterol and Lrp5 expression levels ($p = 0.013$; $r = 0.777$, Fig 4D) showing a cluster of hypercholesterolemic animals mainly displayed to the right reflecting high non-HDL cholesterol levels and upregulated aorta Lrp5 mRNA levels whereas those fed a HC diet supplemented with dietary PSE are found mainly to the left indicating lower non-HDL cholesterol levels and lower Lrp5 expression levels.

4. Discussion

Population studies showed that the LRP5 variant A1330V that causes reduced protein interaction and altered ligand binding [29,30] is associated with hypercholesterolemia. Indeed, the LRP5 A1330V mutation is considered an independent risk factor for hypercholesterolemia in Japanese males [31] and is associated with increased plasma cholesterol levels in the Chinese Han cohort [32]. In this report we describe the relation between plasma lipid concentrations and LRP5 expression levels in a hypercholesterolemic model of LRP5$^{-/-}$ mice challenged with high cholesterol feeding and by a lipid-lowering agent. LRP5$^{-/-}$ mice fed a HC diet showed higher serum cholesterol levels and developed larger aortic lesions than their WT littermates suggesting that LRP5 is required for cholesterol regulation. Moreover, total cholesterol levels correlated with aortic lipid coverage.

Some Wnt proteins and targets have been shown to be upregulated by hypercholesterolemia. Indeed, an up-regulation of β-catenin protein levels has been described in myocardium of hypercholesterolemic rats [33], while an increase in LRP5 gene expression levels has been described in livers of Watanabe rabbits [34] and in aortic valves of ApoE$^{-/-}$ mice [35]. Furthermore, chronic hypercholesterolemia induced an increase in LRP5 and β-catenin protein expression in the aortic valves of Watanabe rabbits [36].

LRP5 deficiency in mice fed a HC diet lead to increased plasma cholesterol levels [13] while NC mice did not develop high cholesterol levels [14]. Consistently, in our study, HC LRP5$^{-/-}$ mice show a mild increase of serum cholesterol (210 mg/dl). Interestingly, in the Rajammanan 2011 study, LRP5 was necessary for the development of valve calcification in experimental hypercholesterolemia as HC LRP5$^{-/-}$ mice had no calcification on the valves, and there was a decreased calcification in LRP5$^{-/-}$:ApoE$^{-/-}$ mice compared with ApoE$^{-/-}$ mice [35], while in our study HC LRP5$^{-/-}$ mice developed larger aortic lesions than WT mice, indicating an atheroprotective role for LRP5. The differences in these results can be explained by mouse strain related differences as the LRP5$^{-/-}$ mice used in the Rajamannan's study were provided by Taconic. Also, ApoE$^{-/-}$:LRP5$^{-/-}$ mice had very high serum cholesterol levels (ApoE$^{-/-}$: 1761 mg/dl) while in our study serum cholesterol levels

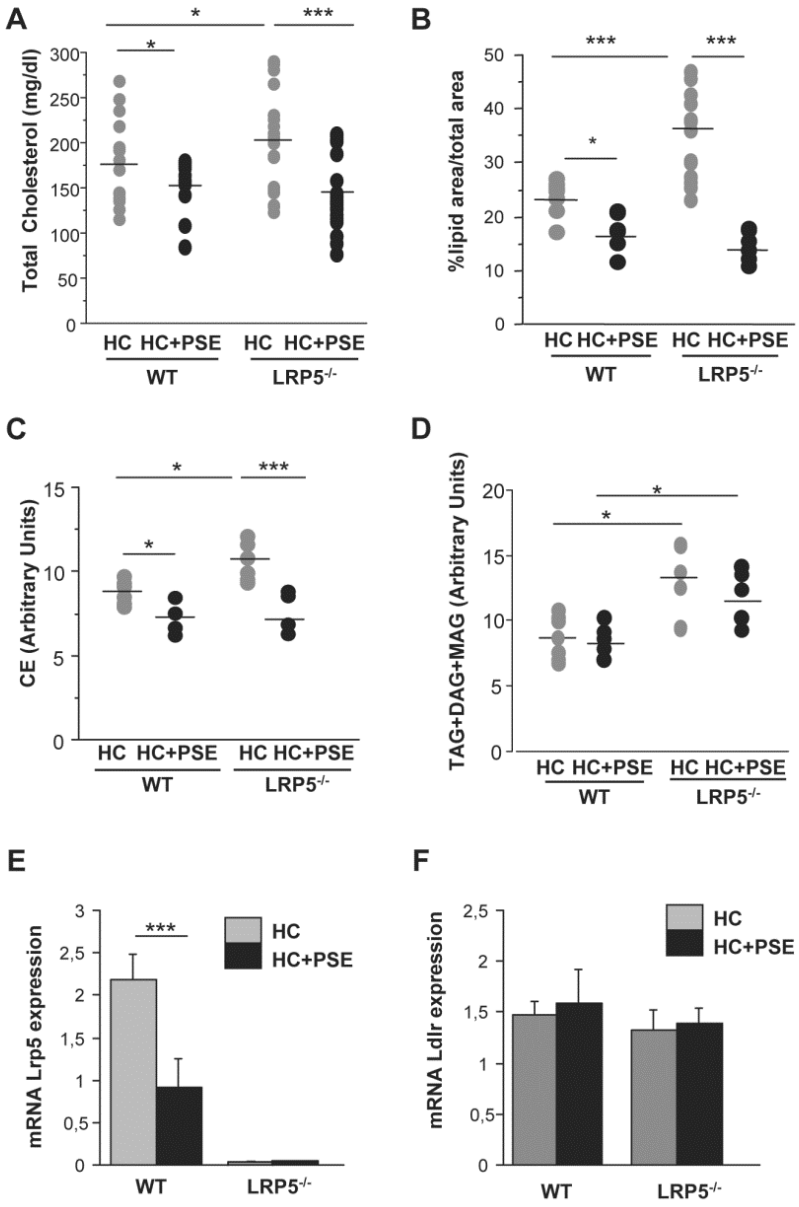

Fig. 3. Lipid composition and gene expression in mice aortas. (A) Serum cholesterol levels of WT and LRP5$^{-/-}$ mice. (B) Lipid accumulation, (C) cholesteryl esters and (D) acylglycerols content in aortas of WT and LRP5$^{-/-}$ mice fed an HC diet with or without dietary PSE. Lrp5 (E) and Ldlr (F) expression levels in aortas of WT and LRP5$^{-/-}$ mice fed a HC or a HC + PSE diet. *$p < 0.05$, ***$p < 0.005$.

were 10 times lower. Finally, the development of aortic valve lesions does not only depend on serum cholesterol levels but also depends on blood pressure and cellular calcium handling and mineralization [35]. Indeed aortic valve calcifications are complex lesions; a study in humans with aortic stenosis did not show benefit from statin treatment and reduction of cholesterol [37].

Our results are in agreement with previous results where ApoE$^{-/-}$:LRP5$^{-/-}$ mice had ~3-fold larger lesions than ApoE$^{-/-}$ mice [14]. Furthermore, unpublished results from our lab show increased aortic expression of LDLR family members and higher macrophage infiltration in HC LRP5$^{-/-}$ mice suggesting that other LDLR members are involved in LRP5$^{-/-}$ mice atherosclerosis progression.

Atherosclerotic plaques are formed by free fatty acids, cholesterol and neutral lipids including acylglycerides and cholesteryl esters [8]. Neutral lipids carry a highly unsaturated pool of fatty acyl groups and they are the main component of LDL particles and atherosclerotic plaques [38]. Since the increase of some neutral lipids is associated with the extent of atherosclerosis progression [39–41] we performed thin layer chromatography and analyzed the CE and acylglyceride lipids content in mice aortas. We found an increase in CE content in aortas of WT mice after HC feeding concomitant with an increase in aortic Lrp5 gene expression. These results support our previous cell culture results where aggregated LDL upregulated macrophage LRP5 gene and protein expression [12]. Indeed, LRP5 upregulation in macrophages due to lipid

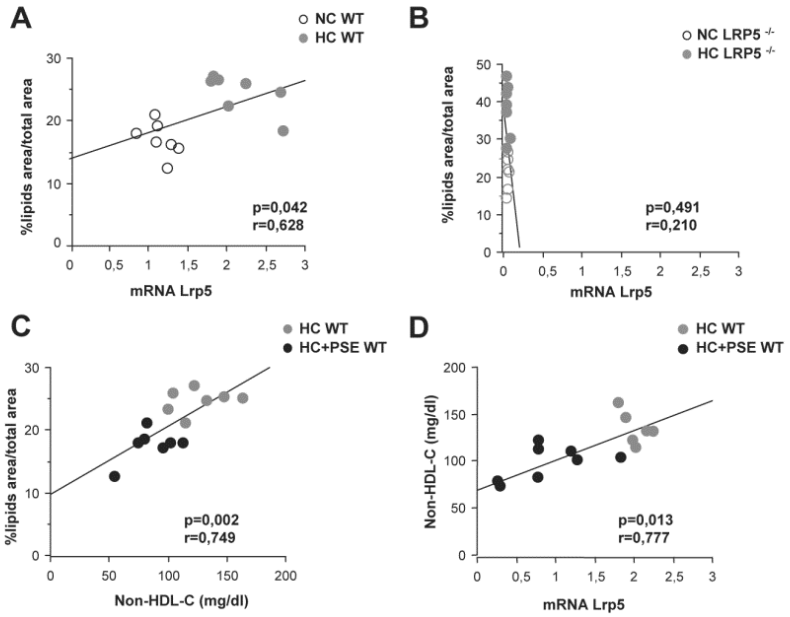

Fig. 4. Linear regression analyses between %lipid area/total area and mRNA Lrp5 expression in (A) WT mice aortas and (B) LRP5$^{-/-}$ mice aortas fed a NC or a HC diet. Linear regression analyses of WT mice fed a HC diet or a HC diet supplemented with 2% PSE between (C) %lipid area/total area and non-HDL cholesterol and (D) non-HDL-C and Lrp5 expression levels in the aorta. *p* statistical significances and *r* correlation coefficients.

treatment increased targets from the Wnt signaling pathway, whereas LRP5-silenced macrophages showed a significant downregulation of Wnt target genes expression resulting in a reduced migratory capacity [12]. LRP5 is also involved in monocyte to macrophage differentiation [42] strongly suggesting that inflammatory cells overexpressing LRP5 in atherosclerotic lesions have mainly migratory functions. Neutral acylglylerides lipids accumulation was also increased in aortas of WT and LRP5$^{-/-}$ after hypercholesterolemic diets. TAG accumulation in the vascular wall is mainly performed by macrophages [43]. There are various mechanisms by which this accumulation can take place, including increasing glucose uptake and incorporation into lipid, increased TAG synthesis and decreased TAG lipolysis [43]. Previous studies have shown that LRP5$^{-/-}$ mice display impaired plasma clearance of intragastrically loaded TAG suggesting that LRP5 modulates plasma clearance of diet derived TAG by triggering TAG hydrolysis [13]. Furthermore, LPS-stimulated macrophages store more TAG and CE [43–45] and TAG-rich lipoproteins are increased during inflammation [46]. Therefore, an increased TAG accumulation in aortas of LRP5$^{-/-}$ mice might be a consequence of an increased inflammatory response supporting an anti-inflammatory role for the canonical Wnt pathway as previously described [47–50]. Decreased TAG plasma levels after PSE feeding have been described in C57Bl6 mice fed a high-fat diet [51], in healthy subjects [52] and in metabolic syndrome patients [53]. Unpublished results from our lab show increased serum TAG and increased expression of hepatic Vldlr in WT mice fed a HC diet. After dietary PSE supplementation, TAG serum levels were reduced and hepatic Vldlr levels returned to normocholesterolemic levels. Interestingly, no changes in TAG serum levels or in hepatic Vldlr gene expression were observed in LRP5$^{-/-}$ mice suggesting LRP5 is necessary to modulate TAG serum levels through interaction with VLDLR in the liver.

Dietary PSE downregulate plasma lipid levels modulating Lrp5 expression levels and aortic CE content in atherosclerotic plaques. Interestingly, a reduction in serum total cholesterol levels and in the extent of aortic plaque coverage was observed in both genotypes after dietary PSE feeding. The ability of PSE to reduce atherosclerotic lesions has been described in ApoE$^{-/-}$ mice fed a HC diet supplemented with 2% phytosterols that show early lesions containing superficial foam cells compared to the advanced atherosclerotic lesions in HC ApoE$^{-/-}$ mice [54]. Furthermore, lipid-loaded foam cell areas in the aortic arch of hamsters receiving an atherogenic diet supplemented with PSE are smaller than in control hamsters [55]. Results from LDLR$^{+/-}$mice also suggest that PSE are not atherogenic since the addition of plant sterols to HC diets inhibits the progression of existing atherosclerotic lesions [56]. Our results also support a beneficial effect of dietary PSE feeding in atherosclerosis progression. The mechanism by which PSE supplementation reduce lipid-rich aortic coverage is cholesterol-dependent. Indeed, eating food products enriched with PSE helps promote healthy blood cholesterol levels. Lipase enzymes, present in the human digestive tract, cleave PSE to free plant sterols in the gastrointestinal tract, which then block gastrointestinal absorption of dietary and biliary cholesterol into the bloodstream, thus lowering serum cholesterol [57]. Therefore, dietary PSE would reduce the plasma lipid concentration, reducing aortic CE accumulation and aortic Lrp5 expression levels.

Lrp5 expression levels in aortas of WT mice were upregulated in HC-fed mice with large aortic atherosclerotic lesions and downregulated after dietary plant sterol supplementation in mice with reduced atherosclerotic plaques. Also, there was a positive correlation between the extent of lipid-rich plaque coverage and aortic Lrp5 gene expression in HC WT mice and this correlation was lost in LRP5$^{-/-}$ mice. Furthermore, after dietary PSE the correlation between the aortic lesions and non-HDL levels was significant in WT mice. More importantly, the correlation remained significant between non-HDL levels and Lrp5 gene expression in WT mice aortas. Although correlation does not equate to causality, these results strongly suggest that Lrp5 gene expression is modulated by plasma lipids levels.

In conclusion, our results show that the modulation of plasma lipid concentrations by plant sterol esters can modulate aortic Lrp5

expression levels that in turn associate to the regulation of CE accumulation and neutral acylclycerides content in aortic atherosclerotic plaques.

5. Funding

This work was supported by grants from the Spanish Ministry of Economy and Competitiveness (SAF 2013-42962-R to LB), Institute of Health Carlos III, ISCIII (TERCEL RD12/0019/0026 and RIC RD12/0042/0027 to LB); Ramon y Cajal Contract (to MBP) and a Danone Institute Fellowship (to CRS).

6. Disclosures

None.

Acknowledgments

We thank Sonia Huertas for technical assistance and Danone for providing plant sterol esters.

Appendix A. Supplementary material

Supplementary data related to this article can be found online at 10.1016/j.atherosclerosis.2014.05.922.

References

[1] Stancu CS, Toma L, Sima AV. Dual role of lipoproteins in endothelial cell dysfunction in atherosclerosis. Cell Tissue Res 2012;349:433–46.
[2] Turkish AR, Sturley SL. The genetics of neutral lipid biosynthesis: an evolutionary perspective. Am J Physiol Endocrinol Metab 2009;297:E19–27.
[3] Berenson GS, Srinivasan SR, Bao W, Newman 3rd WP, Tracy RE, Wattigney WA. Association between multiple cardiovascular risk factors and atherosclerosis in children and young adults. the Bogalusa heart study. N Engl J Med 1998;338:1650–6.
[4] Egusa G, Yamane K. Lifestyle, serum lipids and coronary artery disease: comparison of Japan with the United States. J Atheroscler Thromb 2004;11:304–12.
[5] Nissen SE, Tuzcu EM, Schoenhagen P, Crowe T, Sasiela WJ, Tsai J, et al. Statin therapy, LDL cholesterol, C-reactive protein, and coronary artery disease. N Engl J Med 2005;352:29–38.
[6] Kramsch DM, Franzblau C, Hollander W. The protein and lipid composition of arterial elastin and its relationship to lipid accumulation in the atherosclerotic plaque. J Clin Invest 1971;50:1666–77.
[7] Suarna C, Dean RT, May J, Stocker R. Human atherosclerotic plaque contains both oxidized lipids and relatively large amounts of alpha-tocopherol and ascorbate. Arterioscler Thromb Vasc Biol 1995;15:1616–24.
[8] Mackness B, Hunt R, Durrington PN, Mackness MI. Increased immunolocalization of paraoxonase, clusterin, and apolipoprotein A-I in the human artery wall with the progression of atherosclerosis. Arterioscler Thromb Vasc Biol 1997;17:1233–8.
[9] Lang PD, Insull Jr W. Lipid droplets in atherosclerotic fatty streaks of human aorta. J Clin Invest 1970;49:1479–88.
[10] Hiltunen TP, Luoma JS, Nikkari T, Ylä-Herttuala S. Expression of LDL receptor, VLDL receptor, LDL receptor-related protein, and scavenger receptor in rabbit atherosclerotic lesions: marked induction of scavenger receptor and VLDL receptor expression during lesion development. Circulation 1998;97:1079–86.
[11] Llorente-Cortés V, Otero-Viñas M, Camino-López S, Costales P, Badimon L. Cholesteryl esters of aggregated LDL are internalized by selective uptake in human vascular smooth muscle cells. Arterioscler Thromb Vasc Biol 2006;26:117–23.
[12] Borrell-Pagès M, Romero JC, Juan-Babot O, Badimon L. Wnt pathway activation, cell migration, and lipid uptake is regulated by low-density lipoprotein receptor-related protein 5 in human macrophages. Eur Heart J 2011;32:2841–50.
[13] Fujino T, Asaba H, Kang M-J, Ikeda Y, Sone H, Takada S, et al. Low-density lipoprotein receptor-related protein 5 (LRP5) is essential for normal cholesterol metabolism and glucose-induced insulin secretion. Proc Natl Acad Sci U. S. A 2003;100:229–34.
[14] Magoori K, Kang M-J, Ito MR, Kakuuchi H, Ioka RX, Kamataki A, et al. Severe hypercholesterolemia, impaired fat tolerance, and advanced atherosclerosis in mice lacking both low density lipoprotein receptor-related protein 5 and apolipoprotein E. J Biol Chem 2003;278:11331–6.
[15] Kamal-Eldin A, Moazzami A. Plant sterols and stanols as cholesterol-lowering ingredients in functional foods. Recent Pat Food Nutr Agric 2009;1:1–14.
[16] Othman RA, Moghadasian MH. Beyond cholesterol-lowering effects of plant sterols: clinical and experimental evidence of anti-inflammatory properties. Nutr Rev 2011;69:371–82.
[17] Weingärtner O, Ulrich C, Lütjohann D, Ismail K, Schirmer SH, Vanmierlo T, et al. Differential effects on inhibition of cholesterol absorption by plant stanol and plant sterol esters in apoE-/- mice. Cardiovasc Res 2011;90:484–92.
[18] Rideout TC, Harding SV, Mackay DS. Metabolic and genetic factors modulating subject specific LDL-C responses to plant sterol therapy. Can J Physiol Pharmacol 2012;90:509–14.
[19] Calpe-Berdiel L, Escolà-Gil JC, Ribas V, Navarro-Sastre A, Garcés-Garcés J, Blanco-Vaca F. Changes in intestinal and liver global gene expression in response to a phytosterol-enriched diet. Atherosclerosis 2005;181:75–85.
[20] Weingärtner O, Lütjohann D, Ji S, Weisshoff N, List F, Sudhop T, et al. Vascular effects of diet supplementation with plant sterols. J Am Coll Cardiol 2008;51:1553–61.
[21] Nashed B, Yeganeh B, HayGlass KT, Moghadasian MH. Antiatherogenic effects of dietary plant sterols are associated with inhibition of proinflammatory cytokine production in Apo E-KO mice. J Nutr 2005;135:2438–44.
[22] Sabeva NS, McPhaul CM, Li X, Cory TJ, Feola DJ, Graf GA. Phytosterols differentially influence ABC transporter expression, cholesterol efflux and inflammatory cytokine secretion in macrophage foam cells. J Nutr Biochem 2011;22:777–83.
[23] Bouic PJ, Clark A, Lamprecht J, Freestone M, Pool EJ, Liebenberg RW, et al. The effects of B-sitosterol (BSS) and B-sitosterol glucoside (BSSG) mixture on selected immune parameters of marathon runners: inhibition of post marathon immune suppression and inflammation. Int J Sports Med 1999;20:258–62.
[24] Devaraj S, Autret BC, Jialal I. Reduced-calorie orange juice beverage with plant sterols lowers C-reactive protein concentrations and improves the lipid profile in human volunteers. Am J Clin Nutr 2006;84:756–61.
[25] Holmen SL, Giambernardi TA, Zylstra CR, Buckner-Berghuis BD, Resau JH, Hess JF, et al. Decreased BMD and limb deformities in mice carrying mutations in both Lrp5 and Lrp6. J Bone Min Res Off J Am Soc Bone Min Res 2004;19:2033–40.
[26] Lindvall C, Evans NC, Zylstra CR, Li Y, Alexander CM, Williams BO. The Wnt signaling receptor Lrp5 is required for mammary ductal stem cell activity and Wnt1-induced tumorigenesis. J Biol Chem 2006;281:35081–7.
[27] Cui Y, Niziolek PJ, MacDonald BT, Zylstra CR, Alenina N, Robinson DR, et al. Lrp5 functions in bone to regulate bone mass. Nat Med 2011;17:684–91.
[28] Wu T, Fu J, Yang Y, Zhang L, Han J. The effects of phytosterols/stanols on blood lipid profiles: a systematic review with meta-analysis. Asia Pac J Clin Nutr 2009;18:179–86.
[29] Koh JM, Jung MH, Hong JS, Park HJ, Chang JS, Shin HD, et al. Association between bone mineral density and LDL receptor-related protein 5 gene polymorphisms in young Korean men. J Korean Med Sci 2004;19:407–12.
[30] Urano T, Shiraki M, Usui T, Sasaki N, Ouchi Y, Inoue S. A1330V variant of the low-density lipoprotein receptor-related protein 5 (LRP5) gene decreases Wnt signaling and affects the total body bone mineral density in Japanese women. Endocr J 2009;56:625–31.
[31] Suwazono Y, Kobayashi E, Uetani M, Miura K, Morikawa Y, Ishizaki M, et al. G-protein beta 3 subunit polymorphism C1429T and low-density lipoprotein receptor-related protein 5 polymorphism A1330V are risk factors for hypercholesterolemia in Japanese males–a prospective study over 5 years. Metabolism 2006;55:751–7.
[32] Jiang X-Y, Chen Y, Xu L, Li X, Cao F-F, Li L, et al. Association of LPR5 polymorphism with bone mass density and cholesterol level in population of Chinese Han. Exp Clin Endocrinol Diabetes Off J Ger Soc Endocrinol Ger Diabetes Assoc 2010;118:388–91.
[33] Penumathsa SV, Thirunavukkarasu M, Koneru S, Juhasz B, Zhan L, Pant R, et al. Statin and resveratrol in combination induces cardioprotection against myocardial infarction in hypercholesterolemic rat. J Mol Cell Cardiol 2007;42:508–16.
[34] Kim DH, Inagaki Y, Suzuki T, Ioka RX, Yoshioka SZ, Magoori K, et al. A new low density lipoprotein receptor related protein, LRP5, is expressed in hepatocytes and adrenal cortex, and recognizes apolipoprotein E. J Biochem (Tokyo) 1998;124:1072–6.
[35] Rajamannan NM. The role of Lrp5/6 in cardiac valve disease: experimental hypercholesterolemia in the ApoE-/-/Lrp5-/- mice. J Cell Biochem 2011;112:2987–91.
[36] Rajamannan NM, Subramaniam M, Caira F, Stock SR, Spelsberg TC. Atorvastatin inhibits hypercholesterolemia-induced calcification in the aortic valves via the Lrp5 receptor pathway. Circulation 2005;112:I229–34.
[37] Chan KL, Teo K, Dumesnil JG, Ni A, Tam J. ASTRONOMER investigators. effect of lipid lowering with rosuvastatin on progression of aortic stenosis: results of the aortic stenosis progression observation: measuring effects of rosuvastatin (ASTRONOMER) trial. Circulation 2010;121:306–14.
[38] Hutchins PM, Moore EE, Murphy RC. Electrospray MS/MS reveals extensive and nonspecific oxidation of cholesterol esters in human peripheral vascular lesions. J Lipid Res 2011;52:2070–83.
[39] Kruth HS. Localization of unesterified cholesterol in human atherosclerotic lesions. Demonstration of filipin-positive, oil-red-O-negative particles. Am J Pathol 1984;114:201–8.

[40] Guyton JR, Klemp KF. Development of the atherosclerotic core region. Chemical and ultrastructural analysis of microdissected atherosclerotic lesions from human aorta. Arterioscler Thromb J Vasc Biol Am Heart Assoc 1994;14:1305–14.
[41] Chen Z, Ichetovkin M, Kurtz M, Zycband E, Kawka D, Woods J, et al. Cholesterol in human atherosclerotic plaque is a marker for underlying disease state and plaque vulnerability. Lipids Health Dis 2010;9:61.
[42] Borrell-Pagès M, Romero JC, Badimon L. LRP5 negatively regulates differentiation of monocytes through abrogation of Wnt signalling. J Cell Mol Med 2014;18:314–25.
[43] Feingold KR, Shigenaga JK, Kazemi MR, McDonald CM, Patzek SM, Cross AS, et al. Mechanisms of triglyceride accumulation in activated macrophages. J Leukoc Biol 2012;92:829–39.
[44] Lopes-Virella MF, Klein RL, Stevenson HC. Low density lipoprotein metabolism in human macrophages stimulated with microbial or microbial-related products. Arterioscler Dallas Tex 1987;7:176–84.
[45] Funk JL, Feingold KR, Moser AH, Grunfeld C. Lipopolysaccharide stimulation of RAW 264.7 macrophages induces lipid accumulation and foam cell formation. Atherosclerosis 1993;98:67–82.
[46] Khovidhunkit W, Kim M-S, Memon RA, Shigenaga JK, Moser AH, Feingold KR, et al. Effects of infection and inflammation on lipid and lipoprotein metabolism: mechanisms and consequences to the host. J Lipid Res 2004;45:1169–96.
[47] Martin M, Rehani K, Jope RS, Michalek SM. Toll-like receptor-mediated cytokine production is differentially regulated by glycogen synthase kinase 3. Nat Immunol 2005;6:777–84.
[48] Ahn J, Lee H, Kim S, Ha T. Curcumin-induced suppression of adipogenic differentiation is accompanied by activation of Wnt/beta-catenin signaling. Am J Physiol Cell Physiol 2010;298:C1510–6.
[49] Kim J, Kim J, Kim DW, Ha Y, Ihm MH, Kim H, et al. Wnt5a induces endothelial inflammation via beta-catenin-independent signaling. J Immunol Balt Md 1950;2010(185):1274–82.
[50] Whyte JL, Smith AA, Helms JA. Wnt signaling and injury repair. Cold Spring Harb Perspect Biol 2012;4:a008078.
[51] Rideout TC, Harding SV, Jones PJH. Consumption of plant sterols reduces plasma and hepatic triglycerides and modulates the expression of lipid regulatory genes and de novo lipogenesis in C57BL/6J mice. Mol Nutr Food Res 2010;54(1):S7–13.
[52] Naumann E, Plat J, Kester ADM, Mensink RP. The baseline serum lipoprotein profile is related to plant stanol induced changes in serum lipoprotein cholesterol and triacylglycerol concentrations. J Am Coll Nutr 2008;27:117–26.
[53] Plat J, Brufau G, Dallinga-Thie GM, Dasselaar M, Mensink RP. A plant stanol yogurt drink alone or combined with a low-dose statin lowers serum triacylglycerol and non-HDL cholesterol in metabolic syndrome patients. J Nutr 2009;139:1143–9.
[54] Moghadasian MH, McManus BM, Pritchard PH, Frohlich JJ. "Tall oil"-derived phytosterols reduce atherosclerosis in ApoE-deficient mice. Arterioscler Thromb Vasc Biol 1997;17:119–26.
[55] Ntanios FY, van de Kooij AJ, de Deckere EAM, Duchateau GSMJE, Trautwein EA. Effects of various amounts of dietary plant sterol esters on plasma and hepatic sterol concentration and aortic foam cell formation of cholesterol-fed hamsters. Atherosclerosis 2003;169:41–50.
[56] Plat J, Beugels I, Gijbels MJJ, de Winther MPJ, Mensink RP. Plant sterol or stanol esters retard lesion formation in LDL receptor-deficient mice independent of changes in serum plant sterols. J Lipid Res 2006;47:2762–71.
[57] Weststrate JT, Hop WC, Aalbers AG, Vreeling AW, Bruining HA. The clinical relevance of the waterlow pressure sore risk scale in the ICU. Intensive Care Med 1998;24:815–20.

Supplemental Table 1: Relative changes in serum lipid composition.

mg/dl	WT		LRP5$^{-/-}$	
	↑HC	↓HC+PSE	↑HC	↓ HC+PSE
Total Cholesterol	62 ±6***	22 ±1*	126 ±9***	58 ±8***
HDL-C	27 ±3***	-10 ±0.5	27 ±4***	-26 ±2***
Non-HDL-C	32 ±2***	32 ±3*	90 ±12**	84 ±11
TAG	-1 ±0.2	21 ±2*	20 ±5	6 ±1

Supplemental Table 1: Relative changes in serum lipid composition of WT and LRP5$^{-/-}$ mice at sacrifice. Indicated significances are between the following groups: NC *vs* HC and HC *vs* HC+PSE. *p<0,05; **p<0,01; ***p<0,005.

ARTÍCULO 5

LRP5 and serum cholesterol levels modulate the canonical Wnt pathway in peripheral blood leukocytes.

Autores: María Borrell-Pagés[±], July Carolina Romero[±], Lina Badimon.

Revista: En revisión en Immunology and Cell Biology.

Centro de Investigación Cardiovascular CSIC-ICCC, Hospital de la Santa Creu i Sant Pau, Barcelona, España.

[±] Co-primeros autores

RESUMEN

Los niveles de LRP5 y colesterol en suero modulan la vía canónica de señalización por Wnt en leucocitos de sangre periférica.

Los procesos inflamatorios se activan tras una invasión o daño con el propósito de recuperar la homeostasis celular. Aunque la activación de la señalización Wnt/β-catenina es uno de las primeras respuestas moleculares al daño celular, su participación en la inflamación no se ha definido. Postulamos que LRP5 y la vía de señalización por Wnt están modulados por mecanismos inflamatorios.

Ratones *Wt* y *Lrp5*$^{-/-}$ se alimentaron con una dieta hipercolesterolémica (HC) para provocar dislipidemia e inflamación. Las dietas fueron suplementadas con fitoesteroles esterificados (PSE) para estimular mecanismos anti-inflamatorios. Los ratones *Wt* HC presentaron altos niveles de colesterol plasmático que se correlacionaron con un incremento en la expresión de *Lrp5* y de los genes de la vía de señalización por Wnt en leucocitos, mientras que en ratones *Lrp5*$^{-/-}$ la vía canónica se mantenía inactivada. Funcionalmente, la hipercolesterolemia indujo la expresión de genes pro-inflamatorios en ratones *Lrp5*$^{-/-}$, sugiriendo un rol inhibitorio de la vía de señalización por Wnt en la inflamación. La dieta HC suplementada con PSE muestra niveles reducidos de colesterol en suero tanto en ratones *Wt* como en ratones *Lrp5*$^{-/-}$. Además, en ratones *Wt* la adición de PSE a la dieta HC incrementa la expresión de genes anti-inflamatorios e inhibe la activación de la vía Wnt/β-CATENINA. La expresión hepática de VLDLR, LRP2 y LRP6

incrementa tras la dieta HC en los ratones *Wt* pero no en los *Lrp5*$^{-/-}$ sugiriendo una función para estos receptores en la eliminación de lipoproteínas plasmáticas. Finalmente, demostramos un rol anti-aterogénico para LRP5 ya que los ratones *Lrp5*$^{-/-}$ HC desarrollan lesiones ateroscleróricas aorticas de mayor tamaño que los ratones *Wt*.

Nuestros resultados muestran un rol anti-inflamatorio y de pro-supervivencia para LRP5 y la vía canónica en leucocitos de sangre periférica.

Title: LRP5 and plasma cholesterol levels modulate the canonical Wnt pathway in peripheral blood leukocytes

Authors: Maria Borrell-Pages*, July Carolina Romero*, Lina Badimon

Cardiovascular Research Center, CSIC-ICCC, Hospital de la Santa Creu i Sant Pau, IIB-Sant Pau, Barcelona, Spain, Cardiovascular Research Chair, UAB, Barcelona, Spain.

*Both authors contributed equally to this work

Running title: LRP5 and inflammation.

Address for Correspondence: Prof. Lina Badimon,

Cardiovascular Research Center,

C/ Sant Antoni Maria Claret 167, 08025 Barcelona, Spain,

Tel: 34935565880, FAX: 34935565559,

E-mail:lbadimon@csic-iccc.org

Word Count: 4500 +References

Total Number of Figures and Tables: 5 Figures.

Abbreviations Page:

ABCG: ATP-binding cassette sub-family G

Flt: FMS-like tyrosine kinase

HC: Hypercholesterolemia

HDL: High Density Lipoproteins

Ifn: Interferon

IL: Interleukin

LDL: Low Density Lipoproteins

LRP: Low Density Lipoprotein Receptor related Protein

LPS: Lipopolysaccharide

NC: Normocholesterolemia

PSE: Plant Sterol Ester

TAG: Triglycerides

Tnsfs: Tumor necrosis factor ligand superfamily

WT: Wild type

Abstract

Purpose: Inflammation is triggered after invasion or injury in order to restore homeostasis. Although the activation of Wnt/β-catenin signaling is one of the first molecular responses to cellular damage, its role in inflammation is still unclear. This study tested the hypothesis that the Wnt signaling pathway and its receptor, low-density-lipoprotein receptor-related protein 5 (LRP5), were modulated by inflammatory mechanisms.

Basic Procedures: WT and LRP5$^{-/-}$ mice were fed a hypercholesterolemic diet (HC) to trigger dislipidemia and chronic inflammation. Diets were supplemented with plant sterol esters (PSE) to trigger anti-inflammatory mechanisms.

Main Findings: HC WT mice showed increased serum cholesterol levels that correlated with increased Lrp5 and Wnt/β-catenin genes expression in leukocytes while in LRP5$^{-/-}$ mice Wnt/β-catenin pathway was shut down. Functionally, HC induced proinflammatory gene expression in LRP5$^{-/-}$ mice, suggesting an inhibitory role of the Wnt pathway in inflammation. Dietary PSE were able to downregulate serum cholesterol levels in WT and LRP5$^{-/-}$ mice. Furthermore, in WT mice PSE were able to increase anti-inflammatory genes expression and inhibit Wnt/β-catenin activation. Hepatic gene expression of Vldlr, Lrp2 and Lrp6 were increased after HC feeding in WT mice but not in LRP5$^{-/-}$ mice suggesting a role for these receptors in the clearance of plasmatic lipoproteins. Finally, an antiatherogenic role for LRP5 was demonstrated as HC LRP5$^{-/-}$ mice developed larger aortic atherosclerotic lesions than WT mice.

Principal Conclusions: Our results show an anti-inflammatory, prosurvival role for LRP5 and the Wnt signaling pathway in peripheral blood leukocytes.

Keywords: LRP5, canonical Wnt pathway, lipids, inflammation, plant sterols esters, atherosclerosis

Introduction

Inflammation occurs in response to injury. [1] In some disorders, the inflammatory process becomes continuous and chronic inflammatory diseases may develop including coronary artery disease, obesity and cancer.[1,2] The major components of innate immunity are the leukocytes that are circulating in blood and during tissue injury they invade the wound site in an attempt to phagocytose cells debris and release growth factors and cytokines. [3]

Low-density lipoprotein receptor-related protein 5 (LRP5), is a single-pass transmembrane receptor that participates in the Wnt/β-catenin signaling pathway. LRP5-Wnt ligand binding results in the stabilization of β-catenin that will translocate to the nucleus, trigger TCF/LEF1 transcription factor activation and transcription of Wnt target genes.[4] Wnt/β-catenin signaling is one of the first molecular responses to injury; however its role in inflammation remains controversial. Initial studies showed that exposure to the canonical Wnt ligand Wnt3a resulted in an increase of total β-catenin protein in cultured monocytes. However, no modulation of the inflammatory response was described.[5] Some years later the Wnt/β-catenin pathway was found to inhibit the inflammatory response since inhibitors of β-catenin upregulate inflammatory genes in endothelial cells[6] and administration of an inhibitor of the Wnt/β-catenin pathway, GSK3β, increased proinflammatory cytokine production by Toll-like receptors.[7] However, IL-1β and LPS induced nuclear β-catenin accumulation in human vascular endothelial cells[8] and activation of canonical Wnt genes have been found in endothelial cells of a rejected kidney model[9] suggesting that activation of the pathway triggers the inflammatory response.

Hypercholesterolemia has been widely described to induce vascular inflammation[10–12] by cholesterol internalization in the intima while plant sterol esters (PSE) are known to reduce plasma cholesterol levels.[13] Recent observations from animal and human studies have demonstrated anti-inflammatory effects of phytosterols. Indeed, PSE attenuate the inflammatory response by ameliorating endothelial dysfunction in $ApoE^{-/-}$ mice and decreasing lipid-induced secretion of pro-inflammatory cytokines in cultured human

macrophages.[14,15] Furthermore, PSE have been reported to have anti-inflammatory properties in different cohorts of healthy subjects.[16,17] The cholesterol-lowering activity of plant sterols is because PSE displace cholesterol from mixed micelles as they are more hydrophobic than cholesterol.[18] This replacement causes a reduction of micellar cholesterol concentrations and consequently lowers cholesterol absorption. In the enterocyte, cholesterol is readily esterified by the action of acyl-CoA:cholesterol acyltransferase 2 (ACAT2) and released into lymph in association with chylomicrons. However, some sterols (cholestanols and PSE) are effectively excreted back to the intestinal lumen by heterodimers of the ATP-binding cassette transporters, ABCG5 and ABCG8, present at the apical membrane of the enterocyte.[19,20] The absence of ABCG5 and ABCG8 in sitosterolemic patients is associated with accumulation of sterols and stanols and can lead to severe atherosclerosis already at a very young age.[19,21]

To further understand the role of LRP5 and the Wnt/β-catenin signaling pathway in the inflammatory response we studied inflammatory cytokine levels in blood from WT and LRP5$^{-/-}$ mice fed a hypercholesterolemic diet to induce inflammation, supplemented or not with 2% PSE. Our results support an anti-inflammatory role for LRP5 and the Wnt signaling pathway as LRP5$^{-/-}$ mice show increased expression of proinflammatory genes compared with WT mice in hypercholesterolemic conditions. Also, there is a positive correlation between plasma cholesterol levels and Wnt gene expression in circulating white cells from WT mice. On the contrary, in LRP5$^{-/-}$ mice the correlation is lost and triggering of the Wnt/β-catenin pathway is abolished. Interestingly, plant sterols were able to reduce plasma cholesterol levels, induce the expression of anti-inflammatory genes and downregulate gene expression levels of Lrp5 and Wnt pathway genes in circulating white cells. Abcg5 and Abcg8 increased after hypercholesterolemic diets in the jejunum of WT and LRP5$^{-/-}$ mice independently of plant sterol ingestion. Surprisingly, hepatic gene expression of Lrp2 and Lrp6 were increased only in WT mice and Vldlr expression in the liver was abolished in LRP5$^{-/-}$ mice. Finally we show large lipid deposition in aortas from HC

LRP5$^{-/-}$ mice that are reduced after PSE feeding, supporting a role for LRP5 in atheroclerosis prevention.

Results

Serum lipid concentrations

Total cholesterol, HDL-C and non-HDL-C serum concentrations in WT and LRP5$^{-/-}$ mice fed a hypercholesterolemic diet (HC: 21% fat and 0.25% cholesterol) were significantly increased compared to their normocholesterolemic littermates (NC: 3.5% fat and 0% cholesterol). Indeed, serum levels of total cholesterol, HDL and non-HDL were increased by 62±6mg/dl, 27±3 mg/dl and 32±2 mg/dl respectively in HC WT mice and 126±9mg/dl, 27±4mg/dl and 90±12 mg/dl respectively in HC LRP5$^{-/-}$ mice with respect to their NC littermates (Figure 1). Addition of plant sterol esters to HC diets in WT mice (HC+PSE: 21% fat, 0.25% cholesterol and 2% PSE) reduced total cholesterol and non-HDL-C serum concentrations without affecting HDL-C levels as previously described.[22] However, in HC+PSE LRP5$^{-/-}$ mice there was a 26±2mg/dl increase in HDL-C serum levels respect to HC LRP5$^{-/-}$ mice. Dietary PSE reduced serum triglycerides (TAG) concentrations by 21±2mg/dl with respect to HC in WT mice while TAG levels did not differ significantly among dietary treatment groups in LRP5$^{-/-}$ mice (Figure 1).

Increased inflammatory gene expression in peripheral blood leukocytes of LRP5$^{-/-}$ mice fed a HC diet

High plasma lipid concentration is an instigator of inflammation.[11] To study the role of LRP5 in the inflammatory process we first analyzed the expression of common cytokines by using a PCR array in peripheral blood leukocytes from WT and LRP5$^{-/-}$ mice fed a HC diet. As expected, Lrp5 expression levels were upregulated in HC WT mice compared with HC LRP5$^{-/-}$ mice (Figure 2A). Several pro-inflammatory cytokine genes including FasL, Ifnγ, IL15, IL18 and Tnfsf13b were upregulated in HC LRP5$^{-/-}$ mice compared with HC WT mice (1.92, 3.02, 1.45, 1.99 and 2.12 fold change (FC) increase respectively). An increase in the anti-inflammatory genes Flt3L and IL27 (1.52 and 3.22 FC increase respectively) in HC

LRP5$^{-/-}$ compared with HC WT mice was also observed, supporting a role for LRP5 in inflammation.

Plant Sterol Esters increase the anti-inflammatory response in peripheral blood leukocytes

WT mice fed a HC diet supplemented with 2% PSE showed increased expression levels of anti-inflammatory cytokines gens in circulating white cells compared with HC WT mice. Indeed, a significant fold change increase was observed in Flt3L, IL27, Tnfsf10 and Tnfsf13 (1.70, 2.58, 1.39 and 2.50 respectively, Figure 2B). However, several proinflammatory genes were also upregulated in HC WT mice (Tnfsf9, 1.8 FC) after plant sterol supplementation (FasL, 1.90 FC and IL18, 1.90 FC). Lrp5 was only upregulated in HC WT mice.

HC LRP5$^{-/-}$ mice showed upregulation of inflammatory gene products when compared with HC LRP5$^{-/-}$ mice supplemented with dietary PSE. Indeed an increase was observed in HC LRP5$^{-/-}$ mice in FasL, Ifng and Lta genes respectively (Figure 2C).

Reduced β-catenin translocation into the nucleus in LRP5$^{-/-}$ monocytes.

β-catenin is traslocated to the nucleus upon Wnt pathway activation.[23] By cellular subfractionation experiments we tested whether LRP5 silencing was preventing β-catenin translocation into the nucleus in human monocytes. siRNA-LRP5 monocytes showed a decreased β-catenin translocation into the nucleus respect to control cells (Figure 3A). Additionally, total lysate associated β-catenin levels did not differ in control and LRP5 silenced monocytes. Lrp5 mRNA levels were analyzed showing an efficient inhibition by siRNA-LRP5 (Figure 3B).

High and low cholesterol levels modulate LRP5 and Wnt/β-catenin signaling pathway genes in circulating white cells

We then searched for intracellular pathways modulated by LRP5 and analyzed several canonical Wnt signaling genes in peripheral blood leukocytes of WT and LRP5$^{-/-}$ mice.

Results show that mRNA levels of Lrp5, β-catenin and Lef1 were increased after hypercholesterolemic feeding in WT mice (249.85±1%, 51±2% and 30.7±0.5% respectively, Figure 3C). This increase was significantly reduced when PSE were added to the diets. Downregulation of 209.53±1.5%, 72.3±2% and 74.2±2% were found in Lrp5, β-catenin and Lef1 gene expression levels respectively (Figure. 3C). mRNA expression levels of bone morphogenetic protein 2 (Bmp2) and osteopontin (Opn), two well-known Wnt targets[24,25] were also increased only in the presence of high serum cholesterol levels and their mRNA levels were reduced after dietary sterols intake (69.48±1% in Bmp2 and 90.16±2% in Opn Figure 3C). Taken together, these results show that the cholesterol-lowering effects of dietary PSE abrogate the increased expression levels of Wnt pathway genes observed in mice with high plasma cholesterol levels. We then analyzed the expression levels of Wnt genes in circulating white cells of LRP5$^{-/-}$ mice after the different dietary treatments. Results show that there is no modulation of Lrp5, β-catenin, Lef1, Bmp2 or Opn gene expression levels (Figure 3D) indicating that Lrp5 is necessary for the triggering of the Wnt/β-catenin signaling pathway by high plasma cholesterol levels. To further asses the relevance of total serum cholesterol levels in Wnt signaling pathway we applied a regression model that revealed positive significant values between total cholesterol levels and blood-derived mRNA of Wnt pathway genes in WT mice (Figure 4A) while no significance could be detected in LRP5$^{-/-}$ mice (Figure 4B).

Plant Sterol Esters do not modulate Abcg5 and Abcg8 expression levels

To understand the mechanism by which PSE induce the cholesterol-lowering effect observed in WT and LRP5$^{-/-}$ mice we analyzed the expression levels of Abcg5 and Abcg8 in mice jejunum. In accordance with previous results[19] the expression levels of both genes are coordinately increased in WT mice consuming a high-cholesterol diet (Figure 4C-D). Similar results are observed in HC LRP5$^{-/-}$ mice. Therefore, addition of plant sterol to HC diets in LRP5$^{-/-}$ mice did not modulate Abcg5 or Abcg8 mRNA expression indicating that these receptors are not responsible for the increased serum cholesterol levels in HC LRP5$^{-/-}$ mice.

Receptors expression in the liver

In an attempt to understand why HC LRP5$^{-/-}$ mice show higher plasma cholesterol levels than their HC WT littermates we analyzed protein and gene expression levels of LRP5 and other receptors of the LDLR superfamily of receptors in mice liver. LRP5 gene and protein expression levels were downregulated after HC feeding and with dietary PSE supplementation (Figure 5A). As expected, LDLR mRNA and protein levels were reduced when mice were fed a HC diet in both genotypes (33.4±1.5% in HC WT and 23.6±0.5% in HC LRP5$^{-/-}$ with respect to their NC littermates in Ldlr gene expression; Figure 5B). Interestingly, LRP1 gene and protein levels remained constant among dietary treatment groups although LRP1 levels were lower in LRP5$^{-/-}$ mice than in WT mice (Figure 5C). On the contrary, LRP2 expression was induced by HC diets only in WT mice (Fig. 5D). Lrp6 mRNA expression levels showed a 27±2% increase in HC WT mice with respect to NC WT mice while after dietary plant sterol intake Lrp6 mRNA values returned to normal (Figure 5E). Vldlr increased its mRNA expression levels by 431±21% in HC WT mice and by 151±5% in HC+PSE WT mice with respect to NC WT animals (Figure 5F). Surprisingly VLDLR gene and protein expression levels remained constantly low in LRP5$^{-/-}$ mice liver, independently of diet suggesting a decreased clearance of lipoprotein particles by this receptor, LRP2 and LRP6 in the liver of the LRP5$^{-/-}$ animals.

Lipid deposition in aortas

The measurement of the formation of lipid-rich plaques in mice aortas showed that HC feeding induced a significant increase in aortic plaque in WT and LRP5$^{-/-}$ mice while supplementation with PSE reduced aortic lipid coverage in both groups (Figure 5G). However, the extent of lipid aortic coverage was significantly higher in HC LRP5$^{-/-}$ mice (12.8±1.5%) than in HC WT mice (Figure 5H) indicating a protective role for LRP5 in atherosclerosis progression.

Discussion

We studied Lrp5 and Wnt/β-catenin signaling gene expression variations in an *in vivo* LRP5-deficient mice model challenged with proinflammatory (HC diets) and anti-inflammatory (dietary PSE) stimulus. LRP5$^{-/-}$ mice with high serum cholesterol levels showed increased inflammatory genes expression in circulating leukocytes compared with HC WT mice, suggesting LRP5$^{-/-}$ mice cannot regulate properly the inflammatory response after HC feeding. Several proinflammatory genes were upregulated in HC LRP5$^{-/-}$ mice including FasL, Ifnγ, IL15, IL18 and Tnfsf13b. IL18 induces IFNγ-production from Th1 and natural killers (NK) cells[26] and has been widely described as a potent pro-inflammatory cytokine in atherosclerosis progression.[27] We find an upregulation of IL18 in the absence of Lrp5 supporting an enhanced inflammatory response when Lrp5 is absent.

IL-15 is also upregulated in peripheral blood leukocytes of HC LRP5$^{-/-}$ mice. This cytokine has pro-inflammatory properties, is produced by endothelial cells in response to IFNγ and promotes T-cell migration to sites of inflammation.[28] Other pro-inflamatory genes overexpressed in HC LRP5$^{-/-}$ mice are FasL and Tnfsf13b, members of the tumor necrosis factor (TNF) family. FasL is mainly expressed in activated T-cells, NK cells, macrophages and cancer cells and triggers apoptosis causing tissue damage[29] while Tnfsf13b, also known as B-cell activator factor (BAFF), is mainly produced and secreted by myeloid cells and upregulated by IFNγ, IL10 and CD40L during inflammation and chronic infections.[30]

During the inflammatory response cells try to reestablish control conditions. Two anti-inflammatory cytokines were also upregulated in LRP5$^{-/-}$ mice with high serum cholesterol concentrations, IL-27 and Flt3L. IL-27 inhibits FasL-induced T-cell death and reduce central nervous system inflammation, inflammatory cytokines secretion and joint inflammation in mouse models of multiple sclerosis and rheumatoid arthritis [31,32]. Flt3L signaling is pivotal in the development of early lymphocyte progenitors and is the principal differentiation factor for dendritic cells.[33,34]

Addition of plant sterols to HC diets in WT mice induced upregulation of several anti-inflammatory genes. Indeed, in addition to Flt3L and IL27, Tnfsf10 and Tnfsf13 were

upregulated in HC+PSE WT mice. Tnfsf10 and Tnfsf13 belong to the TNF family, best known for their pro-fibrotic and apoptosis induction functions.[35] However, some of its members can induce prosurvival, anti apoptotic and anti-inflammatory functions. Indeed, Tnfsf10 promotes survival and proliferation of human vascular endothelial cells and reduce leukocyte/endothelial cells adhesion.[36] Furthermore, in a mice model of hypercholesterolemia, Tnfsf10 lowers fasting glucose and pro-inflammatory cytokine levels ameliorating type 2 diabetes mellitus.[37] Similarly, Tnfsf13 transgenic mice have increased T cells proliferation, enhanced Th2 cytokine production and diminished susceptibility to arthritis.[38] In addition to increasing anti-inflammatory cytokines, PSE treatments also reduced the expression levels of Tnfsf9, a potent pro-inflammatory cytokine that triggers T cell activation and survival.[39] The increased expression of anti-inflammatory cytokines after plant sterol feeding in WT mice shows a beneficial effect of PSE in reducing plasma cholesterol-induced inflammation.

To further investigate the mechanisms by which Lrp5 is regulating inflammation, canonical Wnt pathway gene expression were analyzed in peripheral blood leukocytes from WT and $LRP5^{-/-}$ mice. We observed that Lrp5, β-catenin, Lef1, Bmp2 and Opn increased their expression in HC WT mice confirming in vivo that Wnt/β-catenin pathway is activated in high cholesterol niches.[40,41] Furthermore, regression analyses in WT mice revealed that when total cholesterol levels are high, Wnt signaling pathway genes expression are upregulated. However, when Lrp5 is absent there is no variation in canonical Wnt genes expression independently of cholesterol levels. Finally, there was a decreased translocation of β-catenin into the nucleus in $LRP5^{-/-}$ monocytes indicating decreased Wnt signaling.

A major finding in this report is that plant sterol feeding can regulate Wnt signaling genes expression. Indeed, dietary PSE downregulated blood-derived gene expression levels of Lrp5, β-catenin, Lef1, Bmp2 and Opn in HC WT mice. The mechanism by which PSE reduce Wnt/β-catenin activation is most likely cholesterol-dependent. In the literature, there is a general consensus that plant sterols reduce plasma cholesterol in humans because of their ability to displace cholesterol from the mixed micelles in the upper small intestine,

thereby reducing the efficiency of cholesterol absorption.[42] In addition to this micellar mechanism, alternative pathways have been proposed. For instance, it has been reported that plant sterols are able to activate the nuclear receptor LXR upregulating ABC transporters such as ABCG5 and ABCG8 leading to changes in cholesterol transport.[43,44] However, in our study expression levels of these transporters were increased in the jejunum of WT and LRP5$^{-/-}$ mice after HC diets independently of dietary PSE addition.

To study if the increased plasma cholesterol levels in HC LRP5$^{-/-}$ mice with respect to HC WT mice was due to a differential LDLR-mediated LDL clearance, the expression of liver LDLR in WT and LRP5$^{-/-}$ mice was assessed. High-fat diet inhibited LDLR expression in mouse liver independent of genotype. As expected, the addition of dietary PSE in the high-fat diet abolished the decline of LDLR protein levels in WT and LRP5$^{-/-}$ mice. Cre-mediated destruction of LRP1 in LDLR deficient mice resulted in a dramatic increase in chylomicron remnant plasma contents, indicating that LRP1 contributes substantially to hepatic remnant clearance and does not represent an alternative way of remnant uptake only.[45,46] However, the adenoviral mediated transfer of the receptor-associated protein (RAP), which is a repressor of the LRP function[45] or the cre/loxP recombination system to achieve liver-specific LRP1 destruction revealed that there are no consequences on chylomicron remnant clearance in mice with functional LDLR, because it fully compensates for defective LRP1 at the post-transcriptional level.[46] Consistently, hepatic LRP1 expression levels remained constant independently of diets in WT and LRP5$^{-/-}$ mice. LRP2 is a receptor for ApoM, an anti-atherogenic lipoprotein present in HDL particles, chylomicrons, VLDLs and LDLs[47] while LRP6 can regulate LDLR-mediated LDL uptake as LDLR internalization is severely diminished in LRP6$^{-/-}$ cells.[48] HC LRP5$^{-/-}$ mice show reduced expression of both receptors strongly suggesting their participation in the clearance of lipoprotein particles. There is a differential expression of VLDLR in the livers of WT and LRP5$^{-/-}$ mice. While in WT mice there is an upregulation of the VLDLR after hypercholesterolemic diets and even after the addition of plant sterols, LRP5$^{-/-}$ mice have constant VLDLR expression levels. This may explain the increased serum levels of non-HDL (which include LDL and VLDL) in HC LRP5$^{-/-}$ mice that could be due to decreased clearance of lipoprotein particles by the liver.

Studies with adenoviral vectors have shown that ectopic expression of the VLDLR in mouse liver results in enhanced internalization of lipoproteins.[49] Thus, when expressed in the liver, VLDLR seems to act as a clearance receptor for whole lipoprotein particles. Increased VLDL levels in plasma lipoprotein profile in LRP5$^{-/-}$ mice after a high-fat diet have been reported.[50] Furthermore, LRP5 has shown to be required for proper hepatic clearance as the injection of fluorescently labelled chylomicron remnants into LRP5$^{-/-}$ mice and WT littermates fed a high-fat diet revealed that 30 min after injection 80% of labelled chylomicrons remained in the plasma of LRP5$^{-/-}$ mice.[50] However, the authors assumed that this delayed clearance was caused solely by LRP5 and did not analyze other receptors. In our model, we detect that VLDLR, LRP2 and LRP6 could also be participating in the decreased clearance of lipoprotein particles by the liver in LRP5$^{-/-}$ mice.

Our results support a strong link between inflammation and atherosclerosis progression.[51–53]. Indeed, although hypercholesterolemic diets induced higher proinflammatory cytokine secretion and larger atherosclerotic lesions in both genotypes, HC LRP5$^{-/-}$ mice show upregulated proinflammatory cytokine secretion and larger lipid deposition in thoracic aortas than HC WT mice. Furthermore, the addition of PSE to diets increased anti-inflammatory cytokine secretion and decreased aortic lipid deposition, showing that PSE downregulate plasma cholesterol and the inflammatory secretion, effectively reducing atherosclerosis lesion formation.

In conclusion, our results strongly support an anti-inflammatory, prosurvival role for LRP5 and the Wnt signaling pathway in circulating white cells of WT mice. In the absence of LRP5 and in the presence of high levels of cholesterol Wnt signaling remains inactivated and inflammatory genes expression is upregulated. LRP5-expressing WT mice with high plasma cholesterol levels show increased Lrp5 and Wnt/β-catenin pathway genes expression and lower secretion of inflammatory cytokines than their LRP5$^{-/-}$ littermates strongly suggesting a prosurvival role for LRP5 and the Wnt pathway in circulating white cells.

Material and Methods

Animals and experimental design

LRP5$^{-/-}$ mice, a kind gift from Dr. Bart Williams[54,55] were maintained in a C57BL/6 background. Mice were housed in cages under controlled temperature (21±2ºC) on a 12h light/ dark cycle with food and water ad libitum. Homozygous wild-type C57BL/6 mice (WT; n=34) and LRP5$^{-/-}$ C57BL/6 mice (LRP5$^{-/-}$; n=34) were used for the protocols. The presence of LRP5 alleles was assessed by PCR amplification from DNA extracted from tail biopsies in WT, heterozygous and homozygous littermates. Primers used were S17 (GGC TCG GAG GAC AGA CCT GAG), S23 (CTG TCA GTG CCT GTA TCT GTC C) and IRES31 (AGG GGC GGA ATT CGA TAG CT). LRP5$^{-/-}$ and WT mice were fed a normal chow diet (NC, Tekland diet, Harlan Labs, Berkeley, CA, USA) for 10 weeks. Animals were then divided into 3 groups to be fed with NC, high cholesterol diet (HC, TD.88137, Harlan Labs) or HC diet supplemented with 2% Plant Sterol Esters (w/w) for further 8 weeks (n= 8-12/group). Cardiac puncture was performed in mice under terminal anesthesia (1mg/kg Medetomidine and 75mg/kg Ketamine, ip). PSE were provided by Danone (Barcelona, Catalonia, Spain). All sterol analyses were performed by gas liquid chromatography. The study protocol was approved by the local institutional animal research committee (ICCC051 / 5422) and was performed in agreement with the Guide for the Care and Use of Laboratory Animals published by the US National Institutes of Health.

Serum biochemistry and blood-derived mRNA obtainment

Blood samples were collected in serum separator gel tubes and PAX-tubes. Serum was obtained by centrifugation 3500rpm, 20 minutes at 4ºC. Cholesterol, triglycerides and HDL levels were measured enzymatically by using commercially available kits (GERNON reagents; RAL, Barcelona, Catalonia, Spain) and read in a spectrophotometer (MC-15 SOFT; RAL). PAX-tubes were processed for preparation of blood-derived mRNA using PAXgene Blood RNA Kit (QIAGEN Inc., Valencia, CA, USA). Concentration was determined with a NanoDrop ND-1000 spectrophotometer (NanoDrop Technologies Inc., Wilmington,

DE, USA) and purity was checked by the A260/A280 ratio (ratios between 1.8 and 2.1 were considered acceptable).

RNA isolation and Real Time PCR

Jejunum or liver tissues were frozen in liquid nitrogen and RNA was isolated with Trizol® Reagent (Invitrogen, Carlsbad, CA, USA) (N=5-7 mice/group). RNA from transfected human monocytes was isolated using Total RNA extraction kit (QIAGEN Inc.). cDNA was synthesized from 0.5 μg RNA with cDNA Reverse transcription kit (QIAGEN Inc.), the resulting cDNA samples were amplified by real-time polymerase chain reaction (RT-PCR) with the following specific probes from Applied Biosystems (Carlsbad, CA, USA): Lrp5 (Mm_01227476_m1), β-catenin (Mm_00483039_m1), Lef1 (Mm_00550265_m1), Bmp2 (Mm_01340178_m1), Opn (Mm_00436767_m1) and Vldlr (Mm00443298_m1), and from Integrated DNATechnologies, Inc. (Coralville, IA, USA): Ldlr (Mm.PT.49a.9930556), Lrp6 (Mm.PT.56a.6383636), Abcg5 (Mm.PT.56a.8809476) and Abcg8 (Mm.PT.56a.7910478). Results were normalized to 18S probe (Applied Biosystems). Blood-derived RNA was used to perform the RT2 Profiler PCR array PAMM-021 (SABiosciences, QIAGEN Inc.) with RT-PCR thermal cycler (Applied Biosystems 7900HT).

Western blot and antibodies

Sample extracts (100μg or 20 μg protein) were resolved by SDS-PAGE and transferred to nitrocellulose membranes, blocked with 5% skim milk and probed for monoclonal (LRP5, LDLR, LRP2, LRP6, β-actin from Abcam, Cambridge, UK; Histona H1 from Millipore, Bedford, MA, USA; VLDLR from Santa Cruz Biotechnology Inc, Santa Cruz, CA, USA; and LRP1 from Research Diagnostics Inc., Flanders, NJ, USA) or polyclonal (GAPDH and β-catenin from Millipore) primary antibodies. Membranes were then washed and blotted with anti-mouse, anti-rabbit or anti-chicken secondary antibodies (Dako, Glostrup, Denmark). Band densities were determined with the ChemiDoc XRS system (Bio-Rad Laboratories Inc., Hercules, CA, USA) in chemiluminescence detection modus and Quantity-One software (Bio-Rad Laboratories Inc.). Normalization was performed against β-actin.

Subfractionation experiments in human monocytes

Human monocytes were isolated from buffy coats, counted and seeded in BD Primaria™ plates. $10x10^6$ monocytes were suspended in 100µL of Cell Line Nucleofector® Solution V (Amaxa Inc., Gaithersburg, MD, USA) and 300nM of siRNA-Random (Ref. 4390843) or siRNA-LRP5 (Ref.s8293) from Applied Biosystems were transfected with X-001 program. siRNA-Random was used as a control and did not exert any effect on LRP5 expression. For nuclear extracts, cells were PBS washed, scraped with CSK buffer (50nM NaCl, 10mM Pipes pH6.8, 3mM $MgCl_2$, 0.5% Triton X-100, 300mM sucrose and protease inhibitors), incubated 20 minutes shaking at 4ºC and centrifuged. Supernatants (cytoplasmic fractions) were stored at -20ºC. Pellets (nuclear fractions) was suspended in 50uL of Sol/Insol Buffer (15mM pH7.5, 5mM EDTA, 2.5mM EGTA and 1% SDS), heated for 10 minutes at 100ºC when 50uL of CSK buffer was added. Subcellular fractions were analyzed by western blot for β-catenin, GAPDH, Histone H1.

Quantification of atherosclerotic lesions

Mice were anesthetized and aortas were removed, carefully cleaned of adventitial fat under a stereoscopic microscope, and longitudinally cut with the luminal surface facing up (n=6-8 mice/group). Aortas were fixed overnight in 4% paraformaldehyde, washed with ddH_2O 1 hour in gentle shaking and stained with Oil-red-O (ORO) for 30 minutes. Aortas were rinsed with 70% ethanol and ddH_2O; images were captured by Nikon Eclipse 80i microscope and digitized by Retiga 1300i Fast camera. ORO-stained area was quantified with Image J software and results are expressed as percentage of lipid area / total aortic area.

Statistical analysis

Results are expressed as mean ± S.E.M. A Stat View statistical package was used for all the analysis. Comparisons among groups were performed by two way ANOVA analysis. Regression analyses were performed by applying Y= a+b*X lineal pattern besides using

Stat View for Windows program, selecting just highly adjusted equations. Statistical significance was considered when $p<0.05$.

Acknowledgments

We thank Sonia Huertas for technical assistance and Danone for providing plant sterol esters. This work was supported by grants from the Spanish Ministry of Economy and Competitiveness (SAF 2013-42962-R to LB), Institute of Health Carlos III, ISCIII (TERCEL RD12/0019/0026 and RIC RD12/0042/0027 to LB); Ramon y Cajal Contract (to MBP) and a Danone Institute Fellowship (to CRS). The authors declare no conflict of interests.

References

1 Ferrero-Miliani L, Nielsen OH, Andersen PS, Girardin SE. Chronic inflammation: importance of NOD2 and NALP3 in interleukin-1β generation. *Clin Exp Immunol* 2007; **147**: 227–235.

2 O'Shea JJ, Murray PJ. Cytokine signaling modules in inflammatory responses. *Immunity* 2008; **28**: 477–487.

3 Martin P, Leibovich SJ. Inflammatory cells during wound repair: the good, the bad and the ugly. *Trends Cell Biol* 2005; **15**: 599–607.

4 Johnson ML. The high bone mass family--the role of Wnt/Lrp5 signaling in the regulation of bone mass. *J Musculoskelet Neuronal Interact* 2004; **4**: 135–138.

5 Tickenbrock L, Schwäble J, Strey A, Sargin B, Hehn S, Baas M *et al*. Wnt signaling regulates transendothelial migration of monocytes. *J Leukoc Biol* 2006; **79**: 1306–1313.

6 Kim J, Kim J, Kim DW, Ha Y, Ihm MH, Kim H *et al*. Wnt5a induces endothelial inflammation via beta-catenin-independent signaling. *J Immunol* 2010; **185**: 1274–1282.

7 Martin M, Rehani K, Jope RS, Michalek SM. Toll-like receptor-mediated cytokine production is differentially regulated by glycogen synthase kinase 3. *Nat Immunol* 2005; **6**: 777–784.

8 Gelfand BD, Meller J, Pryor AW, Kahn M, Bortz PDS, Wamhoff BR *et al*. Hemodynamic activation of beta-catenin and T-cell-specific transcription factor signaling in vascular endothelium regulates fibronectin expression. *Arterioscler Thromb Vasc Biol* 2011; **31**: 1625–1633.

9 Toerne C von, Schmidt C, Adams J, Kiss E, Bedke J, Porubsky S *et al*. Wnt pathway regulation in chronic renal allograft damage. *Am J Transplant* 2009; **9**: 2223–2239.

10 Stokes KY, Calahan L, Hamric CM, Russell JM, Granger DN. CD40/CD40L contributes to hypercholesterolemia-induced microvascular inflammation. *Am J Physiol Heart Circ Physiol* 2009; **296**: H689–H697.

11 Ridker PM. Hyperlipidemia as an instigator of inflammation: inaugurating new approaches to vascular prevention. *J Am Heart Assoc* 2012; **1**: 3–5.

12 Rajamäki K, Lappalainen J, Oörni K, Välimäki E, Matikainen S, Kovanen PT *et al*. Cholesterol crystals activate the NLRP3 inflammasome in human macrophages: a novel link between cholesterol metabolism and inflammation. *PLoS ONE* 2010; **5**: e11765.

13 Katan MB, Grundy SM, Jones P, Law M, Miettinen T, Paoletti R *et al*. Efficacy and safety of plant stanols and sterols in the management of blood cholesterol levels. *Mayo Clin Proc* 2003; **78**: 965–978.

14 Nashed B, Yeganeh B, HayGlass KT, Moghadasian MH. Antiatherogenic effects of dietary plant sterols are associated with inhibition of proinflammatory cytokine production in Apo E-KO mice. *J Nutr* 2005; **135**: 2438–2444.

15 Sabeva NS, McPhaul CM, Li X, Cory TJ, Feola DJ, Graf GA. Phytosterols differentially influence ABC transporter expression, cholesterol efflux and inflammatory cytokine secretion in macrophage foam cells. *J Nutr Biochem* 2011; **22**: 777–783.

16 Devaraj S, Autret BC, Jialal I. Reduced-calorie orange juice beverage with plant sterols lowers C-reactive protein concentrations and improves the lipid profile in human volunteers. *Am J Clin Nutr* 2006; **84**: 756–761.

17 Othman RA, Moghadasian MH. Beyond cholesterol-lowering effects of plant sterols: clinical and experimental evidence of anti-inflammatory properties. *Nutr Rev* 2011; **69**: 371–382.

18 Trautwein EA, Duchateau GSMJE, Lin Y, Mel'nikov SM, Molhuizen HOF, Ntanios FY. Proposed mechanisms of cholesterol-lowering action of plant sterols. *Eur J Lipid Sci Technol* 2003; **105**: 171–185.

19 Berge KE, Tian H, Graf GA, Yu L, Grishin NV, Schultz J *et al*. Accumulation of dietary cholesterol in sitosterolemia caused by mutations in adjacent ABC transporters. *Science* 2000; **290**: 1771–1775.

20 Brufau G, Kuipers F, Lin Y, Trautwein EA, Groen AK. A reappraisal of the mechanism by which plant sterols promote neutral sterol loss in mice. *PLoS ONE* 2011; **6**: e21576.

21 Lu K, Lee MH, Hazard S, Brooks-Wilson A, Hidaka H, Kojima H *et al*. Two genes that map to the STSL locus cause sitosterolemia: genomic structure and spectrum of mutations involving sterolin-1 and sterolin-2, encoded by ABCG5 and ABCG8, respectively. *Am J Hum Genet* 2001; **69**: 278–290.

22 Wu T, Fu J, Yang Y, Zhang L, Han J. The effects of phytosterols/stanols on blood lipid profiles: a systematic review with meta-analysis. *Asia Pac J Clin Nutr* 2009; **18**: 179–186.

23 Schneider S, Steinbeisser H, Warga RM, Hausen P. Beta-catenin translocation into nuclei demarcates the dorsalizing centers in frog and fish embryos. *Mech Dev* 1996; **57**: 191–198.

24 Dell'Accio F, Bari C De, El Tawil NMF, Barone F, Mitsiadis TA, O'Dowd J, Pitzalis C. Activation of WNT and BMP signaling in adult human articular cartilage following mechanical injury. *Arthritis Res Ther* 2006; **8**: R139.

25 Müller T, Bain G, Wang X, Papkoff J. Regulation of epithelial cell migration and tumor formation by beta-catenin signaling. *Exp Cell Res* 2002; **280**: 119–133.

26 Nakanishi K, Yoshimoto T, Tsutsui H, Okamura H. Interleukin-18 regulates both Th1 and Th2 responses. *Annu Rev Immunol* 2001; **19**: 423–474.

27 Badimon L. Interleukin-18: a potent pro-inflammatory cytokine in atherosclerosis. *Cardiovasc Res* 2012; **96**: 172–175; discussion 176–180.

28 Oppenheimer-Marks N, Brezinschek RI, Mohamadzadeh M, Vita R, Lipsky PE. Interleukin 15 is produced by endothelial cells and increases the transendothelial migration of T cells In vitro

and in the SCID mouse-human rheumatoid arthritis model In vivo. *J Clin Invest* 1998; **101**: 1261–1272.

29 Wu J, Richards MH, Huang J, Al-Harthi L, Xu X, Lin R *et al*. Human FasL gene is a target of β-catenin/T-cell factor pathway and complex FasL haplotypes alter promoter functions. *PLoS ONE* 2011; **6**: e26143.

30 Morimoto S, Nakano S, Watanabe T, Tamayama Y, Mitsuo A, Nakiri Y *et al*. Expression of B-cell activating factor of the tumour necrosis factor family (BAFF) in T cells in active systemic lupus erythematosus: the role of BAFF in T cell-dependent B cell pathogenic autoantibody production. *Rheumatology (Oxford)* 2007; **46**: 1083–1086.

31 Batten M, Li J, Yi S, Kljavin NM, Danilenko DM, Lucas S *et al*. Interleukin 27 limits autoimmune encephalomyelitis by suppressing the development of interleukin 17-producing T cells. *Nat Immunol* 2006; **7**: 929–936.

32 Niedbala W, Cai B, Wei X, Patakas A, Leung BP, McInnes IB *et al*. Interleukin 27 attenuates collagen-induced arthritis. *Ann Rheum Dis* 2008; **67**: 1474–1479.

33 Merad M, Manz MG. Dendritic cell homeostasis. *Blood* 2009; **113**: 3418–3427.

34 Svensson MND, Andersson SEM, Erlandsson MC, Jonsson I-M, Ekwall A-KH, Andersson KME *et al*. Fms-like tyrosine kinase 3 ligand controls formation of regulatory T cells in autoimmune arthritis. *PLoS ONE* 2013; **8**: e54884.

35 Aggarwal BB, Gupta SC, Kim JH. Historical perspectives on tumor necrosis factor and its superfamily: 25 years later, a golden journey. *Blood* 2012; **119**: 651–665.

36 Secchiero P, Corallini F, Iasio MG di, Gonelli A, Barbarotto E, Zauli G. TRAIL counteracts the proadhesive activity of inflammatory cytokines in endothelial cells by down-modulating CCL8 and CXCL10 chemokine expression and release. *Blood* 2005; **105**: 3413–3419.

37 Bernardi S, Zauli G, Tikellis C, Candido R, Fabris B, Secchiero P *et al*. TNF-related apoptosis-inducing ligand significantly attenuates metabolic abnormalities in high-fat-fed mice reducing adiposity and systemic inflammation. *Clin Sci* 2012; **123**: 547–555.

38 Stein JV, López-Fraga M, Elustondo FA, Carvalho-Pinto CE, Rodríguez D, Gómez-Caro R *et al*. APRIL modulates B and T cell immunity. *J Clin Invest* 2002; **109**: 1587–1598.

39 Teijeira Á, Palazón A, Garasa S, Marré D, Aubá C, Rogel A *et al*. CD137 on inflamed lymphatic endothelial cells enhances CCL21-guided migration of dendritic cells. *FASEB J* 2012; **26**: 3380–3392.

40 Borrell-Pagès M, Romero JC, Badimon L. LRP5 negatively regulates differentiation of monocytes through abrogation of Wnt signalling. *J Cell Mol Med* 2014; **18**: 314-325.

41 Borrell-Pagès M, Romero JC, Juan-Babot O, Badimon L. Wnt pathway activation, cell migration, and lipid uptake is regulated by low-density lipoprotein receptor-related protein 5 in human macrophages. *Eur Heart J* 2011; **32**: 2841–2850.

42 Jones PJH, AbuMweis SS. Phytosterols as functional food ingredients: linkages to cardiovascular disease and cancer. *Curr Opin Clin Nutr Metab Care* 2009; **12**: 147–151.

43 Kaneko E, Matsuda M, Yamada Y, Tachibana Y, Shimomura I, Makishima M. Induction of intestinal ATP-binding cassette transporters by a phytosterol-derived liver X receptor agonist. *J Biol Chem* 2003; **278**: 36091–36098.

44 Plat J, Nichols JA, Mensink RP. Plant sterols and stanols: effects on mixed micellar composition and LXR (target gene) activation. *J Lipid Res* 2005; **46**: 2468–2476.

45 Willnow TE, Sheng Z, Ishibashi S, Herz J. Inhibition of hepatic chylomicron remnant uptake by gene transfer of a receptor antagonist. *Science* 1994; **264**: 1471–1474.

46 Rohlmann A, Gotthardt M, Hammer RE, Herz J. Inducible inactivation of hepatic LRP gene by cre-mediated recombination confirms role of LRP in clearance of chylomicron remnants. *J Clin Invest* 1998; **101**: 689–695.

47 Dahlbäck B, Nielsen LB. Apolipoprotein M--a novel player in high-density lipoprotein metabolism and atherosclerosis. *Curr Opin Lipidol* 2006; **17**: 291–295.

48 Ye Z, Go G-W, Singh R, Liu W, Keramati AR, Mani A. LRP6 protein regulates low density lipoprotein (LDL) receptor-mediated LDL uptake. *J Biol Chem* 2012; **287**: 1335–1344.

49 Kobayashi K, Oka K, Forte T, Ishida B, Teng B, Ishimura-Oka K *et al*. Reversal of hypercholesterolemia in low density lipoprotein receptor knockout mice by adenovirus-mediated gene transfer of the very low density lipoprotein receptor. *J Biol Chem* 1996; **271**: 6852–6860.

50 Fujino T, Asaba H, Kang M-J, Ikeda Y, Sone H, Takada S *et al*. Low-density lipoprotein receptor-related protein 5 (LRP5) is essential for normal cholesterol metabolism and glucose-induced insulin secretion. *Proc Natl Acad Sci USA* 2003; **100**: 229–234.

51 Lusis AJ. Atherosclerosis. *Nature* 2000; **407**: 233–241.

52 Moore K J, Sheedy FJ, Fisher EA. Macrophages in atherosclerosis: a dynamic balance. *Nat Rev Immunol* 2013; **13**: 709–721.

53 Libby, P., Ridker, P. M. & Hansson, G. K. Inflammation in atherosclerosis: from pathophysiology to practice. *J Am Coll Cardiol* 2009; **54**: 2129–2138.

54 Holmen SL, Giambernardi TA, Zylstra CR, Buckner-Berghuis BD, Resau JH, Hess JF *et al*. Decreased BMD and limb deformities in mice carrying mutations in both Lrp5 and Lrp6. *J Bone Miner Res* 2004; **19**: 2033–2040.

55 Cui Y, Niziolek PJ, MacDonald BT, Zylstra CR, Alenina N, Robinson DR *et al*. Lrp5 functions in bone to regulate bone mass. *Nat Med* 2011; **17**: 684–691.

FIGURE 1

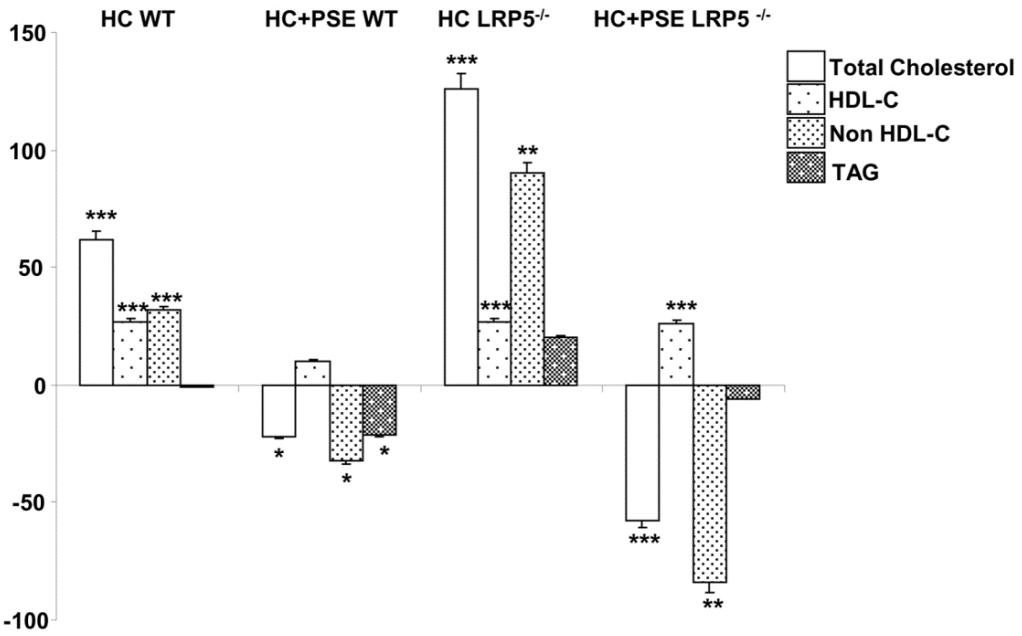

Figure 1: Relative changes in serum lipid composition of WT and LRP5$^{-/-}$ mice at sacrifice. Indicated significances are between the groups: NC *vs* HC and HC *vs* HC+PSE (n=9-12 mice/group). *p<0,05;**p<0,01; ***p<0,005.

FIGURE 2

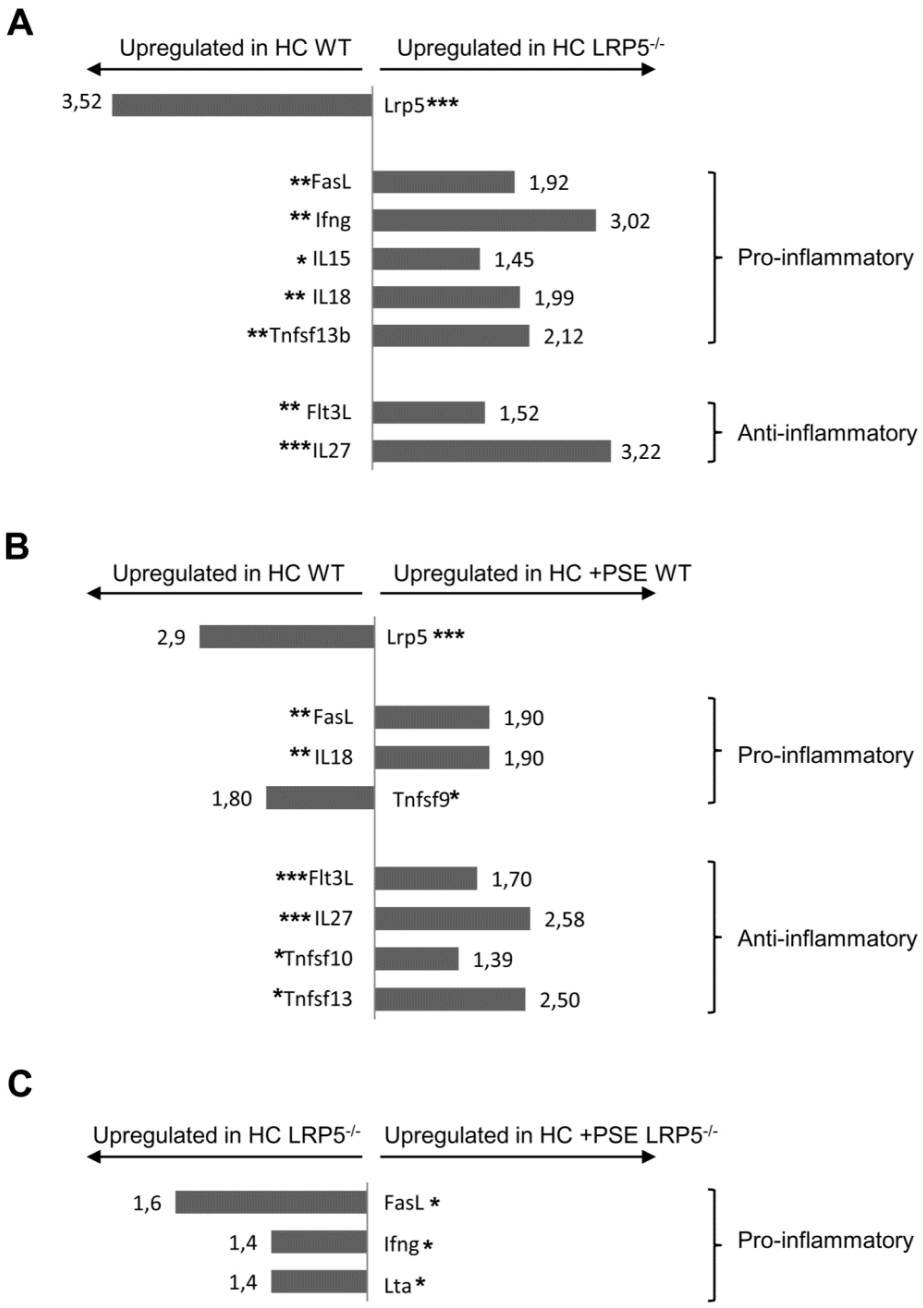

Figure 2: Differential expression of inflammatory genes in peripheral blood leukocytes . Bar chart showing the fold change of modulated genes in (**A**) HC LRP5$^{-/-}$ compared with HC WT mice; (**B**) in HC WT mice versus HC WT supplemented with 2% PSE; (**C**) in HC LRP5$^{-/-}$ mice versus HC LRP5$^{-/-}$ mice supplemented with 2% PSE (n=9-12 mice/group). *p<0,05;**p<0,01; ***p<0,005.

FIGURE 3

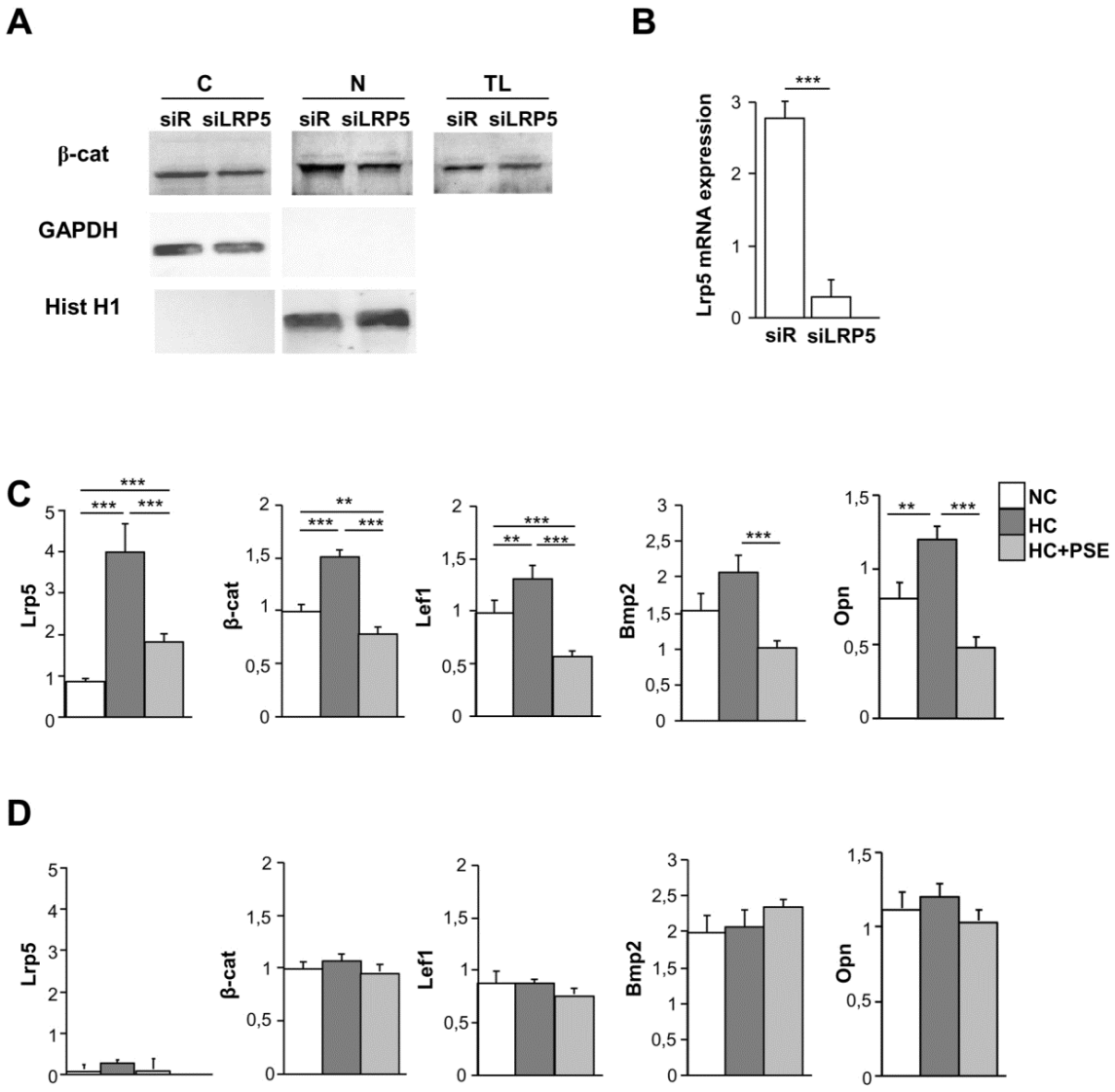

Figure 3: Reduced translocation of β-catenin into the nucleus in monocytes silenced for LRP5. **(A)** Human monocytes were transfected with siRNA-Random (siR) or siRNA-LRP5 (siLRP5) and total lysates (TL), cytoplasmic (C) and nuclear (N) fractions were analyzed by Western blotting using anti-β-catenin antibody. GAPDH and Histone H1 were used as quality controls for cytoplasmic and nuclear fractions respectively; **(B)** Lrp5 gene expression levels of monocytes in (A). Gene expression levels in circulating white cells of Lrp5, β-catenin, Lef1, Bmp2 and Opn genes in (**C**) WT mice or **(D)** LRP5-/- mice fed a NC, HC or a HC diet supplemented with 2% PSE (n= 9-12 mice/group)**.** **p<0,01; ***p<0,005.

FIGURE 4

A **WT mice**

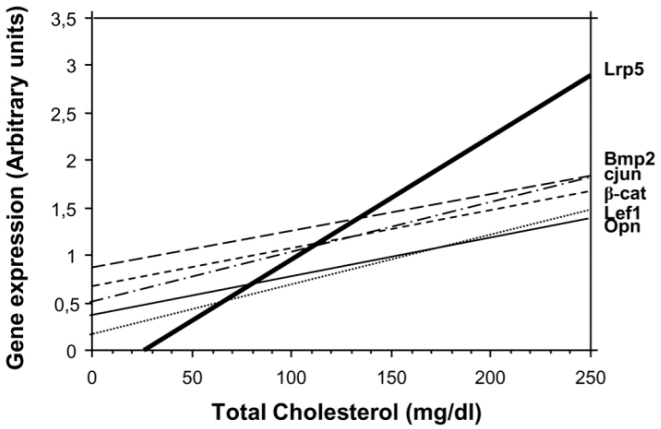

	p-value	r
lrp5	0,0004	0,812
β-catenin	0,009	0,728
lef1	0,056	0,722
opn	0,051	0,795
bmp2	0,059	0,708
c-jun	0,048	0,752

B **LRP5$^{-/-}$ mice**

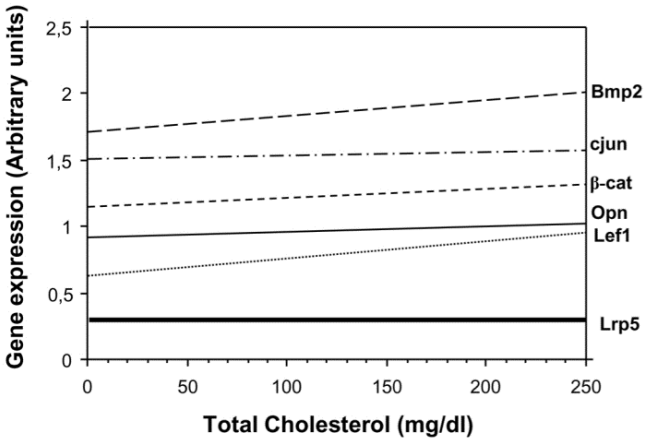

	p-value	r
lrp5	0,861	0,075
β-catenin	0,385	0,221
lef1	0,126	0,385
opn	0,824	0,056
bmp2	0,595	0,134
c-jun	0,808	0,062

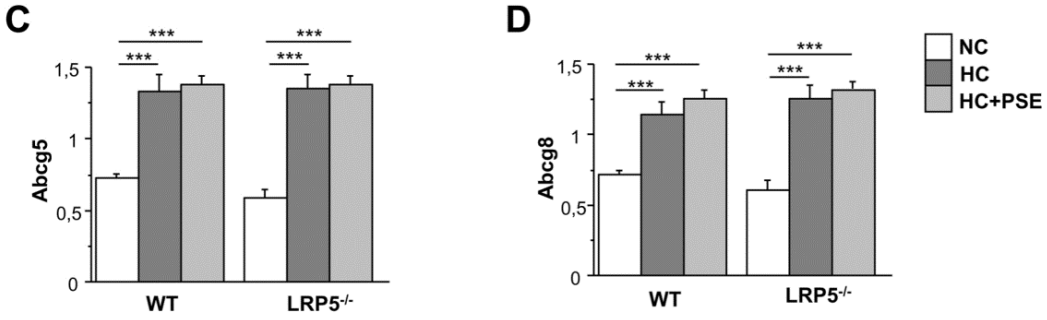

Figure 4: Linear regression analyses showing the correlation between Wnt signaling genes expression in peripheral blood leukocytes and plasma cholesterol concentrations in NC *vs* HC **(A)** WT mice and **(B)** LRP5 $^{-/-}$ mice with statistical significances (p-values) and linear correlation indexes (r). Jejunum gene expression levels of **(C)** Abcg5 and **(D)** Abcg8.

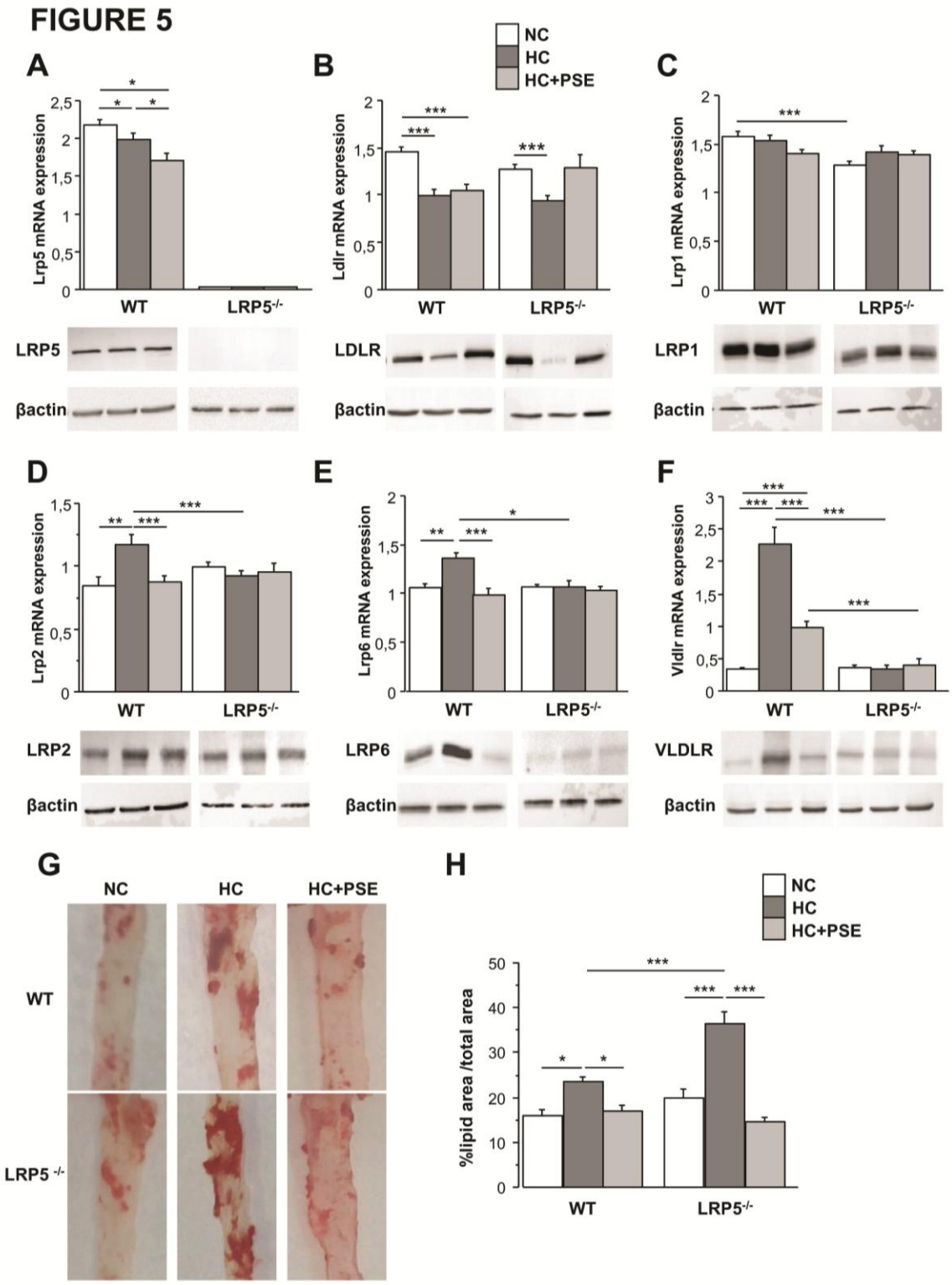

Figure 5: Liver gene and protein expression levels of (**A**) Lrp5, (**B**) Ldlr, (**C**) Lrp1, (**D**) Lrp2, (**E**) Lrp6 and (**F**) Vldlr in WT or LRP5$^{-/-}$ mice fed a NC, HC or a HC diet supplemented with 2% PSE (n= 9-12 mice/group). **(G)** Representative images of mice thoracic aortas stained with ORO. **(H)** Quantification of lipid covered area in mice aortas. *p<0,05; **p<0,01; ***p<0,005.

DISCUSIÓN GLOBAL

La aterosclerosis es la causa subyacente de las enfermedades cardiovasculares (CVD) de origen isquémico[159]. El desarrollo de las lesiones ateroscleróticas está caracterizado por la acumulación de LDL modificadas en la pared vascular[175]. Nuestra hipótesis de partida es que el LRP5, que forma parte de la familia de receptores de las LDL, participa en el desarrollo de las lesiones ateroscleróticas humanas. Para testarla, en primer lugar analizamos la expresión de LRP5 en los 4 tipos celulares presentes en las lesiones: células endoteliales (EC), células musculares lisas vasculares (VSMC), monocitos y macrófagos. Encontramos que LRP5 está expresado en todos los tipos celulares. Sin embargo, al ser tratadas con LDL agregadas (agLDL), una de las modificaciones iniciales de las LDL en la pared vascular, sólo las células inflamatorias (monocitos y macrófagos) muestran un incremento significativo de la expresión de LRP5.

Las agLDL son un potente inductor de la acumulación masiva de ésteres de colesterol (CE) en los macrófagos[176,177]. Inhibimos la expresión de LRP5 en macrófagos humanos tratados con agLDL y demostramos la participación de este receptor en la internalización de lípidos. Mediante cromatografía de capa fina (TLC) observamos que el silenciamiento de LRP5 disminuye la internalización de agLDL, evidenciado por la reducción del contenido total de lípidos en los macrófagos. Estos resultados sugieren la participación de LRP5 en la acumulación de CE en los macrófagos, que es un proceso que tiene lugar durante el desarrollo y progresión de la lesión aterosclerótica y es un regulador clave del comportamiento patológico de la placa[178,179].

Las agLDL incrementan la expresión de LRP1 en los macrófagos y en las VSMC[180,181]. Con el fin de determinar si la internalización de las agLDL por parte de LRP5 en los macrófagos es independiente de LRP1, bloqueamos LRP1 con anticuerpos monoclonales. En este ensayo el aumento de la expresión de LRP5 en los macrófagos inducido por las agLDL se mantiene, demostrando que LRP1 no interfiere en la inducción de la expresión de LRP5 por las agLDL extracelulares. El aumento de la expresión de LRP5 en macrófagos por parte de las agLDL provoca la activación de la vía de señalización canónica de Wnt. Tras la incubación con agLDL, los macrófagos humanos aumentan la expresión de β-CATENINA y LEF1, dos proteínas de la vía de señalización por Wnt. Además, cuatro genes diana de la vía, *C-JUN*, *CICLINA D1*, *BMP2* y *OPN*, también aumentan su expresión sólo en presencia de LRP5, indicando que la activación de la vía canónica de Wnt por las agLDL es dependiente de LRP5 en macrófagos humanos.

BMP2 y *OPN* participan en la progresión de las lesiones ateroscleróticas[182–185]. BMP2 está sobreexpresado en placas ateroscleróticas humanas y participa en la regulación de la biosíntesis del colesterol y en la calcificación aterosclerótica[182,185]. OPN es un potencial biomarcador ya que altos niveles de espresión de OPN en placas ateroscleróticas predicen el riesgo de padecer una nueva complicación vascular[184].La implicación de LRP5 en la internalización de las agLDL y el aumento de la expresión génica y proteica de las dianas de la vía canónica, OPN y BMP2, indican que LRP5 tiene un papel central en la progresión de la aterosclerosis.

C-JUN y CICLINA-D1, dos proteínas adicionales de la vía canónica de señalización por Wnt que aumentan su expresión en los macrófagos humanos después del tratamiento con agLDL, han mostrado su participación en la motilidad celular[186–188]. Todos estos resultados sugieren que LRP5 podría estar implicado en la motilidad de los macrófagos asociada a un proceso aterosclerótico. Ensayos de motilidad en macrófagos silenciados para LRP5 muestran una inhibición de la migración. El mismo ensayo realizado con macrófagos silenciados para LRP1 no mostró ningún cambio en la migración con respecto a los macrófagos control, indicando que el efecto observado en la motilidad de los macrófagos es específico de LRP5. Estos resultados se confirmaron mediante las cámaras Boyden, donde los macrófagos silenciados para LRP5 mostraron una migración menor que el control y que los macrófagos silenciados para LRP1. Evaluamos el efecto de las agLDL en nuestro ensayo de migración celular y observamos que el tratamiento con agLDL induce una reducción en la capacidad migratoria de los macrófagos humanos independientemente de la condición ensayada (siRandom, siLRP5 o siLRP1). Sin embargo, las células tratadas con agLDL y silenciadas para LRP5 muestran una inhibición mayor en la migración que la observada sólo con el tratamiento de agLDL. Estos resultados demuestran una capacidad migratoria reducida en las células inflamatorias deficientes para LRP5.

La aterosclerosis es una patología muy compleja que no sólo consiste en la acumulación de lípidos en la pared vascular, sino que también está influenciada por múltiples procesos que incluyen la inflamación, la diferenciación y la proliferación celular de los estirpes celulares presentes en la lesión[13,31–33,189,190]. Por otra parte, la vía de señalización por Wnt controla la proliferación, la diferenciación y el destino celular durante el desarrollo embrionario y la homeostasis tisular en adultos[103]. De hecho, se ha descrito la participación de la vía canónica de

Wnt en la migración de los monocitos humanos (HM) y en la proliferación de las VSMC[191,192], pero la contribución específica de cada uno de los componentes de la vía en estos procesos no ha sido estudiada. Nosotros postulamos que LRP5 y la vía de señalización por Wnt participan en la regulación de la proliferación y la diferenciación en las células monocíticas, células que son las principales responsables de la respuesta inflamatoria innata y que participan activamente en el proceso aterosclerótico[193,194]. Para probar nuestra hipótesis modulamos la expresión de LRP5 (sobreexpresión/inhibición) en un modelo de células monocíticas humanas (HL60). Así, los análisis de la incorporación celular de BrdU indican que la sobreexpresión de LRP5 en las células HL60 no diferenciadas induce una disminución de la proliferación. Una posible explicación para este hallazgo es la activación de la maquinaria de apoptosis. Se ha demostrado que la vía de señalización por Wnt regula la apoptosis en diferentes tipos celulares[195]. Nuestros estudios de apoptosis en células HL60 no diferenciadas que sobreexpresan LRP5 muestran un aumento de la apoptosis, mientras que el silenciamiento no tiene ningún efecto, indicando que éste podría ser el mecanismo implicado. Estos resultados están respaldados por estudios en ratones *Lrp5*$^{-/-}$, donde la persistencia de la vascularización fetal ocular en ratones *Lrp5*$^{-/-}$ es un resultado de la ausencia de apoptosis en las células epiteliales inducida por los macrófagos[80].

Para confirmar la activación de la apoptosis al sobreexpresar LRP5, analizamos la expresión de varias proteínas apoptóticas. BAX, DUSP6 y G0S2, conocidas por su función pro-apoptótica, aumentan su expresión celular al sobreexpresar LRP5. BAX es un miembro de la familia de BCL2 que interfiere en la función mitocondrial de las células por medio de la formación de poros en la membrana exterior de las mitocondrias[196]. DUSP6 participa en la vía pro-apoptótica ya que su infraexpresión provoca la sobreexpresión de ERK (quinasa regulada por señales extracelulares) y la supervivencia de las células endoteliales[197]. Además, la expresión exógena de DUSP6 induce la apoptosis de células de cáncer pancreático[198]. G0S2 es una proteína mitocondrial que interactúa específicamente con BCL2 y promueve la apoptosis al impedir la formación de los heterodímeros protectores BCL2/BAX[199].

La sobreexpresión de LRP5 provoca una reducción en la expresión de tres proteínas anti-apoptóticas, BCL2, CDK1 y CD180. BCL2 es una proteína de supervivencia con una función esencial en diferentes procesos biológicos[200]. CDK1 interactúa con CICLINA B1 para formar el factor promotor de mitosis, que activa varias vías de supervivencia[201,202] y la inhibición del complejo CDK1-CICLINA B1 resulta en un incremento de la apoptosis en células tumorales

humanas[203]. La proteína CD180 es trasmisora de una señal de activación que resulta en una proliferación celular masiva y en resistencia a la apoptosis[204]. La activación de la maquinaria de apoptosis en las células HL60 con altos niveles de expresión de LRP5 sugiere que este podría ser el mecanismo implicado en la disminución de la proliferación observada en estas células.

A continuación, evaluamos si el efecto negativo de LRP5 en la proliferación celular está restringido a células no diferenciadas. Para esto sobreexpresamos/inhibimos LRP5 en dos líneas celulares de cáncer humanas con altas tasas de proliferación: PC3 Y U87MG. La modulación de LRP5 no tiene ningún efecto en la proliferación de estas células indicando que la inhibición de la proliferación por la sobreexpresión de LRP5 está limitada a células no adheridas y no diferenciadas.

Los monocitos son células inflamatorias circulantes, con el potencial de migrar hacia los tejidos y diferenciarse a macrófagos o células dendríticas y así, participar en la respuesta inflamatoria local. En el caso de la progresión y el desarrollo de la lesión aterosclerótica el influjo de monocitos a áreas de la lesión está muy documentado[205]. Por tanto, analizamos el efecto de la modulación de LRP5 en la diferenciación de las células monocíticas. El silenciamiento de LRP5 en las HL60 provoca un aumento en la diferenciación celular mientras que la sobreexpresión de LRP5 induce un descenso en la diferenciación y una reducción en los niveles de expresión de los marcadores de adhesión y diferenciación *CD11B* y *CD44*. La molécula de adhesión CD11B es un marcador de maduración de células HL60 en respuesta a la diferenciación, ya que más del 90% de las células expresan CD11B después del tratamiento con PMA[206]. La molécula de adhesión CD44 es una glicoproteína transmembrana de la superficie celular y su principal función es mantener la estructura de los órganos y los tejidos por medio de la adhesión matriz-célula y célula-célula[207]. Estos resultados indican una función inhibidora de LRP5 en la diferenciación de las HL60 inducida por PMA que puede estar ocasionada por la interacción directa o indirecta de LRP5 con las moléculas de adhesión celular.

Al obtener estos resultados en una línea celular, investigamos si la función de LRP5 es también inhibidora sobre la diferenciación de monocitos humanos. Para ello realizamos cultivos primarios de monocitos humanos y los dejamos diferenciarse espontáneamente a macrófagos tras 7 días en cultivo. Modulamos la expresión de LRP5 y al igual que en las células HL60, la sobreexpresión de LRP5 en los HM provoca una disminución en su diferenciación. Para

determinar si el efecto en la diferenciación celular de los HM por parte de LRP5 ocurre a través de la modulación de la vía canónica de Wnt, analizamos la expresión de algunos genes diana de esta vía. La expresión de *LEF1, C-JUN y C-MYC* no varía al sobreexpresar LRP5 en los HM, sin embargo, aumenta la expresión de *β-CATENINA*. Este efecto sugiere una regulación inhibidora a nivel de β-CATENINA en monocitos humanos, pero sin afectar las proteínas/genes diana finales de la vía. Por el contrario, los macrófagos (células adheridas y diferenciadas) sí muestran un aumento en la expresión de los genes diana de la vía de señalización por Wnt al sobreexpresar LRP5. Es interesante que la sobreexpresión de LRP5 inhibe la diferenciación osteogénica en las células madre mesenquimales[208] y una represión de la vía canónica se ha descrito en células de carcinoma hepatocelular poco diferenciadas[209]. En conjunto, estos resultados indican una activación de la vía canónica al sobreexpresar LRP5 únicamente en las células diferenciadas.

Investigamos con más detalle los mecanismos que regulan la inhibición de la vía de señalización por Wnt en las células no diferenciadas (HL60 y HM) mediante experimentos de subfraccionamiento celular. La sobreexpresión de LRP5 mantiene el fenotipo de las células no diferenciadas por medio del secuestro de β-CATENINA en la membrana plasmática. Por el contrario, cuando las células están diferenciadas, la sobreexpresión de LRP5 induce la translocación de β-CATENINA al núcleo e incrementa los niveles de expresión de los genes diana de la vía de señalización por Wnt. De hecho, estudios en osteoblastos demuestran que la unión de N-CADHERINA con β-CATENINA en la membrana citoplasmática forma un complejo con AXINA y el dominio citoplasmático de LRP5 provocando la degradación de β-CATENINA y bloqueando la vía canónica de señalización por Wnt[210].

Los resultados obtenidos nos indujeron a considerar que la vía de señalización por Wnt se podría activar al sobreexpresar LRP5 en ausencia de sus ligandos. Varios estudios han mostrado que en la ausencia de sus ligandos, la sobreexpresión del dominio intracelular de LRP5 con o sin su dominio transmembrana, provoca la activación de la vía de señalización por Wnt mediante la dimerización citoplasmática del receptor[86,211,212]. Creemos que este mecanismo es el que explica nuestros resultados en células no diferenciadas que presentan una disminución en la proliferación y diferenciación celular al sobreexpresar el constructo de LRP5 en ausencia de sus ligandos.

Tras la caracterización *in vitro* de la implicación de LRP5 y de la vía canónica de señalización por Wnt en los procesos de proliferación, diferenciación, adhesión, motilidad y captación de lípidos en las células inflamatorias, nos propusimos estudiar la importancia de este receptor en la progresión de la lesión aterosclerótica utilizando un modelo *in vivo* de ratones deficientes para *Lrp5* alimentados con una dieta hipercolesterolémica (HC).

Inicialmente, analizamos los niveles de colesterol en suero de ratones tipo silvestre (*Wt*) y deficientes para *Lrp5* (*Lrp5*$^{-/-}$) alimentados o no con una dieta HC. En ambos genotipos los niveles de colesterol total y colesterol no-HDL en suero aumentan tras la administración de la dieta HC. Sin embargo, los niveles de colesterol total en suero de los ratones *Lrp5*$^{-/-}$ HC son más altos que los de los ratones *Wt* HC, sugiriendo la participación del LRP5 en el desarrollo de la dislipemia. De modo similar, un polimorfismo de un solo nucléotido en el gen de LRP5, rs3736228, que causa la pérdida de su función, provoca un incremento en los niveles de colesterol plasmático en la población China han [67] y es considerado un factor de riesgo independiente para la hipercolesterolemia en la población Japonesa masculina[65].

La participación de LRP5 en el metabolismo de las lipoproteínas se ha descrito en ratones deficientes para Lrp5[82]. Se observó que ratones *Lrp5*$^{-/-}$ alimentados con una dieta HC mostraban una tasa reducida de eliminación de CM residuales, asociados a los altos niveles de colesterol plasmáticos[82]. Postulamos que el incremento de los niveles de colesterol total en nuestros ratones *Lrp5*$^{-/-}$ HC en comparación con los de ratones *Wt* HC podría ser además debido en parte a una eliminación diferencial de LDL en el hígado dependiente de los receptores de LDL. Para probar esta hipótesis, analizamos la expresión hepática de otros miembros de la familia de receptores de LDL que están caracterizados por su participación en el metabolismo de las lipoproteínas, como son LDLR, VLDLR, LRP1, LRP2 y LRP6. Al igual que en otros modelos de animales hipercolesterolémicos[213,214], la administración de la dieta HC en nuestro modelo de ratones deficientes para LRP5 disminuye la expresión hepática de LDLR independientemente del genotipo.

La expresión de LRP2 y LRP6 se ha encontrado reducida en el hígado de ratones *Lrp5*$^{-/-}$ HC lo que nos indica su posible participación en la eliminación de LDL y otras lipoproteínas. LRP2 es un receptor de ApoM, una lipoproteína anti-aterogénica presente en las partículas de HDL, CM, VLDL y LDL[61]. LRP6 regula la captación de LDL mediada por LDLR ya que la internalización de

LDLR es disminuida en células *Lrp6*$^{-/-}$[215]. VLDLR presenta una expresión diferencial en los hígados de ratones *Wt* y *Lrp5*$^{-/-}$. En los ratones *Wt*, la expresión de VLDLR aumenta tras la administración de la dieta HC. Sin embargo, en los ratones *Lrp5*$^{-/-}$ los niveles de expresión de VLDLR permanecen constantes. Éste resultado explicaría el incremento en los niveles de colesterol no-HDL (donde se incluyen LDL y VLDL) en los ratones *Lrp5*$^{-/-}$ HC en comparación con los ratones *Wt* HC. Estos resultados parecen indicar que existe una reducción en la eliminación hepática de lipoproteínas en ausencia de LRP5. Se ha reportado que la expresión ectópica de VLDLR en el hígado de ratón aumenta la internalización de lipoproteínas[216]. De hecho, se observó que LRP5 es necesario para una adecuada eliminación hepática de lipoproteínas ya que 30 minutos después de la inyección de CM residuales marcados con fluorescencia en ratones *Lrp5*$^{-/-}$ y *Wt* alimentados con una dieta HC, el 80% de los CM permanecen en el plasma de los ratones *Lrp5*$^{-/-}$[82]. Sin embargo, los autores asumen que esta eliminación retardada de quilomicrones es causada solamente por la ausencia de LRP5 y no analizan la expresión de otros receptores. En nuestro estudio, hemos descrito que los bajos niveles de expresión de VLDLR, LRP2 y LRP6 contribuyen a la reducida eliminación hepática de lipoproteínas en los ratones *Lrp5*$^{-/-}$ HC y en consecuencia, a sus altos niveles de colesterol.

Al analizar el área cubierta por lípidos en las aortas de los ratones, observamos que los ratones *Lrp5*$^{-/-}$ HC presentan una mayor acumulación de lípidos en la aorta que los ratones *Wt* HC. Con el objetivo de determinar qué receptores de LDL podrían estar participando en la acumulación de lípidos observada en la pared arterial de los ratones *Lrp5*$^{-/-}$ HC, analizamos la expresión génica de miembros de la familia de LRP5 para los que se ha descrito participación en la progresión de la enfermedad cardiovascular. Así, analizamos la expresión de los genes *Ldlr, Vldlr, Lrp1, Lrp2, Lrp8* y *Cd36* en las aortas de los ratones. Los niveles de expresión de *Ldlr*, *Lrp2* y *Lrp8* eran más bajos en las aortas de los ratones *Lrp5*$^{-/-}$ HC indicando que estos receptores no contribuyen a la acumulación de lípidos observada en las aortas. La deficiencia de CD36 se ha asociado con aterosclerosis severa y con un aumento en la incidencia de enfermedad coronaria[217], sin embargo, macrófagos derivados de monocitos de personas deficientes para CD36 presentan una captación de LDL oxidadas reducida[218]. Nuestros resultados no apoyan la contribución de CD36 al fenotipo rico en lípidos de las aortas de ratones *Lrp5*$^{-/-}$, ya que su expresión incrementa en los ratones *Wt* HC pero se reduce en los ratones *Lrp5*$^{-/-}$ HC. La expresión aórtica de *Vldlr*, un receptor que se une a las VLDL y a los CM residuales, no está

modificada por la hipercolesterolemia moderada ni por la deficiencia de *Lrp5*. Por el contrario, Lrp1 esta sobreexpresado en las aortas de los ratones *Lrp5*$^{-/-}$ HC. Este receptor se encuentra sobreexpresado en las VSMC y en macrófagos humanos tras el tratamiento con lípidos extracelulares, así como en las placas ateroscleróticas humanas[180,219]. Además, se han encontrado niveles altos de expresión de LRP1 en las aortas de conejos y cerdos después de una dieta HC, sugiriendo un papel proaterogénico para la sobreexpresión de LRP1[180(p-),220]. Nuestros resultados también muestran un aumento de la expresión de LRP1 en los ratones *Wt* y *Lrp5*$^{-/-}$ hipercolesterolémicos. La expresión de LRP6 aumenta en la aorta de los ratones *Lrp5*$^{-/-}$ HC y este incremento se correlaciona positivamente con el área que cubre la lesión aórtica. *LRP6* se encuentra sobreexpresado en lesiones ateroscleróticas humanas[221] y regula la captación de LDL por parte de LDLR en células derivadas de ovario de hámster adulto (CHO) a través de la formación de un complejo con clatrina, LDLR y la proteína de la hipercolesteromia autosómica recesiva (ARH) que permite la internalización de LDLR tras la estimulación con las LDL[215]. Estos resultados sugieren que *Lrp1* y *Lrp6* contribuyen al incremento de la acumulación de lípidos en las aortas de los ratones *Lrp5*$^{-/-}$ HC, pero son necesarios más estudios sobre las interacciones de LRP1-LRP5 y LRP6-LRP5 para poder completar esta vía de regulación.

Los análisis por inmunohistoquímica (IHC) muestran un mayor número de macrófagos en la capa íntima de las aortas de los ratones *Lrp5*$^{-/-}$ HC en comparación con los *Wt*, apoyando nuestros resultados *in vitro* donde los monocitos que sobreexpresan LRP5 presentan una inhibición de la diferenciación mediante el secuestro de β-CATENINA en la membrana celular. Además, se evidencia una infraexpresión de las proteínas β-CATENINA y MMP7, componentes de la vía de señalización por Wnt, en los ratones deficientes para *Lrp5* confirmando nuestros resultados previos que muestran que el silenciamiento de LRP5 en los macrófagos humanos impide la activación de la vía de señalización Wnt/β-CATENINA. De esta manera, demostramos que los ratones *Lrp5*$^{-/-}$ HC presentan mayor acumulación de macrófagos en la pared vascular probablemente como consecuencia de la falta de activación de la vía canónica de señalización por Wnt.

Los macrófagos activados estimulan la producción y secreción de citoquinas que provocan un estímulo crónico pro-inflamatorio[27,28,34]. Analizamos la expresión de algunas citoquinas pro- y anti-inflamatorias en leucocitos circulantes de los ratones *Wt* y *Lrp5*$^{-/-}$ alimentados con una dieta HC (estímulo pro-inflamatorio) o con una dieta HC suplementada con fitoesteroles

esterificados (PSE, estímulo anti-inflamatorio). Tras la administración de la dieta HC, varios genes pro-inflamatorios incrementan su expresión en leucocitos circulantes de los ratones *Lrp5*$^{-/-}$ en comparación con los ratones *Wt*, sugiriendo que los ratones *Lrp5*$^{-/-}$ no pueden regular apropiadamente la respuesta inflamatoria durante la hipercolesterolemia. IL18 induce la producción de IFNG en las células Th1 y natural killer (NK)[222] y ha sido ampliamente descrita como una citoquina pro-inflamatoria de la progresión de la aterosclerosis[223]. La expresión de *Il18* es mayor en los ratones *Lrp5*$^{-/-}$ HC en comparación con los ratones *Wt* HC, sugiriendo un aumento de la respuesta inflamatoria en ausencia de LRP5.

Il15 está sobreexpresada en leucocitos de sangre periférica de ratones *Lrp5*$^{-/-}$ HC. Ésta citoquina tiene propiedades pro-inflamatorias, es producida por las células endoteliales en respuesta a IFNG y estimula la migración de las células T a los sitios de inflamación[224]. Otros genes pro-inflamatorios que están sobreexpresados en los ratones *Lrp5*$^{-/-}$ HC son *Fasl* y *Tnfsf13b*, miembros de la familia del factor de necrosis tumoral (TNF). FASL está expresado principalmente en las células T activadas, en las células NK, en macrófagos y en las células de cáncer e induce la apoptosis provocando daño tisular[225]; mientras TNFSF13B, también conocido como el factor activador de células B (BAFF), es producido y secretado principalmente por las células mieloides y su expresión es estimulada por IFNG, IL10 y CD40L durante la inflamación e infecciones crónicas[226].

Durante la progresión de la inflamación las células tratan de restablecer sus condiciones normales. En nuestro modelo, dos citoquinas anti-inflamatorias se encuentran sobreexpresadas en los ratones *Lrp5*$^{-/-}$ con altas concentraciones de colesterol en suero, *Il27* y *Flt3l*. La citoquina IL27 inhibe la muerte de las células T inducida por FasL y reduce la inflamación del sistema nervioso central, la secreción de citoquinas inflamatorias y la inflamación de las articulaciones en modelos de ratón con esclerosis múltiple y artritis reumatoide[227,228]. La señalización de FLT3L es crucial en el desarrollo temprano de los linfocitos progenitores y es el principal factor de diferenciación para las células dendríticas[229,230].

La adición de los PSE a la dieta HC, induce la expresión génica de varias citoquinas anti-inflamatorias en leucocitos de los ratones *Wt.* Además de *Flt3l* e *Il27*, las citoquinas *Tnfsf10* y *Tnfsf13* también están sobreexpresadas en ratones Wt alimentados con la dieta HC suplementada con PSE. *Tnfsf10* y *Tnfsf13* pertenecen a la familia de TNF, conocida por sus

funciones inductoras de apoptosis y pro-fibrosis[231]. Sin embargo, algunos de sus miembros pueden inducir funciones anti-inflamatorias, anti-apoptóticas y de supervivencia. TNFSF10 induce la proliferación y supervivencia de las células endoteliales vasculares humanas y reduce la adhesión entre leucocitos y células endoteliales[232,233]. Además, TNFSF10 reduce los niveles de glucosa en ayunas y de citoquinas pro-inflamatorias mejorando la diabetes mellitus tipo 2 en un modelo de ratones hipercolesterolemicos[234]. Ratones deficientes para TNFSF13 presentan un incremento en la proliferación de células T, una elevada producción de citoquinas Th2 y una susceptibilidad reducida a la artritis[235]. La adición de los PSE a la dieta también reduce los niveles de expresión de *Tnfsf9*, una citoquina pro-inflamatoria que estimula la activación y supervivencia de las células T[236]. El aumento en la expresión de citoquinas anti-inflamatorias tras el consumo de los PSE en los ratones *Wt* demuestra su efecto benéfico en la resolución de la inflamación durante la hipercolesterolemia.

Con el objetivo de determinar los mecanismos por los cuales la ausencia de LRP5 participa en la respuesta inflamatoria analizamos la expresión de varios genes diana de la vía canónica de señalización por Wnt en leucocitos de ratones *Wt* y *Lrp5*$^{-/-}$. Observamos que la expresión de *Lrp5, β-catenina, Lef1, Bmp2* y *Opn*, aumenta en los ratones *Wt* HC confirmando nuestros resultados previos *in vitro* que demuestran la activación de la vía canónica en presencia de altos niveles de lípidos en cultivos de macrófagos humanos. Además, análisis de regresión demuestran que los niveles altos de colesterol en suero se correlacionan positivamente con mayores niveles de expresión de los genes de la vía de señalización por Wnt. Por el contrario, la expresión de los genes de la vía de señalización por Wnt en leucocitos de ratones *Lrp5*$^{-/-}$ HC no aumenta a pesar de presentar mayores niveles de colesterol en suero que los ratones *Wt*. Estudios de subfraccionamiento celular en monocitos humanos evidencian una reducción en la cantidad de β-CATENINA translocada al núcleo en ausencia de LRP5, indicando una disminución de la señalización de la vía canónica. Estos resultados apoyan una función anti-inflamatoria y de supervivencia para LRP5 y la vía de señalización por Wnt en leucocitos circulantes de los ratones *Wt*.

A continuación analizamos la expresión de los genes de la vía de señalización por Wnt en los ratones alimentados con la dieta HC suplementada con PSE. Los niveles de expresión de *Lrp5, β-catenina, Lef1, Bmp2* y *Opn* disminuyen significativamente al añadir PSE a la dieta HC en los ratones *Wt*. Probablemente, el mecanismo por el cual los PSE disminuyen la activación de la vía

canónica es dependiente de los niveles de colesterol. Los PSE han sido descritos por su habilidad para disminuir los niveles de colesterol reduciendo su absorción en el duodeno y yeyuno por medio de su integración en las micelas lipídicas con mayor afinidad que el colesterol[237]. Otro mecanismo por el cual los PSE pueden disminuir la concentración del colesterol plasmático implica la reducción de la absorción intestinal del colesterol a través de la regulación de dos receptores transportadores con dominio de unión al ATP, ABCG5 y ABCG8, mediante la activación del receptor nuclear LXR[146,147]. En nuestro modelo, la expresión en el yeyuno de estos dos transportadores incrementa en ambos genotipos por igual tras la dieta HC independientemente de la administración de los PSE, indicando que este mecanismo no es el responsable del incremento del colesterol en suero observado en los ratones *Lrp5*$^{-/-}$ HC.

Por último, nos propusimos demostrar la modulación de LRP5 por parte de los lípidos extracelulares *in vivo* y estudiar el contenido lipídico de las lesiones aórticas presentes en los ratones deficientes para *Lrp5*. Nuestra hipótesis es que la modulación de los niveles de colesterol en suero puede regular la expresión aórtica de LRP5. Las placas ateroscleróticas están formadas por ácidos grasos libres, colesterol y lípidos neutros que incluyen los acilglicéridos y los ésteres de colesterol (CE)[238]. Ya que el incremento de algunos lípidos neutros está asociado con la progresión de la aterosclerosis[239–241], analizamos el contenido de acilglicéridos y CE en las aortas de los ratones mediante cromatografía en capa fina. Encontramos un incremento del contenido de CE en los ratones *Wt* tras ser alimentados con la dieta HC que está correlacionado con un incremento en la expresión aórtica de *Lrp5*, apoyando nuestros estudios previos donde las agLDL aumentan la expresión de LRP5 en macrófagos humanos en cultivo.

La acumulación de acilglicéridos también aumenta en los ratones *Lrp5*$^{-/-}$ y *Wt* tras ser alimentados con la dieta HC. La acumulación de triacilglicéridos (TAG) en la pared vascular es realizada por los macrófagos[242]. Los mecanismos implicados en esta acumulación incluyen el aumento en la captación de glucosa y su incorporación en los lípidos, el aumento en la síntesis de TAG y el descenso en la lipólisis de TAG[242]. Estudios previos han demostrado que los ratones *Lrp5*$^{-/-}$ tienen una insuficiencia en la eliminación de TAG del plasma sugiriendo que LRP5 modula su eliminación al estimular la hidrólisis de TAG[82]. Se ha descrito que macrófagos estimulados con lipopolisacáridos (LPS) almacenan más TAG y CE[242–244] y que la cantidad de lipoproteínas ricas en TAG aumenta durante la inflamación[245]. Por esto, un incremento en la acumulación de

TAG en las aortas de los ratones *Lrp5*$^{-/-}$ puede ser consecuencia de una respuesta inflamatoria incrementada apoyando una función anti-inflamatoria para la vía de señalización canónica por Wnt[115,118,119,246].

Una reducción en los niveles de TAG en suero tras el consumo de PSE se ha descrito en los ratones C57Bl6 alimentados con una dieta HC[134], en personas sanas[247] y en pacientes con síndrome metabólico[248]. Hemos observado un incremento en los niveles de TAG en suero y un aumento en la expresión hepática de VLDLR en los ratones *Wt* HC. Tras la suplementación de la dieta HC con PSE, los niveles de TAG en suero disminuyen y los niveles de expresión hepática de VLDLR vuelven a los observados en normocolesterolemia. Sin embargo, no se observa ningún cambio en la concentración de TAG en suero ni en los niveles de la expresión hepática de VLDLR en los ratones *Lrp5*$^{-/-}$ HC sugiriendo que LRP5 es necesario para modular los niveles de TAG en suero a través de la interacción con VLDLR en el hígado.

El consumo de PSE disminuye los niveles de lípidos en suero modulando la expresión de *Lrp5* y el contenido de CE en las lesiones ateroscleróticas. De hecho, observamos una reducción en los niveles de colesterol total en suero y en el área de las lesiones en la aorta tras la administración de la dieta HC suplementada con PSE. La habilidad de los PSE para reducir lesiones ateroscleróticas se ha descrito en los ratones *Apoe*$^{-/-}$ alimentados con una dieta HC suplementada con fitoesteroles al 2%, los cuales presentan lesiones tempranas con células espumosas superficiales a diferencia de las lesiones avanzadas encontradas en los ratones *Apoe*$^{-/-}$ HC[148]. De modo similar, el área de células espumosas en el arco aórtico de hámsteres alimentados con una dieta proaterogénica suplementada con PSE es menor que en los hámsteres control[149]. Estudios en ratones *Ldlr*$^{+/-}$ también sugieren que los PSE no son aterogénicos ya que la adición de los PSE a la dieta HC inhibe la progresión de las lesiones ateroscleróticas existentes[150]. Así, nuestros resultados respaldan un efecto benéfico del consumo de PSE en la progresión de la aterosclerosis y demuestran la modulación de la expresión aórtica de LPR5 por parte de los niveles de colesterol en suero.

Los niveles de expresión aórtica de *Lrp5* aumentan en los ratones *Wt* HC con grandes lesiones ateroscleróticas y disminuye tras el consumo de PSE en ratones con lesiones ateroscleróticas de menor tamaño. Además, existe una correlación positiva entre el tamaño del área cubierta por lípidos y la expresión génica de Lrp5 en la aorta de ratones *Wt* HC que no se observa en los

ratones *Lrp5*$^{-/-}$. Tras el consumo de los PSE, se observa una correlación entre los niveles de colesterol no-HDL y las lesiones aórticas de los ratones *Wt*, y la correlación entre los niveles de colesterol no-HDL y los niveles de expresión de *Lrp5* en la aorta de los ratones *Wt* observada con la dieta HC continua siendo significativa. Estos resultados sugieren que la expresión de *Lrp5* en la pared vascular esta modulada por los niveles de lípidos en plasma.

En resumen, este trabajo describe la implicación de LRP5 en diferentes procesos celulares claves durante la formación de la lesión, como son la infiltración y diferenciación de las células monocíticas, la adhesión y migración celular y la captación de lípidos. Además, demostramos que la ausencia de este receptor durante la hipercolesterolemia ocasiona una deficiencia en la respuesta inflamatoria y en el metabolismo de las lipoproteínas a nivel sistémico. En conjunto, nuestros resultados demuestran la participación de LRP5 en el desarrollo de la lesión aterosclerótica y evidencian un papel ateroprotector y de supervivencia para LRP5 y la vía canónica de señalización por Wnt.

CONCLUSIONES

- Los macrófagos deficientes para LRP5 presentan una menor acumulación intracelular de lípidos y una capacidad migratoria reducida.
- La sobreexpresión de LRP5 en monocitos activa la maquinaria de apoptosis y disminuye su capacidad de proliferación y diferenciación a macrófagos debido al secuestro de β-CATENINA en la membrana celular.
- Un incremento de los lípidos extracelulares provoca un incremento en la expresión celular de LRP5 y la activación de la vía canónica de señalización por Wnt en cultivos primarios de macrófagos humanos y en la aorta de ratones alimentados con una dieta HC.
- Ratones deficientes para *Lrp5* alimentados con una dieta HC presentan mayores niveles de colesterol en plasma, mayor acumulación de lípidos en las aortas y mayor expresión de proteínas pro-inflamatorias en leucocitos circulantes en comparación con los ratones WT HC, sugiriendo un rol anti-inflamatorio y protector para LRP5 durante la progresión de la lesión aterosclerótica.
- La deficiencia de *Lrp5* impide la activación de la vía canónica de señalización por Wnt en respuesta a la dieta HC, ocasionando el aumento de la infiltración de lípidos y monocitos en la pared vascular e incrementando la inflamación sistémica.
- LRP5 y la vía de señalización por Wnt tienen un papel anti-inflamatorio durante la progresión de la lesión aterosclerótica ya que ratones *Wt* con elevados niveles de colesterol en sangre presentan una mayor expresión de LRP5 y proteínas de la vía de señalización por Wnt en leucocitos circulantes y una menor expresión de citoquinas inflamatorias en comparación con los ratones $Lrp5^{-/-}$ HC.
- La adición de los PSE a la dieta HC disminuye la formación de lesiones ateroscleróticas mediante la reducción de los niveles de colesterol en suero, la reducción de CE en las aortas de los ratones y la secreción en sangre de citoquinas anti-inflamatorias.
- LRP5 y la vía canónica de señalización por Wnt son protectores contra el desarrollo de lesiones ateroscleróticas.

PARTICIPACIÓN DEL DOCTORANDO EN LOS ARTÍCULOS PUBLICADOS

La Dra. Lina Badimon y la Dra. Maria Borrell-Pagés, como codirectoras de la tesis doctoral de July Carolina Romero Sandoval, certifican que la participación de la doctoranda en los artículos presentados en esta tesis ha sido la siguiente:

Artículo 1: Realizó los experimentos de las figuras 2 y 4.

Artículo 2: Realizó los experimentos de las figuras 1, 2, 3, 4, 5, 6 y 7 y colaboró con la redacción de los materiales y métodos y en la corrección del artículo.

Artículo 3: Realizó los experimentos de las figuras 1, 2, 3A, 3D, 5 y 6 y participó en la escritura y corrección del artículo.

Artículo 4: Realizó los experimentos de las figuras 1, 2, 3, 4 y 5 y participó en la escritura y corrección del artículo.

Artículo 5: Realizó los experimentos de las figuras 1, 2, 3 y 4 y participó en la escritura y corrección del artículo.

Además, certifican que ninguna de estas publicaciones ha sido incluida en otra tesis doctoral.

Firmado,

Prof. Lina Badimon Dra. Maria Borrell-Pagés

OTRAS PUBLICACIONES

Thrombosis Research 130 (2012) S12–S15

Contents lists available at SciVerse ScienceDirect

Thrombosis Research

journal homepage: www.elsevier.com/locate/thromres

Circulating Biomarkers

L. Badimon [a,b,c,*], J.C. Romero [a], J. Cubedo [a], M. Borrell-Pagès [a]

[a] Cardiovascular Research Center, CSIC-ICCC, Hospital de la Santa Creu i Sant Pau, IIB-Sant Pau, Barcelona, Spain
[b] CIBERobn, Fisiopatología de la Obesidad y Nutrición, Instituto de Salud Carlos III, Spain
[c] Cardiovascular Research Chair, UAB, Barcelona, Spain

ARTICLE INFO

Keywords:
cardiovascular disease
biomarker
myocardial infarction
risk factor
atherosclerosis

ABSTRACT

Cardiovascular diseases (CVD) remain a leading cause of death worldwide. In the past years new biomarkers have drawn the clinician's attention for their use in primary prevention and in the identification of individuals at cardiovascular risk. Biomarkers also provide information on the progression and possible recurrence of cardiovascular events, and include inflammatory markers (C-reactive protein and interleukin-18), endothelial dysfunction markers (intercellular adhesion molecule-1 and vascular cell adhesion molecule-1), neurohormonal markers (brain natriuretic peptide and copeptine), ischemia biomarkers (apolipoprotein J) and necrosis markers (troponins). Although biomarkers provide utility for predicting cardiovascular risk, the identification and characterization of new biomarkers to achieve increasing diagnosis and prognostic efficiency in CVD prevention is of high clinical interest. In this review we will discuss on recently discovered biomarkers and their clinical applications.

Introduction

Cardiovascular diseases (CVD) are the leading cause of death in industrialized countries [1]. Effective primary prevention relies on the accurate identification of individuals at risk of developing heart disease [2]. Traditional risk factors including age, gender, dyslipemia, hypertension, diabetes and smoking are useful, but the identification of new cardiovascular risk factors to improve our understanding of disease biology and clinical disease manifestation as well as therapeutic efficacy are still needed.

Biomarkers are analytical tools used to assess biological parameters. An NIH working group standardized the definition of a biomarker as "a characteristic that is objectively measured and evaluated as an indicator of normal biological processes, pathogenic processes, or pharmacologic responses to a therapeutic intervention" [3]. Biomarkers are currently used to identify high-risk individuals, to diagnose disease conditions promptly and accurately, and to effectively prognosticate and treat patients with disease [4]. It is of clinical value only if it is accurate, reproducible in a standardized manner, adequate to the patient, easy to interpret by clinicians and has high specificity and sensitivity for the parameter it is expected to identify [5].

Atherosclerosis, myocardial infarction and other CVD have complex progression so it is simplistic to assume that a group of biomarkers can determine the inter-individual variation and susceptibility to develop a certain disease manifestation. Scientific approaches should involve the analysis of multiple biomarkers that cover different aspects of the physiopathological processes associated to disease progression.

In this review we will describe cardiovascular biomarkers already implemented in clinical diagnosis and novel biomarkers that are under evaluation for future medical applications. We will also describe the different contributions of each biomarker to the progression of CVD.

Cardiovascular Disease Biomarkers

Several biomarkers have been highlighted for their ability to predict cardiovascular events. These include inflammation, endothelial dysfunction, neurohormonal activation, ischemia biomarkers and necrosis biomarkers (Table 1).

Inflammation and Endothelial Dysfunction biomarkers

Atherosclerosis is usually initiated by endothelium damage that releases soluble forms of cellular adhesion molecules. These proteins are accepted as markers of endothelial dysfunction and vascular disease [5]. Indeed, trans-endothelial migration of leukocytes is regulated by soluble cell adhesion molecules including intercellular adhesion molecule-1 (ICAM-1), vascular adhesion molecule-1 (VCAM-1) and E-selectin. When endothelial cells are activated by pro-inflammatory stimuli such as bacterial endotoxins, interleukin 1b (Il-1b), tumour necrosis factor-α (TNF-α), C reactive protein (CRP), oxidized low-density lipoproteins (LDL) or hemodynamic forces related to blood flow, adhesion molecule expression is increased. Therefore adhesion molecules are considered early systemic inflammation and endothelial cell activation markers [5].

* Corresponding author at: Cardiovascular Research Center, C/Sant Antoni Maria Claret 167, 08025 Barcelona, Spain. Tel.: +34 935565880; fax: +34 935565559.
E-mail address: lbadimon@csic-iccc.org (L. Badimon).

0049-3848/$ – see front matter © 2012 Elsevier Ltd. All rights reserved.
http://dx.doi.org/10.1016/j.thromres.2012.08.262

Other molecules including soluble CD40 ligand (sCD40L), interleukin-18 (Il-18), monocyte chemotactic protein-1 (MCP1), fibrinogen and CRP are inflammatory biomarkers that result in endothelial activation [1]. sCD40L belongs to the TNFα family and is involved in the pathogenesis of atherosclerosis through its inflammatory and pro-thrombotic properties [1,6]. IL-18 is highly expressed in atherosclerotic plaques when compared to healthy arteries and high serum levels are found in individuals who have suffered a myocardial infarction or unstable angina episode [7]. MCP1 promotes plaque instability by recruiting monocytes to sites of inflammation [8]. Fibrinogen is related to atherosclerosis and thrombosis by its participation in the coagulation cascade where it increases blood viscosity, promotes platelet aggregation and stimulates smooth muscle cells migration [1,9]. High CRP plasmatic levels are associated to risk of stroke, angina and myocardial infarction and are predictors of atherosclerosis and vascular death [10]. Besides acting as an inflammation biomarker, CRP is also a vascular disease mediator as it can alter endothelial cells phenotype contributing to lesion formation, plaque rupture and coronary thrombosis [1]. A monomeric form of CRP displays a pro-thrombotic phenotype enhancing not only platelet deposition, but also thrombus growth; however, it is mainly attached to vascular components [11].

Myeloperoxidase (MPO) has emerged as a potential participant in the promotion and/or propagation of atherosclerosis and other CVD [12]. It is an enzyme present in activated neutrophils, monocytes and tissue macrophages that catalyzes the formation of reactive oxygen species (ROS). MPO and ROS are abundant in human atherosclerotic plaques [13] and show increased expression levels in the infarct area after an acute myocardial infarction (AMI) [14]. High plasmatic MPO levels predict endothelial dysfunction and coronary artery disease [15] while low plasmatic levels and certain specific MPO polymorphisms have been described as cardioprotective [16].

The molecular and cellular features associated with vulnerable plaques are considered potential diagnostic markers for plaque rupture and for the identification of patients at risk. The Athero-Express vascular bio-bank has been used to prospectively study atherosclerotic plaque in relation to future local and systemic vascular outcomes. This proteomic search of atherosclerotic plaque-derived biomarkers has identified osteopontin (OPN) as a potential plaque biomarker. High plasma levels of OPN strongly predict the risk of a new vascular complication [17].

There is an increasing interest on the role of free fatty acids (FFA) on early steps of atherogenesis and their implications on the prevention and treatment of CVD. FFA can increase the generation of ROS by the production of cytokines in mononuclear cells. They can also induce the activation of pro-inflammatory NF-κB pathways in human endothelial cells [18]. To prove the clinical relevance of FFA a group of healthy subjects received a 48-hour infusion of low-dose lipid to increase plasma FFA to levels of obesity and diabetes. Plasmatic levels of endothelial activation biomarkers (ICAM and VCAM), systemic inflammation biomarkers (MPO) and thrombosis biomarkers (total plasminogen inhibitor-1 -tPAI-1-) were increased providing direct evidence in humans that mild short-term lipid-oversupply is sufficient to initiate early vascular abnormalities that may lead to atherosclerosis and CVD [5].

Table 1
Traditional risk factors and biomarkers in CVD.

Traditional risk factors		Known and Novel Biomarkers			
Modifiables	Non modifiables	Inflammation and Endothelial Dysfunction	Neurohormonal activation	Ischemia	Necrosis
Dyslipemia Hypertension Diabetes Smoking Obesity Physical Inactivity	Age Gender Family History	ICAM-1 VCAM-1 E-selectin CRP sCD40L IL-18 MCP-1 Fibrinogen MPO ROS OPN FFA	BNP NT-proBNP ADM MR-proADM Copeptin	FFA IMA ApoJ	cTnT cTnI

Neurohormonal activation biomarkers

Activation of neurohormonal pathways is essential for homeostasis in the normal heart. In acute heart failure these systems have beneficial effects but in chronic heart failure their activation produces deleterious effects by increasing the load on the left ventricle and promoting structural remodelling. Interventions that have favourable hemodynamic but unfavourable neurohormonal effects can actually exacerbate cardiac disease and may increase cardiovascular morbidity and mortality. As neurohormonal activation appears to parallel the severity of heart failure, an understanding of neurohormonal activation and its interaction with hemodynamic factors is essential for optimizing pharmacologic therapies for CVD [19].

Elevated levels of B-type natriuretic peptide (BNP) are associated with adverse clinical outcomes in acute coronary syndrome [20] and in coronary heart disease (CHD) [21]. BNP is released from cardiomyocytes in response to high arterial pressure or cardiac dilatation [1]. Recent experiments have shown that bedside BNP measurement enhances the prediction of cardiovascular risk at 10 months, independently of any traditional echocardiography assessment of dysfunction, suggesting that BNP should be measured in addition to echocardiography for accurate prognosis [20].

The biological activity of adrenomedullin (ADM) in the cardiovascular system is similar to that of BNP causing vasodilatation and hypotension with activation effects on platelet cAMP production [22]. Plasma ADM is elevated in CHD and after AMI. The ADM precursor, MR-proADM may represent a clinically useful marker of prognosis after AMI as it is a powerful predictor of adverse outcome, especially in those subjects with elevated NT-proBNP (BNP precursor) [23].

Copeptin is the C-terminal fragment of the vasopressin precursor hormone with a longer half-life in circulation which makes it easier to measure [24]. Copeptin is a prognostic biomarker as its levels are peaked early after AMI and are associated with the incidence of death or heart failure during follow-up [24]. When used together with cardiac troponin, copeptin may improve the sensitivity for diagnosing AMI [25]. Copeptin is also a good marker of neurohormonal stress, making it useful in risk stratification in sepsis and other diseases and hence is not specific to the cardiovascular system [26].

Biomarkers of Ischemia

One of the most important challenges in the diagnosis of an acute ischemic event is the identification of biomarkers that will allow the early detection of the ischemic process before an irreversible injury occurs [27]. Serum levels of FFA increase after ischemia as a result of an increased adipose tissue lipolysis and of a decrease in fatty acid consumption. Therefore, the measurement of FFA serum levels has been proposed for early detection of cardiac injury as its change is previous to that of necrosis biomarkers [28,29].

Serum albumin from patients with myocardial ischemia exhibit low metal-binding capacity for cobalt than albumin from healthy subjects [30]. However, increased ischemia-modified albumin (IMA) levels have also been found in relation to non-cardiac ischemic processes [31] making IMA measurement in need of further studies.

Recently, a proteomic approach has detected changes in the serum profile of Apolipoprotein J (Apo J) in patients in the early phase

post-AMI. ApoJ is an HDL-related glycoprotein with anti-inflammatory properties that has less glycosylated serum isoforms after an ischemic process [32].

Cardiac necrosis biomarkers

The measurement of the cardiac troponins, cardiac troponin T and cardiac troponin I, is the current diagnostic reference standard for myocardial necrosis. Troponins have myocardial tissue specificity and sensitivity as well as a demonstrated capacity for therapeutic decision making [24]. Troponins are released from cardiomyocytes following irreversible myocardial damage. The acute release of cardiac troponins is considered to mirror cardiomyocyte death, while a sustained increase in its plasmatic levels is related to the initiation of ventricular remodelling [33]. The sensitive nature of troponins have revealed that myocardial necrosis is found in AMI and in a range of other clinical situations, highlighting the need to use all other clinical information available (BNP, echocardiography etc) for diagnosis of AMI [34].

Traditional Risk Factor vs Biomarkers

There are conflicting results regarding how much information biomarkers add to the information provided by traditional risk factors in cardiovascular risk assessment. For instance, studies with the biomarkers CRP [10], MPO [13], BNP [20] or MR-proADM [23] have concluded that the biomarker aids to risk prediction; however, other reports maintain that the contribution of biomarkers to increase the information obtained with traditional risk factors is little (reviewed in [35]). Several factors can influence the outcome predicted by a biomarker including the population studied. While high-risk populations often yield favourable estimates of biomarkers performance, low-to-intermediate risk populations usually show conflicting data [36].

There is an increasing interest on the investigation of circulating biomarkers of cardiovascular risk in adults and their association with established traditional risk factors in metabolic syndrome progression. Indeed, increased levels of angiogenic plasmatic biomarkers (vascular endothelial growth factor and placental growth factor), inflammation biomarkers (CRP and NT-proBNP) and necrosis biomarkers (TnT) mirror the pathophysiological changes occurring in the cardiovascular system in metabolic syndrome [37].

Other studies analyze the associations between traditional risk factors and relevant biomarkers to enrich and improve cardiovascular risk prediction models. An example is the contribution of two traditional risk factors (abdominal obesity and physical inactivity) to the circulating levels of inflammation biomarkers in CHD [38]. Inflammatory biomarkers including CRP, adiponectin, secretory phospholipase A2 (sPLA2) and fibrinogen were shown to be linearly associated with increasing waist circumference and physical inactivity while lipoprotein phospholipase A2 and MPO were not. Furthermore, only CRP, MPO, sPLA2 and fibrinogen were associated with an increased CHD risk, showing that the association between abdominal obesity and CHD risk and physical inactivity and CHD risk cannot be explained by concomitant variation in inflammatory biomarkers. Moreover, several inflammatory biomarkers contribute to an increased CHD independently of the two traditional risk factors [38].

In conclusion, although biomarkers provide utility for predicting cardiovascular risk, the hope that existed a few years ago that new biomarkers would vastly improve cardiovascular risk prevention has still not materialized. The current challenge is to find new biomarkers that alone or in combination with pre-existing biomarkers, can improve risk evaluation processes with significant statistic and clinical outcomes. A better understanding of the information flux in pathological situations will increase the opportunity of interventions that limit CVD impact.

Conflict of Interest

None declared.

Funding

This work was supported by grants from the Spanish Ministry of Science and Innovation (SAF 2010–16549 to LB), Institute Carlos III (CIBEROBN-CB06/03 and TERCEL – RD06/0010/0017 to LB), Foundation Jesus Serra Fellowship (to JC) , Danone Institute Fellowship (to CRS) and MICINN- Ramon y Cajal Investigator Contract (RYC-2007-01466 to MBP).

References

[1] Straface E, Lista P, Gambardella L, Franconid F, Malorni W. Gender-specific features of plasmatic and circulating cell alterations as risk factors in cardiovascular disease. Fundam Clin Pharmacol 2010;24:665-74.
[2] Wang T. New cardiovascular risk factors exist, but are they clinically useful? Eur Heart J 2008;29:441-4.
[3] Biomarkers Definitions Working Group. Biomarkers and surrogate end-points: preferred definitions and conceptuals framework. Clin Pharmacol Ther 2001;69: 89-95.
[4] Vasan RS. Biomarkers of cardiovascular disease. Circulation 2006;113:2335-62.
[5] Mathew M, Tay E. Cusi. Elevated plasma free fatty acids increase cardiovascular risk by inducing plasma biomarkers of endothelial activation, myeloperoxidase and PAI-1 in healthy subjects. Cardiovasc Diabetol 2010;9:1-9.
[6] André P, Nannizzi-Alaimo L, Prasad SK, Phillips DR. Platelet-derived CD40L: the switch-hitting player of cardiovascular disease. Circulation 2002;106:896-9.
[7] Blankenberg S, Tiret L, Bickel C, Peetz D, Cambien F, Meyer J, et al. Interleukin-18 is a strong predictor of cardiovascular death in stable and unstable angina. Circulation 2002;106:24-30.
[8] de Lemos JA, Morrow DA, Sabatine MS, Murphy SA, Gibson CM, Antman EM, et al. Association between plasma levels of monocyte chemoattractant protein-1 and long-term clinical outcomes in patients with acute coronary syndromes. Circulation 2003;107:690-5.
[9] Mosesson MW. Fibrinogen and fibrin structure and functions. J Thromb Haemost 2005;3:1894-904.
[10] Danesh J, Wheeler JG, Hirschfield GM, Eda S, Eiriksdottir G, Rumley A, et al. C-reactive protein and other circulating markers of inflammation in the prediction of coronary heart disease. N Engl J Med 2004;350:1387-97.
[11] Molins B, Peña E, Vilahur G, Mendieta C, Slevin M, Badimon L. C-reactive protein isoforms differ in their effects on thrombus growth. Arterioscler Thromb Vasc Biol Dec. 2008;28(12):2239-46.
[12] Nicholls S, Hazen S. Myeloperoxidase and cardiovascular disease. Arterioscler Thromb Vasc Biol 2005;25:1102-11.
[13] Thukkani AK, McHowat J, Hsu FF, Brennan ML, Hazen SL. DA F. Identification of alpha-chloro fatty aldehydes and unsaturated lysophosphatidylcholine molecular species in human atherosclerotic lesions. Circulation 2003;108:3128-33.
[14] Askari AT, Brennan ML, Zhou X, Drinko J, Thomas J, Topol E, Hazen S, Penn M. Myeloperoxidase and plasminogen activator inhibitor 1 play a central role in ventricular remodeling after myocardial infarction. J Exp Med 2003;197(5):615.
[15] Zhang R, Brennan ML, Fu X, Aviles RJ, Pearce GL, Penn MS, Topol EJ, Sprecher DL, Hazen SL. Association between myeloperoxidase levels and risk of coronary artery disease. JAMA 2001;286:2136-42.
[16] Kutter D, Devaquet P, Vanderstocken G, Paulus JM, Marchal V, Gothot A. Consequences of total and subtotal myeloperoxidase deficiency: risk or benefit? Acta Haematol 2000;104:10-5.
[17] de Kleijn DVP, Moll FL, Hellings WE, Ozsarlak-Sozer G, de Bruin P, Doevendans PA. Local atherosclerotic plaques are a source of prognostic biomarkers for adverse cardiovascular events. Arterioscler Thromb Vasc Biol 2010;30 [00-00].
[18] Shoelson SE. Inflammation and insulin resistance. J Clin Invest 2006;116(7):1793.
[19] Pool PE. The clinical significance of neurohormonal activacion. Clin Ther 1997;19: 53-73.
[20] Ang DS, Kong CF, Kao MP, Struthers AD. Serial bedside B-type natriuretic peptide strongly predicts prognosis in acute coronary syndrome independent of echocardiographic abnormalities. Am Heart J 2009;158:133-40.
[21] Cowie MR, Struthers AD, Wood DA, Coats AJ, Thompson SG, Poole-Wilson PA, et al. Value of natriuretic peptides in assessment of patients with possible new heart failure in primary care. Lancet 1997;350:1349-53.
[22] Hinson JP, Kapas S, Smith DM. Adrenomedullin, a multifunctional regulatory peptide. Endocr Rev 2000;21:138-67.
[23] Takahashi K, Satoh F, Hara E, Sone M, Murakami O, Kayama T, Yoshimoto T, Shibahara S. Production and secretion of adrenomedullin from glial cell tumors and its effects on cAMP production. Peptides 1997;18:1117-24.
[24] Hochholzer W, Morrow DA, Giugliano RP. Novel biomarkers in cardiovascular disease: Update 2010. Am Heart J 2010;160:583-94.
[25] Khan SQ, Dhillon OS, O'Brien RJ, Struck J, Quinn PA, Morgenthaler NG, Squire IB, Davies JE, Bergmann A, Ng LL. C-terminal provasopressin (copeptin) as a novel and prognostic marker in acute myocardial infarction: Leicester Acute Myocardial Infarction Peptide (LAMP) study. Circulation 2007;115:2103-10.
[26] Chan D, Ng LL. Biomarkers in acute myocardial infarction. BMC Med 2010;8:34-44.

[27] Morrow DA, de Lemos JA, Sabatine MS, Antman EM. The search for a biomarker of cardiac ischemia. Clin Chem 2003;49(4):537-9.
[28] Kleinfeld AM, Prothro D, Brown DL, Davis RC, Richieri GV, DeMaria A. Increases in serum unbound free fatty acid levels following coronary angioplasty. Am J Cardiol 1996;78(12):1350-4.
[29] Panteghini M. Role and importance of biochemical markers in clinical cardiology. Eur Heart J 2004;25(14):1187-96.
[30] Bar-Or D, Lau E, Winkler JV. A novel assay for cobalt-albumin binding and its potential as a marker for myocardial ischemia-a preliminary report. J Emerg Med 2000;19(4):311-5.
[31] Apple FS, Quist HE, Otto AP, Mathews WE, Murakami MM. Release characteristics of cardiac biomarkers and ischemia-modified albumin as measured by the albumin cobalt-binding test after a marathon race. Clin Chem 2002;48(7):1097-100.
[32] Cubedo J, Padro T, García-Moll X, Pintó X, Cinca J, Badimon L. Proteomic signature of Apolipoprotein J in the early phase of new-onset myocardial infarction. J Proteome Res 2011;10(1):211-20.
[33] Emdin M, Vittorini S, Passino C, Clerico A. Old and new biomarkers of heart failure. Eur J Heart Fail 2009;11:331-5.
[34] Collinson PO, Gaze DC. Biomarkers of cardiovascular damage. Med Princ Pract 2007;16:247-61.
[35] Melander O, Newton-Cheh C, Almgren P, Hedblad B, Berglund G, Engström G. Novel and conventional biomarkers for prediction of incident cardiovascular events in the community. J Am Med Assoc 2009;302:49-57.
[36] Smith GD, Ebrahim S. Mendelian randomization: prospects, potentials and limitations. Int J Epidemiol 2004;33(1):30-42.
[37] Siervo M, Ruggiero D, Sorice R, Nutile T, Aversano M, Stephan BCM, Ciullo M. Angiogenesis and biomarkers of cardiovascular risk in adults with metabolic syndrome. J Intern Med 2010;268:338-47.
[38] Rana JS, Arsenault BJ, Després JP, Côté M, Talmud PJ, Ninio E, et al. Inflammatory biomarkers, physical activity, waist circumference, and risk of future coronary heart disease in healthymen and women. Eur Heart J 2011;32:336-44.

BIBLIOGRAFÍA

1. World Health Organization. World Health Statistics 2013. A wealth of information on global public health. 2013.

2. World Health Organization, World Heart Federation, World Stroke Organization. Global atlas on cardiovascular disease prevention and control. 2011. Available at: http://www.who.int/cardiovascular_diseases/publications/atlas_cvd/en/index.html.

3. Mackay, J, Mensah, G. *The Atlas of Heart Disease and Stroke*. World Health Organization; 2004.

4. Cannon B. Cardiovascular disease: Biochemistry to behaviour. *Nature* 2013;493(7434):S2-3. doi:10.1038/493S2a.

5. World Health Organization. Global health risks: Mortality and burden of disease attributable to selected major risks. 2009.

6. World Health Organization. Prevention of cardiovascular disease: Guidelines for assessment and management of cardiovascular risk. 2007.

7. Kivimäki M, Leino-Arjas P, Luukkonen R, Riihimäki H, Vahtera J, Kirjonen J. Work stress and risk of cardiovascular mortality: prospective cohort study of industrial employees. *BMJ* 2002;325(7369):857.

8. Lett HS, Blumenthal JA, Babyak MA, Sherwood A, Strauman T, Robins C, Newman MF. Depression as a risk factor for coronary artery disease: evidence, mechanisms, and treatment. *Psychosom. Med.* 2004;66(3):305-315.

9. Rosengren A, Hawken S, Ounpuu S, Sliwa K, Zubaid M, Almahmeed WA, Blackett KN, Sitthi-amorn C, Sato H, Yusuf S, INTERHEART investigators. Association of psychosocial risk factors with risk of acute myocardial infarction in 11119 cases and 13648 controls from 52 countries (the INTERHEART study): case-control study. *Lancet* 2004;364(9438):953-962. doi:10.1016/S0140-6736(04)17019-0.

10. Gump BB, Matthews KA, Eberly LE, Chang Y, MRFIT Research Group. Depressive symptoms and mortality in men: results from the Multiple Risk Factor Intervention Trial. *Stroke J. Cereb. Circ.* 2005;36(1):98-102. doi:10.1161/01.STR.0000149626.50127.d0.

11. Badimon L, Romero JC, Cubedo J, Borrell-Pagès M. Circulating biomarkers. *Thromb. Res.* 2012;130 Suppl 1:S12-15. doi:10.1016/j.thromres.2012.08.262.

12. Ross R. Atherosclerosis--an inflammatory disease. *N. Engl. J. Med.* 1999;340(2):115-126. doi:10.1056/NEJM199901143400207.

13. Lusis AJ. Atherosclerosis. *Nature* 2000;407(6801):233-241. doi:10.1038/35025203.

14. Moore KJ, Sheedy FJ, Fisher EA. Macrophages in atherosclerosis: a dynamic balance. *Nat. Rev. Immunol.* 2013;13(10):709-721. doi:10.1038/nri3520.

15. Ishibashi S, Brown MS, Goldstein JL, Gerard RD, Hammer RE, Herz J. Hypercholesterolemia in low density lipoprotein receptor knockout mice and its reversal by adenovirus-mediated gene delivery. *J. Clin. Invest.* 1993;92(2):883-893. doi:10.1172/JCI116663.

16. Meikle PJ, Wong G, Barlow CK, Kingwell BA. Lipidomics: Potential role in risk prediction and therapeutic monitoring for diabetes and cardiovascular disease. *Pharmacol. Ther.* 2014;143(1):12-23. doi:10.1016/j.pharmthera.2014.02.001.

17. Mathews CK, Holde KKEV, Ahern KG. *Biochemistry*. Benjamin Cummings; 2000.

18. Turley SD, Dietschy JM. Sterol absorption by the small intestine. *Curr. Opin. Lipidol.* 2003;14(3):233-240. doi:10.1097/01.mol.0000073503.41685.8e.

19. Ostlund RE, Bosner MS, Stenson WF. Cholesterol absorption efficiency declines at moderate dietary doses in normal human subjects. *J. Lipid Res.* 1999;40(8):1453-1458.

20. Pikuleva IA, Curcio CA. Cholesterol in the retina: The best is yet to come. *Prog. Retin. Eye Res.* 2014. doi:10.1016/j.preteyeres.2014.03.002.

21. Tabas I, Williams KJ, Borén J. Subendothelial lipoprotein retention as the initiating process in atherosclerosis: update and therapeutic implications. *Circulation* 2007;116(16):1832-1844. doi:10.1161/CIRCULATIONAHA.106.676890.

22. Meaney S, Bodin K, Diczfalusy U, Björkhem I. On the rate of translocation in vitro and kinetics in vivo of the major oxysterols in human circulation: critical importance of the position of the oxygen function. *J. Lipid Res.* 2002;43(12):2130-2135.

23. Rader DJ, Daugherty A. Translating molecular discoveries into new therapies for atherosclerosis. *Nature* 2008;451(7181):904-913. doi:10.1038/nature06796.

24. Stenmark KR, Yeager ME, El Kasmi KC, Nozik-Grayck E, Gerasimovskaya EV, Li M, Riddle SR, Frid MG. The adventitia: essential regulator of vascular wall structure and function. *Annu. Rev. Physiol.* 2013;75:23-47. doi:10.1146/annurev-physiol-030212-183802.

25. Perrotta I. Ultrastructural features of human atherosclerosis. *Ultrastruct. Pathol.* 2013;37(1):43-51. doi:10.3109/01913123.2011.592721.

26. Gasser TC, Ogden RW, Holzapfel GA. Hyperelastic modelling of arterial layers with distributed collagen fibre orientations. *J. R. Soc. Interface R. Soc.* 2006;3(6):15-35. doi:10.1098/rsif.2005.0073.

27. Libby P, Ridker PM, Hansson GK. Inflammation in atherosclerosis: from pathophysiology to practice. *J. Am. Coll. Cardiol.* 2009;54(23):2129-2138. doi:10.1016/j.jacc.2009.09.009.

28. Badimon L, Storey RF, Vilahur G. Update on lipids, inflammation and atherothrombosis. *Thromb. Haemost.* 2011;105 Suppl 1:S34-42. doi:10.1160/THS10-11-0717.

29. Shi C, Pamer EG. Monocyte recruitment during infection and inflammation. *Nat. Rev. Immunol.* 2011;11(11):762-774. doi:10.1038/nri3070.

30. Steinberg D. Atherogenesis in perspective: hypercholesterolemia and inflammation as partners in crime. *Nat. Med.* 2002;8(11):1211-1217. doi:10.1038/nm1102-1211.

31. Lang JK, Cimato TR. Cholesterol and hematopoietic stem cells: inflammatory mediators of atherosclerosis. *Stem Cells Transl. Med.* 2014;3(5):549-552. doi:10.5966/sctm.2013-0205.

32. Swirski FK, Libby P, Aikawa E, Alcaide P, Luscinskas FW, Weissleder R, Pittet MJ. Ly-6Chi monocytes dominate hypercholesterolemia-associated monocytosis and give rise to macrophages in atheromata. *J. Clin. Invest.* 2007;117(1):195-205. doi:10.1172/JCI29950.

33. Shi N, Chen S-Y. Mechanisms simultaneously regulate smooth muscle proliferation and differentiation. *J. Biomed. Res.* 2014;28(1):40-46. doi:10.7555/JBR.28.20130130.

34. Shalhoub J, Falck-Hansen MA, Davies AH, Monaco C. Innate immunity and monocyte-macrophage activation in atherosclerosis. *J. Inflamm. Lond. Engl.* 2011;8:9. doi:10.1186/1476-9255-8-9.

35. Passlick B, Flieger D, Ziegler-Heitbrock HW. Identification and characterization of a novel monocyte subpopulation in human peripheral blood. *Blood* 1989;74(7):2527-2534.

36. Shantsila E, Wrigley B, Tapp L, Apostolakis S, Montoro-Garcia S, Drayson MT, Lip GYH. Immunophenotypic characterization of human monocyte subsets: possible implications for cardiovascular disease pathophysiology. *J. Thromb. Haemost. JTH* 2011;9(5):1056-1066. doi:10.1111/j.1538-7836.2011.04244.x.

37. Sunderkötter C, Nikolic T, Dillon MJ, Van Rooijen N, Stehling M, Drevets DA, Leenen PJM. Subpopulations of mouse blood monocytes differ in maturation stage and inflammatory response. *J. Immunol. Baltim. Md 1950* 2004;172(7):4410-4417.

38. Hilgendorf I, Swirski FK. Making a difference: monocyte heterogeneity in cardiovascular disease. *Curr. Atheroscler. Rep.* 2012;14(5):450-459. doi:10.1007/s11883-012-0274-8.

39. Ingersoll MA, Spanbroek R, Lottaz C, Gautier EL, Frankenberger M, Hoffmann R, Lang R, Haniffa M, Collin M, Tacke F, Habenicht AJR, Ziegler-Heitbrock L, Randolph GJ. Comparison of gene expression profiles between human and mouse monocyte subsets. *Blood* 2010;115(3):e10-19. doi:10.1182/blood-2009-07-235028.

40. Ghattas A, Griffiths HR, Devitt A, Lip GYH, Shantsila E. Monocytes in Coronary Artery Disease and Atherosclerosis: Where Are We Now? *J. Am. Coll. Cardiol.* 2013;62(17):1541-1551. doi:10.1016/j.jacc.2013.07.043.

41. Jeon H, Blacklow SC. Structure and physiologic function of the low-density lipoprotein receptor. *Annu. Rev. Biochem.* 2005;74:535-562. doi:10.1146/annurev.biochem.74.082803.133354.

42. Li Y, Cam J, Bu G. Low-density lipoprotein receptor family: endocytosis and signal transduction. *Mol. Neurobiol.* 2001;23(1):53-67. doi:10.1385/MN:23:1:53.

43. Go G-W, Mani A. Low-density lipoprotein receptor (LDLR) family orchestrates cholesterol homeostasis. *Yale J. Biol. Med.* 2012;85(1):19-28.

44. Brown MS, Goldstein JL. Receptor-mediated control of cholesterol metabolism. *Science* 1976;191(4223):150-154.

45. Hobbs HH, Russell DW, Brown MS, Goldstein JL. The LDL receptor locus in familial hypercholesterolemia: mutational analysis of a membrane protein. *Annu. Rev. Genet.* 1990;24:133-170. doi:10.1146/annurev.ge.24.120190.001025.

46. Van Craeyveld E, Jacobs F, Gordts SC, De Geest B. Gene therapy for familial hypercholesterolemia. *Curr. Pharm. Des.* 2011;17(24):2575-2591.

47. Gent J, Braakman I. Low-density lipoprotein receptor structure and folding. *Cell. Mol. Life Sci. CMLS* 2004;61(19-20):2461-2470. doi:10.1007/s00018-004-4090-3.

48. Sakai J, Hoshino A, Takahashi S, Miura Y, Ishii H, Suzuki H, Kawarabayasi Y, Yamamoto T. Structure, chromosome location, and expression of the human very low density lipoprotein receptor gene. *J. Biol. Chem.* 1994;269(3):2173-2182.

49. Takahashi S, Suzuki J, Kohno M, Oida K, Tamai T, Miyabo S, Yamamoto T, Nakai T. Enhancement of the binding of triglyceride-rich lipoproteins to the very low density lipoprotein receptor by apolipoprotein E and lipoprotein lipase. *J. Biol. Chem.* 1995;270(26):15747-15754.

50. Yuan G, Liu Y, Sun T, Xu Y, Zhang J, Yang Y, Zhang M, Cianflone K, Wang DW. The therapeutic role of very low-density lipoprotein receptor gene in hyperlipidemia in type 2 diabetic rats. *Hum. Gene Ther.* 2011;22(3):302-312. doi:10.1089/hum.2010.038.

51. Eck MV, Oost J, Goudriaan JR, Hoekstra M, Hildebrand RB, Bos IST, van Dijk KW, Van Berkel TJC. Role of the macrophage very-low-density lipoprotein receptor in atherosclerotic lesion development. *Atherosclerosis* 2005;183(2):230-237. doi:10.1016/j.atherosclerosis.2005.03.045.

52. Borrell-Pagès M, Romero JC, Juan-Babot O, Badimon L. Wnt pathway activation, cell migration, and lipid uptake is regulated by low-density lipoprotein receptor-related protein 5 in human macrophages. *Eur. Heart J.* 2011;32(22):2841-2850. doi:10.1093/eurheartj/ehr062.

53. Boucher P, Herz J. Signaling through LRP1: Protection from atherosclerosis and beyond. *Biochem. Pharmacol.* 2011;81(1):1-5. doi:10.1016/j.bcp.2010.09.018.

54. Cal R, Castellano J, Revuelta-López E, Aledo R, Barriga M, Farré J, Vilahur G, Nasarre L, Hove-Madsen L, Badimon L, Llorente-Cortés V. Low-density lipoprotein receptor-related protein 1 mediates hypoxia-induced very low density lipoprotein-cholesteryl ester uptake and accumulation in cardiomyocytes. *Cardiovasc. Res.* 2012;94(3):469-479. doi:10.1093/cvr/cvs136.

55. Cal R, Juan-Babot O, Brossa V, Roura S, Gálvez-Montón C, Portoles M, Rivera M, Cinca J, Badimon L, Llorente-Cortés V. Low density lipoprotein receptor-related protein 1 expression correlates with cholesteryl ester accumulation in the myocardium of ischemic cardiomyopathy patients. *J. Transl. Med.* 2012;10:160. doi:10.1186/1479-5876-10-160.

56. Camino-López S, Llorente-Cortés V, Sendra J, Badimon L. Tissue factor induction by aggregated LDL depends on LDL receptor-related protein expression (LRP1) and Rho A translocation in human vascular smooth muscle cells. *Cardiovasc. Res.* 2007;73(1):208-216. doi:10.1016/j.cardiores.2006.10.017.

57. Camino-López S, Badimon L, González A, Canals D, Peña E, Llorente-Cortés V. Aggregated low density lipoprotein induces tissue factor by inhibiting sphingomyelinase activity in human vascular smooth muscle cells. *J. Thromb. Haemost. JTH* 2009;7(12):2137-2146. doi:10.1111/j.1538-7836.2009.03638.x.

58. Castellano J, Farré J, Fernandes J, Bayes-Genis A, Cinca J, Badimon L, Hove-Madsen L, Llorente-Cortés V. Hypoxia exacerbates Ca(2+)-handling disturbances induced by very low density lipoproteins (VLDL) in neonatal rat cardiomyocytes. *J. Mol. Cell. Cardiol.* 2011;50(5):894-902. doi:10.1016/j.yjmcc.2011.02.002.

59. Yancey PG, Ding Y, Fan D, Blakemore JL, Zhang Y, Ding L, Zhang J, Linton MF, Fazio S. Low-density lipoprotein receptor-related protein 1 prevents early atherosclerosis by limiting lesional apoptosis and inflammatory Ly-6Chigh monocytosis: evidence that the effects are not apolipoprotein E dependent. *Circulation* 2011;124(4):454-464. doi:10.1161/CIRCULATIONAHA.111.032268.

60. Overton CD, Yancey PG, Major AS, Linton MF, Fazio S. Deletion of macrophage LDL receptor-related protein increases atherogenesis in the mouse. *Circ. Res.* 2007;100(5):670-677. doi:10.1161/01.RES.0000260204.40510.aa.

61. Dahlbäck B, Nielsen LB. Apolipoprotein M--a novel player in high-density lipoprotein metabolism and atherosclerosis. *Curr. Opin. Lipidol.* 2006;17(3):291-295. doi:10.1097/01.mol.0000226122.10005.88.

62. Faber K, Hvidberg V, Moestrup SK, Dahlbäck B, Nielsen LB. Megalin is a receptor for apolipoprotein M, and kidney-specific megalin-deficiency confers urinary excretion of apolipoprotein M. *Mol. Endocrinol. Baltim. Md* 2006;20(1):212-218. doi:10.1210/me.2005-0209.

63. Dugué-Pujol S, Rousset X, Château D, Pastier D, Klein C, Demeurie J, Cywiner-Golenzer C, Chabert M, Verroust P, Chambaz J, Châtelet F-P, Kalopissis A-D. Apolipoprotein A-II is catabolized in the kidney as a function of its plasma concentration. *J. Lipid Res.* 2007;48(10):2151-2161. doi:10.1194/jlr.M700089-JLR200.

64. Koh JM, Jung MH, Hong JS, Park HJ, Chang JS, Shin HD, Kim SY, Kim GS. Association between bone mineral density and LDL receptor-related protein 5 gene polymorphisms in young Korean men. *J. Korean Med. Sci.* 2004;19(3):407-412.

65. Urano T, Shiraki M, Usui T, Sasaki N, Ouchi Y, Inoue S. A1330V variant of the low-density lipoprotein receptor-related protein 5 (LRP5) gene decreases Wnt signaling and affects the total body bone mineral density in Japanese women. *Endocr. J.* 2009;56(4):625-631.

66. Suwazono Y, Kobayashi E, Uetani M, Miura K, Morikawa Y, Ishizaki M, Kido T, Nakagawa H, Nogawa K. G-protein beta 3 subunit polymorphism C1429T and low-density lipoprotein receptor-related protein 5 polymorphism A1330V are risk factors for hypercholesterolemia in Japanese males--a prospective study over 5 years. *Metabolism.* 2006;55(6):751-757. doi:10.1016/j.metabol.2006.01.011.

67. Jiang X-Y, Chen Y, Xu L, Li X, Cao F-F, Li L, Lu M, Jin L, Wang X-F. Association of LPR5 polymorphism with bone mass density and cholesterol level in population of Chinese Han. *Exp. Clin. Endocrinol. Diabetes Off. J. Ger. Soc. Endocrinol. Ger. Diabetes Assoc.* 2010;118(6):388-391. doi:10.1055/s-0029-1225613.

68. Mani A, Radhakrishnan J, Wang H, Mani A, Mani M-A, Nelson-Williams C, Carew KS, Mane S, Najmabadi H, Wu D, Lifton RP. LRP6 mutation in a family with early coronary disease and metabolic risk factors. *Science* 2007;315(5816):1278-1282. doi:10.1126/science.1136370.

69. Shen G-Q, Li L, Girelli D, Seidelmann SB, Rao S, Fan C, Park JE, Xi Q, Li J, Hu Y, Olivieri O, Marchant K, Barnard J, Corrocher R, Elston R, Cassano J, Henderson S, Hazen SL, Plow EF, Topol EJ, Wang QK. An LRP8 variant is associated with familial and premature coronary artery disease and myocardial infarction. *Am. J. Hum. Genet.* 2007;81(4):780-791. doi:10.1086/521581.

70. Shen G-Q, Girelli D, Li L, Olivieri O, Martinelli N, Chen Q, Topol EJ, Wang QK. Multi-allelic haplotype association identifies novel information different from single-SNP analysis: a new protective haplotype in the LRP8 gene is against familial and early-onset CAD and MI. *Gene* 2013;521(1):78-81. doi:10.1016/j.gene.2013.03.022.

71. Jiang M, Bujo H, Ohwaki K, Unoki H, Yamazaki H, Kanaki T, Shibasaki M, Azuma K, Harigaya K, Schneider WJ, Saito Y. Ang II-stimulated migration of vascular smooth muscle cells is dependent on LR11 in mice. *J. Clin. Invest.* 2008;118(8):2733-2746. doi:10.1172/JCI32381.

72. Takahashi M, Bujo H, Jiang M, Noike H, Saito Y, Shirai K. Enhanced circulating soluble LR11 in patients with coronary organic stenosis. *Atherosclerosis* 2010;210(2):581-584. doi:10.1016/j.atherosclerosis.2009.12.010.

73. Ogita M, Miyauchi K, Dohi T, Tsuboi S, Miyazaki T, Yokoyama T, Yokoyama K, Shimada K, Kurata T, Jiang M, Bujo H, Daida H. Increased circulating soluble LR11 in patients with acute coronary syndrome. *Clin. Chim. Acta* 2013;415:191-194. doi:10.1016/j.cca.2012.10.047.

74. Hey PJ, Twells RC, Phillips MS, Yusuke Nakagawa, Brown SD, Kawaguchi Y, Cox R, Guochun Xie, Dugan V, Hammond H, Metzker ML, Todd JA, Hess JF. Cloning of a novel member of the low-density lipoprotein receptor family. *Gene* 1998;216(1):103-111.

75. Herz J, Hamann U, Rogne S, Myklebost O, Gausepohl H, Stanley KK. Surface location and high affinity for calcium of a 500-kd liver membrane protein closely related to the LDL-receptor suggest a physiological role as lipoprotein receptor. *EMBO J.* 1988;7(13):4119-4127.

76. Brown MS, Herz J, Goldstein JL. LDL-receptor structure. Calcium cages, acid baths and recycling receptors. *Nature* 1997;388(6643):629-630. doi:10.1038/41672.

77. Vincent V, Goffin V, Rozakis-Adcock M, Mornon JP, Kelly PA. Identification of cytoplasmic motifs required for short prolactin receptor internalization. *J. Biol. Chem.* 1997;272(11):7062-7068.

78. Figueroa DJ, Hess JF, Ky B, Brown SD, Sandig V, Hermanowski-Vosatka A, Twells RC, Todd JA, Austin CP. Expression of the type I diabetes-associated gene LRP5 in macrophages, vitamin A system cells, and the Islets of Langerhans suggests multiple potential roles in diabetes. *J. Histochem. Cytochem. Off. J. Histochem. Soc.* 2000;48(10):1357-1368.

79. Gong Y, Slee RB, Fukai N, Rawadi G, Roman-Roman S, Reginato AM, Wang H, Cundy T, Glorieux FH, Lev D, Zacharin M, Oexle K, Marcelino J, Suwairi W, Heeger S, Sabatakos G, Apte S, Adkins WN, Allgrove J, Arslan-Kirchner M, Batch JA, Beighton P, Black GC, Boles RG, Boon LM, Borrone C, Brunner HG, Carle GF, Dallapiccola B, De Paepe A, Floege B, Halfhide ML, Hall B, Hennekam RC, Hirose T, Jans A, Jüppner H, Kim CA, Keppler-

Noreuil K, Kohlschuetter A, LaCombe D, Lambert M, Lemyre E, Letteboer T, Peltonen L, Ramesar RS, Romanengo M, Somer H, Steichen-Gersdorf E, Steinmann B, Sullivan B, Superti-Furga A, Swoboda W, van den Boogaard MJ, Van Hul W, Vikkula M, Votruba M, Zabel B, Garcia T, Baron R, Olsen BR, Warman ML. LDL receptor-related protein 5 (LRP5) affects bone accrual and eye development. *Cell* 2001;107(4):513-523.

80. Kato M, Patel MS, Levasseur R, Lobov I, Chang BH-J, Glass DA 2nd, Hartmann C, Li L, Hwang T-H, Brayton CF, Lang RA, Karsenty G, Chan L. Cbfa1-independent decrease in osteoblast proliferation, osteopenia, and persistent embryonic eye vascularization in mice deficient in Lrp5, a Wnt coreceptor. *J. Cell Biol.* 2002;157(2):303-314. doi:10.1083/jcb.200201089.

81. Little RD, Carulli JP, Del Mastro RG, Dupuis J, Osborne M, Folz C, Manning SP, Swain PM, Zhao S-C, Eustace B, Lappe MM, Spitzer L, Zweier S, Braunschweiger K, Benchekroun Y, Hu X, Adair R, Chee L, FitzGerald MG, Tulig C, Caruso A, Tzellas N, Bawa A, Franklin B, McGuire S, Nogues X, Gong G, Allen KM, Anisowicz A, Morales AJ, Lomedico PT, Recker SM, Van Eerdewegh P, Recker RR, Johnson ML. A mutation in the LDL receptor-related protein 5 gene results in the autosomal dominant high-bone-mass trait. *Am. J. Hum. Genet.* 2002;70(1):11-19. doi:10.1086/338450.

82. Fujino T, Asaba H, Kang M-J, Ikeda Y, Sone H, Takada S, Kim D-H, Ioka RX, Ono M, Tomoyori H, Okubo M, Murase T, Kamataki A, Yamamoto J, Magoori K, Takahashi S, Miyamoto Y, Oishi H, Nose M, Okazaki M, Usui S, Imaizumi K, Yanagisawa M, Sakai J, Yamamoto TT. Low-density lipoprotein receptor-related protein 5 (LRP5) is essential for normal cholesterol metabolism and glucose-induced insulin secretion. *Proc. Natl. Acad. Sci. U. S. A.* 2003;100(1):229-234. doi:10.1073/pnas.0133792100.

83. Magoori K, Kang M-J, Ito MR, Kakuuchi H, Ioka RX, Kamataki A, Kim D-H, Asaba H, Iwasaki S, Takei YA, Sasaki M, Usui S, Okazaki M, Takahashi S, Ono M, Nose M, Sakai J, Fujino T, Yamamoto TT. Severe hypercholesterolemia, impaired fat tolerance, and advanced atherosclerosis in mice lacking both low density lipoprotein receptor-related protein 5 and apolipoprotein E. *J. Biol. Chem.* 2003;278(13):11331-11336. doi:10.1074/jbc.M211987200.

84. Xia C, Lu E, Zeng J, Gong X. Deletion of LRP5 in VLDLR knockout mice inhibits retinal neovascularization. *PloS One* 2013;8(9):e75186. doi:10.1371/journal.pone.0075186.

85. Shin Y, Huh YH, Kim K, Kim S, Park KH, Koh J-T, Chun J-S, Ryu J-H. Low-density lipoprotein receptor-related protein 5 governs Wnt-mediated osteoarthritic cartilage destruction. *Arthritis Res. Ther.* 2014;16(1):R37. doi:10.1186/ar4466.

86. Mao J, Wang J, Liu B, Pan W, Farr GH 3rd, Flynn C, Yuan H, Takada S, Kimelman D, Li L, Wu D. Low-density lipoprotein receptor-related protein-5 binds to Axin and regulates the canonical Wnt signaling pathway. *Mol. Cell* 2001;7(4):801-809.

87. Hashimoto L, Habita C, Beressi JP, Delepine M, Besse C, Cambon-Thomsen A, Deschamps I, Rotter JI, Djoulah S, James MR. Genetic mapping of a susceptibility locus for insulin-dependent diabetes mellitus on chromosome 11q. *Nature* 1994;371(6493):161-164. doi:10.1038/371161a0.

88. Nakagawa Y, Kawaguchi Y, Twells RC, Muxworthy C, Hunter KM, Wilson A, Merriman ME, Cox RD, Merriman T, Cucca F, McKinney PA, Shield JP, Tuomilehto J, Tuomilehto-Wolf E, Ionesco-Tirgoviste C, Nisticò L, Buzzetti R, Pozzilli P, Joner G, Thorsby E, Undlien DE, Pociot F, Nerup J, Rönningen KS, Bain SC, Todd JA, Bart's-Oxford Family Study Group. Fine mapping of the diabetes-susceptibility locus, IDDM4, on chromosome 11q13. *Am. J. Hum. Genet.* 1998;63(2):547-556.

89. Ai M, Heeger S, Bartels CF, Schelling DK. Clinical and molecular findings in osteoporosis-pseudoglioma syndrome. *Am. J. Hum. Genet.* 2005;77(5):741-753. doi:10.1086/497706.

90. Babij P, Zhao W, Small C, Kharode Y, Yaworsky PJ, Bouxsein ML, Reddy PS, Bodine PVN, Robinson JA, Bhat B, Marzolf J, Moran RA, Bex F. High bone mass in mice expressing a mutant LRP5 gene. *J. Bone Miner. Res. Off. J. Am. Soc. Bone Miner. Res.* 2003;18(6):960-974. doi:10.1359/jbmr.2003.18.6.960.

91. Papathanasiou I, Malizos KN, Tsezou A. Low-density lipoprotein receptor-related protein 5 (LRP5) expression in human osteoarthritic chondrocytes. *J. Orthop. Res. Off. Publ. Orthop. Res. Soc.* 2010;28(3):348-353. doi:10.1002/jor.20993.

92. Li C, Huang Z, Kingsley R, Zhou X, Li F, Parke DW 2nd, Cao W. Biochemical alterations in the retinas of very low-density lipoprotein receptor knockout mice: an animal model of retinal angiomatous proliferation. *Arch. Ophthalmol.* 2007;125(6):795-803. doi:10.1001/archopht.125.6.795.

93. Willert K, Brown JD, Danenberg E, Duncan AW, Weissman IL, Reya T, Yates JR, Nusse R. Wnt proteins are lipid-modified and can act as stem cell growth factors. *Nature* 2003;423(6938):448-452. doi:10.1038/nature01611.

94. Takada R, Satomi Y, Kurata T, Ueno N, Norioka S, Kondoh H, Takao T, Takada S. Monounsaturated fatty acid modification of Wnt protein: its role in Wnt secretion. *Dev. Cell* 2006;11(6):791-801. doi:10.1016/j.devcel.2006.10.003.

95. Logan CY, Nusse R. The Wnt signaling pathway in development and disease. *Annu. Rev. Cell Dev. Biol.* 2004;20:781-810. doi:10.1146/annurev.cellbio.20.010403.113126.

96. Port F, Basler K. Wnt trafficking: new insights into Wnt maturation, secretion and spreading. *Traffic Cph. Den.* 2010;11(10):1265-1271. doi:10.1111/j.1600-0854.2010.01076.x.

97. Nusse R, Fuerer C, Ching W, Harnish K, Logan C, Zeng A, ten Berge D, Kalani Y. Wnt signaling and stem cell control. *Cold Spring Harb. Symp. Quant. Biol.* 2008;73:59-66. doi:10.1101/sqb.2008.73.035.

98. Clevers H. Wnt/beta-catenin signaling in development and disease. *Cell* 2006;127(3):469-480. doi:10.1016/j.cell.2006.10.018.

99. Angers S, Moon RT. Proximal events in Wnt signal transduction. *Nat. Rev. Mol. Cell Biol.* 2009;10(7):468-477. doi:10.1038/nrm2717.

100. Caliceti C, Nigro P, Rizzo P, Ferrari R. ROS, Notch, and Wnt Signaling Pathways: Crosstalk between Three Major Regulators of Cardiovascular Biology. *BioMed Res. Int.* 2014;2014:318714. doi:10.1155/2014/318714.

101. George SJ. Wnt pathway: a new role in regulation of inflammation. *Arterioscler. Thromb. Vasc. Biol.* 2008;28(3):400-402. doi:10.1161/ATVBAHA.107.160952.

102. Gumbiner BM. Carcinogenesis: a balance between beta-catenin and APC. *Curr. Biol. CB* 1997;7(7):R443-446.

103. Kim W, Kim M, Jho E. Wnt/β-catenin signalling: from plasma membrane to nucleus. *Biochem. J.* 2013;450(1):9-21. doi:10.1042/BJ20121284.

104. MacDonald BT, Tamai K, He X. Wnt/beta-catenin signaling: components, mechanisms, and diseases. *Dev. Cell* 2009;17(1):9-26. doi:10.1016/j.devcel.2009.06.016.

105. Van der Heyden MA, Rook MB, Hermans MM, Rijksen G, Boonstra J, Defize LH, Destrée OH. Identification of connexin43 as a functional target for Wnt signalling. *J. Cell Sci.* 1998;111 (Pt 12):1741-1749.

106. Howe LR, Subbaramaiah K, Chung WJ, Dannenberg AJ, Brown AM. Transcriptional activation of cyclooxygenase-2 in Wnt-1-transformed mouse mammary epithelial cells. *Cancer Res.* 1999;59(7):1572-1577.

107. Mann B, Gelos M, Siedow A, Hanski ML, Gratchev A, Ilyas M, Bodmer WF, Moyer MP, Riecken EO, Buhr HJ, Hanski C. Target genes of beta-catenin-T cell-factor/lymphoid-enhancer-factor signaling in human colorectal carcinomas. *Proc. Natl. Acad. Sci. U. S. A.* 1999;96(4):1603-1608.

108. Shtutman M, Zhurinsky J, Simcha I, Albanese C, D'Amico M, Pestell R, Ben-Ze'ev A. The cyclin D1 gene is a target of the beta-catenin/LEF-1 pathway. *Proc. Natl. Acad. Sci. U. S. A.* 1999;96(10):5522-5527.

109. Müller T, Bain G, Wang X, Papkoff J. Regulation of epithelial cell migration and tumor formation by beta-catenin signaling. *Exp. Cell Res.* 2002;280(1):119-133.

110. Dell'Accio F, De Bari C, El Tawil NMF, Barone F, Mitsiadis TA, O'Dowd J, Pitzalis C. Activation of WNT and BMP signaling in adult human articular cartilage following mechanical injury. *Arthritis Res. Ther.* 2006;8(5):R139. doi:10.1186/ar2029.

111. Takada I, Kouzmenko AP, Kato S. Wnt and PPARgamma signaling in osteoblastogenesis and adipogenesis. *Nat. Rev. Rheumatol.* 2009;5(8):442-447. doi:10.1038/nrrheum.2009.137.

112. Krishnan V, Bryant HU, Macdougald OA. Regulation of bone mass by Wnt signaling. *J. Clin. Invest.* 2006;116(5):1202-1209. doi:10.1172/JCI28551.

113. Baron R, Rawadi G, Roman-Roman S. Wnt signaling: a key regulator of bone mass. *Curr. Top. Dev. Biol.* 2006;76:103-127. doi:10.1016/S0070-2153(06)76004-5.

114. Bennett CN, Longo KA, Wright WS, Suva LJ, Lane TF, Hankenson KD, MacDougald OA. Regulation of osteoblastogenesis and bone mass by Wnt10b. *Proc. Natl. Acad. Sci. U. S. A.* 2005;102(9):3324-3329. doi:10.1073/pnas.0408742102.

115. Whyte JL, Smith AA, Helms JA. Wnt signaling and injury repair. *Cold Spring Harb. Perspect. Biol.* 2012;4(8):a008078. doi:10.1101/cshperspect.a008078.

116. Gelfand BD, Meller J, Pryor AW, Kahn M, Bortz PDS, Wamhoff BR, Blackman BR. Hemodynamic activation of beta-catenin and T-cell-specific transcription factor signaling in vascular endothelium regulates fibronectin expression. *Arterioscler. Thromb. Vasc. Biol.* 2011;31(7):1625-1633. doi:10.1161/ATVBAHA.111.227827.

117. Von Toerne C, Schmidt C, Adams J, Kiss E, Bedke J, Porubsky S, Gretz N, Lindenmeyer MT, Cohen CD, Gröne H-J, Nelson PJ. Wnt pathway regulation in chronic renal allograft damage. *Am. J. Transplant. Off. J. Am. Soc. Transplant. Am. Soc. Transpl. Surg.* 2009;9(10):2223-2239. doi:10.1111/j.1600-6143.2009.02762.x.

118. Martin M, Rehani K, Jope RS, Michalek SM. Toll-like receptor-mediated cytokine production is differentially regulated by glycogen synthase kinase 3. *Nat. Immunol.* 2005;6(8):777-784. doi:10.1038/ni1221.

119. Kim J, Kim J, Kim DW, Ha Y, Ihm MH, Kim H, Song K, Lee I. Wnt5a induces endothelial inflammation via beta-catenin-independent signaling. *J. Immunol. Baltim. Md 1950* 2010;185(2):1274-1282. doi:10.4049/jimmunol.1000181.

120. Zhang P, Katz J, Michalek SM. Glycogen synthase kinase-3beta (GSK3beta) inhibition suppresses the inflammatory response to Francisella infection and protects against tularemia in mice. *Mol. Immunol.* 2009;46(4):677-687. doi:10.1016/j.molimm.2008.08.281.

121. Ma J, Wang R, Fang X, Sun Z. β-catenin/TCF-1 pathway in T cell development and differentiation. *J. Neuroimmune Pharmacol. Off. J. Soc. NeuroImmune Pharmacol.* 2012;7(4):750-762. doi:10.1007/s11481-012-9367-y.

122. Yu Q, Sharma A, Oh SY, Moon H-G, Hossain MZ, Salay TM, Leeds KE, Du H, Wu B, Waterman ML, Zhu Z, Sen JM. T cell factor 1 initiates the T helper type 2 fate by inducing the transcription factor GATA-3 and repressing interferon-gamma. *Nat. Immunol.* 2009;10(9):992-999. doi:10.1038/ni.1762.

123. Bedel A, Nègre-Salvayre A, Heeneman S, Grazide M-H, Thiers J-C, Salvayre R, Maupas-Schwalm F. E-cadherin/beta-catenin/T-cell factor pathway is involved in smooth muscle cell proliferation elicited by oxidized low-density lipoprotein. *Circ. Res.* 2008;103(7):694-701. doi:10.1161/CIRCRESAHA.107.166405.

124. Sarzani R, Salvi F, Bordicchia M, Guerra F, Battistoni I, Pagliariccio G, Carbonari L, Dessì-Fulgheri P, Rappelli A. Carotid artery atherosclerosis in hypertensive patients with a functional LDL receptor-related protein 6 gene variant. *Nutr. Metab. Cardiovasc. Dis. NMCD* 2011;21(2):150-156. doi:10.1016/j.numecd.2009.08.004.

125. Shao J-S, Cheng S-L, Pingsterhaus JM, Charlton-Kachigian N, Loewy AP, Towler DA. Msx2 promotes cardiovascular calcification by activating paracrine Wnt signals. *J. Clin. Invest.* 2005;115(5):1210-1220. doi:10.1172/JCI24140.

126. Shao J-S, Aly ZA, Lai C-F, Cheng S-L, Cai J, Huang E, Behrmann A, Towler DA. Vascular Bmp Msx2 Wnt signaling and oxidative stress in arterial calcification. *Ann. N. Y. Acad. Sci.* 2007;1117:40-50. doi:10.1196/annals.1402.075.

127. Marinou K, Christodoulides C, Antoniades C, Koutsilieris M. Wnt signaling in cardiovascular physiology. *Trends Endocrinol. Metab. TEM* 2012;23(12):628-636. doi:10.1016/j.tem.2012.06.001.

128. Kim DH, Inagaki Y, Suzuki T, Ioka RX, Yoshioka SZ, Magoori K, Kang MJ, Cho Y, Nakano AZ, Liu Q, Fujino T, Suzuki H, Sasano H, Yamamoto TT. A new low density lipoprotein receptor related protein, LRP5, is expressed in hepatocytes and adrenal cortex, and recognizes apolipoprotein E. *J. Biochem. (Tokyo)* 1998;124(6):1072-1076.

129. Zhang SH, Reddick RL, Piedrahita JA, Maeda N. Spontaneous hypercholesterolemia and arterial lesions in mice lacking apolipoprotein E. *Science* 1992;258(5081):468-471.

130. Ostlund RE Jr. Phytosterols in human nutrition. *Annu. Rev. Nutr.* 2002;22:533-549. doi:10.1146/annurev.nutr.22.020702.075220.

131. Kamal-Eldin A, Moazzami A. Plant sterols and stanols as cholesterol-lowering ingredients in functional foods. *Recent Pat. Food Nutr. Agric.* 2009;1(1):1-14.

132. Othman RA, Moghadasian MH. Beyond cholesterol-lowering effects of plant sterols: clinical and experimental evidence of anti-inflammatory properties. *Nutr. Rev.* 2011;69(7):371-382. doi:10.1111/j.1753-4887.2011.00399.x.

133. Weingärtner O, Ulrich C, Lütjohann D, Ismail K, Schirmer SH, Vanmierlo T, Böhm M, Laufs U. Differential effects on inhibition of cholesterol absorption by plant stanol and plant sterol esters in apoE-/- mice. *Cardiovasc. Res.* 2011;90(3):484-492. doi:10.1093/cvr/cvr020.

134. Rideout TC, Harding SV, Mackay DS. Metabolic and genetic factors modulating subject specific LDL-C responses to plant sterol therapy. *Can. J. Physiol. Pharmacol.* 2012;90(5):509-514. doi:10.1139/y2012-060.

135. Gylling H, Plat J, Turley S, Ginsberg HN, Ellegård L, Jessup W, Jones PJ, Lütjohann D, Maerz W, Masana L, Silbernagel G, Staels B, Borén J, Catapano AL, De Backer G, Deanfield J, Descamps OS, Kovanen PT, Riccardi G, Tokgözoglu L, Chapman MJ, European Atherosclerosis Society Consensus Panel on Phytosterols. Plant sterols and plant stanols in the management of dyslipidaemia and prevention of cardiovascular disease. *Atherosclerosis* 2014;232(2):346-360. doi:10.1016/j.atherosclerosis.2013.11.043.

136. Weingärtner O, Böhm M, Laufs U. Controversial role of plant sterol esters in the management of hypercholesterolaemia. *Eur. Heart J.* 2009;30(4):404-409. doi:10.1093/eurheartj/ehn580.

137. Devaraj S, Autret BC, Jialal I. Reduced-calorie orange juice beverage with plant sterols lowers C-reactive protein concentrations and improves the lipid profile in human volunteers. *Am. J. Clin. Nutr.* 2006;84(4):756-761.

138. De Smet E, Mensink RP, Plat J. Effects of plant sterols and stanols on intestinal cholesterol metabolism: suggested mechanisms from past to present. *Mol. Nutr. Food Res.* 2012;56(7):1058-1072. doi:10.1002/mnfr.201100722.

139. Miettinen TA, Gylling H. Regulation of cholesterol metabolism by dietary plant sterols. *Curr. Opin. Lipidol.* 1999;10(1):9-14.

140. Calpe-Berdiel L, Escolà-Gil JC, Ribas V, Navarro-Sastre A, Garcés-Garcés J, Blanco-Vaca F. Changes in intestinal and liver global gene expression in response to a phytosterol-enriched diet. *Atherosclerosis* 2005;181(1):75-85. doi:10.1016/j.atherosclerosis.2004.11.025.

141. Rideout TC, Harding SV, Jones PJH. Consumption of plant sterols reduces plasma and hepatic triglycerides and modulates the expression of lipid regulatory genes and de novo lipogenesis in C57BL/6J mice. *Mol. Nutr. Food Res.* 2010;54 Suppl 1:S7-13. doi:10.1002/mnfr.201000027.

142. Lottenberg AM, Bombo RPA, Ilha A, Nunes VS, Nakandakare ER, Quintão ECR. Do clinical and experimental investigations support an antiatherogenic role for dietary phytosterols/stanols? *IUBMB Life* 2012;64(4):296-306. doi:10.1002/iub.1006.

143. Berge KE, Tian H, Graf GA, Yu L, Grishin NV, Schultz J, Kwiterovich P, Shan B, Barnes R, Hobbs HH. Accumulation of dietary cholesterol in sitosterolemia caused by mutations in adjacent ABC transporters. *Science* 2000;290(5497):1771-1775.

144. Brufau G, Kuipers F, Lin Y, Trautwein EA, Groen AK. A reappraisal of the mechanism by which plant sterols promote neutral sterol loss in mice. *PloS One* 2011;6(6):e21576. doi:10.1371/journal.pone.0021576.

145. Van der Velde AE, Brufau G, Groen AK. Transintestinal cholesterol efflux. *Curr. Opin. Lipidol.* 2010;21(3):167-171. doi:10.1097/MOL.0b013e3283395e45.

146. Plat J, Nichols JA, Mensink RP. Plant sterols and stanols: effects on mixed micellar composition and LXR (target gene) activation. *J. Lipid Res.* 2005;46(11):2468-2476. doi:10.1194/jlr.M500272-JLR200.

147. Kaneko E, Matsuda M, Yamada Y, Tachibana Y, Shimomura I, Makishima M. Induction of intestinal ATP-binding cassette transporters by a phytosterol-derived liver X receptor agonist. *J. Biol. Chem.* 2003;278(38):36091-36098. doi:10.1074/jbc.M304153200.

148. Moghadasian MH, McManus BM, Pritchard PH, Frohlich JJ. "Tall oil"-derived phytosterols reduce atherosclerosis in ApoE-deficient mice. *Arterioscler. Thromb. Vasc. Biol.* 1997;17(1):119-126.

149. Ntanios FY, van de Kooij AJ, de Deckere EAM, Duchateau GSMJE, Trautwein EA. Effects of various amounts of dietary plant sterol esters on plasma and hepatic sterol concentration and aortic foam cell formation of cholesterol-fed hamsters. *Atherosclerosis* 2003;169(1):41-50.

150. Plat J, Beugels I, Gijbels MJJ, de Winther MPJ, Mensink RP. Plant sterol or stanol esters retard lesion formation in LDL receptor-deficient mice independent of changes in serum plant sterols. *J. Lipid Res.* 2006;47(12):2762-2771. doi:10.1194/jlr.M600346-JLR200.

151. Nashed B, Yeganeh B, HayGlass KT, Moghadasian MH. Antiatherogenic effects of dietary plant sterols are associated with inhibition of proinflammatory cytokine production in Apo E-KO mice. *J. Nutr.* 2005;135(10):2438-2444.

152. Calpe-Berdiel L, Escolà-Gil JC, Benítez S, Bancells C, González-Sastre F, Palomer X, Blanco-Vaca F. Dietary phytosterols modulate T-helper immune response but do not induce apparent anti-inflammatory effects in a mouse model of acute, aseptic inflammation. *Life Sci.* 2007;80(21):1951-1956. doi:10.1016/j.lfs.2007.02.032.

153. Wilund KR, Yu L, Xu F, Vega GL, Grundy SM, Cohen JC, Hobbs HH. No association between plasma levels of plant sterols and atherosclerosis in mice and men. *Arterioscler. Thromb. Vasc. Biol.* 2004;24(12):2326-2332. doi:10.1161/01.ATV.0000149140.00499.92.

154. Ratnayake WM, L'Abbé MR, Mueller R, Hayward S, Plouffe L, Hollywood R, Trick K. Vegetable oils high in phytosterols make erythrocytes less deformable and shorten the life span of stroke-prone spontaneously hypertensive rats. *J. Nutr.* 2000;130(5):1166-1178.

155. Miettinen TA. Phytosterolaemia, xanthomatosis and premature atherosclerotic arterial disease: a case with high plant sterol absorption, impaired sterol elimination and low cholesterol synthesis. *Eur. J. Clin. Invest.* 1980;10(1):27-35.

156. Sudhop T, Gottwald BM, von Bergmann K. Serum plant sterols as a potential risk factor for coronary heart disease. *Metabolism* 2002;51(12):1519-1521. doi:10.1053/meta.2002.36298.

157. Assmann G, Cullen P, Erbey J, Ramey DR, Kannenberg F, Schulte H. Plasma sitosterol elevations are associated with an increased incidence of coronary events in men: results of a nested case-control analysis of the Prospective Cardiovascular Münster (PROCAM) study. *Nutr. Metab. Cardiovasc. Dis. NMCD* 2006;16(1):13-21. doi:10.1016/j.numecd.2005.04.001.

158. Weingärtner O, Lütjohann D, Ji S, Weisshoff N, List F, Sudhop T, von Bergmann K, Gertz K, König J, Schäfers H-J, Endres M, Böhm M, Laufs U. Vascular effects of diet supplementation with plant sterols. *J. Am. Coll. Cardiol.* 2008;51(16):1553-1561. doi:10.1016/j.jacc.2007.09.074.

159. Mendis S, Nordet P, Fernandez-Britto JE, Sternby N. Atherosclerosis in children and young adults: An overview of the World Health Organization and International Society and Federation of Cardiology study on Pathobiological Determinants of Atherosclerosis in Youth study (1985–1995). *Prev. Control* 2005;1(1):3-15. doi:10.1016/j.precon.2005.02.010.

160. Varela O, Martínez-González J, Badimon L. The response of smooth muscle cells to alpha-thrombin depends on its arterial origin: comparison among different species. *Eur. J. Clin. Invest.* 1998;28(4):313-323.

161. Murao S, Gemmell MA, Callaham MF, Anderson NL, Huberman E. Control of macrophage cell differentiation in human promyelocytic HL-60 leukemia cells by 1,25-dihydroxyvitamin D3 and phorbol-12-myristate-13-acetate. *Cancer Res.* 1983;43(10):4989-4996.

162. Collins SJ. The HL-60 promyelocytic leukemia cell line: proliferation, differentiation, and cellular oncogene expression. *Blood* 1987;70(5):1233-1244.

163. Oliveira NL, Kalf GF. Induced differentiation of HL-60 promyelocytic leukemia cells to monocyte/macrophages is inhibited by hydroquinone, a hematotoxic metabolite of benzene. *Blood* 1992;79(3):627-633.

164. Holmen SL, Giambernardi TA, Zylstra CR, Buckner-Berghuis BD, Resau JH, Hess JF, Glatt V, Bouxsein ML, Ai M, Warman ML, Williams BO. Decreased BMD and limb deformities in mice carrying mutations in both Lrp5 and Lrp6. *J. Bone Miner. Res. Off. J. Am. Soc. Bone Miner. Res.* 2004;19(12):2033-2040. doi:10.1359/JBMR.040907.

165. Lindvall C, Evans NC, Zylstra CR, Li Y, Alexander CM, Williams BO. The Wnt signaling receptor Lrp5 is required for mammary ductal stem cell activity and Wnt1-induced tumorigenesis. *J. Biol. Chem.* 2006;281(46):35081-35087. doi:10.1074/jbc.M607571200.

166. Cui Y, Niziolek PJ, MacDonald BT, Zylstra CR, Alenina N, Robinson DR, Zhong Z, Matthes S, Jacobsen CM, Conlon RA, Brommage R, Liu Q, Mseeh F, Powell DR, Yang Q, Zambrowicz B, Gerrits H, Gossen JA, He X, Bader M, Williams BO, Warman ML, Robling AG. Lrp5 functions in bone to regulate bone mass. *Nat. Med.* 2011;17(6):684-691. doi:10.1038/nm.2388.

167. Havel RJ, Eder HA, Bragdon JH. The distribution and chemical composition of ultracentrifugally separated lipoproteins in human serum. *J. Clin. Invest.* 1955;34(9):1345-1353. doi:10.1172/JCI103182.

168. Lowry OH, Rosebrough NJ, Farr AL, Randall RJ. Protein measurement with the Folin phenol reagent. *J. Biol. Chem.* 1951;193(1):265-275.

169. Guyton JR, Klemp KF, Mims MP. Altered ultrastructural morphology of self-aggregated low density lipoproteins: coalescence of lipid domains forming droplets and vesicles. *J. Lipid Res.* 1991;32(6):953-962.

170. Llorente-Cortés V, Martínez-González J, Badimon L. LDL receptor-related protein mediates uptake of aggregated LDL in human vascular smooth muscle cells. *Arterioscler. Thromb. Vasc. Biol.* 2000;20(6):1572-1579.

171. Llorente-Cortés V, Otero-Viñas M, Badimon L. Differential role of heparan sulfate proteoglycans on aggregated LDL uptake in human vascular smooth muscle cells and mouse embryonic fibroblasts. *Arterioscler. Thromb. Vasc. Biol.* 2002;22(11):1905-1911.

172. Friedewald WT, Levy RI, Fredrickson DS. Estimation of the concentration of low-density lipoprotein cholesterol in plasma, without use of the preparative ultracentrifuge. *Clin. Chem.* 1972;18:499-502.

173. Bligh EG, Dyer WJ. A rapid method of total lipid extraction and purification. *Can. J. Biochem. Physiol.* 1959;37(8):911-917.

174. Stary HC, Blankenhorn DH, Chandler AB, Glagov S, Insull W Jr, Richardson M, Rosenfeld ME, Schaffer SA, Schwartz CJ, Wagner WD. A definition of the intima of human arteries and of its atherosclerosis-prone regions. A report from the Committee on Vascular Lesions of the Council on Arteriosclerosis, American Heart Association. *Circulation* 1992;85(1):391-405.

175. Tertov VV, Orekhov AN, Sobenin IA, Gabbasov ZA, Popov EG, Yaroslavov AA, Smirnov VN. Three types of naturally occurring modified lipoproteins induce intracellular lipid accumulation due to lipoprotein aggregation. *Circ. Res.* 1992;71(1):218-228.

176. Khoo JC, Miller E, McLoughlin P, Steinberg D. Enhanced macrophage uptake of low density lipoprotein after self-aggregation. *Arterioscler. Dallas Tex* 1988;8(4):348-358.

177. Kruth HS. Sequestration of aggregated low-density lipoproteins by macrophages. *Curr. Opin. Lipidol.* 2002;13(5):483-488.

178. Choudhury RP, Lee JM, Greaves DR. Mechanisms of disease: macrophage-derived foam cells emerging as therapeutic targets in atherosclerosis. *Nat. Clin. Pract. Cardiovasc. Med.* 2005;2(6):309-315. doi:10.1038/ncpcardio0195.

179. Webb NR, Moore KJ. Macrophage-derived foam cells in atherosclerosis: lessons from murine models and implications for therapy. *Curr. Drug Targets* 2007;8(12):1249-1263.

180. Llorente-Cortés V, Otero-Viñas M, Sánchez S, Rodríguez C, Badimon L. Low-density lipoprotein upregulates low-density lipoprotein receptor-related protein expression in vascular smooth muscle cells: possible involvement of sterol regulatory element binding protein-2-dependent mechanism. *Circulation* 2002;106(24):3104-3110.

181. Llorente-Cortés V, Royo T, Juan-Babot O, Badimon L. Adipocyte differentiation-related protein is induced by LRP1-mediated aggregated LDL internalization in human vascular smooth muscle cells and macrophages. *J. Lipid Res.* 2007;48(10):2133-2140. doi:10.1194/jlr.M700039-JLR200.

182. Dhore CR, Cleutjens JP, Lutgens E, Cleutjens KB, Geusens PP, Kitslaar PJ, Tordoir JH, Spronk HM, Vermeer C, Daemen MJ. Differential expression of bone matrix regulatory proteins in human atherosclerotic plaques. *Arterioscler. Thromb. Vasc. Biol.* 2001;21(12):1998-2003.

183. Lund SA, Giachelli CM, Scatena M. The role of osteopontin in inflammatory processes. *J. Cell Commun. Signal.* 2009;3(3-4):311-322. doi:10.1007/s12079-009-0068-0.

184. De Kleijn DPV, Moll FL, Hellings WE, Ozsarlak-Sozer G, de Bruin P, Doevendans PA, Vink A, Catanzariti LM, Schoneveld AH, Algra A, Daemen MJ, Biessen EA, de Jager W, Zhang H, de Vries J-P, Falk E, Lim SK, van der Spek PJ, Sze SK, Pasterkamp G. Local atherosclerotic plaques are a source of prognostic biomarkers for adverse cardiovascular events. *Arterioscler. Thromb. Vasc. Biol.* 2010;30(3):612-619. doi:10.1161/ATVBAHA.109.194944.

185. Derwall M, Malhotra R, Lai CS, Beppu Y, Aikawa E, Seehra JS, Zapol WM, Bloch KD, Yu PB. Inhibition of bone morphogenetic protein signaling reduces vascular calcification and atherosclerosis. *Arterioscler. Thromb. Vasc. Biol.* 2012;32(3):613-622. doi:10.1161/ATVBAHA.111.242594.

186. Neumeister P, Pixley FJ, Xiong Y, Xie H, Wu K, Ashton A, Cammer M, Chan A, Symons M, Stanley ER, Pestell RG. Cyclin D1 governs adhesion and motility of macrophages. *Mol. Biol. Cell* 2003;14(5):2005-2015. doi:10.1091/mbc.02-07-0102.

187. Jiao X, Katiyar S, Willmarth NE, Liu M, Ma X, Flomenberg N, Lisanti MP, Pestell RG. c-Jun induces mammary epithelial cellular invasion and breast cancer stem cell expansion. *J. Biol. Chem.* 2010;285(11):8218-8226. doi:10.1074/jbc.M110.100792.

188. Zhong Z, Yeow W-S, Zou C, Wassell R, Wang C, Pestell RG, Quong JN, Quong AA. Cyclin D1/cyclin-dependent kinase 4 interacts with filamin A and affects the migration and invasion potential of breast cancer cells. *Cancer Res.* 2010;70(5):2105-2114. doi:10.1158/0008-5472.CAN-08-1108.

189. Golledge J, Van Campenhout A, Pal S, Rush C. Bone marrow–derived cells and arterial disease. *J. Vasc. Surg.* 2007;46(3):590-600. doi:10.1016/j.jvs.2007.04.031.

190. Iwata H, Manabe I, Nagai R. Lineage of Bone Marrow–Derived Cells in Atherosclerosis. *Circ. Res.* 2013;112(12):1634-1647. doi:10.1161/CIRCRESAHA.113.301384.

191. Tickenbrock L, Schwäble J, Strey A, Sargin B, Hehn S, Baas M, Choudhary C, Gerke V, Berdel WE, Müller-Tidow C, Serve H. Wnt signaling regulates transendothelial migration of monocytes. *J. Leukoc. Biol.* 2006;79(6):1306-1313. doi:10.1189/jlb.0905539.

192. Mill C, George SJ. Wnt signalling in smooth muscle cells and its role in cardiovascular disorders. *Cardiovasc. Res.* 2012;95(2):233-240. doi:10.1093/cvr/cvs141.

193. Ley K, Miller YI, Hedrick CC. Monocyte and Macrophage Dynamics During Atherogenesis. *Arterioscler. Thromb. Vasc. Biol.* 2011;31(7):1506-1516. doi:10.1161/ATVBAHA.110.221127.

194. Moore KJ, Tabas I. Macrophages in the pathogenesis of atherosclerosis. *Cell* 2011;145(3):341-355. doi:10.1016/j.cell.2011.04.005.

195. Li F, Chong ZZ, Maiese K. Winding through the WNT pathway during cellular development and demise. *Histol. Histopathol.* 2006;21(1):103-124.

196. Danial NN, Korsmeyer SJ. Cell death: critical control points. *Cell* 2004;116(2):205-219.

197. Rössig L, Haendeler J, Hermann C, Malchow P, Urbich C, Zeiher AM, Dimmeler S. Nitric oxide down-regulates MKP-3 mRNA levels: involvement in endothelial cell protection from apoptosis. *J. Biol. Chem.* 2000;275(33):25502-25507. doi:10.1074/jbc.M002283200.

198. Furukawa T, Sunamura M, Motoi F, Matsuno S, Horii A. Potential tumor suppressive pathway involving DUSP6/MKP-3 in pancreatic cancer. *Am. J. Pathol.* 2003;162(6):1807-1815. doi:10.1016/S0002-9440(10)64315-5.

199. Welch C, Santra MK, El-Assaad W, Zhu X, Huber WE, Keys RA, Teodoro JG, Green MR. Identification of a protein, G0S2, that lacks Bcl-2 homology domains and interacts with and antagonizes Bcl-2. *Cancer Res.* 2009;69(17):6782-6789. doi:10.1158/0008-5472.CAN-09-0128.

200. Kelly GL, Strasser A. The essential role of evasion from cell death in cancer. *Adv. Cancer Res.* 2011;111:39-96. doi:10.1016/B978-0-12-385524-4.00002-7.

201. Bernhard EJ, McKenna WG, Muschel RJ. Cyclin expression and G2-phase delay after irradiation. *Radiat. Res.* 1994;138(1 Suppl):S64-67.

202. Maity A, Hwang A, Janss A, Phillips P, McKenna WG, Muschel RJ. Delayed cyclin B1 expression during the G2 arrest following DNA damage. *Oncogene* 1996;13(8):1647-1657.

203. Yuan J, Yan R, Krämer A, Eckerdt F, Roller M, Kaufmann M, Strebhardt K. Cyclin B1 depletion inhibits proliferation and induces apoptosis in human tumor cells. *Oncogene* 2004;23(34):5843-5852. doi:10.1038/sj.onc.1207757.

204. Porakishvili N, Memon A, Vispute K, Kulikova N, Clark EA, Rai KR, Nathwani A, Damle RN, Chiorazzi N, Lydyard PM. CD180 functions in activation, survival and cycling of B chronic lymphocytic leukaemia cells. *Br. J. Haematol.* 2011;153(4):486-498. doi:10.1111/j.1365-2141.2011.08605.x.

205. Hume DA. The mononuclear phagocyte system. *Curr. Opin. Immunol.* 2006;18(1):49-53. doi:10.1016/j.coi.2005.11.008.

206. Sokoloski JA, Sartorelli AC, Rosen CA, Narayanan R. Antisense oligonucleotides to the p65 subunit of NF-kappa B block CD11b expression and alter adhesion properties of differentiated HL-60 granulocytes. *Blood* 1993;82(2):625-632.

207. Slevin M, Krupinski J, Gaffney J, Matou S, West D, Delisser H, Savani RC, Kumar S. Hyaluronan-mediated angiogenesis in vascular disease: uncovering RHAMM and CD44 receptor signaling pathways. *Matrix Biol. J. Int. Soc. Matrix Biol.* 2007;26(1):58-68. doi:10.1016/j.matbio.2006.08.261.

208. Baksh D, Boland GM, Tuan RS. Cross-talk between Wnt signaling pathways in human mesenchymal stem cells leads to functional antagonism during osteogenic differentiation. *J. Cell. Biochem.* 2007;101(5):1109-1124. doi:10.1002/jcb.21097.

209. Yuzugullu H, Benhaj K, Ozturk N, Senturk S, Celik E, Toylu A, Tasdemir N, Yilmaz M, Erdal E, Akcali KC, Atabey N, Ozturk M. Canonical Wnt signaling is antagonized by noncanonical Wnt5a in hepatocellular carcinoma cells. *Mol. Cancer* 2009;8:90. doi:10.1186/1476-4598-8-90.

210. Haÿ E, Laplantine E, Geoffroy V, Frain M, Kohler T, Müller R, Marie PJ. N-cadherin interacts with axin and LRP5 to negatively regulate Wnt/beta-catenin signaling, osteoblast function, and bone formation. *Mol. Cell. Biol.* 2009;29(4):953-964. doi:10.1128/MCB.00349-08.

211. Hay E, Faucheu C, Suc-Royer I, Touitou R, Stiot V, Vayssière B, Baron R, Roman-Roman S, Rawadi G. Interaction between LRP5 and Frat1 mediates the activation of the Wnt canonical pathway. *J. Biol. Chem.* 2005;280(14):13616-13623. doi:10.1074/jbc.M411999200.

212. Shahi P, Park D, Pond AC, Seethammagari M, Chiou S-H, Cho K, Carstens JL, Decker WK, McCrea PD, Ittmann MM, Rosen JM, Spencer DM. Activation of Wnt signaling by chemically induced dimerization of LRP5 disrupts cellular homeostasis. *PloS One* 2012;7(1):e30814. doi:10.1371/journal.pone.0030814.

213. Sheng Z, Otani H, Brown MS, Goldstein JL. Independent regulation of sterol regulatory element-binding proteins 1 and 2 in hamster liver. *Proc. Natl. Acad. Sci.* 1995;92(4):935-938.

214. Singh AB, Kan CFK, Shende V, Dong B, Liu J. A novel posttranscriptional mechanism for dietary cholesterol-mediated suppression of liver LDL receptor expression. *J. Lipid Res.* 2014;55(7):1397-1407. doi:10.1194/jlr.M049429.

215. Ye Z, Go G-W, Singh R, Liu W, Keramati AR, Mani A. LRP6 protein regulates low density lipoprotein (LDL) receptor-mediated LDL uptake. *J. Biol. Chem.* 2012;287(2):1335-1344. doi:10.1074/jbc.M111.295287.

216. Kobayashi K, Oka K, Forte T, Ishida B, Teng B, Ishimura-Oka K, Nakamuta M, Chan L. Reversal of hypercholesterolemia in low density lipoprotein receptor knockout mice by adenovirus-mediated gene transfer of the very low density lipoprotein receptor. *J. Biol. Chem.* 1996;271(12):6852-6860.

217. Yuasa-Kawase M, Masuda D, Yamashita T, Kawase R, Nakaoka H, Inagaki M, Nakatani K, Tsubakio-Yamamoto K, Ohama T, Matsuyama A, Nishida M, Ishigami M, Kawamoto T, Komuro I, Yamashita S. Patients with CD36 deficiency are associated with enhanced atherosclerotic cardiovascular diseases. *J. Atheroscler. Thromb.* 2012;19(3):263-275.

218. Nozaki S, Kashiwagi H, Yamashita S, Nakagawa T, Kostner B, Tomiyama Y, Nakata A, Ishigami M, Miyagawa J, Kameda-Takemura K. Reduced uptake of oxidized low density lipoproteins in monocyte-derived macrophages from CD36-deficient subjects. *J. Clin. Invest.* 1995;96(4):1859-1865. doi:10.1172/JCI118231.

219. Llorente-Cortés V, Badimon L. LDL receptor-related protein and the vascular wall: implications for atherothrombosis. *Arterioscler. Thromb. Vasc. Biol.* 2005;25(3):497-504. doi:10.1161/01.ATV.0000154280.62072.fd.

220. Llorente-Cortes V, Casani L, Cal R, Llenas A, Juan-Babot O, Camino-López S, Sendra J, Badimon L. Cholesterol-lowering strategies reduce vascular LRP1 overexpression induced by hypercholesterolaemia. *Eur. J. Clin. Invest.* 2011;41(10):1087-1097. doi:10.1111/j.1365-2362.2011.02513.x.

221. Keramati AR, Singh R, Lin A, Faramarzi S, Ye Z, Mane S, Tellides G, Lifton RP, Mani A. Wild-type LRP6 inhibits, whereas atherosclerosis-linked LRP6R611C increases PDGF-dependent vascular smooth muscle cell proliferation. *Proc. Natl. Acad. Sci. U. S. A.* 2011;108(5):1914-1918. doi:10.1073/pnas.1019443108.

222. Nakanishi K, Yoshimoto T, Tsutsui H, Okamura H. Interleukin-18 regulates both Th1 and Th2 responses. *Annu. Rev. Immunol.* 2001;19:423-474. doi:10.1146/annurev.immunol.19.1.423.

223. Badimon L. Interleukin-18: a potent pro-inflammatory cytokine in atherosclerosis. *Cardiovasc. Res.* 2012;96(2):172-175; discussion 176-180. doi:10.1093/cvr/cvs226.

224. Oppenheimer-Marks N, Brezinschek RI, Mohamadzadeh M, Vita R, Lipsky PE. Interleukin 15 is produced by endothelial cells and increases the transendothelial migration of T cells In vitro and in the SCID mouse-human rheumatoid arthritis model In vivo. *J. Clin. Invest.* 1998;101(6):1261-1272. doi:10.1172/JCI1986.

225. Wu J, Richards MH, Huang J, Al-Harthi L, Xu X, Lin R, Xie F, Gibson AW, Edberg JC, Kimberly RP. Human FasL gene is a target of β-catenin/T-cell factor pathway and complex FasL haplotypes alter promoter functions. *PloS One* 2011;6(10):e26143. doi:10.1371/journal.pone.0026143.

226. Morimoto S, Nakano S, Watanabe T, Tamayama Y, Mitsuo A, Nakiri Y, Suzuki J, Nozawa K, Amano H, Tokano Y, Kobata T, Takasaki Y. Expression of B-cell activating factor of the tumour necrosis factor family (BAFF) in T cells in active systemic lupus erythematosus: the role of BAFF in T cell-dependent B cell pathogenic autoantibody production. *Rheumatol. Oxf. Engl.* 2007;46(7):1083-1086. doi:10.1093/rheumatology/kem097.

227. Batten M, Li J, Yi S, Kljavin NM, Danilenko DM, Lucas S, Lee J, de Sauvage FJ, Ghilardi N. Interleukin 27 limits autoimmune encephalomyelitis by suppressing the development of interleukin 17-producing T cells. *Nat. Immunol.* 2006;7(9):929-936. doi:10.1038/ni1375.

228. Niedbala W, Cai B, Wei X, Patakas A, Leung BP, McInnes IB, Liew FY. Interleukin 27 attenuates collagen-induced arthritis. *Ann. Rheum. Dis.* 2008;67(10):1474-1479. doi:10.1136/ard.2007.083360.

229. Merad M, Manz MG. Dendritic cell homeostasis. *Blood* 2009;113(15):3418-3427. doi:10.1182/blood-2008-12-180646.

230. Svensson MND, Andersson SEM, Erlandsson MC, Jonsson I-M, Ekwall A-KH, Andersson KME, Nilsson A, Bian L, Brisslert M, Bokarewa MI. Fms-like tyrosine kinase 3 ligand controls formation of regulatory T cells in autoimmune arthritis. *PloS One* 2013;8(1):e54884. doi:10.1371/journal.pone.0054884.

231. Aggarwal BB, Gupta SC, Kim JH. Historical perspectives on tumor necrosis factor and its superfamily: 25 years later, a golden journey. *Blood* 2012;119(3):651-665. doi:10.1182/blood-2011-04-325225.

232. Secchiero P, Gonelli A, Carnevale E, Milani D, Pandolfi A, Zella D, Zauli G. TRAIL promotes the survival and proliferation of primary human vascular endothelial cells by activating the Akt and ERK pathways. *Circulation* 2003;107(17):2250-2256. doi:10.1161/01.CIR.0000062702.60708.C4.

233. Secchiero P, Corallini F, di Iasio MG, Gonelli A, Barbarotto E, Zauli G. TRAIL counteracts the proadhesive activity of inflammatory cytokines in endothelial cells by down-modulating CCL8 and CXCL10 chemokine expression and release. *Blood* 2005;105(9):3413-3419. doi:10.1182/blood-2004-10-4111.

234. Bernardi S, Zauli G, Tikellis C, Candido R, Fabris B, Secchiero P, Cooper ME, Thomas MC. TNF-related apoptosis-inducing ligand significantly attenuates metabolic abnormalities in high-fat-fed mice reducing adiposity and systemic inflammation. *Clin. Sci. Lond. Engl. 1979* 2012;123(9):547-555. doi:10.1042/CS20120176.

235. Stein JV, López-Fraga M, Elustondo FA, Carvalho-Pinto CE, Rodríguez D, Gómez-Caro R, De Jong J, Martínez-A C, Medema JP, Hahne M. APRIL modulates B and T cell immunity. *J. Clin. Invest.* 2002;109(12):1587-1598. doi:10.1172/JCI15034.

236. Teijeira Á, Palazón A, Garasa S, Marré D, Aubá C, Rogel A, Murillo O, Martínez-Forero I, Lang F, Melero I, Rouzaut A. CD137 on inflamed lymphatic endothelial cells enhances CCL21-guided migration of dendritic cells. *FASEB J. Off. Publ. Fed. Am. Soc. Exp. Biol.* 2012;26(8):3380-3392. doi:10.1096/fj.11-201061.

237. Jones PJH, AbuMweis SS. Phytosterols as functional food ingredients: linkages to cardiovascular disease and cancer. *Curr. Opin. Clin. Nutr. Metab. Care* 2009;12(2):147-151.

238. Mackness B, Hunt R, Durrington PN, Mackness MI. Increased immunolocalization of paraoxonase, clusterin, and apolipoprotein A-I in the human artery wall with the progression of atherosclerosis. *Arterioscler. Thromb. Vasc. Biol.* 1997;17(7):1233-1238.

239. Kruth HS. Localization of unesterified cholesterol in human atherosclerotic lesions. Demonstration of filipin-positive, oil-red-O-negative particles. *Am. J. Pathol.* 1984;114(2):201-208.

240. Guyton JR, Klemp KF. Development of the atherosclerotic core region. Chemical and ultrastructural analysis of microdissected atherosclerotic lesions from human aorta. *Arterioscler. Thromb. J. Vasc. Biol. Am. Heart Assoc.* 1994;14(8):1305-1314.

241. Chen Z, Ichetovkin M, Kurtz M, Zycband E, Kawka D, Woods J, He X, Plump AS, Hailman E. Cholesterol in human atherosclerotic plaque is a marker for underlying disease state and plaque vulnerability. *Lipids Health Dis.* 2010;9:61. doi:10.1186/1476-511X-9-61.

242. Feingold KR, Shigenaga JK, Kazemi MR, McDonald CM, Patzek SM, Cross AS, Moser A, Grunfeld C. Mechanisms of triglyceride accumulation in activated macrophages. *J. Leukoc. Biol.* 2012;92(4):829-839. doi:10.1189/jlb.1111537.

243. Lopes-Virella MF, Klein RL, Stevenson HC. Low density lipoprotein metabolism in human macrophages stimulated with microbial or microbial-related products. *Arterioscler. Dallas Tex* 1987;7(2):176-184.

244. Funk JL, Feingold KR, Moser AH, Grunfeld C. Lipopolysaccharide stimulation of RAW 264.7 macrophages induces lipid accumulation and foam cell formation. *Atherosclerosis* 1993;98(1):67-82.

245. Khovidhunkit W, Kim M-S, Memon RA, Shigenaga JK, Moser AH, Feingold KR, Grunfeld C. Effects of infection and inflammation on lipid and lipoprotein metabolism: mechanisms and consequences to the host. *J. Lipid Res.* 2004;45(7):1169-1196. doi:10.1194/jlr.R300019-JLR200.

246. Ahn J, Lee H, Kim S, Ha T. Curcumin-induced suppression of adipogenic differentiation is accompanied by activation of Wnt/beta-catenin signaling. *Am. J. Physiol. Cell Physiol.* 2010;298(6):C1510-1516. doi:10.1152/ajpcell.00369.2009.

247. Naumann E, Plat J, Kester ADM, Mensink RP. The baseline serum lipoprotein profile is related to plant stanol induced changes in serum lipoprotein cholesterol and triacylglycerol concentrations. *J. Am. Coll. Nutr.* 2008;27(1):117-126.

248. Plat J, Brufau G, Dallinga-Thie GM, Dasselaar M, Mensink RP. A plant stanol yogurt drink alone or combined with a low-dose statin lowers serum triacylglycerol and non-HDL cholesterol in metabolic syndrome patients. *J. Nutr.* 2009;139(6):1143-1149. doi:10.3945/jn.108.103481.